550
R-4

THE GEOLOGICAL SOCIETY OF AMERICA

BULLETIN

PUBLISHED BY THE SOCIETY

NOVEMBER 1961

THE JOHN CRERAR LIBRARY
NOV 27 1961

Council

PRESIDENT

THOMAS B. NOLAN, *Washington, D. C.*

VICE-PRESIDENT

M. KING HUBBERT, *Houston, Texas*

SECRETARY

FREDERICK BETZ, JR., 419 *West* 117 *Street, New York* 27, *N. Y.*

TREASURER

J. EDWARD HOFFMEISTER, *Rochester, N. Y.*

COUNCILORS

1960–1961 HOLLIS D. HEDBERG (PAST PRESIDENT) *Princeton, N. J.*

1959–1961

JOHN C. FRYE	ROBERT P. SHARP	CHARLES F. PARK, JR.	E. F. OSBORN
Urbana, Ill.	*Pasadena, Calif.*	*Stanford, Calif.*	*University Park, Pa.*

1960–1962

NORMAN D. NEWELL	VINCENT C. KELLEY	GEORGE P. WOOLLARD	HAROLD L. JAMES
New York, N. Y.	*Albuquerque, N. M.*	*Madison, Wis.*	*Menlo Park, Calif.*

1961–1963

EDUARDO J. GUZMAN	J. M. HARRISON	E. B. ECKEL	CARL TOLMAN
Mexico City, Mex.	*Ottawa, Ontario*	*Denver, Colo.*	*St. Louis, Mo.*

COMMITTEE ON PUBLICATIONS

WILLIAM C. KRUMBEIN, *Chairman*
E. N. GODDARD
J. E. ARMSTRONG

Conferees
FREDERICK BETZ, JR., *Secretary*
AGNES CREAGH, *Managing Editor*

EDITORIAL STAFF

AGNES CREAGH
Managing Editor

BARBARA ANNE FLYNN
Assistant Editor

UNIVERSITY OF ILLINOIS LIBRARY

The Geological Society of America Bulletin

Volume 72 November 1961 Number 11

CONTENTS

Theory of folding of stratified viscoelastic media and its implications in tectonics and orogenesis . . . . . *M. A. Biot* 1595–1620

Experimental verification of the theory of folding of stratified viscoelastic media . . . . . *M. A. Biot, H. Odé, and W. L. Roever* 1621–1632

Paleoecology of an early Oligocene biota from Douglass Creek basin, Montana . . . . . *R. L. Konizeski* 1633–1642

Origin of Pennsylvanian underclay and related seat rocks . . . . . *John W. Huddle and Sam H. Patterson* 1643–1660

Breccia pipe near Cameron, Arizona . . . . *Jonathan Barrington and Paul F. Kerr* 1661–1674

Stochastic variables of geologic search and decision . . . . . *Bahngrell W. Brown* 1675–1686

SHORT NOTES

Two tills in southern Connecticut . . . . . *Richard Foster Flint* 1687–1692

Seismic refraction profiles on the continental shelf south of Bellport, Long Island, New York . . . . . *M. V. Brown, John Northrop, Roberto Frassetto, and L. H. Grabner* 1693–1706

Late Quaternary sea level: A discussion . . . . . *Joseph R. Curray* 1707–1712

Clay minerals in sediments of Owens, China, Searles, Panamint, Bristol, Cadiz, and Danby lake basins, California . . . . . *John B. Droste* 1713–1722

Zoned granitic intrusions—an alternative hypothesis of origin . . . . . *Joseph A. Vance* 1723–1728

Subscriptions $15.00 per year. Printing Office: Burlington, Vt. Second-class postage paid at Burlington, Vermont
Published monthly.
Communications regarding publications should be addressed to The Geological Society of America, Dr. Frederick Betz, Jr., Secretary, 419 West 117 Street, New York 27, N. Y.
Please give notice of change of address 4 weeks in advance. Claims for nonreceipt of the Bulletin of a given month must be sent to the Secretary of the Society before the end of the second succeeding month.

PAPERS IN PRESS FOR FORTHCOMING ISSUES

Distribution of Cu, Ni, Co, V, and Cr in Rocks of the Hindubagh Igneous Complex, Zhob Valley, West Pakistan. S. A. Bilgrami

K-Ar Age Studies of Mississippi and Other River Sediments. P. M. Hurley, D. G. Brookins, W. H. Pinson, S. R. Hart, and H. W. Fairbairn

Petrology and Structural Geometry of the Pre-granitic Rocks in the Sierra Nevada, Alpine County, California. R. B. Parker

Upper Paleozoic Stratigraphy of East-central Idaho. J. Philip Shannon, Jr.

Chemical and Mineralogical Composition of Fossil Molluscan Shells from the Fox Hills Formation, South Dakota. K. K. Turekian and R. L. Armstrong

Submarine Geology of the Tasman Sea. J. C. Standard

Stratigraphy of the Cambrian Sedimentary Rocks of Eastern Pennsylvania. Bradford Willard

Reconnaissance Study of Quaternary Faults In and South of Yellowstone National Park, Wyoming. J. D. Love

Corona Development in Norwegian Hyperites and its Bearing on the Metamorphic Facies Concept. R. C. Reynolds, Jr., and A. F. Frederickson

Late Quaternary History of the Snake River in American Falls Region, Idaho. Donald E. Trimble and Wilfred J. Carr

TECTONIC MAP OF MEXICO

Compiled by Zoltan de Cserna. Scale 1:2,500,000. In full color.
Price, $5.50
Special price to Fellows and Members of GSA, $4.00

NEW MEMOIR

85. X-Ray Powder Data for the Ore Minerals: The Peacock Atlas. L. G. Berry and R. M. Thompson
Price, $8.25
Special price to Fellows and Members of GSA, $6.00

REVIEW VOLUMES IN ENGINEERING GEOLOGY IN PRESS

Volume 1. Thomas Fluhr and R. F. Legget, *Editors*

Contains eight papers covering fields of engineering seismology, petrography applied to portland-cement concrete, sand and gravel, photo analysis and interpretation in engineering geology, engineering aspects of sediment transport, engineering geology of radioactive waste material, rock bolting, recent U.S.S.R. publications in selected fields of soil science.
Price, $7.00
Special price to Fellows and Members of GSA, $5.00

NEW CODE OF STRATIGRAPHIC NOMENCLATURE

Authors of papers to be submitted to GSA for publication are requested to follow the usage for stratigraphic nomenclature recommended in the new Code of Stratigraphic Nomenclature (See May 1961 issue of the Bulletin of the American Association of Petroleum Geologists).

M. A. BIOT *Shell Development Company, Houston, Texas*

Theory of Folding of Stratified Viscoelastic Media and Its Implications in Tectonics and Orogenesis[1]

Abstract: This paper presents an introduction to the theory of folding of stratified viscoelastic media under compression and discusses its significance in the context of tectonics and orogenesis. Simplified derivations are given for results obtained earlier by the writer as particular cases of more elaborate theories. The writer emphasizes the mechanism involved in folding. The paper begins with a discussion of the buckling of an elastic rod that is under axial compression and is restrained laterally by viscous dashpots. The analysis then proceeds to the analogous problem for an elastic and a viscous plate surrounded by a viscous medium. Results of some of the more complex problems previously analyzed by the writer are also applied and discussed. Experimental verification of the theory by model tests is presented in a companion paper (Biot, Odé, and Roever, 1961).

A new feature of the present approach is the emphasis on rate phenomena and time histories in tectonic folding. In purely static problems of elastic buckling, a sharply defined wavelength is associated with the instability. By contrast, for viscoelastic media, the present theory leads to the concept of dominant wavelength and band width selectivity in analogy with the theory of electric wave filters. This is well illustrated by the gradual appearance of near-regular folds when a purely viscous layer surrounded by a viscous medium of lower viscosity is subjected to a compression in a direction tangent to the layer.

The theory is applied to specific examples of geological interest. These include the case of a single layer or a superposition of layers. Previous theoretical work by the writer is applied to the discussion of folding, under the simultaneous action of gravity forces and a horizontal compression, for a single layer or a superposition of layers lying at the surface of a deep substratum of lower viscosity. The case of a continuously inhomogeneous medium under similar forces is also included.

Using accepted values of rock viscosity and elastic moduli, the writer finds that the time required for significant folding to take place agrees very well with the geological time scale. Folding may occur under tectonic stresses that are small in comparison with the crushing strength of the rock. The time history of folding depends, of course, on initial irregularities of the layers, but after sufficient time the folding becomes fairly insensitive to the magnitude and the distribution of the initial disturbances. The writer concludes that the viscous mechanism tends to predominate in tectonic folding. As a theoretical consequence, the wavelength of the folds will, in general, not be sensitive to the magnitude of the tectonic stresses unless gravity forces become important. The calculated wavelengths are in good agreement with the range of observed values. The point at which plastic or brittle failure occurs is found to depend primarily not on the magnitude of the strain but on deformation rates. The theory can be applied to materials with nonlinear stress-strain characteristics, and the procedure to accomplish this is briefly discussed. Certain nonlinear features resulting from the geometry of deformation are shown to have a bearing on the regularity of the folds.

[1] Work carried out under the sponsorship of the Exploration and Production Research Division (Houston, Texas), where the author is a consultant for the Shell Development Company

CONTENTS

1. Introduction and acknowledgments 1596
2. Buckling of an elastic rod with viscous lateral restraint 1599
3. Buckling of an elastic plate in a viscous medium 1601
4. Folding instability of a compressed viscous plate in a viscous medium 1603
5. Amplification and selectivity of folding . . . 1604
6. Geological aspects of the folding theory . . . 1607
7. Folding of multiple layers 1611
8. Influence of gravity on folding 1614
9. Concluding remarks 1618
References cited 1619

Figure
1. Instability of a thin rod under an axial compression *F*. 1599

Geological Society of America Bulletin, v. 72, p. 1595–1620, 13 figs., November 1961

2. Balance of forces in a rod that buckles under an axial compression F and is laterally restrained by viscous dashpots 1600
3. Elastic plate of effective rigidity $E/(1-\nu^2)$ or viscous layer of viscosity η embedded in a viscous medium of viscosity η_1 1602
4. Deflection of the viscous embedding medium at the surface of contact with the layer and the restraining force, q', of the medium 1603
5. Amplification of the folding as a function of the wave number 1605
6. Folding of a layer 2 feet thick before and after yielding at the bends 1610
7. Folding of a composite layer. 1612
8. Sharpening of bends due to local yielding in the later phase of folding of the multiple-layered system of Figure 7 1613
9. Single layer of viscosity η on top of soft substratum of viscosity η_1 and density ρ_1 under a compressive stress P 1614
10. Dominant wavelength, L_d, plotted as the ratio L_d/h for the surface layer of Figure 9, when the combined effect of compressive stress, P, gravity, g, and viscosity ratio, η/η_1, is taken into account 1615
11. Layer embedded between two media of different viscosities and densities 1616
12. Multiple superposed layers lying at the surface of a medium subject to gravity . . 1616
13. Inhomogeneous viscous solid with a viscosity decreasing exponentially with the depth 1617

Table
1. Band width $(\Delta l/l_d)_e$ for the elastic layer in a viscous medium as a function of the amplification factor A_d 1605
2. Band width $(\Delta l/l_d)_v$ for the viscous layer in the viscous medium as a function of the amplification factor A_d 1606
3. Amplifications of the amplitude of folding at times $t = t_1/6$, $t = t_1/3$, and $t = t_1$, as a function of the viscosity ratio, η/η_1, and corresponding ratios of the dominant wavelength, L_d, to the layer thickness, h. 1607
4. Time in years required for explosive folding for a viscous layer in a viscous medium for various compressive loads, P, and viscosities 1608
5. Time in years required for explosive folding of an elastic layer in a viscous medium for various compressive loads, P, in the layer and viscosities, η_1, of the medium 1609

1. INTRODUCTION AND ACKNOWLEDGMENTS

A quantitative approach to the mechanics of folding of stratified sedimentary rock and, on a larger scale, of the earth's crust has attracted the attention of many investigators. Past attempts in this direction have been based primarily on the buckling theory of elastic media. These studies were restricted to static stability, and time was not considered.

This paper presents some simple geological implications based on a new approach. The theory has been verified by model tests, and the results are presented in a companion paper (Biot, Odé, and Roever, 1961). In contrast with past theories, this theory considers the deformation of viscoelastic media that exhibit either elastic, viscous, or heredity properties. Moreover, the writer has developed exact quantitative theories. The problem of calculating folding under a compressive stress extends far beyond the concepts of purely static instability, and rate processes and time histories play a dominant role.

The writer calls attention to the particular type of folding mechanism considered in the present theory. He deals only with the spontaneous folding caused by *instability* under a compressive load acting in a direction parallel with the layer and does not discuss other types of folding.

The purpose here is not to present specific geological applications but rather to discuss certain aspects of the theory that are significant in the context of geology.

Smoluchowski (1909a; 1909b; 1910) carried out the first detailed investigation based on elastic theory. He analyzed the buckling of an elastic plate lying on top of a heavy fluid and subject to a horizontal compression. He found that when a certain critical compression is reached, the plate buckles in sinusoidal waves. The load and the wavelength depend on the elasticity of the plate and the gravity buoyancy of the underlying fluid. Smoluchowski discusses many geological implications of this theory. Subsequently Goldstein (1926) published the same mathematical analysis. Later investigators—Kienow (1942) and Gunn (1937) among others—have developed applications of the theory to geology. In an extensive memoir on the mechanics of deformation in the earth's crust, Goguel (1943) devoted two chapters to the problem of folding. He based his analysis on concepts of energy dissipation. The results obtained by Goguel's method are most interesting but, on the whole, are qualitative. The theory of buckling of an elastic plate embedded in a medium that is elastic has been established by a number of authors in connection with technological problems such as the design of sandwich panels. Analytical work on this problem has been done by Bijlaard (1939; 1947), Van der Neut (1943), and Gough, Elam, and DeBruyne (1940). The last-named in-

cluded an experimental verification by model tests. From the viewpoint of geology, this purely elastic theory is of somewhat remote interest: the contrast between elastic rigidities of rock is not sufficient to permit explanation of folding of an embedded layer on a purely elastic basis.

The writer has investigated viscoelastic properties during the last 10 years: the results have been published in a series of theoretical papers. He developed a general theory of the folding of a compressed plate embedded in an indefinite medium, both viscoelastic, in a paper published in 1957. The writer used simplified equations for the bending of a viscoelastic plate in analogy with the same elastic equations for the purely elastic plate. The results were supported by comparison with the treatment of this problem by an exact theory for the stability of a viscoelastic continuum (Biot, 1959a). The writer (1959b) then investigated the problem of interfacial adherence between the layer and the surrounding medium and showed that the influence of this adherence in the case of a single layer is not significant and can be neglected. The influence of gravity on folding is important in certain situations with density contrasts and for a layer situated at the surface and was taken into account in another paper (Biot, 1959c). Finally, the writer (1960) investigated the stability for a medium limited by a horizontal surface whose rigidity and viscoelastic properties vary continuously in such a way that the medium tends to become a perfect fluid at large depth. The medium was subjected simultaneously to the action of a horizontal compression and to gravity. The writer found that gravity is important in the mechanics of folding of the surface. The writer (1958b) presented a short account of this first phase of his program at a recent colloquium.

The more elaborate and exact form of the theory results from two earlier developments. The first is based on a series of publications in which the writer (1934; 1938; 1939a; 1939b) developed a systematic theory of stability of a continuum under initial stress. An important feature of this theory is its applicability to either elastic or nonelastic media (Biot, 1956). The central idea which permits the extension of the theory to viscoelastic media is represented by the introduction of a *correspondence principle* (Biot, 1954; 1956). This provides a standard procedure for generalizing to viscoelasticity the solution of an elasticity problem. The other development deals with the application of a new thermodynamics of irreversible processes to the mechanical properties of viscoelastic media. In particular, the writer (1954) has developed some very general expressions for the relationships between stress and strain in materials that exhibit heredity properties and obey complicated creep laws. The writer (1958a) has given a general account of the thermodynamic theories in a recent lecture.

The writer has found that for materials that exhibit complex viscoelastic properties, consideration of the thermodynamics is important in stability problems.

Chandrasekhar (1955) and Hide (1955) have treated the problem of stability in a gravity field of an inhomogeneous, incompressible viscous fluid. Their theories are based on the classical equations of fluid mechanics and are restricted to the imcompressible viscous medium; no initial stresses other than the hydrostatic gravity stress are considered.

The writer herein presents a simplified rederivation of some of the significant results of the theory, along with a discussion of their implication in geodynamics. To simplify the mathematical analysis, the writer has considered only the two cases of an elastic or a viscous layer in a viscous medium. Thermodynamic considerations do not enter in these simpler cases. The emphasis has been put on a clear understanding of the mechanics of folding. The reader interested in the more advanced treatment is referred to the papers mentioned previously.

To clarify the mechanics of dynamic folding, the writer first analyzes, in Section 2, the problem of buckling under axial compression of a slender elastic rod restrained laterally by viscous dashpots. This leads to a better understanding of the folding of an axially compressed elastic layer submerged in a viscous medium. This problem is treated in Section 3. In Section 4, the writer analyzes the folding of a viscous layer under compression in a viscous medium.

In all these cases, there is, of course, no sudden buckling, as would occur, for instance, in an elastic plate with elastic lateral restraint. The folding depends on the imperfections present in the plate, *i.e.*, on its departure from a perfect plane. The deformation will grow as a function of time. The important result, however, is that the rate of growth of the deflection is very sensitive to the wavelength of the folds, *i.e.*, their distance from crest to

crest. The theory shows that there is a wavelength that grows at the fastest rate; this is referred to as the *dominant wavelength*. After sufficient time, this dominant wavelength appears in the form of more or less regular sinusoidal waves. In other words, the mechanics of folding is similar to the function of a filter amplifier when certain wavelengths present in a noise signal are amplified selectively.

The writer analyzes the regularity of the folding based on the concept of selectivity and band width of the amplification in Section 5.

In applying these concepts to geology, one must bear in mind that viscosity properties of rock vary widely. The coefficient of viscosity may, for instance, be of the order of 10^{17} poises and go up to 10^{22} poises. This is in contrast with the elastic rigidity, which ranges only from about 10^{11} to 10^{12} dynes/cm^2. From the standpoint of rate processes and viscoelasticity, the earth's crust is therefore highly heterogeneous. In relation to higher-viscosity rock, the solids of lower viscosity will even tend to behave as liquids. This points to enormous differences between the behavior of stratified structures when considered, on the one hand, as elastic materials susceptible only to static instability and, on the other hand, as viscoelastic materials with strain-rate effects. The writer gives a quantitative analysis of the folding of rock strata in Section 6. Because of the exponential time dependence of folding, the time required for significant amplitudes to be produced is not sensitive to the magnitude of the initial irregularities. Also, folding will occur within lengths of time that agree well with the known geological time scale. Moreover, such folding may take place within relatively short periods on the geological scale, even for compressive stresses that are very small in comparison with the yield point of the rock. Another interesting conclusion is that, in the mechanism of folding, the viscous properties of the rock will tend to overshadow the effect of elasticity. Stress will affect the rate of folding, but the wavelength will remain about the same, of the order of about 20 to 50 times the thickness. Of particular interest is the result that failure of the rock with the appearance of cracks or plastic yielding *does not depend primarily on the magnitude of bending of the layer but on deformation rates*. At low stress, large deformations will be possible without the occurrence of failure.

The writer reaches similar conclusions in Section 7, where he has analyzed the folding of multiple superposed layers. This is intended as a preliminary evaluation based on certain simplifying assumptions regarding interfacial slip. The writer will present a more elaborate theory for this case at a later date.

The writer considers the influence of gravity for the case of a layer lying at the surface or embedded in materials of different densities on top and bottom in Section 8. He also considers the case of multiple layers lying at the surface. He concludes that larger-scale folding is not incompatible with the viscous mechanism of the present theory if we assume that we are dealing with a system of multiple layers with interfacial slip. However, final conclusions regarding the bearing of the present theories on orogenesis will have to wait for further applications based on a more realistic model.

Finally, the writer analyzes the folding of a medium whose viscosity decreases continuously with depth in exponential fashion. This provides a continuous transition from a solid at the surface to a fluid at a certain depth. The medium is also under the influence of gravity. The thought here was to determine how this case differs from the discontinuous case, where a layer lies on top of a less viscous material. Also, this model embodies one characteristic feature for the earth's crust as a whole, since the effect of pressure and temperature tend to produce a gradual decrease of viscosity with depth. The discussion of this case is based on a more elaborate theory (Biot, 1960). The writer found that large-scale folding is not compatible with this model.

In the present paper, the writer emphasizes the linear aspects of the theory. However, the theory can easily be extended to apply to *nonlinear materials* in two ways. First, in the incipient phase of folding, the stress in the layer may be high enough to be in the range where the relationship between creep rate and stress is nonlinear. In this case, the theory will apply for incipient folding, provided that a viscosity coefficient that represents the linear dependence between stress increments and small creep-rate increments is used. This "*effective viscosity coefficient*" will be stress-dependent. The next phase will be characterized by the *local* appearance of plasticity, fracture, and high creep rates. The occurrence of this phase will generally be associated with large deformations, unless the initial compression itself is very high. The point at which these effects become significant can be evaluated by calculating the stresses on the basis

of the linear theory. When localized yielding or fracture occurs, one can extend the calculation to this phase by applying the present linear theory, taking into account the local inhomogeneities, and by using the concept of "effective viscosity." In addition to the "physical" nonlinearities just mentioned, which originate in the physical nature of the materials, other nonlinear features are involved. They might be called geometrical, since they arise when deflections are "large." The result, for instance, is to shorten the distance between crests of the folds over the value given by the linear theory. Such corrections are easily introduced by elementary considerations. These points are discussed briefly at the end of Section 6. Other features arising from nonlinearity are of geometric origin and are due to the amplitude limitation of the folds. As explained at the end of section 5 this limitation tends to increase the regularity of the folds. Further development of the theory along this line is in progress and will be presented later.

The writer owes recognition to Prof. F. Kaisin, Sr., who was his teacher of geology at the University of Louvain during the years 1927–1929, for the motivating ideas that instigated the development of the present theory.

He is also indebted to M. King Hubbert for many stimulating discussions in connection with the geological aspects of the theory, and to J. Handin for information on the rheological properties of rock.

2. BUCKLING OF AN ELASTIC ROD WITH VISCOUS LATERAL RESTRAINT

To illustrate the qualitative aspect of the various problems treated hereafter, the writer discusses first a simple problem of instability. Let a thin rod be pinned at both ends A and B and be subjected to a total axial compressive load, F. Such a rod buckles under an axial compression given by the well-known Euler formula

$$F = \pi^2 \frac{EI}{a^2}, \tag{2.1}$$

where E is Young's modulus of the elastic material, I the moment of inertia of the rod's cross section, and $a = AB$, its length.

The deflection between points A and B is a half wave, and, within the limitations of a linear theory, equilibrium is maintained for an arbitrary amplitude of the deflection, *i.e.*, the equilibrium is neutral. Another way of stating this is by saying that under the axial compression (2.1), the rod deflects laterally by a finite amount under an infinitesimal lateral load.

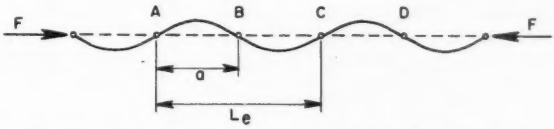

Figure 1. Instability of a thin rod under an axial compression F. The rod will buckle in many waves, provided it is restrained at the nodes A, B, C, and D.

Instead of a rod of length a, let us consider a rod of infinite length that is subject to the same compressive load, F. Let the rod be pinned at equidistant points A, B, C, D, *etc.* (Fig. 1), the distance between the points being equal to a. Each section can then be assimilated to the pinned rod of length a, which we have just considered, and each of these sections will buckle in a half sine wave. This rod of indefinite length will then exhibit a sinusoidal deflection of wavelength

$$L_e = 2a. \tag{2.2}$$

We shall refer to this length as the Euler wavelength associated with the compressive load F. Note that the rod exerts no lateral force on the pins at points A, B, C, D, *etc.* The restraint is therefore introduced only to indicate how an experiment could actually be performed showing such a sinusoidal deflection. Without the pins, of course, the system would be unstable, and the rod would immediately collapse with the appearance of larger buckling wavelengths.

Let us now maintain a fixed compressive load, F, but vary the distance between pins, *i.e.*, vary the wavelength, L. For wavelengths smaller than the Euler wavelength, L_e, the deflection cannot be maintained and will

suddenly disappear. For wavelengths larger than L_e, the deflection will increase and the rod will collapse, unless we introduce a lateral load to prevent this. To evaluate the magnitude of the lateral force required to do this, we shall use the familiar equations for the deflection of a beam in the theory of structures. We shall assume that the rod can deflect only in the plane of the figure. The x co-ordinate lies along the axis of the undeformed rod, and w denotes the deflection perpendicular to this direction. The bending moment, M, is proportional to the curvature, d^2w/dx^2, of the rod. This relationship is

$$EI\frac{d^2w}{dx^2} = -M. \tag{2.3}$$

The sign conforms to the directions indicated in Figure 2 for positive bending moments. The bending moment is made up of two parts,

$$M = M_1 + M_2. \tag{2.4}$$

The term M_1 is the bending moment due to the axial load F_1;

$$M_1 = Fw. \tag{2.5}$$

The term M_2 is the bending moment due to the lateral restraining forces. These forces are assumed to act perpendicularly to the rod axis. The magnitude of this force per unit length is designated by q, and the sign is chosen positive when q is acting in the positive direction of the deflection w. The following relationships can be written:

$$\frac{dS}{dx} = -q, \quad \frac{dM_2}{dx} = S, \tag{2.6}$$

where S represents the shearing force on the rod cross section due to q, and

$$\frac{d^2M_2}{dx^2} = -q. \tag{2.7}$$

Combining equations (2.3), (2.4), (2.5), and (2.7), we derive

$$q = F\frac{d^2w}{dx^2} + EI\frac{d^4w}{dx^4}. \tag{2.8}$$

The sinusoidal deflection of the rod is represented by

$$w = w_0 \cos lx, \tag{2.9}$$

where the wavelength of the deformation is

$$L = \frac{2\pi}{l}. \tag{2.10}$$

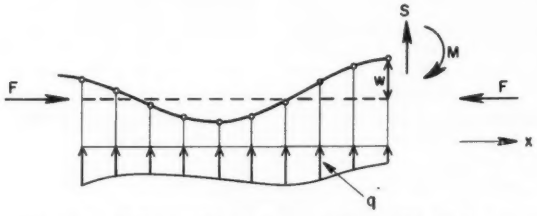

Figure 2. Balance of forces in a rod that buckles under an axial compression F and is laterally restrained by viscous dashpots

The transversal load necessary to maintain this deflection is also distributed sinusoidally, *i.e.*,

$$q = q_0 \cos lx. \tag{2.11}$$

Relation (2.8) can therefore be written

$$-q = Fl^2w - EIl^4w. \tag{2.12}$$

The quantity $-q$ represents the force with which the rod is pushing against the lateral constraint. It is represented by two terms. The first, Fl^2w, is a driving force generated by the compression, F, and the curvature of the rod. The second term, EIl^4w, represents the restraint against deformation due to the bending rigidity. There is a wavelength for which these two terms are equal, *i.e.*, for which $q = 0$. The value of l for which this occurs corresponds to the Euler wavelength

$$L_e = 2\pi\sqrt{\frac{EI}{F}}. \tag{2.13}$$

This corresponds to equation (2.1), if we put $2a = L_e$. For wavelengths larger than this value, the rod pushes against the lateral constraint, and it can be seen that there is a certain wavelength for which the magnitude of this push will be a maximum.

Finally, we shall specify the nature of the lateral constraint. We shall assume that it is made up of a continuous distribution of viscous dashpots, such that the restraining force is proportional to the time derivative of the deflection, namely,

$$-q = b\frac{dw}{dt}. \tag{2.14}$$

Substituting in equation (2.12) yields

$$b\frac{dw}{dt} = w(Fl^2 - EIl^4). \tag{2.15}$$

This is a differential equation for w, and its general solution is

$$w = Ce^{pt}, \tag{2.16}$$

with

$$p = \frac{1}{b}(Fl^2 - EIl^4). \tag{2.17}$$

For wavelengths smaller than L_e, the value of p is negative, and the deflection will die out. Any sinusoidal deflection of wavelength larger than L_e is unstable, since p is then positive. Its amplitude increases exponentially.

The value of l for which p is a maximum is

$$l_d = \sqrt{\frac{F}{2EI}}. \tag{2.18}$$

This corresponds to the wavelength for which the rate of increase of the amplitude is maximum. We shall call this the dominant wavelength, L_d. Its value is

$$L_d = 2\pi\sqrt{\frac{2EI}{F}} = \sqrt{2}\,L_e. \tag{2.19}$$

The dominant wavelength is $\sqrt{2}$ times the Euler wavelength, is a function of the compressive load, and is independent of the viscosity of the lateral constraint.

The physical significance of this dominant wavelength lies in the fact that the initial deviations of the rod axis from a perfect straight line can be expanded in a Fourier series. Each component is characterized by its own wavelength, and its amplitude will increase exponentially at a certain rate. The dominant wavelength will possess a much larger rate of deformation than others and is therefore the one most likely to be observed in practice. A certain amount of scatter of the observed wavelengths around the value L_d must be expected, owing to the randomness of the initial irregularities. The writer calls attention to the physical significance of the Euler wavelength, L_e, which acts as a cutoff wavelength. For all wavelengths smaller than L_e, the value of p (equation 2.17) is negative. The Euler wavelength depends on the load, and if the load is suddenly decreased, all wavelengths which had appeared and are now smaller than the new value of L_e will gradually disappear.

In deriving these equations, we have neglected all inertia forces. This is justified, since we have in mind applications to viscous solids in which rates of deformation are very small.

3. BUCKLING OF AN ELASTIC PLATE IN A VISCOUS MEDIUM

We consider now an elastic plate of thickness h embedded in an infinite viscous continuum. The geometry is illustrated in Figure 3. We choose the x axis parallel to the plate and the y axis perpendicular to it. The plate is infinitely extended. A uniform compression, P, per unit area is acting in the plate in the x direction. We are interested in the buckling of this plate and in the appearance of a sinusoidal deflection along x. The deformation is one of two-dimensional strain in the x,y plane. In analyzing such a deformation, we may imagine that the plate is represented by a strip of unit thickness in the direction perpendicular to x,y. We can then treat the problem of buckling of this strip in a manner entirely analogous to that of the rod analyzed heretofore. There are, however, two essential differences.

The first difference arises from the fact that we are dealing with two-dimensional strain. The stress-strain relationships in the x,y plane are

$$\begin{aligned}\sigma_{xx} &= 2\mu e_{xx} + \lambda(e_{xx} + e_{yy}),\\ \sigma_{yy} &= 2\mu e_{yy} + \lambda(e_{xx} + e_{yy}),\end{aligned} \tag{3.1}$$

where λ and μ are Lamé coefficients. In the bending deformation of the plate, we can put

$$\sigma_{yy} = 0. \tag{3.2}$$

We derive

$$\sigma_{xx} = Be_{xx}, \tag{3.3}$$

with

$$B = \frac{4\mu(\mu + \lambda)}{2\mu + \lambda} = \frac{E}{1 - \nu^2}. \tag{3.4}$$

In this expression, E is Young's modulus and ν is Poisson's ratio for the plate. We see that for two-dimensional strain, Young's modulus must

be replaced by B. On the other hand, the moment of inertia, I, of the cross section is, in this case,

$$I = \frac{h^3}{12}. \tag{3.5}$$

Equation (2.3) is therefore replaced by

$$\frac{1}{12} Bh^3 \frac{d^2w}{dx^2} = -M. \tag{3.6}$$

The total compressive load which plays the role of F is

$$F = Ph. \tag{3.7}$$

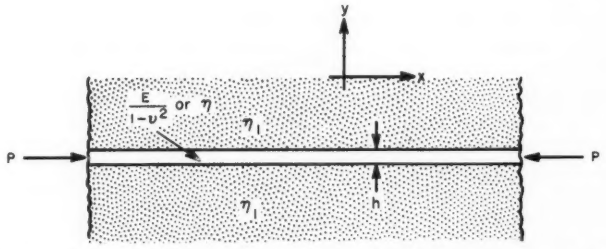

Figure 3. Elastic plate of effective rigidity $E/(1-\nu^2)$ (E, Young's modulus; ν, Poisson's ratio) or viscous layer of viscosity η embedded in a viscous medium of viscosity η_1

Equation (2.8) must, therefore, be replaced by

$$q = \frac{Ph\, d^2w}{dx^2} + \frac{1}{12} Bh^3 \frac{d^4w}{dx^4}. \tag{3.8}$$

This is the load, q, per unit area required to maintain a deflection, w, of the plate under the axial compression, P. For a sinusoidal deflection (equation 2.9), we write

$$-q = Phl^2w - B\frac{h^3}{12} l^4w. \tag{3.9}$$

The second difference from the problem in the previous section is that the lateral constraint is due to a viscous continuum instead of to local dampers. The load per unit area required to deflect a semi-infinite viscoelastic medium has been evaluated in previous work (Biot, 1957; 1959a; 1959b). The result is expressed as follows.

The normal load, q', per unit area acting at the surface is assumed to be distributed sinusoidally (Fig. 4). We write

$$q' = q'_0 \cos lx. \tag{3.10}$$

The deflection, w, of the surface is also distributed sinusoidally. Its positive direction is chosen the same as that of q'. If the material is an incompressible viscous solid of viscosity η_1, the relationship between load and deflection is

$$q' = 2\eta_1 l \frac{dw}{dt}. \tag{3.11}$$

The plate acts upon two such half-spaces, one on each side; therefore, we can write

$$-q = 2q' \tag{3.12}$$

or

$$-q = 4\eta_1 l \frac{dw}{dt}. \tag{3.13}$$

Comparing this with equation (2.14), we note an essential difference in the fact that the viscous-resistance factor $4\eta_1 l$ of an equivalent dashpot contains the quantity l. Hence, the viscous resistance of the medium per unit area is inversely proportional to the wavelength. This is essentially due to a similarity law for the half-space. In that respect, it is entirely analogous to the case of an elastic half-space. In the latter case, if the same specific load is distributed over similar areas of different dimensions, the deflection is proportional to the linear dimension of the area.

Combining equations (3.9) and (3.13), we derive

$$4\eta_1 \frac{dw}{dt} = Phlw - \frac{1}{12} Bh^3 l^3 w. \tag{3.14}$$

The solution of this differential equation is again given by the general formula (2.16). The exponential rate of deformation is measured by

$$p = \frac{1}{4\eta_1}\left(Phl - \frac{1}{12} Bh^3 l^3\right). \tag{3.15}$$

The rate is zero for the value of l that cancels

the right-hand side, *i.e.*, for the Euler wavelength,

$$L_e = \pi h \sqrt{\frac{B}{3P}} = \pi h \sqrt{\frac{E}{3(1-\nu^2)P}}. \quad (3.16)$$

The value of p is a maximum for $l = l_d$, where

$$l_d h = 2\sqrt{\frac{P}{B}}. \quad (3.17)$$

This yields the dominant wavelength

$$L_d = \pi h \sqrt{\frac{B}{P}} = \pi h \sqrt{\frac{E}{(1-\nu^2)P}}, \quad (3.18)$$

or $L_d = \sqrt{3}\, L_e$.

at a uniform constant rate in a direction parallel with the plate. We are concerned here with the stability of this state of uniform deformation of the plate and the medium. In particular, we shall investigate the possibility of sinusoidal folding of the plate when a small perturbation is introduced in the system. Such a perturbation is, for instance, a deviation of the plate from a perfectly flat surface. By Fourier expansion of such deviation, this amounts to examining how a perturbation constituted by a single sinusoidal wave in the deflection of the plate will grow in amplitude as a function of time. In analyzing this problem, we shall neglect the compressive stress, P_1, in

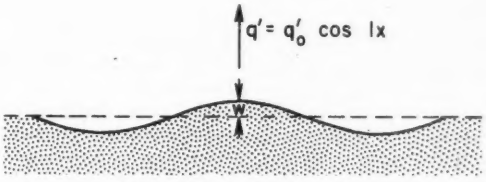

Figure 4. Deflection of the viscous embedding medium at the surface of contact with the layer and the restraining force, q', of the medium

In this case of a plate restrained by a viscous continuum, the ratio of L_d/L_e is $\sqrt{3}$, as compared to $\sqrt{2}$ for the rod restrained by dashpots. This is due to the dependence of the viscous resistance on the wavelength in expression (3.13).

As mentioned in the previous section, the Euler wavelength, L_e, acts as a cutoff wavelength. Its value depends on the compressive load, and any wavelength component smaller than L_e present in the deformation at any particular instant will tend to disappear.

4. FOLDING INSTABILITY OF A COMPRESSED VISCOUS PLATE IN A VISCOUS MEDIUM

We shall now consider the case in which the elastic plate of the previous problem is replaced by a layer of incompressible, purely viscous solid of viscosity coefficient η. The plate of thickness h (Fig. 3) is subject to a longitudinal compression, P, per unit area. It is embedded in an incompressible, purely viscous, indefinite medium of considerably lower viscosity, η_1. We can visualize an experiment in which the plate and the medium are squeezed together the surrounding medium. The writer (1959a) has shown that this assumption is justified in a much more elaborate analysis of the problem.

To analyze the deformation in this problem, we must consider the stress-strain relationships for an incompressible viscous medium in two-dimensional strain. The stress and strain in the plane are related by the equations

$$\sigma_{xx} - \sigma = 2\eta \frac{\partial e_{xx}}{\partial t}, \quad \sigma_{yy} - \sigma = 2\eta \frac{\partial e_{yy}}{\partial t}, \quad (4.1)$$

where

$$\sigma = \frac{1}{2}(\sigma_{xx} + \sigma_{yy}). \quad (4.2)$$

The x axis is shown parallel with the plate. If free expansion is allowed in the y direction, *i.e.*, normal to the plate, we can put $\sigma_{yy} = 0$. Then

$$\sigma_{xx} = 4\eta \frac{\partial e_{xx}}{\partial t}. \quad (4.3)$$

Hence, a uniform rate of strain, $\partial e_{xx}/\partial t$, will produce a constant compressive stress in the plate:

$$P = -4\eta \frac{\partial e_{xx}}{\partial t}. \quad (4.4)$$

The same rate of strain in the surrounding medium produces a compressive stress

$$P_1 = -4\eta_1 \frac{\partial e_{xx}}{\partial t}. \tag{4.5}$$

This is the initial steady state of the system upon which we shall now superpose a sinusoidal bending deformation of the plate.

The bending of a viscous plate can be treated in a manner entirely analogous to that of an elastic plate. The appearance of bending introduces a bending moment, M, in the viscous plate proportional to the rate of change of its curvature. The following relationship is easily derived:

$$\frac{1}{3}\eta h^3 \frac{\partial^3 w}{\partial x^2 \partial t} = -M. \tag{4.6}$$

This equation is formally the same as relationship (3.6), provided that we introduce the formal identity

$$B = 4\eta \frac{\partial}{\partial t}. \tag{4.7}$$

Proceeding exactly as in the case of an elastic plate, we establish the analogue of expression (3.8) for the transversal load, q, acting on the plate:

$$q = Ph \frac{\partial^2 w}{\partial x^2} + \frac{1}{3}\eta h^3 \frac{\partial^5 w}{\partial t \partial x^4}. \tag{4.8}$$

For a sinusoidal deformation, this becomes

$$-q = Phl^2 w - \frac{1}{3}\eta h^3 l^4 \frac{dw}{dt}. \tag{4.9}$$

The load, $-q$, is the reaction of the viscous medium to deformation. Its expression is given by equation (3.13). Hence, we derive

$$4\eta_1 l \frac{dw}{dt} = Phl^2 w - \frac{1}{3}\eta h^3 l^4 \frac{dw}{dt}. \tag{4.10}$$

This is a differential equation for the deflection w. As before, the solution for w is proportional to the exponential e^{pt}, and p is given by

$$p = \frac{P}{\frac{4\eta_1}{hl} + \frac{1}{3}\eta h^2 l^2}. \tag{4.11}$$

This expression depends on the wavelength through the nondimensional variable lh. For zero and infinite wavelength, *i.e.*, for $l = \infty$ and $l = 0$, the value of p is zero and the rate of deformation of any sinusoidal bending is zero. For an intermediate value of l, the value of p goes through a maximum. The value of l at which this happens is given by $l = l_d$, where

$$l_d h = \sqrt[3]{\frac{6\eta_1}{\eta}}. \tag{4.12}$$

The corresponding dominant wavelength is

$$L_d = 2\pi h \sqrt[3]{\frac{\eta}{6\eta_1}}. \tag{4.13}$$

The ratio of dominant wavelength to thickness, L_d/h, is shown in Table 3 as a function of the viscosity ratio, η/η_1.

The value of $p = p_m$ for the dominant wavelength is found by putting $l = l_d$ in expression (4.11). We find

$$p_m = \frac{P}{6\eta_1} \sqrt[3]{\frac{6\eta_1}{\eta}}. \tag{4.14}$$

This expression determines the rate of growth of the amplitude of folding at the dominant wavelength.

We note the important fact that for a viscous plate in a viscous medium, the *dominant wavelength is independent of the compressive load, P.* This is in contrast with the case of the elastic plate. The load, of course, affects the rate of deformation, but, as shown by relation (4.11), all wavelengths are equally affected.

The case of the viscous plate also differs from that of the elastic plate by the absence of a cutoff wavelength, *i.e.*, all wavelengths are amplified.

5. AMPLIFICATION AND SELECTIVITY OF FOLDING

The writer must call attention to certain important features of folding, which are characterized by two aspects. One is the degree of amplification, *i.e.*, the magnitude of the factor by which a certain wavelength amplitude initially present in the layer is multiplied after a given time. Another is the selectivity of the amplification. This can be characterized by the band width representing those wavelengths that are selectively amplified. These concepts are entirely analogous to those encountered in the theory of electronic wave filters.

Let us first consider the case of an elastic layer in a viscous medium. The amplification factor, after an interval of time, is

$$A = e^{pt}, \tag{5.1}$$

where p is a function of the wavelength given by equation (3.15). The maximum value, A_d, of this amplification occurs for the dominant

wavelength, *i.e.*, for $l = l_d$. We write

$$A_d = e^{p_m t}, \tag{5.2}$$

where p_m is the maximum value of p, *i.e.*,

$$p_m = \frac{1}{6} l_d h \frac{P}{\eta_1} = \frac{1}{3} \frac{P}{\eta_1} \sqrt{\frac{P}{B}}. \tag{5.3}$$

We can plot the amplification at any given time as a function of the wavelength or, more conveniently, as a function of the wave number,

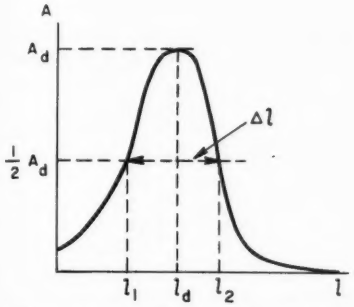

Figure 5. Amplification, A, of the folding as a function of the wave number

l (Fig. 5). There are two wave numbers, l_1 and l_2, for which the amplification is one-half the maximum value, *i.e.*, for which

$$A = \frac{1}{2} A_d. \tag{5.4}$$

This is an equation for l_1 and l_2 which is equivalent to

$$1 - \frac{p}{p_m} = \frac{\log 2}{p_m t} = \frac{\log 2}{\log A_d}. \tag{5.5}$$

(log denotes the natural logarithm.)

The selectivity is determined by the relative band width

$$\frac{\Delta l}{l_d} = \frac{l_2 - l_1}{l_d}. \tag{5.6}$$

Equation (5.5) can be solved approximately by expanding the left-hand side in the vicinity of its minimum and retaining only the term that corresponds to the osculating parabola. We find

$$\frac{\Delta l}{l_d} = 2\sqrt{\frac{2}{3} \frac{\log 2}{p_m t}} = \frac{1.36}{\sqrt{\log A_d}}. \tag{5.7}$$

There are two immediate conclusions. The band width decreases as $1/\sqrt{t}$ and depends only on the amplification, A_d, of the dominant wavelength.

For decreasing values of $\Delta l/l_d$, the selectivity increases, and the folding more closely approaches a pure sine wave. The significance of the band width is illustrated by the fact that two waves of wave numbers $l_d + 1/2\ \Delta l$ and $l_d - 1/2\ \Delta l$ will, by superposition, produce amplitude beats. The interval between the beats is denoted by D, and we can write

$$\frac{L_d}{D} = \frac{\Delta l}{l_d}. \tag{5.8}$$

Table 1 shows the band width for various amplifications.

Table 1. Band Width $(\Delta l/l_d)_e$ For the Elastic Layer in a Viscous Medium as a Function of the Amplification Factor A_d

A_d	$(\Delta l/l_d)_e$
10	0.896
10^2	0.635
10^3	0.516
10^4	0.448
10^5	0.400

As can be seen, the selectivity varies slowly with the amplification. A certain regularity in the waves will begin to appear at amplifications of 10^2. Theoretically, of course, the amplification may grow to infinity. Since the amplitude of the folding remains finite, this can be the case only when the folding is initiated in a layer in which initial imperfections are smaller and smaller. The closer we come to an initially perfectly flat layer, the smaller will be the band width, and the more regular will be the appearance of the folding.

Let us now turn to the case of a viscous layer in a viscous medium. According to (4.14), the maximum value of p is

$$p_m = \frac{P}{6\eta_1} \sqrt[3]{\frac{6\eta_1}{\eta}} = \frac{P}{\eta} \left[\frac{\eta}{6\eta_1}\right]^{2/3}. \tag{5.9}$$

We can represent the selectivity by a band width, as above. We write an equation identical to (5.5), except that p_m is given by (5.9) and p by (4.11). Proceeding as above, and using the same type of approximate solution of

equation (5.5) to determine the band width, we find

$$\frac{\Delta l}{l_d} = 2\sqrt{\frac{\log 2}{p_m t}} = \frac{1.66}{\sqrt{\log A_d}}. \qquad (5.10)$$

This expression differs only by a constant factor for the similar formula (5.7) for the elastic layer. The band width for the viscous layer at various amplifications, as given by (5.10), is shown in Table 2.

Comparing Table 2 with expression (5.7) and with Table 1 for the selectivity of the elastic layer, we note that the viscous layer has

TABLE 2. BAND WIDTH $(\Delta l/l_d)_v$ FOR THE VISCOUS LAYER IN THE VISCOUS MEDIUM AS A FUNCTION OF THE AMPLIFICATION FACTOR A_d

A_d	$(\Delta l/l_d)_v$
10	1.095
10^2	0.775
10^3	0.632
10^4	0.548
10^5	0.490

a larger band width. For the elastic layer, Table 1 indicates that a band width $\Delta l/l_d = 0.635$ is attained for an amplification of $A_d = 100$. Table 2 shows that for the same band width to be obtained in the case of the viscous layer, we must reach an amplification about 10 times larger. As a consequence, the elastic layer will tend to fold more regularly—a result that has been confirmed by model tests.

There is another interesting aspect by which the viscous layer differs from the elastic layer. For the elastic layer, by starting with layers that contain less and less initial distortion from the ideal plane surface, we can attain arbitrarily larger amplification factors, provided we wait long enough. This is not so for the viscous layer, since the compressive load, P, produces a shortening of the layer that at a constant rate. If a significant amplification requires too long a time, the shortening of the layer will become so large that the folding phenomenon will be completely masked.

This can be brought out very clearly by a consideration of the time required for a given amplification to be obtained. This time is given by

$$t = \frac{1}{p_m} \log A_d . \qquad (5.11)$$

When the value for p_m given in equation (5.9) is introduced, the time becomes

$$t = \frac{\eta}{P}\left[\frac{6\eta_1}{\eta}\right]^{2/3} \log A_d . \qquad (5.12)$$

The quantity η/P is a time that has the following physical interpretation. Under the load P, the uniform compressive strain rate is given by equation (4.4), and the total compressive strain after a time t is

$$-e_{xx} = \frac{P}{4\eta} t . \qquad (5.13)$$

When the compressive strain corresponds to a shortening of 25 per cent, the time elapsed is

$$t_1 = \frac{\eta}{P}. \qquad (5.14)$$

With the reference time t_1, expression (5.12) becomes

$$\frac{t}{t_1} = \left[\frac{6\eta_1}{\eta}\right]^{2/3} \log A_d . \qquad (5.15)$$

It is of interest to show the dependence of the amplification factor, A_d, on the viscosity ratio and the time ratio. This is shown in Table 3 for three values of the time, *i.e.*, $t = t_1/6$, $t = t_1/3$, and $t = t_1$.

These three values of t correspond to a shortening of the layer of 4.2, 8.8, and 25 per cent, respectively.

One important feature is immediately apparent from Table 3. Beyond a certain amplification, the amplitude of folding will increase at an explosive rate. This happens when $A_d \geqq 1000$, and we can adopt this value as a standard. The time required for explosive amplification to occur is then given by relating (5.15) after $A_d = 1000$ is substituted. We find

$$\frac{t}{t_1} = 6.90\left[\frac{6\eta_1}{\eta}\right]^{2/3}. \qquad (5.16)$$

This time ratio for explosive amplification is a function only of the viscosity ratio.

As indicated in the discussion of band width, good selectivity also begins to appear for amplifications of about 1000; hence, sharp definition of the wavelength is also to be expected at these amplifications.

Another important feature brought out by Table 3 is the small amplification exhibited for viscosity ratios (η/η_1) smaller than 100.

Larger amplifications would, of course, appear for times t larger than t_1. However, this would imply a shortening of the layer larger

than 25 per cent. Such a large compressive strain would then overshadow the folding itself. We can conclude, therefore, that a clearcut folding with sharp definition requires that the viscosity of the layer be at least 100 times that of the medium.[2]

Finally, at large viscosity ratios, the wavelength definition becomes very sharp. For instance, for $\eta/\eta_1 = 2000$, the amplification at the instant $t = t_1/3$ is of the order $A_d = 10^7$. Substituting this value of A_d in expression (5.10) for the band width, we find

$$\frac{\Delta l}{l} = 0.415 . \qquad (5.17)$$

Using this value in equation (5.8) indicates that regular folds will appear over a distance D equal to about 2 1/2 times the wavelength. Of course, such large amplification can be achieved only for a layer whose initial deviation from a perfect plane is of the order of 10^{-7} of the wavelength.

The previous considerations on selectivity are applicable only within the range of validity of the linear theory. Attention should be called to a type of nonlinearity of geometric origin whose effect is to *increase the regularity of the folds*. This can be seen by considering a case of folding with uneven amplitude of the folds. Since the amplitude is limited by the geometry, the folds of greater amplitude will reach their limit first, while those of smaller amplitude will continue to grow. This will result in smoothing out of the uneven amplitudes and corresponds to an increase in selectivity. Here again we find an analogy in electronics. The phenomenon is not unlike the increase of selectivity obtained in the FM receivers by the use of amplitude limitation.

6. GEOLOGICAL ASPECTS OF THE FOLDING THEORY

We shall briefly discuss some of the previous results in the context of tectonics.

TABLE 3. AMPLIFICATIONS OF THE AMPLITUDE OF FOLDING AT TIMES $t = t_1/6$, $t = t_1/3$, AND $t = t_1$, AS A FUNCTION OF THE VISCOSITY RATIO, η/η_1, AND CORRESPONDING RATIOS OF THE DOMINANT WAVELENGTH, L_d, TO THE LAYER THICKNESS, h

$\frac{\eta}{\eta_1}$	$\frac{L_d}{h}$	A_d $t = t_1/6$	A_d $t = t_1/3$	A_d $t = t_1$
12	7.9	1.30	1.70	4.9
36	11.4	1.73	3.01	27.1
72	14.4	2.39	5.74	1.89×10^2
100	16.0	2.97	8.80	6.8×10^2
144	18.1	4.01	16.0	4.1×10^3
288	22.9	9.04	81.7	5.4×10^5
500	27.4	24.0	5.7×10^2	1.9×10^8
1,000	34.5	1.5×10^2	2.4×10^4	1.4×10^{13}
2,000	43.5	3.0×10^3	9.1×10^6	7.5×10^{20}
10,000	74.5	1.5×10^{10}	2.2×10^{20}	1.1×10^{61}

Let us first consider the case of a viscous layer embedded in a viscous medium. It is reasonable to assume that for very low stresses acting over long periods of time, the behavior of most rock is in the nature of a viscous medium.[3] The analysis of Section 4, which neglects gravity, indicates that the existence of a very small compressive stress in the layer will immediately initiate folding. The wavelength of the folding will be characterized entirely by the ratio of the viscosity coefficients of the layer and of the medium and will be independent of the compressive load, P.

Viscosity coefficients of rock range widely. Accepted magnitudes of viscosity (Birch, Schairer, and Spicer, 1942; Griggs, 1939) range from 10^{17} to 10^{22} poises.[4] The figure 10^{17}

[2] As pointed out in Section 6, this may not be the case for materials with strongly nonlinear properties.

[3] As pointed out hereafter the validity of the theory is not dependent on such an assumption since nonlinear physical properties may be introduced.

[4] The same orders of magnitude are derived from observations communicated to the writer by M. King Hubbert on deformation of pillars in salt mines and the sagging of marble slabs in old cemeteries under low stress and over long periods of time. Such deformations have also been observed by Kaisin (1927), who stressed the importance of these phenomena in tectonics.

is the order of magnitude of the viscosity for halite. These values correspond to pressures and temperatures near the surface of the earth. Some materials have lower values of viscosity. Viscosities will also be lower at higher pressure and temperature. The earth is, therefore, a highly heterogeneous medium from the standpoint of its flow properties. This is in contrast with the elastic properties, since the elastic moduli of rock generally range from 10^{11} to 10^{12} dynes/cm^2. It is clear, therefore, that folding in the earth must primarily reflect the large differences in viscous or viscoelastic properties.

As an example, let us consider a layer of viscosity $\eta = 10^{21}$ poises (dynes cm^{-2} sec^{-1}) embedded in a medium of viscosity $\eta_1 = 10^{18}$ poises. Let us assume also that the compressive load is $P = 10^3$ dynes/cm^2. This is about 1450 psi, *i.e.*, of the order of a fraction of the compressive strength of hard rock. The time required for the layer to shorten by 25 per cent is

$$t_1 = \frac{\eta}{P} = 10^{13} \text{ sec} = 317{,}000 \text{ years}. \quad (6.1)$$

The dominant wavelength (*See* Table 3) is

$$L_d = 34.5\, h\,, \quad (6.2)$$

where h is the layer thickness. The time, t, required for explosive folding to begin is given by equation (5.16); we find

$$\frac{t}{t_1} = 0.218\,. \quad (6.3)$$

Hence,

$$t = 72{,}000 \text{ years}\,. \quad (6.4)$$

At this time, the shortening of the layer is $t/4t_1$, or 5 per cent.

Let us keep the same ratio of the viscosities, $\eta/\eta_1 = 1000$, and consider other values for the viscosities and the compressive load, P. Table 4 shows the time required to reach explosive folding.

The time is shown in years, the load in pounds per square inch, and the viscosity in poise (cgs) units. These results fit in very well with the geological time scale[5].

If the viscosity ratio is $\eta/\eta_1 = 100$, a similar table could be constructed in which the viscosities would be replaced by

$$\eta = 10^{22},\ 10^{21},\ 10^{20} \text{ cgs} \qquad \eta_1 = 10^{20},\ 10^{19},\ 10^{18} \text{ cgs}\,. \quad (6.5)$$

[5] Kulp (1959) has evaluated this time scale on the basis of radioactivity measurements.

When the same values for the compressive load are used, the time intervals are simply multiplied by the factor 4.65. The dominant wavelength in this case is

$$L_d = 16\, h\,. \quad (6.6)$$

It can be seen that for periods of the order of 10^5 or 10^6 years, a *relatively small load may produce explosive folding, even in hard rock.*

The wavelengths predicted are also within the range of observed values.

Table 4. Time in Years Required for Explosive Folding for a Viscous Layer in a Viscous Medium for Various Compressive Loads, P, and Viscosities

P	η 10^{22}	10^{21}	10^{20} cgs
psi	η_1 10^{19}	10^{18}	10^{17} cgs
	years	years	years
14.5	7.2×10^7	7.2×10^6	720,000
145.0	7.2×10^6	720,000	72,000
1,450.0	720,000	72,000	7,200
14,500.0	72,000	7,200	720

Our next step is to introduce the influence of the elasticity of the layer. We shall therefore examine the magnitude of the folding of a purely elastic layer in a viscous medium. The amplification factor, A_d, is related to the time by equations (5.2) and (5.3). They can be combined to read

$$t = t_e \log A_d\,, \quad (6.7)$$

with a characteristic time

$$t_e = \frac{3\eta_1}{P}\sqrt{\frac{B}{P}}\,. \quad (6.8)$$

The modulus B of the layer is defined by expression (3.4) and is close to Young's modulus of the material. The elastic moduli of rock are in the range 10^{11} to 10^{12} dynes/cm^2, the latter value being close to the modulus of quartz. For the purpose of comparison, we shall adopt the highest value, $B = 10^{12}$ dynes/cm^2. Since t is proportional to $\sqrt{B}$, the variations of B within the allowable range for rock do not affect the order of magnitude of t_e. The viscosity, η_1, of the surrounding medium is assumed, as it was previously, to lie in the range $\eta_1 = 10^{17}$ to $\eta_1 = 10^{20}$ poises. In analogy with our treatment of the viscous layer and also by examination of equations (5.2) and (5.3), it can be seen that explosive folding will start

for the same value, $A_d = 1000$, for the amplification factor. Hence, the time at which explosive folding appears is given by

$$t = 6.90\, t_e = 20.7 \frac{\eta_1}{P} \sqrt{\frac{B}{P}}. \qquad (6.9)$$

This time is shown in years in Table 5, with $B = 10^{12}$ dynes/cm^2, for different values of the viscosity, η_1, of the surrounding medium and of the compression, P, in the layer.

Comparison of these time intervals with those of Table 4 shows that much more time is required for the layer to fold as an elastic layer. This is particularly true for the smaller values of the compression, where the viscous phenomenon clearly predominates. At high values of the compression, of the order of 14,000 psi, the elastic property begins to influence the folding. We must remember, however, that such high loads are near the crushing strength, where plastic deformation and rupture will be introduced and will be superposed to the purely elastic deformation. Actually, of course, the rock will possess combined elastic and viscous properties, *i.e.*, it will be *viscoelastic*. It will tend to deform as a viscous solid at low rates of deformation, and, as this rate increases, the elasticity property will gradually enter into play. Calculation of the rate of folding for the more complex case of a viscoelastic layer can be carried out by applying the more elaborate theory (Biot, 1957; 1959b). These considerations lead to the conclusion that the viscosity of the layer will, in general, tend to predominate over its elasticity.

On the other hand, at high loads the viscoelastic properties will tend to be masked by rupture and plastic deformation, particularly in regions of maximum bending. In this connection, we should also evaluate the bending stresses in the layer during the process of folding. The maximum stress will occur at the point of maximum amplitude, which is also the point of maximum curvature. Consider the folding of a viscous layer. The bending moment is given by equation (4.6). A sinusoidal deflection at the dominant wavelength is

$$w = w_t \cos l_d x\,, \qquad (6.10)$$

where

$$w_t = w_{0e}{}^{p_m t} \qquad (6.11)$$

is the maximum amplitude at $x = 0$. The values of l_d and p_m are given by expressions (4.12) and (4.14). Using these values and substituting w in equation (4.6) for the bending moment, we find

$$M = \frac{1}{3} h w_t P\,. \qquad (6.12)$$

By a well-known formula of plate theory, the maximum bending stress is

$$\sigma_m = \frac{6M}{h^2}\,; \qquad (6.13)$$

hence,

$$\sigma_m = 2 \frac{w_t}{h} P\,. \qquad (6.14)$$

This stress is a traction on the stretched side of the layer and a compression on the other. The stress must be superposed, of course, to the original compression in the layer. On the compressed side, the stresses due to bending and the initial compression are added, and the total compression is

$$\sigma_c = P\left[\frac{2w_t}{h} + 1\right]. \qquad (6.15)$$

On the stretched side, the stresses are subtracted, and we obtain a tensile stress

$$\sigma_t = P\left[\frac{2w_t}{h} - 1\right]. \qquad (6.16)$$

TABLE 5. TIME IN YEARS REQUIRED FOR EXPLOSIVE FOLDING OF AN ELASTIC LAYER IN A VISCOUS MEDIUM FOR VARIOUS COMPRESSIVE LOADS, P, IN THE LAYER AND VISCOSITIES, η_1, OF THE MEDIUM
Elastic modulus of the layer is $B = 10^{12}$

P psi	η_1 cgs 10^{20}	10^{19}	10^{18}	10^{17}
	years	years	years	years
14.5	6.5×10^{10}	6.5×10^{9}	6.5×10^{8}	6.5×10^{7}
145.0	2.0×10^{9}	2.0×10^{8}	2.0×10^{7}	2.0×10^{6}
1,450.0	6.5×10^{7}	6.5×10^{6}	650,000	65,000
14,500.0	2.0×10^{6}	200,000	20,000	2,000

In the actual geological case, these stresses must also be superposed on the over-all hydrostatic pressure prevailing at the depth of the layer.

To illustrate the significance of this formula, let us consider the case of a layer of viscosity $\eta = 10^{21}$ poises embedded in a medium of viscosity $\eta_1 = 10^{18}$ poises. For a layer 2 feet thick, the dominant wavelength will be 70 feet. Assume also a compressive load of 1450 psi in the layer and an initial deviation of the layer from a plane surface of the order of 0.1 inch over a distance of a wavelength, *i.e.*, over a distance of 70 feet. From Table 4, we see that the time required for the layer to reach the state of explosive folding is of the order of 70,000 years. At that moment, the amplification factor is 1000, and the amplitude of the folds will be 100 inches. The folds will have the aspect shown in Figure 6*a*.

Consider the stress at a point of maximum amplitude, as given by equation (6.16). Substituting the values $P = 1450$ psi, $h = 24$ inches, and $w_t = 100$ inches, we find

$$\sigma_t = 10{,}600 \text{ psi} . \qquad (6.17)$$

At such stress, cracks are likely to appear, or some form of plastic deformation will occur, with a considerable increase in the creep rate equivalent to a decrease of the "effective" coefficient of viscosity as the stress increases. The stress at which this will occur depends not only on the nature of the rock but also on the hydrostatic pressure and temperature. In any case, a weakening of the layer is to be expected at points A and B of maximum amplitude. Further deformation will progress as though the layer were hinged at these points, producing a sharpening of the bends, as indicated in Figure 6*b*.

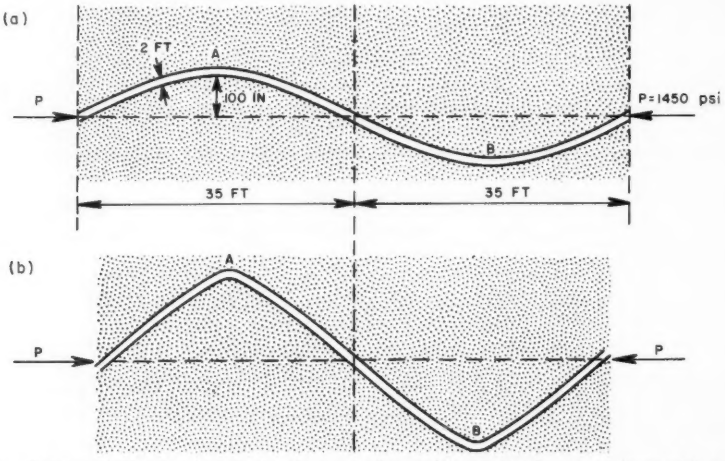

Figure 6. Folding of a layer 2 feet thick before and after yielding at the bends. (*a*) layer with a viscosity of $\eta = 10^{21}$ poises in a medium of viscosity $\eta_1 = 10^{18}$ poises under a compressive stress $P = 1450$ psi. The amplitude is shown after 70,000 years. The assumed initial amplitude is one-tenth of an inch. (*b*) further deformation produces a sharpening of the folds due to yielding of the material at the bends.

At the lower stress shown in Table 4, *e.g.*, 145 psi, considerably more folding will have to occur before this type of failure will develop. On the other hand, at the higher stress, *e.g.*, 14,500 psi, plasticity and fracture will occur almost immediately. At such high stresses, a theory based on elastic or viscous deformation can still be applied as an approximation if we assume that plastic deformations for incremental stresses obey relationships that on the average, can be represented by an "incremental elastic modulus" or an "incremental coefficient of viscosity." In technological problems, a theory of buckling that makes use of the so-called "tangent modulus" has been successfully applied. Similarly, we could use the

theories for either the viscous or the elastic layer, as developed above, provided that we substitute the appropriate coefficient representing average incremental properties.

The weakening of the layer at the point of maximum curvature would then be represented by a decrease in the effective elastic modulus or the effective viscosity coefficient as the stress increases. The significance of an effective viscosity is illustrated by considering a material whose rate of compressive deformation, $-\dot{e}$, is a certain function of the compressive stress, P. We can write this relationship as

$$-\dot{e} = f(P)\,, \tag{6.18}$$

where $f(P)$ represents an empirical function. In the vicinity of a stress, P_0, a small variation, dP, of the stress will produce a corresponding variation, $-d\dot{e}$, of the strain rate. The effective viscosity coefficient, η, is then defined by

$$\frac{1}{4\eta} = -\frac{d\dot{e}}{dP} = \frac{df(P_0)}{dP}\,. \tag{6.19}$$

The right-hand side represents the slope of the function $f(P)$ at the stress P_0. In order to make the equation conform with the assumptions of the plate-bending theory, the strain, e, is taken as that of a plate whose deformation is free in the direction of the compression and in the direction normal to its plane but is restrained in its plane in the direction normal to the stress.

At this point, we must consider the significance of the characteristic time, t_1, if the material is nonlinear. In this case, t_1, as defined by equation (6.1), does not represent the time in which an over-all shortening of 25 per cent of the layer takes place, since η represents the viscosity for incremental stresses. Actually, the time required for a 25 per cent shortening will be longer than t_1 by a factor $(df/dP) \times (P/f)$. This means that appreciable folding may occur for effective viscosity ratios smaller than 100. *Hence, when nonlinearity is introduced, significant folding may still occur for dominant wavelengths which are smaller than about 15 times the thickness.*

By contrast, other nonlinear effects that are introduced here will primarily depend on the geometry or kinematics of the deformation for large displacements. Such an effect will, for instance, be a shortening of the distance between crests of the folding. This will appear if the slope of the folding becomes appreciable. We have taken this into account in Figure 6*b*. An additional shortening of the distance between crests is a consequence of the shortening of the layer itself due to the constant action of the compressive stress. This shortening is proportional to t/t_1, as defined previously. We have neglected this effect in our discussion, and it should be introduced as a correction depending on the magnitude of t/t_1. For nonlinear materials, t_1 should be corrected according to our remark in the preceding paragraph.

It is of considerable interest to note that the stress in a viscous layer depends not on the magnitude of the strain but on its rate. This means that considerable bending can occur under a low compressive stress, P, without the appearance of cracks or plastic yielding.

Before concluding this section, we should also mention the magnitude of the dominant wavelength for the case of an elastic layer. Applying formula (3.18), assuming $B = 10^{11}$ dynes/cm^2 and $P = 14{,}500$ psi, we find

$$L_d \cong 30h\,. \tag{6.20}$$

We have assumed a compressive stress near the crushing strength; hence, the wavelength due to elastic bending of the layer will, in general, be larger than that given in equation (6.20). On the other hand, the observed wavelengths are usually smaller and tend to be closer to the values predicted from the assumption of purely viscous bending. This further confirms the conclusion that the viscous mechanism of folding tends to predominate.

7. FOLDING OF MULTIPLE LAYERS

We shall now consider the important case of a multiplicity of superposed layers that are separated by softer materials at their interfaces (Fig. 7*a*). To acquire an insight into the nature of this problem, let us first analyze the case of n superposed layers of equal thickness, h, and viscosity, η, assuming that perfect lubrication exists between the layers. This stack of layers is embedded in a medium of viscosity η_1 and is subject to a horizontal compression, P, per unit area.

This case is readily analyzed by making use of the previous results for a single layer. All transversal forces acting on each layer must add up, so that if q is the transversal load with which the surrounding medium reacts on the whole stack, the load on each layer is q/n. Hence, the deflection, w, must satisfy the same equation (4.9) as for the single plate, except that q must now be replaced by q/n. This

is also equivalent to replacing η_1 by η_1/n in all equations obtained above for the single viscous layer in a viscous medium. The dominant wavelength (4.13) becomes

$$L_d = 2\pi h \sqrt[3]{\frac{n\eta}{6\eta_1}}. \qquad (7.1)$$

A stack of $n = 10$ layers will show a dominant wavelength equal to $\sqrt[3]{10} = 2.16$ times the wavelength for a single layer.

All conclusions for a single layer are applicable to multiple layers, provided we change the viscosity ratio accordingly. For instance, in the numerical example just considered, assume a layer of thickness $h = 2$ feet and viscosity $\eta = 10^{21}$. We superpose 10 such layers, for a total thickness of 20 feet, and assume that they are embedded in a medium of viscosity $\eta_1 = 10^{18}$. The single layer then behaves as though it were embedded in a medium of viscosity 10 times smaller, *i.e.*, it behaves as the single layer with a viscosity ratio $\eta/\eta_1 = 10{,}000$. Using this ratio, we find that the length of time required for explosive folding, given by equation (5.16), is 15,500 years. The value of t_1 is the same as that given by equation (6.1). The dominant wavelength will be 150 feet. If we assume initial deviations of about one-quarter of an inch from the perfect plane over a distance of one wavelength, the aspect of the folding after 15,000 years will resemble that shown in Figure 7*b*.

The conclusions drawn for the single layer regarding further development of the folding beyond the linear range are applicable. We can use equations (6.15) and (6.16) to calculate the bending stresses. These stresses depend only on the compressive load, P, and the maximum deflection, w_1. After 15,000 years, this deflection is about 11 feet. From equation (6.16), we derive the existence of a bending stress at that time of the order of

$$\sigma_t = 14{,}000 \text{ psi}. \qquad (7.2)$$

At such a stress, cracks or plastic flow will begin to appear, along with a sharpening of the folds at the bend, as shown in Figure 8.

Since the stress is given by equation (6.16), it should be kept in mind that the appearance of cracks is associated not only with the ampli-

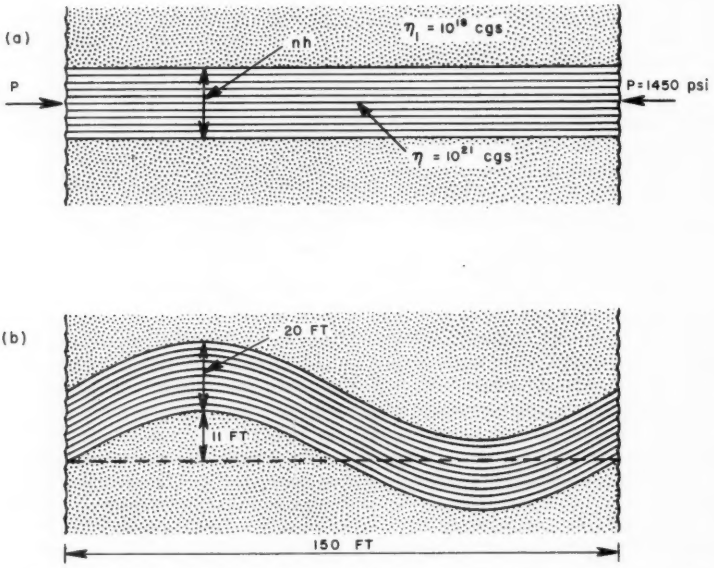

Figure 7. Folding of a composite layer. (*a*) layer made of the superposition of 10 individual layers with a total thickness of 20 feet. Viscosities and compressive stresses the same as in Figure 6. (*b*) Aspect of the folding after 15,500 years, assuming an initial deflection of one-quarter of an inch.

tude of the deformation but also with the total compressive load, P, *i.e.*, it will depend on the rate of deformation. If the load is much smaller than assumed here, the folding will take longer and cracks may not appear at all, or they may appear only at a much later stage when the folds are practically collapsed.

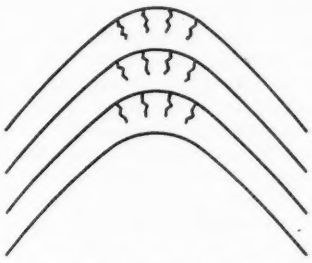

Figure 8. Sharpening of bends due to local yielding in the later phase of folding of the multiple-layered system of Figure 7

We have assumed that the layers are of identical thickness and property, but this is not required, as shown hereafter. Consider a number of layers of thickness h_i and viscosity η_i. The compression acting in each of these layers is P_i, and the total thickness of the stack is H. The total transverse load, q, produced by the superposed layers is obtained by adding these loads for each layer. In other words, equation (4.10) for the single layer is replaced by

$$4\eta_1 l \frac{dw}{dt} = l^2 w \Sigma P_i h_i - \frac{1}{3} l^4 \frac{dw}{dt} \Sigma \eta_i h^2{}_i . \quad (7.3)$$

If we introduce the quantities

$$\begin{aligned} h &= \sqrt{\frac{\Sigma \eta_i h^3{}_i}{\Sigma \eta_i h_i}} \\ \eta &= \frac{\Sigma \eta_i h_i}{H} \\ P &= \Sigma \frac{P_i h_i}{H} \\ n &= \frac{H}{h} , \end{aligned} \quad (7.4)$$

equation (7.3) reduces to

$$\frac{4\eta_1}{n} l \frac{dw}{dt} = P h l^2 w - \frac{1}{3} \eta h^3 l^4 \frac{dw}{dt} . \quad (7.5)$$

This is the same as the equation of folding for a single layer that has a thickness h, a viscosity η, is subject to a load P, and is surrounded by a medium of viscosity η_1/n. The rate of compressive strain of this fictitious layer under the load P is also the same as the actual system. A heterogeneous layered system of this type can, therefore, be analyzed by the methods exemplified heretofore. Once the over-all deformation has been determined, the bending stresses must be individually evaluated for each particular layer. The stress can easily be evaluated by calculating the bending moment in each layer, as is done for the case of the single layer.

It should be kept in mind that the present treatment of folding of multiple layers is approximate. We have assumed that the layer thickness remains constant. This, of course, is not the case. Because the normal loads in the layer add up, there is a limit in the present theory to the number of layers that can be stacked.

To complete this analysis, we shall also briefly mention the case of superposed elastic layers. By the same reasoning as before, examination of equation (3.14) leads to the conclusion that n superposed layers behave as a single one in a medium of viscosity η_1/n. Since the dominant wavelength for the elastic layer is independent of the viscosity, it has the same value (equation 3.18) as for the single layer. The rate of deformation is increased, however, but this does not change the comparison of the elastic case with the viscous case, as illustrated by the time scales of Tables 4 and 5, because both cases are affected by the same factor.

Although the assumption of perfect slip between layers will not be justified in general, one should keep in mind that, in many cases, layers of rock of low viscosity will alternate with layers of much higher viscosity. The latter will play the role of the actual layers considered in the theory, whereas the low-viscosity rock will behave more or less as an interfacial lubricant. We should also keep in mind the possibility of interfacial lubrication by the mechanism of hydraulic lifting in fluid-filled porous rock, as suggested by Hubbert and Rubey (1959) and Rubey and Hubbert (1959) for overthrust faulting. The present analysis of the folding of multiple layers is a simplified one intended as a preliminary attack on the problem. A more elaborate treatment of the problem, which does not assume perfect interfacial slip, has been in preparation and will be presented at a later date.

It should be noted that if friction occurs be-

tween layers, the value for the dominant wavelength lies between that of a single solid layer of thickness $H = nh$ and that given by equation (7.1). The adherence will tend to increase the dominant wavelength somewhat above the latter value.

8. INFLUENCE OF GRAVITY ON FOLDING

In the geological scale the influence of gravity is of course a dominant factor. Its importance will vary, depending on the size of the folds, the density differences of the rock, and the proximity to the surface. We have

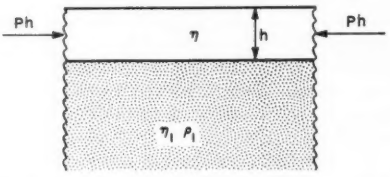

Figure 9. Single layer of viscosity η on top of soft substratum of viscosity η_1 and density ρ_1 under a compressive stress P

limited outselves to an analysis of the influence of gravity for two simple cases.

In one case, the layer lies on top of an infinitely deep medium. In the other, the layer lies between two infinite media of different densities. These two cases are closely related, and results from the first can be derived for the other. The problem has been analyzed in detail in a previous publication (Biot, 1959c). A brief account of the results and elaboration on some applications follows.

Consider the case of a layer of viscosity η lying on top of an infinitely deep medium of viscosity η_1 and density ρ_1 (Fig. 9).

Equation (4.10) for the deflection, w, of the layer is replaced by

$$Phl^2 w - \frac{1}{3}\eta h^3 l^4 \frac{dw}{dt} = 2\eta_1 \frac{dw}{dt} + \rho g w \,. \quad (8.1)$$

If we compare this equation with equation (4.10), we notice that there is an additional term, $\rho_1 g w$. This term introduces the effect of gravity and represents a "weight addition," positive or negative, associated with the rise or fall of the surface as it folds. Another difference is the replacement of the factor 4 by half its value. The latter change is due to the fact that the infinite medium lies only on one side of the layer, so that the lateral restraint to folding is reduced by half.

In the absence of gravity, the dominant wavelength for this case is given by

$$L_d = 2\pi h \sqrt[3]{\frac{\eta}{3\eta_1}} \,. \quad (8.2)$$

Comparing this with expression (4.13), we notice that the factor 6 is replaced by 3. This is again a consequence of the fact that the layer is restrained only on one side. The influence of gravity can be derived from the diagrams in the earlier paper (Biot, 1959c). Let us assume a certain viscosity ratio, say, $\eta/\eta_1 = 500$. The ratio of the dominant wavelength of the layer to its thickness (L_d/h) is then a function only of the parameter $P/\rho_1 gh$ which embodies the influence of gravity. The value of L_d/h is shown in Figure 10 as a function of $\sqrt{P/\rho_1 gh}$. The square root of the parameter is represented along the abscissa because this yields a more convenient graph. Similar curves are also plotted for three other values of the viscosity ratio, η/η_1.

We see from these results that gravity makes the dominant wavelength dependent on the load. A particular case of interest is that of a layer lying on a substratum whose viscosity is very small relative to that of the medium, *i.e.*, $\eta_1/\eta = 0$. The dominant wavelength for this case is

$$L_d = \pi h \sqrt{\frac{2P}{\rho_1 gh}} \,. \quad (8.3)$$

This equation is represented by the limiting straight line in Figure 10 ($\eta_1 = 0$). We also note that there is no theoretical lower limit for the compression, P. Folding will occur no matter how low the compression. This is in contrast with the case of a purely elastic layer lying on a heavy fluid, discussed by Smoluchowski (1909a; 1909b; 1910) and Goldstein (1926), and shows the existence of a lower limit for P below which no instability appears.[6] However, although there is no theoretical lower limit for P in the case of a viscous layer, there is a practical one which brings into consideration the rate of folding. Below a certain value of $P/\rho_1 gh$, the writer (1959c) has shown that the amplification of the folding becomes

[6] It is interesting to note that the buckling wavelength for the elastic plate is given by the same formula (8.3), where P is the buckling load.

insignificant. This region may be defined approximately by

$$\frac{P}{\rho_1 g h} \lesssim 9 \tag{8.4}$$

and corresponds to the left side of the shaded line in Figure 10. This fact leads to an interesting conclusion. Suppose that we apply the highest possible load, *i.e.*, let it be of the order of the crushing strength, P = 14,500 psi ($P = 10^9$ dynes/cm^2). If the thickness of the layer is such that the inequality (8.4) is satisfied, we have

$$h > \frac{P}{9\rho_1 g}. \tag{8.5}$$

For a density $\rho_1 = 2.5$ of the underlying material, this becomes

$$h \gtrsim 1500 \text{ feet}. \tag{8.6}$$

Hence, for a thickness larger than 1500 feet, no significant folding will occur. With a lower value for P, say, 1450 psi, this limiting thickness would be reduced to 150 feet. As pointed out hereafter, this conclusion must be modified if we introduce the influence of surface erosion.

Another interesting conclusion can be drawn if we consider the wavelength. If we assume again that the compressive load is of the order of 14,500 psi, the longest possible wavelength corresponds to a thickness of 1500 feet. As shown by Figure 10, the wavelength at this limiting point is fairly independent of the viscosity ratio and is of the order of about 10 times the thickness, *i.e.*, L_d = 15,000 feet. Wavelengths that are much larger than this will not occur in a single surface layer by the present mechanism of purely viscous folding.

We should point out that the analysis neglects the important factor of surface erosion. The effect of erosion is to remove matter from the crests while the troughs are filled by deposits. As indicated by Gunn (1937), the effect is approximately equivalent to a decrease in density. Hence, previous results can be used if

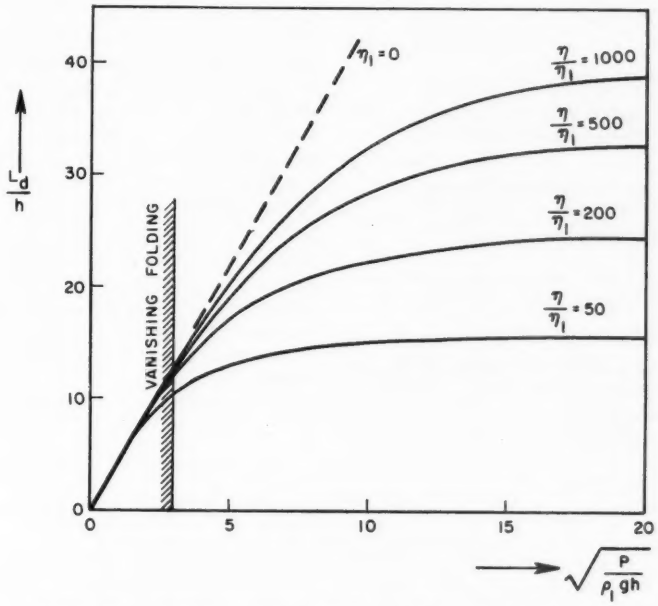

Figure 10. Dominant wavelength, L_d, plotted as the ratio L_d/h for the surface layer of Figure 9, when the combined effect of compressive stress, P, gravity, g, and viscosity ratio, η/η_1, is taken into account

we replace ρ_1 by an effective density $\alpha\rho_1$, with $\alpha < 1$. From Figure 10, we can see that this will generally increase the instability and the dominant wavelengths. Hence, if erosion is taken into account, wavelengths considerably larger than 15,000–20,000 feet are possible. Estimation of how large these can actually be in the earth on the basis of viscous folding requires the development of a more elaborate theory.

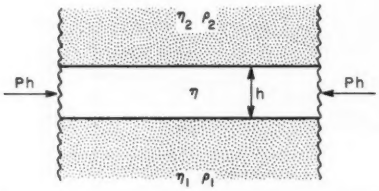

Figure 11. Layer embedded between two media of different viscosities and densities

The size of possible wavelengths is also increased if we consider the folding of multiple layers, as discussed hereafter.

In a more qualitative way, the mechanism of viscous folding in a gravity field can be explained as follows. A decrease in compressive load, P, or an increase in thickness will produce the same effect. Both cases correspond to a relative increase of the influence of gravity. The results just discussed lead to the conclusion that for a decrease in load below a certain value, which depends on the layer thickness, the effect of gravity takes over completely. The mechanism involved here is one of balance between the forces due to the compressive load, which produce the folding tendency, and the stabilizing influence of the gravity force, whose action tends to flatten out the folds. It is clear that in the absence of compression, a layer that is initially folded in a wavy surface will gradually be evened out and will approach a flat surface under its own weight. This last effect becomes predominant for the smaller values of the parameter $P/\rho_1 gh$, and the magnitude of the folding becomes insignificant compared to the over-all viscous shortening of the layer under the compression, P, which occurs during the same time.

The writer has discussed (1959c) the case of a layer sandwiched between two infinite media of different densities in detail. Let us denote by ρ_1 and η_1 the density and viscosity of the bottom medium and by ρ_2 and η_2 the corresponding quantities for the top medium (Fig. 11). We must distinguish two cases. In one, the bottom medium is heavier, *i.e.*,

$$\rho_1 > \rho_2 . \tag{8.7}$$

In this case, the effect of gravity is stabilizing, and we can readily treat the problem by using the above results. We can repeat the same discussion used for the layer lying on top of the infinite medium and simply replace η_1 by $\eta_1 + \eta_2$ and ρ_1 by $\rho_1 - \rho_2$.

When the top medium is the heavier, *i.e.*,

$$\rho_2 > \rho_1 , \tag{8.8}$$

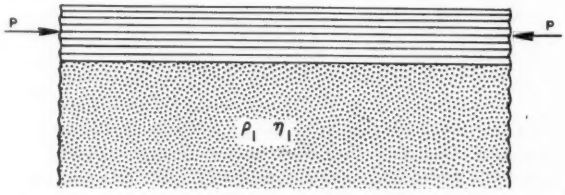

Figure 12. Multiple superposed layers lying at the surface of a medium subject to gravity

the effect of gravity is destabilizing, and spontaneous folding may occur without the compressive load. (For a discussion of this case, *see* Biot, 1959c.)

Of interest also is the influence of gravity in the case of a multiplicity of superposed layers; this was considered previously in this paper without gravity. Assume that we have such a system of superposed layers lying on top of an infinite medium of density ρ_1 and viscosity η_1 (Fig. 12).

Let us proceed as in the derivation of equation (7.5). We shall use the same definitions for the factor n and the average quantities h, η,

and P expressed by equations (7.4). When all layers have the same thickness, h represents the thickness of each layer and n the number of layers. We apply the same reasoning as used in the derivation of equation (7.5), except that we now start from equation (8.1), which includes the effect of gravity. For multiple layers, this equation becomes

$$Phl^2w - \frac{1}{3}\eta h^3 l^4 \frac{dw}{dt} = \frac{2\eta_1}{n}\frac{dw}{dt} + \frac{\rho_1 g w}{n}. \quad (8.9)$$

Comparison with equation (8.1) shows that the result is the same as that for the single layer of thickness h, except that the viscosity of the bottom medium and the gravity, g, are both divided by n. We can therefore repeat exactly the same analysis, using the diagram of Figure 10 for the single layer. We can see that the effect of stacking layers is to increase the dominant wavelength proportionally to $\sqrt[3]{n}$ for cases where viscosity predominates and proportionally to $\sqrt{n}$ for cases where gravity predominates.

We must also replace g by g/n in the inequality (8.4). Correspondingly, the higher limit for the wavelength of viscous folding becomes of the order of 15,000 n feet. By the same reasoning used for the case of a single layer, we can see that the effect of erosion will increase. This will increase the higher limit even more. Regarding the assumption of perfect slip between layers, we refer to our remark at the end of Section 7 on the action of layers of low-viscosity rock and the mechanism of hydraulic lifting in fluid-filled porous rock suggested by Hubbert and Rubey, (1959) and Rubey and Hubbert (1959). It can therefore be concluded that the large-scale folding associated with orogenesis is not incompatible with the mechanism of purely viscous folding of multiple layers.

As a matter of general interest, the problem of folding of an inhomogeneous but continuous solid (Fig. 13) was also analyzed. In particular, we have considered a purely viscous and incompressible solid that is infinitely deep and such that its viscosity coefficient decreases exponentially with depth,

$$\eta = \eta_0 e^{-\gamma y}. \quad (8.10)$$

This means that as we go deeper, the solid approaches the liquid state in a continuous manner. Originally, the material is in equilibrium under gravity, with a hydrostatic pressure, $\rho g y$, proportional to the depth. We then assume that it is compressed horizontally at a uniform rate. This superimposes a horizontal compressive stress, P, which has a value of P_0 at the surface and which also decreases exponentially with depth:

$$P = P_0 e^{-\gamma y}. \quad (8.11)$$

Under these conditions, the surface is found to be unstable, and folding will develop. The dominant wavelength of these folds is a function of a characteristic nondimensional parameter

$$G = \frac{\rho g}{P_0 \gamma}. \quad (8.12)$$

(ρ is the mass density of the solid, and g is the acceleration of gravity.) The dominant wavelength can be expressed as

$$L_d = \frac{2\pi}{r\delta}. \quad (8.13)$$

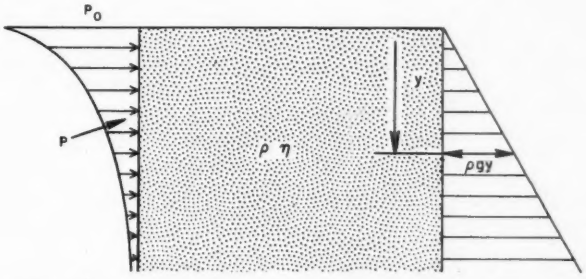

Figure 13. Inhomogeneous viscous solid with a viscosity decreasing exponentially with the depth y. The initial stress is the hydrostatic pressure, $\rho g y$, and a horizontal compression, P, function of depth.

The nondimensional quantity δ is a function of G, which has been determined numerically. The dependence of G on δ can be approximated by

$$\delta = 2.2\, G^{6/10}. \qquad (8.14)$$

We conclude from this result that the presence of gravity is required in order for folding to occur. This can be seen by putting $g = 0$. In this case, the dominant wavelength, L_d, becomes infinite, and the folding disappears. This last conclusion depends, of course, on the assumption that the material is of infinite extent in the horizontal direction. If the surface extends over a distance D and is restrained at the ends, the wavelength will be determined by equation (8.13) if $L_d < D$. For larger wavelengths, or in the absence of gravity, the wavelength will be determined by the geometry of the constraint, and the surface will tend to bend in one-half wave of length D. The writer has discussed a numerical application of this result to examine the possibility of folding in the earth's crust as a whole by a purely viscous mechanism, based on a viscosity coefficient decreasing exponentially with depth (Biot, 1960). He assumes that this constitutes an approximation for the viscosity of rock due to the increase of temperature and pressure with depth. For significant folding to occur, the viscosity must decrease by a factor smaller than $1/e$ in a depth of about 200 feet and the wavelength must not exceed 6000 feet. Such a viscosity gradient is considerably steeper than occurs on the average in the earth. Hence this model is not adequate to explain large-scale folding.

9. CONCLUDING REMARKS

The purpose of this paper has been to present a simplified and intuitive treatment of the theory of folding of stratified viscoelastic media along with specific examples that are relevant in a geologic framework. The writer realizes that the geologic implications of the theory deserve a more elaborate discussion than has been given here. However, such a task lies beyond his particular field of competence.

In its present state the theory represents the first phase of a program. Its extension to materials and configurations of a more complex nature has been under development and will be presented at a later date.

It is difficult to assign specific values to the viscosity coefficients of rock except within one order of magnitude. Laboratory tests are restricted to time intervals that are extremely short in comparison with the geological time scale. On the other hand, a few observations have been reported of deformations occurring under natural conditions and known gravity forces over periods of the order of a century. Viscosities derived from such data agree in order of magnitude with the results from laboratory tests. The range of values, 10^{17}–10^{22} poises, considered herein is probably on the high side if we take into account the fact that the viscosity drops quite rapidly with increasing pressure and temperature. Hence, the time required for folding at appreciable depth may be even smaller on the average than the figures given herein. Another feature involved here lies in the nature of the "effective viscosity coefficient" that must be introduced in the present theory when applied to materials of nonlinear properties as, for instance, when deformation rates increase faster than proportionally to the stress. As regards the viscosity contrast, values of 100 to 1000 for the ratio of the viscosity of the layer to that of the embedding medium may be reasonably assumed as a representative order of magnitude for materials such as limestone or sandstone embedded in shale.

Within a lower stress range rocks are elastic for fast deformation and tend to behave approximately like a viscous medium for slow deformations. Results of the theory indicate that the viscous behavior predominates in tectonic folding. This leads to large deformations without fracture, and the dependence of fracture on deformation rates. This paper gives the time histories and rate processes and evaluates them numerically.

If one assumes that rocks behave as a purely viscous solid, significant folding may appear under relatively low tectonic stresses. However, in such a case the influence of gravity becomes important near the surface and may be sufficient to prevent folding. Even deep folds may be blocked by the presence of a stabilizing density gradient.

The theory is developed in the context of linear phenomena but is applicable to materials with nonlinear stress-strain relations. The linear theory may be looked upon as describing incipient folding in a state of initial plastic stress. The rheological behavior in this case may be described by an "effective viscosity coefficient". In any case the incipient folding that is governed by the linear theory determines a wave length that is "frozen-in". As the folding proceeds, high stresses are produced at the

crests. Cracks or accelerated creep are generated at these points, thus introducing another nonlinear feature. Owing to weakening at the bends, the bends tend to behave like hinges, and the folding then proceeds by a different mechanism that brings the crests closer together. The writer has also discussed another nonlinear feature of purely geometric origin by which folding tends to become more regular than predicted by the linear theory. This is due to the geometric limitation on folding beyond a certain amplitude: the waves of small amplitudes continue to grow at an exponential rate. In the light of the present remarks it should be remembered that wavelength predictions from the linear theory apply only to incipient folding. Therefore, any application to field observations when the folds are sharp requires an evaluation of the incipient configuration through an "unfolding process".

The time required for significant folding to occur has been evaluated. This evaluation is based on a range of acceptable tectonic stresses and rock viscosities. The results are in excellent agreement with the geological time scale based on radioactivity data.

The geometric patterns of the folding derived from the present theory show a striking similarity to observed geological structures. This seems partly a consequence of two fundamental results of the theory. It was shown that for purely viscous deformations and when the influence of gravity is not important the dominant wave length is independent of the tectonic stress. This will, of course, remain approximately true for the case where viscous deformations play the important part. The other theoretical result involved here is the dependence of the dominant wave length on the cubic root of the viscosity ratio with the consequence that it is not sensitive to large variations in viscosity contrast.

Large-scale folding is compatible with the present theory, and the writer has shown that distances of a few miles between crests are possible by viscous deformation under the combined action of a horizontal compression and gravity. This conclusion, however, is not applicable if the crust is assumed to be of isotropic properties with a viscosity decreasing continuously with depth and a gradient corresponding to average properties in the earth. This is consistent with the usual assumption that stratification and discontinuities play an essential part in orogenic folding.

REFERENCES CITED

Bijlaard, P. P., 1939, Het plooien van een vlakke plaat die op een elastisch-isotrope half-ruimte is opgelegd: De Ingenieur in Ned. Indie., no. 9, p. 215–226

—— 1947, On the elastic stability of thin plates supported by a continuous medium: Koninkl. Nederlandse Akad. Wetensch. Proc., v. L, nos. 1 and 2, p. 79–193

Biot, M. A., 1934, Sur la stabilité de l'equilibre elastique, equations de l'elasticité d'un milieu soumis à tension initiale: Ann. Soc. Sci. de Bruxelles, tome 54, ser. B, pt. 1, p. 18–21

—— 1938, Theory of elasticity with large displacements and rotations: 5th Internat. Cong. Applied Mechanics Proc., p. 117–122

—— 1939a, Théorie de l'elasticité du second ordre avec application à la theorie du Flambage: Ann. Soc. Sci. de Bruxelles, tome 59, ser. 1, p. 104–112

—— 1939b, Non-linear theory of elasticity and the linearized case for a body under initial stress: Philos. Mag., v. 27, sec. 7, p. 468–489

—— 1940, Elastizitats Theorie Zweiter Ordnung mit Anwendungen: Zeitschr. angew. Math. und Mech., bd. 20, no. 2, p. 89–99

—— 1954, Theory of stress-strain relations in anisotropic viscoelasticity and relaxation phenomena: Jour. Applied Physics, v. 25, no. 11, p. 1385–1391

—— 1956, Variational and Lagrangian methods in viscoelasticity: Berlin, Springer-Verlag, IUTAM Proc., Colloquium on deformation and flow of solids (Madrid, 1955), p. 251–263

—— 1957, Folding instability of a layered viscoelastic medium under compression: Royal Soc. London Proc., ser. A, v. 242, p. 444–454

—— 1958a, Linear thermodynamics and the mechanics of solids: 3d U.S. Natl. Cong. Applied Mechanics, American Soc. Mechanical Engineers Proc., p. 1–18

—— 1958b, Stability problems of inhomogeneous viscoelastic media: New York, Pergamon Press, IUTAM Proc., Colloquium on inhomogeneity in elasticity and plasticity (Warsaw, September 1958), p. 311–321

Biot, M. A., 1959a, Folding of a layered viscoelastic medium derived from an exact stability theory of a continuum under initial stress: Applied Mathematics Quart., v. XVII, no. 2, p. 185–204

—— 1959b, On the instability and folding deformation of a layered viscoelastic medium in compression: Jour. Applied Mechanics, ser. E, v. 26, p. 393–400

—— 1959c, The influence of gravity on the folding of a layered viscoelastic medium under compression: Jour. Franklin Inst., v. 267, no. 3, p. 211–228

—— 1960, Instability of a continuously inhomogeneous viscoelastic half-space under initial stress: Jour. Franklin Inst., v. 270, no. 3, p. 190–201

Biot, M. A., Odé, H., and Roever, W. L., 1961, Experimental verification of the theory of folding of stratified viscoelastic media: Geol. Soc. America Bull., v. 72, p. 1621–1632

Birch, Francis, Schairer, J. F., and Spicer, H. Cecil, 1942, Handbook of physical constants: Geol. Soc. America Special Paper 36, 325 p.

Chandrasekhar, S., 1955, The character of the equilibrium of an incompressible heavy viscous fluid of variable density: Cambridge Philos. Soc. Proc., v. 51, pt. 1, p. 162–178

Goguel, J., 1943, Introduction a l'étude mécanique des déformations de l'écorce terrestre: Paris, Mémoire, Ministère de la Production Industrielle et des Communications, Imprimerie Nationale, 514 p.

Goldstein, S., 1926, The stability of a strut under thrust when buckling is resisted by a force proportional to the displacement: Cambridge Philos. Soc. Proc., v. 23, p. 120–129

Gough, G. S., Elam, C. F., and DeBruyne, N. A., 1940, The stabilization of a thin sheet by a continuous supporting medium: Jour. Royal Aeronautical Soc., v. 44, p. 12–43

Griggs, D. T., 1939, Creep of rocks: Jour. Geology, v. 47, p. 225–251

—— 1940, Experimental flow of rocks under conditions favoring recrystallization: Geol. Soc. America Bull., v. 51, p. 1001–1022

Gunn, Ross, 1937, A quantitative study of mountain building on an unsymmetrical earth: Jour. Franklin Inst., v. 224, no. 1, p. 19–53

Hide, R., 1955, The character of the equilibrium of an incompressible viscous fluid of variable density: an approximate theory: Cambridge Philos. Soc. Proc., v. 51, pt. 1, p. 179–201

Hubbert, M. King, and Rubey, William W., 1959, Mechanics of fluid-filled porous solids and its applications to overthrust faulting: Geol. Soc. America Bull., v. 70, p. 115–166

Kaisin, F., 1927, Déformation de Plaques de Marbre dans des Monuments Anciens de Bruges: Ann. Soc. Sci. de Bruxelles, tome 47, ser. B, pt. 1, p. 192–194

Kienow, S., 1942, Grundzüge einer Theorie der Faltungs- und Schieferungsvorgänge: Berlin, Bornträger, Fortschritte der Geologie und Paleontologie, bd. XIV, h. 46

Kulp, J. Laurence, 1959, Absolute age determination of sedimentary rocks: 5th World Petroleum Cong., sect. 1, Paper 37, p. 689–704

Rubey, William W., and Hubbert, M. King, 1959, Overthrust belt in geosynclinal area of western Wyoming in light of fluid-pressure hypothesis: Geol. Soc. America Bull., v. 70, p. 167–205

Smoluchowski, M., 1909a, Über ein gewisses—Stabilitätsproblem der Elastizitätslehre: Akad. Wiss. Krakau. Math. Kl., p. 3–20

—— 1909b, Kilka Uwag o Fizycznych Podstawach Theoryi Gorotworczych (Einige Bemerkungen über die Physikalischen Grundlagen der Theorien der Gebirgsbildung): Kosmos, v. XXXIV, p. 547–579 (Annals of the Copernicus Society published by Gubrynowicz and Schmidt, Lwow)

—— 1910, Versuche über Faltungs-erscheinungen Schwimmender Elasticher Platten: Akad. Wiss. Krakau. Math. Kl., p. 727–734

Van der Neut, 1943, Die Stabilität Geschichteter Streifen: Natl. Luchtvaart Laboratorium, Bericht S. 284

Manuscript Received by the Secretary of the Society, May 9, 1960

M. A. BIOT
H. ODÉ
W. L. ROEVER
Shell Development Company, Houston, Texas

Experimental Verification of the Theory of Folding of Stratified Viscoelastic Media

Abstract: An experimental check has been obtained for the stability theory of stratified viscoelastic media in compression. Model tests have been conducted for both an elastic layer and a viscous layer embedded in a viscous medium and subject to a compression parallel with the layer. The appearance of the folds and the measured wavelengths are in good agreement with the theoretical predictions. For a better interpretation of the tests, the writers present a theoretical evaluation of the time history of deformation for a layer whose folding develops from a given initial departure from perfect flatness. The calculated folding of the layer at various intervals is plotted for different values of the significant parameter.

CONTENTS

1. Introduction and acknowledgments 1621
2. Analytical evaluation of the time history of folding 1622
3. Numerical evaluation of the time history of folding 1623
4. Description of experiments 1627
5. Discussion of experimental results 1629
References cited 1630
Appendix: Evaluation of the integral (2.7) . . . 1631

Figure
1. Layer of thickness h and viscosity η under compressive stress P in a medium of viscosity η_1 1622
2. Shape of assumed initial disturbance of the layer 1623
3. Time history of folding for a viscosity ratio $\eta/\eta_1 = 1000$ 1624
4. Time history of folding for a viscosity ratio $\eta/\eta_1 = 144$ 1625
5. Amplitude $w(0,t)$ at the center ($x = 0$) for the time histories shown in Figures 3 and 4 1626
6. Example of folding of a viscous layer in a viscous medium 1626
7. Graph of results of buckling of elastic layers in a viscous medium 1628

Plate Facing
1. Deformation tank 1628
2. Elastic and viscous layers buckling in a viscous medium 1629

Table
1. Dimensions and constants used 1628
2. Dependence of wavelength on viscosity ratio . 1629

1. INTRODUCTION AND ACKNOWLEDGMENTS

Biot (1957; 1959a; 1959b) has described theoretical analyses of the folding of a viscoelastic layer under compression in a viscoelastic medium. The particular cases of a viscous or elastic layer in a viscous medium have been rederived and discussed by elementary methods in a companion paper (Biot, 1961). The writers here establish an experimental verification of these results by model tests in the laboratory. The tests covered the cases of both the elastic layer and the viscous layer embedded in a viscous medium. It may be assumed that such simplified models embody the significant aspects of the physics and furnish a crucial check of the theory.

To prepare adequately the qualitative, as well as the quantitative, interpretation of the tests, the writers evaluate the time history of the folding from the theory. Since folding cannot occur in a geometrically perfect plane layer, the writers have introduced an initial disturbance in the form of a kink and have calculated the subsequent deformation and development of folds that appear as a result of compression in the layer. This is accomplished in sections 2 and 3. Only the case of a viscous layer was evaluated. The theory indicates that similar results will be obtained for an elastic layer. The appearance of the dominant wave-

Geological Society of America Bulletin, v. 72, p. 1621–1632, 7 figs., 2 pls., November 1961

length and the qualitative aspect of the folds predicted by the theory are well verified by the tests. The experiments are described in Section 4, their results discussed in Section 5. Results for the elastic layer show good agreement with the theoretical prediction regarding the dependence of the dominant wavelength on the compression load and its independence of the viscosity of the medium. Satisfactory agreement is also obtained for the case of a viscous layer, in which the dominant wavelengths are close to the calculated values and are independent of the compression loads, as predicted.

The authors wish to acknowledge the valuable assistance of Mr. T. J. Shankland in the experimental phase of this work.

2. ANALYTICAL EVALUATION OF THE TIME HISTORY OF FOLDING

Consider the case of a viscous layer of thickness h embedded in an infinite viscous medium (Fig. 1). The layer is under an initial compression P per unit area. In the companion paper, Biot (1961) derived an equation for the lateral deflection, w, of the layer[1] and investigated the stability of the layer. He restricted the analysis to an infinite wave of constant wavelength. He found that an initial sinusoidal deflection, w, of the layer, represented by

$$w = W_0 \cos lx \,, \tag{2.1}$$

increases exponentially with time. After a time t, the deflection (2.1) becomes[2]

$$w = W_0 e^{pt} \cos lx \,, \tag{2.2}$$

where

$$p = \frac{P}{\dfrac{4\eta_1}{hl} + \dfrac{1}{3}\eta h^2 l^2} \tag{2.3}$$

(h = thickness of the layer, η_1 = viscosity coefficient of the medium, η = viscosity coefficient of the layer).

The wavelength L is related to l by

$$L = \frac{2\pi}{l} \,. \tag{2.4}$$

In the present analysis, this result will be used to solve a more complex problem. Instead of starting with an initial deflection (2.1) that is perfectly sinusoidal, the writers will consider the case in which the initial deflection, $w_0(x)$, is localized. The problem will then be to evaluate the time history of the folding under the compression P. This can be done by using the principle of superposition. The initial deflection can be represented as a superposition of cosine functions by a Fourier integral. Consider an initial deflection represented by the expression

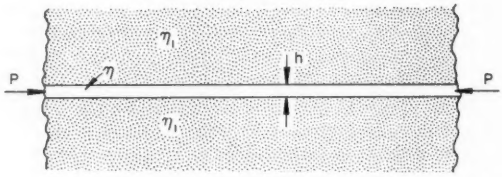

Figure 1. Layer of thickness h and viscosity η under compressive stress P in a medium of viscosity η_1

$$w_0(x) = \frac{b}{1 + \left(\dfrac{x}{a}\right)^2} \,. \tag{2.5}$$

This is a bell-shaped curve, as Figure 2 shows. Expression (2.5) can be written as a Fourier integral by the well-known identity

$$\frac{b}{1 + \left(\dfrac{x}{a}\right)^2} = ba \int_0^\infty e^{-la} \cos lx \, dl \,. \tag{2.6}$$

For any given wavelength, any sinusoidal component under the integral sign will be multiplied by the factor e^{pt}, as expressed by equation (2.2). The deflection $w(x,t)$ after a time t is thus obtained by multiplying each component under the integral sign in equation (2.6) by this factor, *i.e.*,

$$w(x,t) = ba \int_0^\infty e^{pt-la} \cos lx \, dl \,. \tag{2.7}$$

[1] The equation was also derived as a particular case of a more elaborate theory (Biot, 1957).

[2] *See* equation (4.11) of the companion paper (Biot, 1961).

The quantity p is a function of l, given by equation (2.3).

The computation of this integral was done numerically. It is convenient to make use of the time t_1 already introduced in earlier work (Biot, 1959a; 1959b; 1961):

$$t_1 = \frac{\eta}{P}. \tag{2.8}$$

As pointed out, t_1 is the time required for the layer to shorten by 25 per cent if it remained straight while under the constant pressure P.

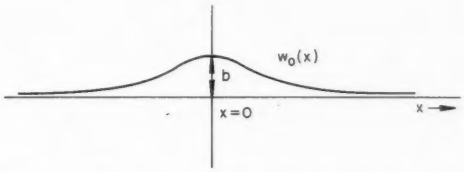

Figure 2. Shape of assumed initial disturbance of the layer

It is convenient to use t_1 as a reference time. In the calculations and in plotting the results, the writers will represent the time by means of the dimensionless ratio t/t_1. The method used for the numerical evaluation of the integral (2.7) is explained in the Appendix.

3. NUMERICAL EVALUATION OF THE TIME HISTORY OF FOLDING

Let us consider the parameters and variables of the problem. As shown by equation (A.2) in the Appendix, the deflection w is a function of a/h, t/t_1, and the viscosity ratio η/η_1. It is also proportional to the maximum initial deflection, b. Computations were carried out for three values of the viscosity ratio, but results are presented in detail only for the two values $\eta/\eta_1 = 1000$ and 144, since these adequately point out the significant features. For each ratio, three different values of the parameter a/h were so chosen that the average wavelength content of the initial perturbation is related in a definite way to the physically dominant wavelength of the system. The latter is the wavelength of fastest rate of growth under a given load P. It tends to obliterate all others. As shown earlier (Biot, 1957; 1959a; 1961), the dominant wavelength for the present case is given by

$$L_d = 2\pi h \sqrt[3]{\frac{\eta}{6\eta_1}}. \tag{3.1}$$

In this case, L_d is independent of the load. For viscosity ratios $\eta/\eta_1 = 1000$ and 144, $L_d = 34.57\,h$ and $18.12\,h$, respectively. On the other hand, the average wave number of the initial perturbation can be defined as

$$l_{\text{av.}} = \frac{\int_0^\infty l e^{-la}\,dl}{\int_0^\infty e^{-la}\,dl} = \frac{1}{a}, \tag{3.2}$$

so that the average wavelength, $L_{\text{av.}}$, of the initial perturbation is, by equations (2.4) and (3.2),

$$L_{\text{av.}} = 2\pi a. \tag{3.3}$$

For the computation, a was so chosen that, approximately,

$$L_d = \frac{1}{2} L_{\text{av.}}, L_{\text{av.}}, 2L_{\text{av.}}. \tag{3.4}$$

From equations (3.1), (3.3), and (3.4), the values of a/h corresponding to equation (3.4) can be computed. They are, approximately,

$$a/h = 11, 5.50, 2.75 \tag{3.5}$$

for the ratio $\eta/\eta_1 = 1000$, and

$$a/h = 5.60, 2.80, 1.50 \tag{3.6}$$

for $\eta/\eta_1 = 144$.

The three cases (3.5) for the viscosity ratio $\eta/\eta_1 = 1000$ are plotted in Figure 3. The shape of the deformed layer is plotted at various instants. The abscissa represents the ratio x/h of the distance x along the layer to the thickness h. The deformation is symmetric with respect to the origin because the initial perturbation is symmetric about this point. Hence, only the deformation on one side of the axis of symmetry is shown ($x > 0$). The ordinates are proportional to the deflections of the layer but do not represent the actual magnitude. The point of maximum deflection is on the axis of

symmetry ($x = 0$), and all deflections at that point are reduced to the same value, taken as unity. The graphs therefore show the gradual development of the folds of a half-portion of the layer. The shape of the layer is shown at four instants—at $t = 0$, where the shape is the initial disturbance in the ratio 1:4. This introduces very little difference in the time history of the folding. A definite wavelength is measurable that is very close to the dominant wavelength, $L_d = 34.57\ h$.

A similar plot is shown in Figure 4 for the

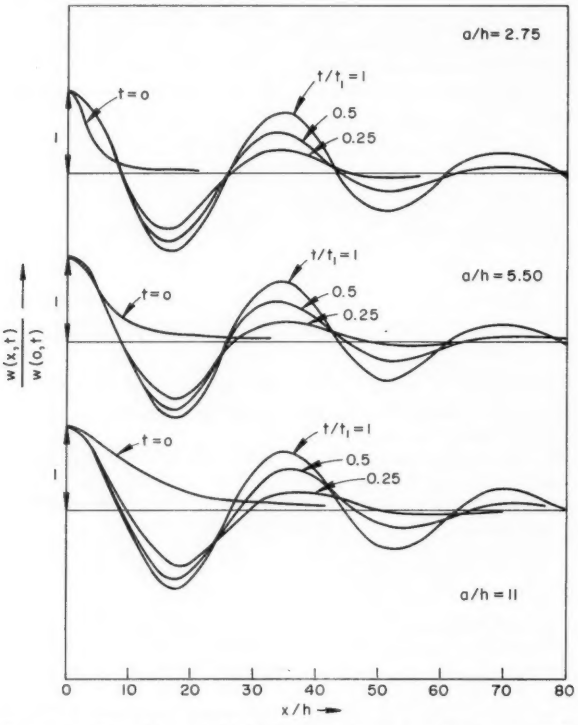

Figure 3. Time history of folding for a viscosity ratio $\eta/\eta_1 = 1000$. Three types of initial disturbances (at $t = 0$) are considered. All amplitudes are reduced to unity at the center ($x = 0$). Only the right half of the symmetric figure is shown.

assumed initial disturbance itself as represented by equation (2.5), and subsequently at

$$t = 0.25t_1,\ 0.50t_1, \text{ and } t_1 . \qquad (3.7)$$

The magnitude of the deflection at any point is known, once it has been calculated at $x = 0$. This is discussed hereafter.

Figure 3 also indicates that after sufficient time a very definite wavelength appears that is quite sharp. The three values of a/h for which the deflections have been evaluated correspond to a variation of the width of the three cases in which the viscosity ratio $\eta/\eta_1 = 144$ (3.6); here also, the curves have been plotted for the instants (3.7).

Again, the result is fairly insensitive to the width of the initial disturbance. Although the definition in this case is less sharp, a characteristic wavelength appears that is close to the dominant wavelength, $L_d = 18.12\ h$, at least in the later phase of the folding. The observed wavelength in this case tends to shift slightly toward longer waves when the width of the initial perturbation increases.

We shall now consider the amplitude of the folding. We must evaluate the amplitude on the axis of symmetry of the initial disturbance, *i.e.*, at $x = 0$. The initial deflection at that point is equal to b. At time t, it is found by putting $x = 0$ in equation (2.7); *i.e.*,

$$w(0,t) = ba\int_0^\infty e^{pt-la}\,dl\,. \qquad (3.8)$$

In Figure 5, we have plotted the ratio $w(0,t)/b$, *i.e.*, the amplification factor at $x = 0$ as a function of t/t_1, for the values of the viscosity ratio η/η_1 and a/h given heretofore.

It can be verified that the amplification given by equation (3.8) is not very sensitive to the width of the initial perturbation and that it is closely approximated by the amplification factor A_d, which Biot (1961) derived for a purely sinusoidal deformation of dominant wavelength. The amplification factor A_d is given by equation (5.15) of Biot (1961):

$$\log A_d = \frac{t}{t_1}\left(\frac{\eta}{6\eta_1}\right)^{2/3}, \qquad (3.9)$$

where log is the natural logarithm.

Figures 3 and 4 confirm the conclusions of Biot's analysis (1961) regarding band width and selectivity of the folding. Biot found that regular waves can be expected to appear over a distance

$$D = \frac{L_d}{\Delta l/l_d}$$

when $\Delta l/l_d$ is the band width as given by Table 2 of the Biot (1961) paper. For an

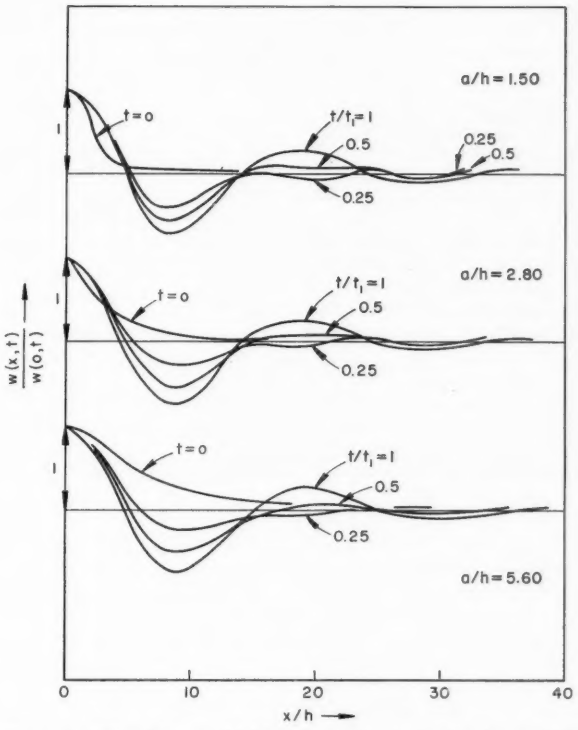

Figure 4. Time history of folding for a viscosity ratio $\eta/\eta_1 = 144$. Three types of initial disturbances (at $t = 0$) are considered. All amplitudes are reduced to unity at the center ($x = 0$). Only the right half of the symmetric figure is shown.

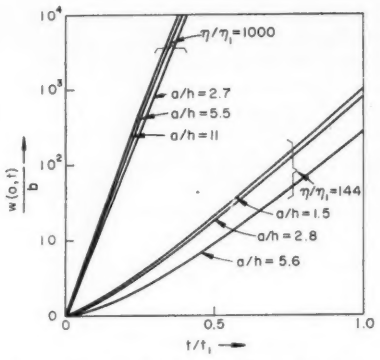

Figure 5. Amplitude $w(0, t)$ at the center ($x = 0$) for the time histories shown in Figures 3 and 4 (b = amplitude at the center of the initial disturbance)

amplification factor $A_d = 1000$, this yields the value $\triangle l/l_d = 0.632$, indicating that $D = 1.58\ L_d$. As shown by Figure 5 for the case in which $\eta/\eta_1 = 1000$, the amplification $A_d = 1000$ corresponds to $t/t_1 \cong 0.3$. Figure 3 shows that folding at this instant is regular over a distance of about 1.5 L_d, as calculated. We must, of course, consider the fact that the figure shows only half of the complete picture.

The significance of these results can be illustrated by a specific example. Consider a layer of thickness $h = 2$ feet and viscosity $\eta = 10^{21}$ cgs. This layer is subject to a compression $P = 1450$ psi and is embedded in a medium of viscosity $\eta_1 = 10^{18}$ cgs. The initial deflection is assumed to correspond to $a/h = 5.50$ (hence, $a = 11$ feet), and its maximum value at the center is shown as $b = 0.24$ inch. The time t_1 is

$$t_1 = \frac{\eta}{P} = 319{,}000 \text{ years}.$$

The folding deformation of this layer at the time

$$t = 0.3t_1 = 95{,}700 \text{ years}$$

can be derived from Figures 3 and 5. Figure 6 shows the shape and amplitude. The maximum amplitude at the center is

$$w(0, t) \cong 1000b = 20 \text{ feet}.$$

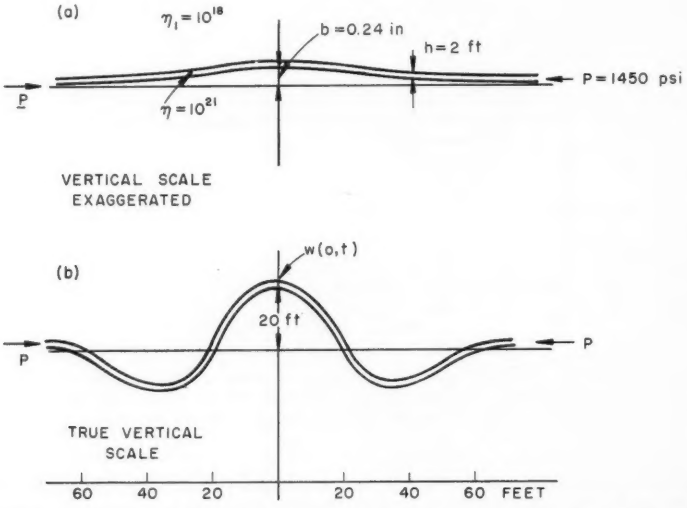

Figure 6. Example of folding of a viscous layer in a viscous medium. (*a*) layer of thickness $n = 2$ feet with initial disturbance of maximum amplitude $b = 0.24$ inch under horizontal compression $P = 1450$ psi. (*b*) deformation and folding of the layer after 95,700 years. At that time, the amplitude of folding is 20 feet at the center. (The figure does not take into account the shortening between crests due to the geometry of folding at finite amplitude. *See* Section 6 of Biot's (1961) companion paper.)

The analysis presented is based on the assumption of an initial bell-shaped disturbance, represented by equation (2.5). A much more complicated type of initial irregularity can be represented by a superposition of bell-shaped curves of various widths and locations. The resulting deformation of the layer is then obtained by superposition of the folding due to each initial bell-shaped component. Time histories with such composite initial disturbances were evaluated. The results do not differ significantly from those given heretofore, except for the very special case in which the spacing of the disturbances is such that the folds tend to cancel each other by being exactly out of phase.

At the larger amplitudes of folding, the rate of folding becomes much slower than predicted by the present linear theory. This is due to a nonlinear effect of geometric origin. Therefore, the folding amplitudes will tend to equalize and exhibit more regular behavior at large strain, as already pointed out by Biot (1961).

Time histories for the case of an elastic layer or for problems with more complex viscoelastic properties can be computed by the same method. As shown by the previous analysis of band width, the folding for the elastic layer can be expected to show more regularity of the waves. This conclusion is borne out by the model tests discussed in the following section.

4. DESCRIPTION OF EXPERIMENTS

Laboratory tests of the buckling theory have been conducted for two cases—an elastic layer in a viscous medium, and a viscous layer in a viscous medium. As derived previously (Biot, 1957), the dominant wavelength for an elastic layer in a viscous medium is

$$L_d = \pi h \sqrt{\frac{E}{(1 - \nu^2)P}}, \qquad (4.1)$$

where E and ν are Young's modulus and Poisson's ratio of the layer, respectively; the dominant wavelength for the viscous layer is given by equation (3.1).

The tests were designed to verify these formulas and to show that the type of deformation observed conforms with the predictions of the previous sections.

The experiments were performed in a tank 1 m high, 1 m wide, and 20 cm front to back. A narrow plate-glass window was provided in the center of the front and back for observation and photography. The tank was filled with the viscous medium, and the layers were lowered into it in a vertical position and were compressed vertically by weights (Pl. 1). Weights were placed on a platform that moved vertically on guide rails above the tank. Application of the load to the layer tripped a microswitch, which started the clock used to read loading time to fractions of a second. Another clock, used to read to the nearest second, was started manually.

Results were observed photographically by a 35-mm Robot camera with spring-loaded rapid film advance. With this device, up to five pictures per second could be taken. An attempt was made to record still faster deformations with a 16-mm movie camera. At these higher deformation rates, the inertial forces become important in the experiment, and the theory is no longer applicable.

Corn syrup was chosen as the viscous medium because it has relatively high viscosity at room temperature and is transparent, water soluble, nontoxic, and inexpensive. Two grades of syrup manufactured by the Corn Products Company were used—their most viscous grade, No. 1152, and a less viscous grade, No. 1132.

A locally obtained grade of roofing tar was selected for the viscous layers because it could be readily cast into shape and yet was sufficiently viscous so that the layers could be handled into and out of the tank. The mold was lined with thin sheets of Teflon, which enabled the cast layers to be removed from the mold without damage. Elastic layers were made of sheet aluminum and of cellulose acetate butyrate, which were chosen primarily on the basis of availability.

The viscosity of the two grades of syrup was determined both by using a Hoeppler viscometer and by timing the rate of fall of ball bearings through the syrup and applying the Stokes law. These measurements were in close agreement and are summarized in Table 1.

The quantity $E/(1 - \nu^2)$ was obtained for the aluminum and cellulose acetate butyrate layers by direct measurement from the bending of small strips, approximately 2 cm by 10 cm, cut from the sheets. Each strip was measured in two ways—as a cantilever beam loaded at the end, and as a beam freely supported on the ends and loaded in the center. The strip was assumed to be sufficiently wide in relation to its thickness (20 to 1 minimum) to bend as a plate into a cylindrical surface. In that case, the effective modulus used in the

TABLE 1. DIMENSIONS AND CONSTANTS USED

Material	Viscosity (poises)	Density
Pitch (25° C)	3.0×10^7	1.253
1132 corn syrup (24.8° C)	7.0×10^2	1.4
1152 corn syrup (24.9° C)	1.35×10^4	1.45

Sheet used	Thickness h (cm)	Width (cm)	$E/(1-\nu^2)$ (dynes/cm^2)	Viscosity (poises)
Cellulose acetate butyrate	0.102	19.72	1.25×10^{10}	
	0.0787	19.72	1.76×10^{10}	
	0.0510	19.72	2.42×10^{10}	
	0.0254	19.72	2.43×10^{10}	
Aluminum	0.0531	19.70	5.79×10^{11}	
Pitch	0.35	19.70		3.0×10^7
	0.37	19.70		3.0×10^7
	0.87	19.70		3.0×10^7
	1.08	19.70		3.0×10^7

standard beam formulas is $E/(1-\nu^2)$. Results of these measurements, which agreed within $\pm$ 20 per cent, are averaged together and are summarized in Table 1.

The viscosity of the tar was determined by a standard method, called the rod-viscometer method, which involves the shearing of a 2-cm by 2-cm by 10-cm beam of the material (Saal, 1933).

From measurements with several different loads, the rate of deformation was found to be proportional to the applied load, indicating true Newtonian behavior. In addition, no yield point was apparent, since the material would eventually flow to a plane surface under the influence of gravity.

The measurement subject to the largest error in these experiments is that of the wavelength of the buckling. The method used here was merely to measure the distance from the first

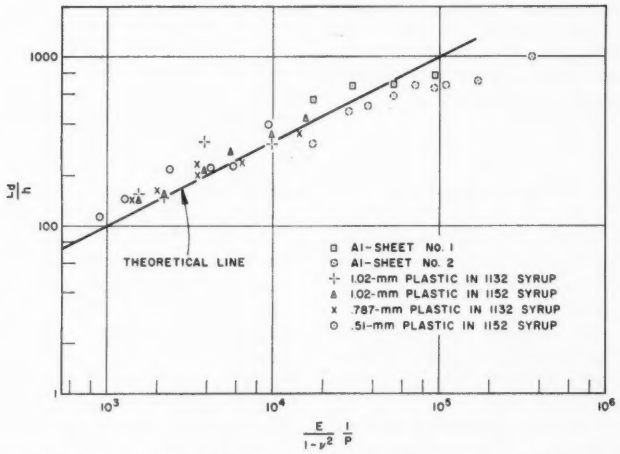

Figure 7. Graph of results of buckling of elastic layers in a viscous medium. L_d = measured wavelength; h = layer thickness; P = compressive load; E = Young's modulus of layer; ν = Poisson's ratio of layer.

SO_3	S	Alkalies	Total	Source of data
....	....	....	100.1	Grim, Bradley, and White (1957, p. 20)
....	....	....	100.35	Grim (1953, p. 372)
....	Tr	....	99.78	McMillan (1956, p. 214)
....	0.02	....	....	McMillan (1956, p. 214)
0.29	.02	....	99.92	McMillan (1956, p. 214)
....	.87	....	....	Stout *et al.* (1923, p. 374)
....	2.32	....	....	Stout *et al.* (1923, p. 374)
....	.02	....	99.32	McMillan (1956, p. 214)
....	....	....	99.27	Keller, Wescott, and Bledsoe (1954, p. 20)
....	.39	....	....	Stout (1923, p. 374)
....	....	0.88	99.15	Waagé (1950, p. 160)
....	....	1.0	99.89	Waagé (1950, p. 160)
....	....	....	99.29	Keller, Wescott, and Bledsoe (1954, p. 20)
....	....	....	98.25	Waagé (1950, p. 160)
....	....	....	....	Patterson and Hosterman (1960, p. 186)
....	....	....	99.07	Keller, Wescott, and Bledsoe (1954, p. 20)
....	....	....	100	Patterson and Hosterman (Written communication, 1959)
....	Tr	....	....	Stout, *et al.* (1923, p. 374)
....	....	.81	99.82	Waagé (1950, p. 160)
....	....	....	99	Patterson and Hosterman (1960, p. 186)
....	....	....	100	Patterson and Hosterman (1960, p. 186)
....	....	.96	....	Foose (1944, p. 568)
....	....	....	100.18	Keller, Wescott, and Bledsoe (1954, p. 20)
....	....	....	....	Grim (1953, p. 47)
....	....	....	....	Greaves-Walker (1907, p. 470)
....	....	....	....	Greaves-Walker (1907, p. 470)
....	....	....	....	Greaves-Walker (1907, p. 470)
....	....	....	100.16	McQueen (1943, p. 156)
....	....	....	100.75	McQueen (1943, p. 156)
....	....	....	....	Greaves-Walker (1907, p. 470)
....	....	....	101.40	Foose (1944, p. 568)
....	....	....	....	McQueen (1943, p. 156)
....	....	....	....	Foose (1944, p. 568)
....	....	....	101.00	McQueen (1943, p. 163)
....	....	....	101.34	McQueen (1943, p. 163)
....	....	....	99.77	Foose (1944, p. 568)
....	....	....	100.33	McQueen (1943, p. 163)
....	....	....	....	

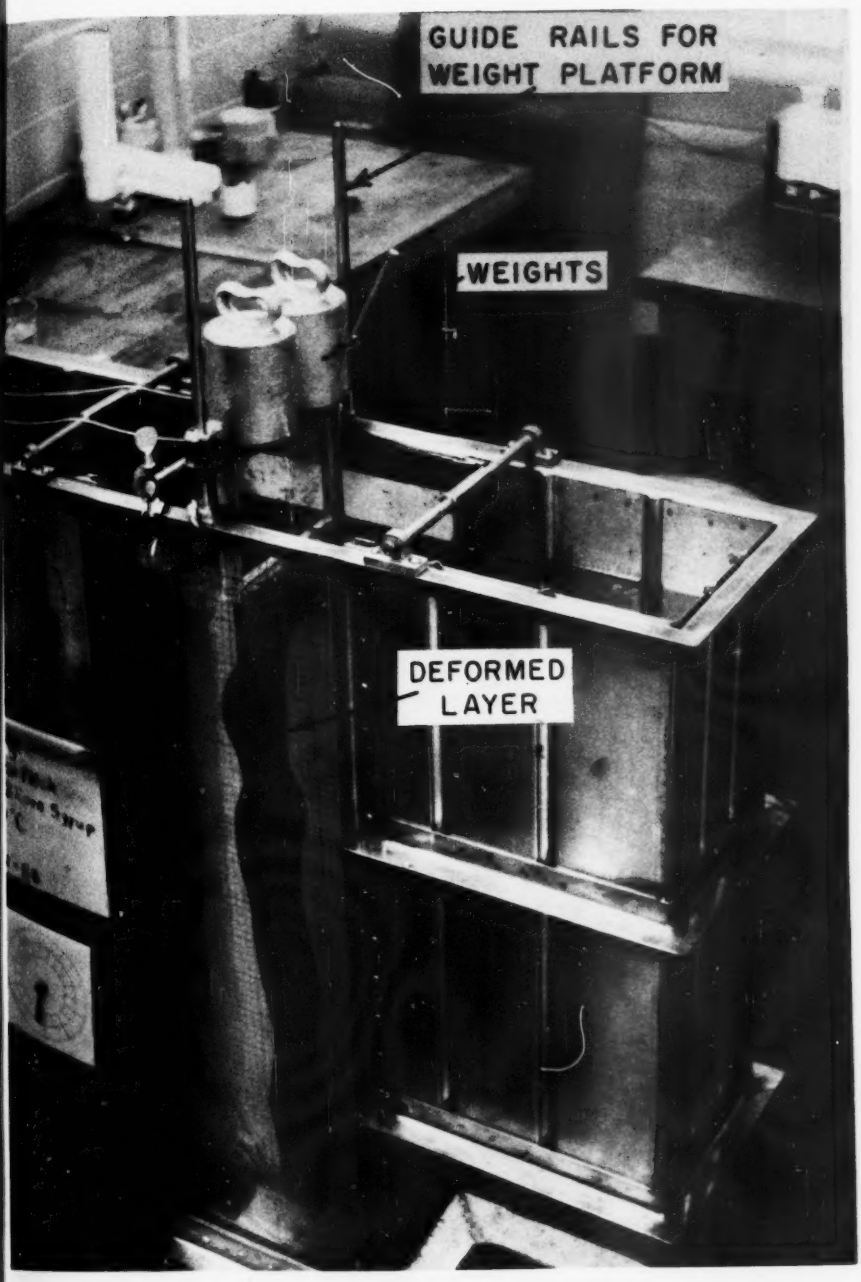

DEFORMATION TANK

BIOT, ODÉ, AND ROEVER, PLATE 1
Geological Society of America Bulletin, volume 72

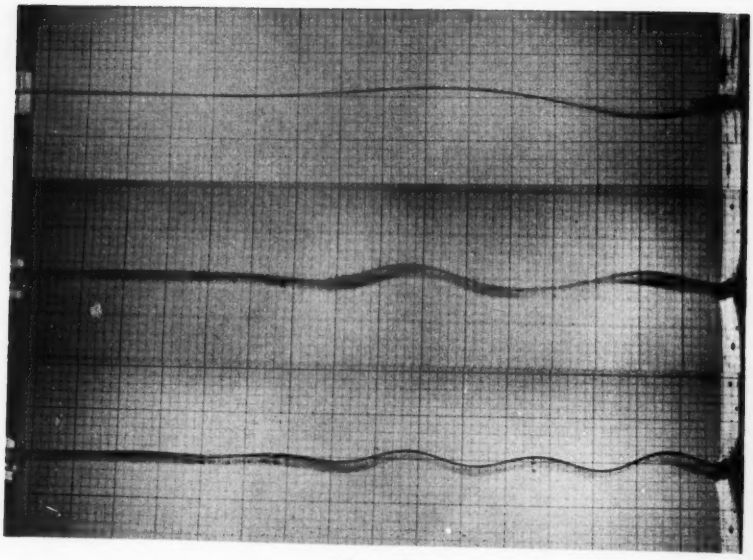

Figure 1

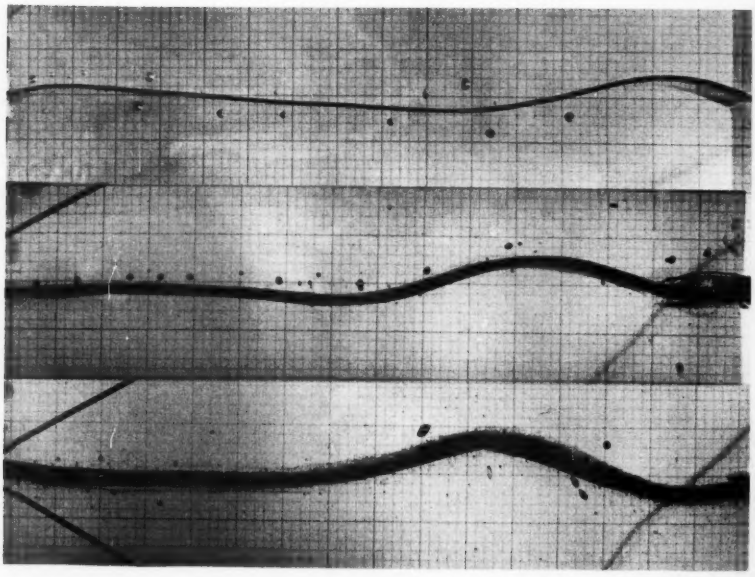

Figure 2

ELASTIC AND VISCOUS LAYERS BUCKLING IN A VISCOUS MEDIUM

peak or trough to the last (a centimeter scale is superposed on each photograph) and divide by the number of cycles observed. This was very straightforward in the case of the elastic layers (Pl. 2, fig. 1), in which a number of well-defined peaks and troughs existed, but became somewhat more ambiguous in the case of the viscous layers, in which the buckling damped out rapidly away from the end where the load was applied (Pl. 2, fig. 2). In all cases, however, the writers attempted to measure the distance between the better developed peaks and troughs and to average these measurements to obtain the wavelength used in the results.

Elastic layers were buckled in both of the viscous media (viscosity ratio approximately 20) with no consistent change in observed wavelength, as predicted by the theory.

TABLE 2. DEPENDENCE OF WAVELENGTH ON VISCOSITY RATIO

η_1 (poises)	η/η_1	h (cm)	L_d/h (calc.)	L_d/h (exp.)
700	4.28×10^4	0.37	121.0	119 – 127
1.35×10^4	2.22×10^3	0.35	45.1	35.3 – 51.4
1.35×10^4	2.22×10^3	0.87	45.1	39.1 – 47.1
1.35×10^4	2.22×10^3	1.08	45.1	35.2 – 48.1

5. DISCUSSION OF EXPERIMENTAL RESULTS

Results for the elastic layer are shown in Figure 7. The ratio of dominant wavelength to layer thickness is plotted against E/P $1 - \nu^2$), where E is Young's modulus, P is the compressive stress, and ν is Poisson's ratio. The results demonstrate the predicted dependence of wavelength upon load over most of the range but show more deviation at longer wavelengths. This is in the region in which the observed wavelength is influenced by the length of the layer used in the experiments, which will be discussed presently.

Experiments with the layers under an initial long bend showed that the observed wavelength was influenced by the preset bend whenever the expected value was within about one to one-half times the preset bend. Shorter wavelengths, however, simply superimposed themselves upon the longer bends with no change in observed wavelength from previous initially undistorted cases.

A much smaller number of experiments were made with viscous layers. One set of four experiments was made to demonstrate the predicted dependence of wavelength on viscosity ratio (Table 2). Another set of experiments was performed in which the load was varied by a factor of 4. This did not change the wavelength, which is in accord with the theory.

To obtain an idea of the magnitude of the amplification involved in these tests, we can compute A_d from equations (2.8) and (3.9). For the folding shown in Figure 2A of Plate 2, $P = 2.153 \times 10^5$ dynes/cm^2, $t/t_1 = 0.054$, and $\eta/\eta_1 = 4.28 \times 10^4$, so that $A_d = 92$. For the folding shown in Figure 2C of Plate 2, $P = 5.348 \times 10^5$ dynes/cm^2, $t/t_1 = 0.339$, and $\eta/\eta_1 = 2.22 \times 10^3$, so that $A_d \cong 44$. These

PLATE 2. ELASTIC AND VISCOUS LAYERS BUCKLING IN A VISCOUS MEDIUM

Figure 1. Buckling of elastic layers in a viscous medium under various loads. 1-mm acetate layer in 1132 corn syrup. (A) 1.6-kg load; (B) 6.6-kg load; (C) 11.6 kg- load. All loads applied from right side.

Figure 2. Buckling of viscous layers in a viscous medium

	Load (kg)	Time applied (sec)	Layer thickness (cm)	η/η_1
A	1.6	7.5	0.37	40,000
B	11.6	49	0.87	2,000
C	11.6	19	1.08	2,000

All loads applied from right side

values appear to be reasonable, since they imply an initial waviness of the layer having an amplitude of the order of 1 mm or less.

There are several obvious difficulties in these experiments. In the first place, the boundary condition of an infinite layer and a surrounding medium is far from attained. Friction occurs as the edge of the plate is forced to shear a thin layer of fluid between the sheet and the glass windows. The extent to which this friction affects the results was not evaluated. Other difficulties with boundary conditions occur in cases in which the dominant wavelength is longer than about half the depth of the tank, because the ends of the plate have to be restrained, thereby forcing nodes. For this reason, whenever possible, measurements were made in the range in which the wavelength was less than half the length of the layer. In addition, with very thin plates it was necessary to clamp the upper and lower ends, thus imposing a zero slope at the end nodes.

Secondly, the various layers suffered from defects of one kind or another. The aluminum was slightly prestressed and tended to assume a single wavelength. The plastic sheets, especially the thinnest ones, had an inherent transverse bend, which increased the effective rigidity. To counteract this tendency, the writers clamped the ends.

The tar layers were less dense than the syrup and hence floated unless restrained. Since they would eventually deform and flow from any clamp, a different kind of restraint was necessary. Before the tar was cast, two strings were run down the length of the mold so that they occupied a position as near as possible to the neutral fiber. When the tar layer was in the tank, the strings were tied to a weight at the bottom; after the run, they were used to lift the tar from the tank. Nonetheless, they must have increased the stiffness of the tar and, to some extent, must have altered its experimental behavior.

Thirdly, the insertion of very thin sheets into the syrup invariably distorted the sheets; in the case of the thinnest tar layer in the thickest syrup, the sheets were distorted irreparably.

The results from these rather crude experiments seem to show surprisingly good quantitative agreement with the theory, but a somewhat more elegant experiment might show more dramatic results. Particularly, an experiment that uses as the viscous medium a material of sufficiently high viscosity that it can be handled as a solid with the layer cast inside it might circumvent many of the difficulties encountered in these experiments. However, this method would lose the advantage of repeatability inherent in the present technique, in which the same layer can be deformed several times.

REFERENCES CITED

Biot, M. A., 1957, Folding instability of a layered viscoelastic medium under compression: Royal Soc. London Proc., ser. A, v. 242, p. 444–454

—— 1959a, On the instability and folding deformation of a layered viscoelastic medium in compression: Jour. Applied Mechanics, ser. E, v. 26, p. 393–400

—— 1959b, Folding of a layered viscoelastic medium derived from an exact stability theory of a continuum under initial stress: Applied Mathematics Quart., v. XVII, no. 2, p. 185–204

—— 1961, Theory of folding of stratified viscoelastic media and its implications in tectonics and orogenesis: Geol. Soc. America Bull., v. 72, p. 1595–1620

Filon, N. L., 1928, On a quadrature formula for trigonometric integrals: Royal Soc. Edinburgh Proc., ser. A, v. 49, p. 38–47

Saal, R. N. J., 1933, Determinations regarding the plastic properties of asphaltic bitumen: 1st World Petroleum Cong. (London) Proc., pt. II, p. 515–523

MANUSCRIPT RECEIVED BY THE SECRETARY OF THE SOCIETY, MAY 9, 1960

APPENDIX: EVALUATION OF THE INTEGRAL (2.7)

By putting

$$s = lh\,, \tag{A.1}$$

we can write the integral (2.7) as

$$\frac{w(x,t)}{b} = \frac{a}{h}\int_0^\infty \exp\left[\frac{-as}{h} + \frac{t}{t_1} f^{-1}(s)\right] \cos\left(\frac{sx}{h}\right) ds\,, \tag{A.2}$$

in which

$$f(s) = \frac{4\eta_1}{s\eta} + \frac{1}{3}s^2\,. \tag{A.3}$$

For a given value of t/t_1, the factor exp $[(-as/h) + (t/t_1) f^{-1}(s)]$, considered as a function of s, is replaced by straight-line intervals.

Equation (A.2) then becomes

$$\frac{w(x,t)}{b} = \frac{a}{h}\sum^{k} \int_{A_k}^{A_{k+1}} (a_k s + b_k) \cos\left(\frac{sx}{h}\right) ds$$

$$= \frac{a}{h}\sum^{k}\left[(a_k s + b_k)\frac{\sin(xs/h)}{x/h}\Bigg|_{A_k}^{A_{k+1}} + \frac{a_k}{(x/h)^2}\cos\frac{xs}{h}\Bigg|_{A_k}^{A_{k+1}}\right],$$

in which a_k and b_k are given for the interval. Because $a_k A_{k+1} + b_k = a_{k+1}A_{k+1} + b_{k+1}$, all but two terms due to the first bracketed term disappear; those also disappear, however, because $\sin(xs/h)/(x/h)$ tends to zero for s vanishing, and $a_k s + b_k$ tends to zero for k tending to infinity. Thus,

$$\frac{w(x,t)}{b} = \frac{a}{h}\sum^{k} \frac{a_k}{(x/h)^2} \cdot \left(\cos A_{k+1}\frac{x}{h} - \cos A_k \frac{x}{h}\right).$$

For small values of x, this expression has to be expanded into powers of x. The method used here for the computation of integrals of the type (A.2) was first proposed by Filon (1928).

R. L. KONIZESKI *U. S. Geological Survey, c/o Montana State University, Missoula, Mont.*

Paleoecology of an Early Oligocene Biota from Douglass Creek Basin, Montana

Abstract: Douglass Creek basin lies west of the Continental Divide in the northern part of the Rocky Mountain physiographic province. Numerous minor environmental differences exist between the Douglass Creek area and the Pipestone Springs and Canyon Ferry areas east of the Divide. In the 19th century, however, the three areas had identical mammalian species representation, although not equally dense populations.

Fossils of an early Oligocene biota have been collected from the Douglass Creek basin. Presence of all but one of the Douglass Creek mammalian species in the Pipestone Springs–Canyon Ferry early Oligocene fauna suggests that the three ancient ecosystems resembled each other in much the same way as the 19th century systems.

The early Oligocene deposits and biota of the Douglass Creek basin indicate a moist, temperate climate with seasonal variations. Sediment size and distribution suggest that the cross-valley relief was no greater than it is now. The fish and invertebrate faunas show that a shallow, hard-water lake existed in the area. The flora included a lowland, lake-border association and an upland coniferous forest. Although the ancient Douglass Creek biota doubtless included many species not represented in the fossil collections, most of the mammalian species are probably represented in the combined Douglass Creek, Pipestone Springs, and Canyon Ferry fossil assemblages. If so, the number of mammalian species was about the same as in the 19th century ecosystem.

CONTENTS

Introduction 1633
Acknowledgments 1634
Nineteenth century ecosystem 1634
Topography and climate 1634
Habitat zones and vertebrate fauna 1634
Physical geology 1634
Geologic history 1638
Early Oligocene biota and inferred climatological data 1638
Flora 1638
Invertebrate fauna 1639
Vertebrate fauna 1639
Early Oligocene ecosystem 1641
References cited 1642

Figure
1. Continental Divide and problem area 1635
2. Douglass Creek basin and section A–A′ . . . 1636
3. Generalized distribution of 19th century habitat zones, and inferred distribution of early Oligocene habitat zones 1637

INTRODUCTION

PURPOSE: This paper attempts to describe the interacting environmental and biotic systems peculiar to the Douglass Creek basin in early Oligocene time. A description of the 19th century Douglass Creek basin ecosystem and its relationships to those of Pipestone Springs and Canyon Ferry are included as a standard for comparison.

PROBLEM AREA: The Douglas Creek basin (Fig. 1), as here defined, includes the area of Tertiary deposition now drained by Douglass, Murray, Spring, Bear, Sturgeon, Sheep, and Morris creeks. The basin lies about 25 miles west of the Continental Divide on the northeastern slopes of the Garnet Range. It is roughly subcircular but trends northward through Tps. 11 and 12 N., R. 12 W., Powell County, Montana (Fig. 2). It covers about 20 square miles and slopes from an altitude of 5200 feet at its head to 4550 feet at the drainage exit. Irregular mountain slopes rise from a few hundred to more than 1000 feet above the basin and partly isolate it from the regional intermontane valley system. However, the basin is connected with the Clark Fork valley by a narrow canyon and with the Nevada Creek valley across low terraces a few hundred feet above the floor of the basin.

Geological Society of America Bulletin, v. 72, p. 1633–1642, 3 figs., November 1961

The Continental Divide, which lies between the Douglass Creek basin and the Canyon Ferry-Pipesone Springs areas, rises above 7000 feet along most of its extent between the regional eastern and western intermontane valley systems of the northern part of the Rocky Mountain physiographic province. However, its uniformity is interrupted by many passes (Fig. 1); Marias pass, about 100 miles north of the problem area, is the lowest at 5213 feet.

Pipestone Springs and Canyon Ferry are located in the valleys of the Jefferson and Missouri rivers, 65–70 miles from Douglass Creek basin and 20–30 miles east of the Continental Divide (Fig. 1). Valley-floor elevations range from 4550 to 5000 feet at Pipestone Springs and 3500 to 4000 feet at Canyon Ferry. Parts of early Oligocene biota have been collected from Douglass Creek basin by this writer; from Pipestone Springs by Burke (1936, p. 1), Donohoe (1956, p. 264), Douglass (1901, p. 238; 1908), Matthew (1903, p. 197), Reed (1954, p. 105); and from Canyon Ferry by Douglass (1903, p. 149) and White (1954, p. 395).

ACKNOWLEDGMENTS

The author did field work during the summers of 1955–1957; a grant from the Penrose Bequest of the Geological Society of America financed the work. The author expresses his thanks to the Society and to all who aided in the investigation, especially Dr. Philip L. Wright of the University of Montana for his advice on modern mammalian distribution, Dr. D. I. Axelrod of the University of California for his review of the Douglass Creek early Oligocene flora, Dr. D. W. Taylor and Mr. I. G. Sohn of the U. S. Geological Survey for invertebrate identifications and environmental interpretations, and Drs. J. R. Beerbower of Lafayette College and Frank A. Swenson of the U. S. Geological Survey for reviewing the manuscript.

NINETEENTH CENTURY ECOSYSTEM

Topography and Climate

Douglass Creek and its tributaries drain most of Douglass Creek basin. These streams have cut an asymmetrical system of inner valleys 50–75 feet below benchland-forming remnants of the ancient Douglass Creek basin Tertiary fill (Fig. 2). The benchlands extend over about 90 per cent of the basin. They slope gently away from the mountains toward the valley axis which dips north at about 40 feet to the mile.

The growing season in the valley averages about 70 days compared to 80 and 130 days at Pipestone Springs and Canyon Ferry (U.S. Dept. Agriculture, 1941, p. 955). Average annual precipitation is about 17 inches, compared to 12 and 11 inches at Pipestone Springs and Canyon Ferry in the rainshadow of the Continental Divide. The bottomlands of all three localities have a fairly persistent year-round water supply; the bordering benchlands are semiarid.

Habitat Zones and Vertebrate Fauna

Three major habitat zones apparently existed within the 19th century ecosystem (Fig. 3). An upland coniferous zone existed along the mountain slopes in all but the northeastern areas and extended into the valley along the upper courses of the principal drainages. A lowland, mesohydrophytic plant zone existed along the bottoms of the inner valleys. A benchland, xerophytic plant zone existed principally along the benchlands but also on the mountain slopes northeast of the basin.

A near approach to total-species representation of the 19th century Douglass Creek biota in some conjectural future fossil assemblage could be expected only if numerically large collections were made from each of these three zones. Forty genera of mammals, including 49 species, were represented. The mammalian distribution was determined from studies by Wright (1951 and personal communication); Anthony (1928); Burt *et al.* (1952); and from information given by early settlers, especially Mr. H. Morgan; and from the writer's observations. Despite the certainty of numerous minor environmental differences between the Douglass Creek and Pipestone Springs-Canyon Ferry areas, and the partial barrier to faunal migration interposed by the highlands along the Continental Divide, the same species apparently inhabited the three localities. It follows that similar or identical fossil vertebrate faunas could be expeced in the three areas if the ancient environments had been even as grossly similar as they are today.

PHYSICAL GEOLOGY

The highlands around Douglass Creek basin are formed mostly of Early Tertiary volcanic rocks, with some Mississippian limestone and Precambrian shale. Early Tertiary volcanic

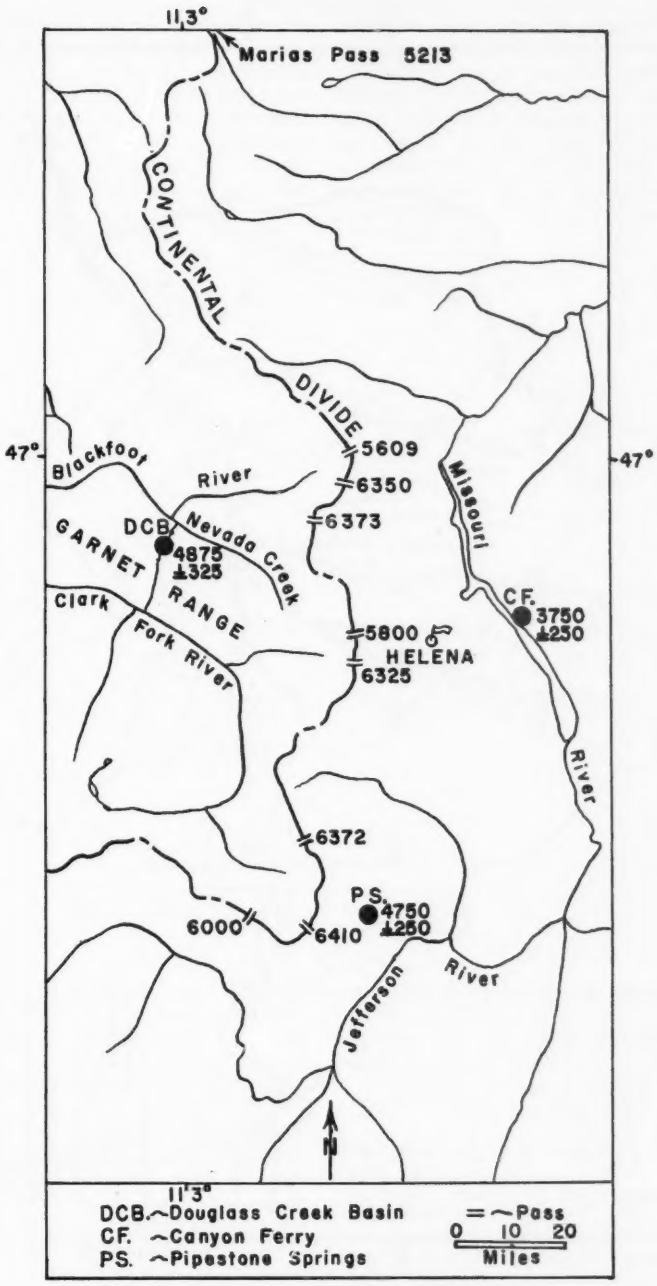

Figure 1. Continental Divide and problem area

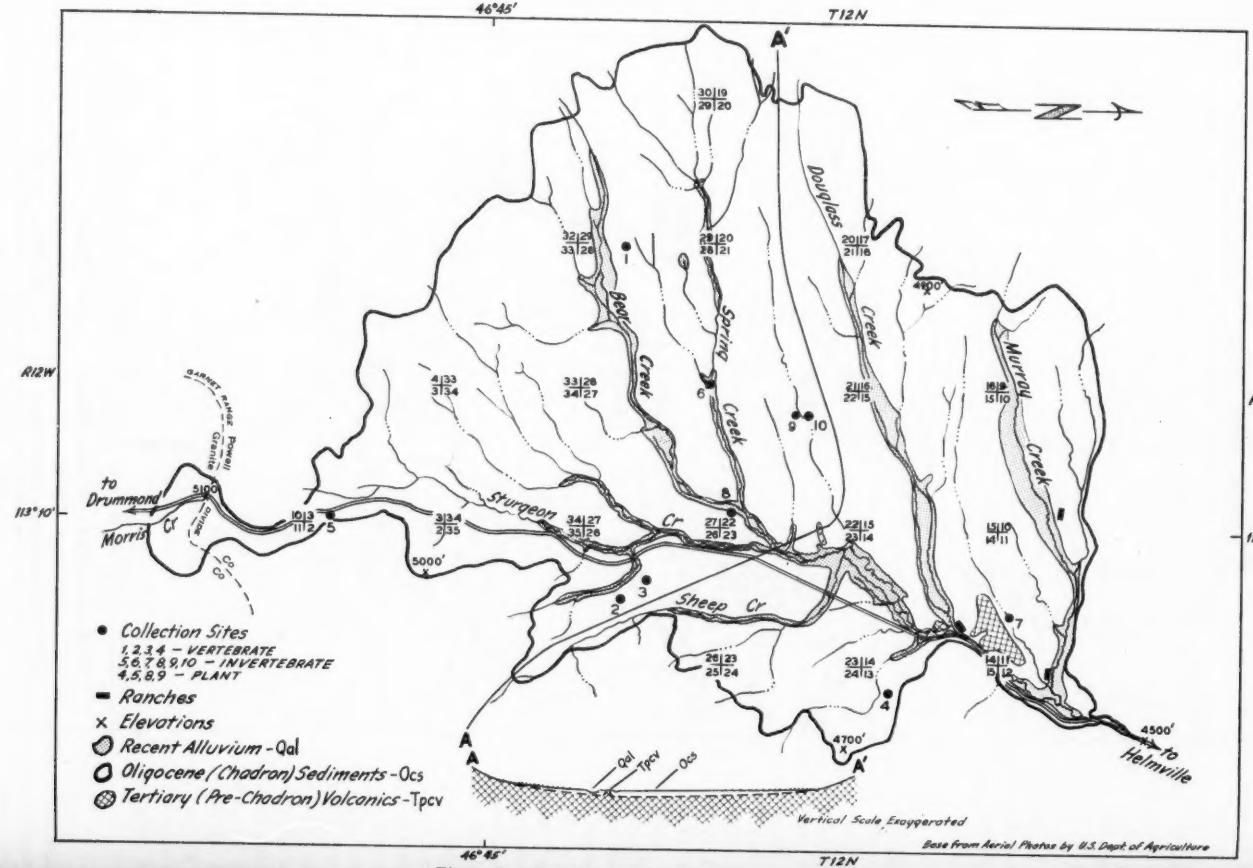

Figure 2. Douglass Creek basin and section A–A′

rocks also underlie Cenozoic fill within the basin, and local inliers are beveled to the surface profile (Fig. 2). The basin is partly filled with more than 200 feet of early Oligocene deposits. On the margins of the basin these are covered with a few feet of Pleistocene debris derived from adjacent mountain slopes. In the center of the basin they are covered by a thin soil.

basin, but some exposures show reverse dips of up to 15°. Local folding of the plant shale of locality 5 may be related to tectonics or to differential compaction. Field relationships indicate that plant shale occurs both above and below the principal mammal-bearing blocky-clay horizon. The bentonite-rich deposits have been greatly disrupted near the surface because of excessive expansion and

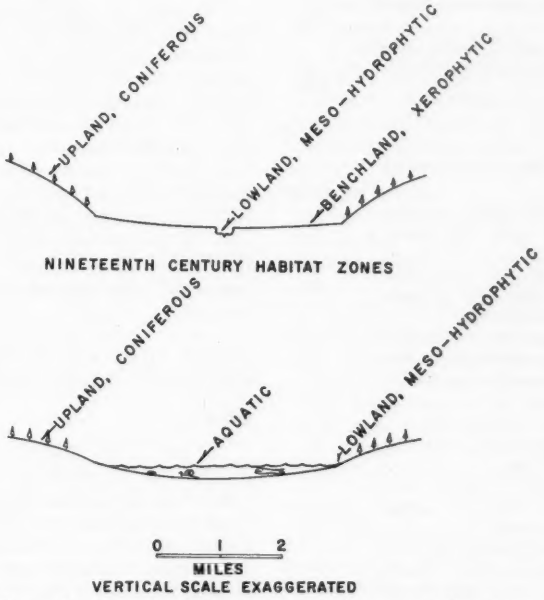

Figure 3. Generalized distribution of 19th century habitat zones, and inferred distribution of early Oligocene habitat zones

Near the margins of the basin the Oligocene deposits consist mostly of semiconsolidated blocky bentonitic clay (mammal clay) and laminated shale (plant shale) with a few thin beds of limestone and some thin lenses of gypsum. Forty feet of massive, marly limestone crops out near the center of the basin. Shale and clay are exposed locally. The thin limestone beds in the marginal areas may thicken toward the center of the basin, or central basin beds may underlie the visible marginal section. The central basin plant shale of locality 8 (Fig. 2) is apparently equivalent to that in locality 4 in the marginal section. The marginal beds generally dip 1°–10° toward the axis of the

contraction that resulted from alternating wet and dry periods. Because of this it is difficult to determine their intravalley relationships; the following section is tentative.

Tentative composite Douglass Creek basin Oligocene section

	Feet
Shale (plant shale), buff, laminated; contains plants, myriad ostracodes, few gastropods, pelecypods; best exposures at locality 5	35
Clay (mammal clay), cream when dry, greenish gray when wet, blocky, moderately indurated, expands when moist, crumbles on drying; constituents montmorillonite (95 per cent), quartz and	

Base from Aerial Photos by U.S. Dept. of Agriculture
T12N
46°45'
Figure 2. Douglass Creek basin and section A–A'

feldspar (5 per cent)[1]; contains vertebrates; best exposures at locality 3 . .	65
Limestone, buff to white, thin-bedded, ripple-marked, contains many gastropods, a few ostracodes; best exposures in second draw 1 mile north of locality 3 .	1
Shale, brown, similar to plant shale but bedding poor to moderate; contains few ostracodes	10
Clay, gray, blocky, bentonitic, similar to mammal clay but unfossiliferous . . .	3
Shale, gray, laminated	2
Clay, gray, blocky, bentonitic, similar to mammal clay	15
Limestone, light gray, marly, massive, contains gastropods; best exposures at locality 10	100
	231.0

Plant-shale section at locality 5

	Feet	Inches
Limestone, light gray, marly; contains fish scales and teeth, pelecypods, myriad ostracodes	1	3
Shale, chocolate brown, calcareous, laminated; contains two gypsum beds, myriads of ostracodes	1	6
Clay, olive, unctuous, bentonitic; constituents montmorillonite (90 per cent), gypsum (10 per cent), quartz (? per cent)	0	7
Shale, yellow brown; contains rare (1–2-inch) argillaceous beds and one (1-inch) gypsum bed	6	8
Limestone, light brown, marly, thin-bedded; contains abundant ostracodes, some gastropods	0	11
Shale, yellow brown, laminated; constituents mixed-layered (illite-montmorillonite) (85 per cent), calcite (13 per cent), quartz (1 per cent), gypsum (? per cent)	13	8
Shale, chocolate brown, laminated; contains plants, abundant ostracodes	1	0
Limestone, chocolate brown, marly, petroliferous	0	3
Limestone lens, yellow brown . . .	0	4
Shale, ferruginous, thin-bedded . . .	0	7

(Total section 25 feet, 11 inches)

GEOLOGIC HISTORY

The writer suggests that the history of the area was as follows:

(1) Extrusion of pre-Oligocene, early Tertiary volcanic rocks

(2) Development of the ancestral Douglass Creek basin by erosion and/or diastrophism

(3) Ponding of the ancient Douglass Creek with concomitant submersion of the basin and deposition of early Oligocene sediments

(4) Initiation of a new erosional cycle accompanied by pedimentation of Douglass Creek basin sediments and pre-Oligocene inliers

(5) Deposition of Pleistocene debris along the margins of the basin

(6) Slight eastward tilting of the basin and initiation of modern inner valley system.

The inliers of early Tertiary volcanic rocks show that the initial, pre-Oligocene floor of Douglass Creek basin was very irregular, in contrast to the modern profile. The fine-grained, bentonitic, Oligocene sediments indicate that relief in the immediate area was low and that explosive volcanism occurred intermittently in adjacent areas. The sediment distribution shows that an early Oligocene lake, here named Lake Douglass, existed. The water in the lake was hard, as is indicated by the beds of limestone near the center of the basin and calcareous silt and clay along its margins.

EARLY OLIGOCENE BIOTA AND INFERRED CLIMATOLOGICAL DATA

Flora

The plant shale of locality 5 is best exposed in road cuts immediately north and downvalley from the Garnet Range Divide (Fig. 2). Plant material is present throughout much of the exposed section. Some fragments occur in the tailings of animal burrows in the bentonitic shale of localities 8 and 9. A single specimen was noted in the calcareous clay of locality 4. Owing to the large coefficient of expansion of bentonite, the highly bentonitic plant shale swells and contracts excessively upon alternate wetting and drying. Because of this, identifiable plant specimens were obtainable only in recently exposed, relatively unweathered outcrops, notably the roadcuts of locality 5. Eleven species were found, six of them common to the early or middle Oligocene Florissant flora of Colorado (MacGinitie, 1953, p. 167)[2]. Dr. D. I. Axelrod (personal communication) describes the Douglass Creek basin collection as follows:

"The material from the Douglass Creek section . . . is quite scrappy and not easy to evaluate be-

[1] Figures obtained by X-ray analyses of single specimens by R. I. Smith, Butte School of Mines, and Dr. J. Hower, Montana State University

[2] Numerous specimens of *Typha* sp. (cattail) have since been collected.

cause most of it is not well preserved. The collection appears to include the following plants:

Fossil species	*Similar living species*
EQUISETACEAE	
Equisetum sp.	*E.* spp.
PINACEAE	
Pinus cf. *florissanti*	*P. ponderosa* (group)
Picea magna	*P. neoveitchii*
TAXODIACEAE	
Sequoia affinis	*S. empervirens*
CYPERACEAE	
Cyperacites sp.	*Cyperus*
SALICACEAE	
Populus heeri (?)	*P. angustifolia*
Salix venosuiscula	*S. caudata*
Salix taxifoloides	*S. exigua* (group)
FAGACEAE	
Quercus predayana	*Q. chrysolepis*
ULMACEAE	
Ulmus tenuinervis	*U. divaricata*
ACERACEAE	
Acer arida	*A. grandidentatum*

"This assemblage is chiefly a lake-border association, as shown by the presence of *Equisetum*, *Cyperacites*, *Salix* and *Populus*. The nearby slopes supported a conifer forest of *Pinus*, *Picea* and *Sequoia*, with associates of *Acer*, *Quercus* and *Ulmus*. Several poorly preserved angiosperms that cannot be determined may also represent a part of the forest community.

"Since the collection is so small, and is not an adequate sample, it is difficult to infer any of the details of climate in the region. No doubt climate was temperate, but whether it was warm temperate like Florissant (as the oak and elm suggest), with a number of types in it whose nearest relatives now occur in Mexico, is not now known.

"Rainfall was distributed in summer and winter, and was not less than 30 to 35 inches. Winters appear to have been comparatively mild, but the frequence of frost or snow cannot be determined from the material at hand."

Invertebrate Fauna

I. G. Sohn, of the U. S. Geological Survey, has identified two species of ostracodes, *Candona sp.* and *Cypridopsis*(?) and noted a large, smooth unidentifiable form; all three are abundant in the plant shale of locality 5. They are present in lesser, varying, amounts throughout much of the section, excepting the mammal-bearing blocky clay and some of the calcareous and gypsum lenses. Little is known about the North American nonmarine Oligocene ostracodes. The modern species seem to have wide ecological valences, tolerating, in general, the normal ranges of temperature and water chemistry. Most species occur in water less than 1 m deep.

Dr. Dwight W. Taylor, of the U.S. Geological Survey, has identified *Lymnaea* n. sp., *Hippeutis*(?) n. sp., and *Biomphalaria* cf. *B. pseudoammonia* (Scholotheim); and noted several unidentifiable species of fresh-water gastropods. Dr. Taylor notes, "The species suggest quiet, shallow water, such as the borders of streams, oxbow lakes, ponds, etc. The bodies of water in question were probably perennial, but may have dried up in part during some of the year." Specimens were most abundant in the central valley limestone and marl of locality 10 and were much less abundant in the plant shale of locality 5. None were found in the mammal-bearing blocky clay or the calcareous and gypsum lenses.

Modern fresh-water pulmonate gastropods have attained worldwide distribution and are known at elevations up to 18,000 feet above sea level. Most species and individuals occur in water less than 3 m deep. Perennially cold bodies of water and bodies with a continuous temperature of more than 30°C contain few species and individuals. Pennak (1953, p. 145) states "It is generally true that soft waters contain few species and individuals, while hard waters contain many species and individuals." This writer noted that the maximum number of early Oligocene specimens in the Douglass Creek basin occured in the calcareous parts of the section.

A single, unidentified pelecypod was collected from the plant shale of locality 5.

Vertebrate Fauna

Unidentifiable fish teeth and spines are numerous in the plant shale of locality 5. Twenty-nine specimens of a single species of lizard and 12 species of mammals were collected from early Oligocene (mammal-clay) beds in the marginal areas of the valley (Fig. 2). Only one specimen was found in the central valley beds. Most of the fossils are so fragmentary that specific identification is difficult.

Douglass Creek basin local fauna

Class OSTEICHTHYES
Subclass ACTINOPTERYGII
Superorder TELEOSTEI

Uncatalogued teeth, spines, and scales collected from locality 5

Class REPTILIA
Order SQUAMATA
Suborder SAURIA
Family ANGUIDAE
Glyptosaurus sp.

C[hicago] N[atural] H[istory] M[useum] PR 401, dermal scute; collected from locality 3

Class MAMMALIA
Order INSECTIVORA
Family SOLENODONTINAE
Apternodus Mediaevus Matthew

CNHM PM 3832, left mandible with P_3–M_3 and lacking anterior parts, coronoid, angular, and condyles; collected from locality 3

CNHM PM 3833, left mandibular fragment with P_4M_1; collected locality 3

Order RODENTIA
Family ISCHYROMIDAE
Titanotheriomys?

CNHM PM 3834, symphysial region of lower jaws with proximal parts of incisors; collected from locality 3

Family APLODONTIDAE

CNHM PM 3831, 3830, left P_4–M_2 and right M_2 in mandibular fragments; collected from localities 2 and 3. These specimens are from aged individuals, and the teeth are worn nearly to the roots. Donohoe (1956) describes a Pipestone Springs form, "*Pipestoneomys bisulcatus*," as the only known Oligocene aplodontid. Unfortunately its lower dentition is unknown, and its specific relationships to the Douglass Creek basin specimens are at present indeterminate.

Family EOMYIDAE
Paradjidaumo minor Douglass

CNHM PM 3835, 3836, right M_1M_2, and right M_1 in mandibular fragments; collected from locality 3

Order CARNIVORA
Family CANIDAE
Hesperocyon paterculus Matthew

CNHM PM 3828, 3843; right mandibular fragments with P_3–M_1, and P_2–M_1; collected from localities 1 and 3. These specimens agree in tooth pattern with the Canyon Ferry form described by White (1954, p. 416) but are slightly smaller.

Order PERISSODACTYLA
Family EQUIDAE
Mesohippus sp.

CNHM PM 3816, 3825, 3819, 3824, 3826, 3821, 3823, 3820, 3818, 3822, 3817, 3827, right M_1, left P^2 badly worn with protoloph, metaloph; collected from locality 2; left P_2, M_1, M_2, right M_1, M_1, M_2, P_2, collected from locality 3, right P_4, right M_1, collected from locality 4.

Stirton (1940, p. 169) notes "*Mesohippus* and *Miohippus* are very closely related and cannot be differentiated by individual teeth." These specimens are referred to *Mesohippus* by reason of their stratigraphic position.

Family BRONTOTHERIIDAE

CNHM PM 3829, tooth fragments; collected from locality 2

Family RHINOCEROTIDAE
Caenopus cf. *C. mitis* Cope

CNHM PM 3844, partial right P^2 with protoloph, metaloph, and adjacent areas of ectoloph; collected from locality 3. This specimen compares closely with *C. mitis* but is slightly smaller. *C. mitis* A.M.N.H. No. 6325, P^2 ant.-post. = 18mm, *versus* CNHM PM 3844 = 16mm.

Order ARTIODACTYLA
Family AGRIOCHOERIDAE
Agriochoerus sp.

CNHM PM 3841, 3842, left ungual phalanx, talonid lower left M_3; collected from locality 3

Family HYPERTRAGULIDAE
Leptomeryx cf. *C. evansi* Leidy

CNHM PM 3837, 3838, left P_4–M_1, M_1–M_2 in mandibular fragments, collected from locality 3

Leptomeryx? sp.?

CNHM PM 3839, 3840, Talonid of right lower M_3, left M_1; collected from locality 3. These specimens are about 50 per cent larger than *L. evansi* and are certainly specifically if not generically distinct. They compare closely with several undescribed Pipestone Springs specimens in the collections of the Chicago Natural History Museum.

Leptomeryx sp.?

Uncatalogued, (A)-left M_1–M_2, (B)-P_4–M_1, in mandibular fragments; collected from localities 2 and 3. Unfortunately these specimens have been misplaced. They are included in the faunal list for completeness and because of their relatively small size.

Measurements of teeth of *L. Evansi* (in mm):

	Princeton Museum no. 12,962	Douglass Creek (A)	Douglass Creek (B)
P^4 ant.-post. diam.	6.0	..	5.5
P^4 trans. diam.	3.0	..	3.0
M_1 ant.-post. diam.	7.0	5.5	6.0
M_2 ant.-post. diam.	7.0	6.0	..
M_1 trans. diam.	5.0	4.5	5.0
M_2 trans. diam.	5.0	4.5	..

The detail in which the early Oligocene Douglass Creek basin ecosystem can be described depends largely on the completeness of representation of the ancient biota. One method of approximating complete species representation of the vertebrate fauna, which must be used judiciously, is by comparison with the stratigraphically and supposedly ecologically equivalent Pipestone Springs and Canyon Ferry faunas. White (1954, p. 429) describes the Pipestone Springs and Canyon Ferry areas as being close both geographically and ecologically and ascribes any faunal differences between them to accidents of preservation. The early Oligocene deposits in those localities and in the Douglass Creek basin are generally of the finer grades. This is in accordance with the commonly held concept of relatively low mid-Tertiary Rocky Mountain

relief (Van Houten, 1952, p. 74, 78, Table 1). On this basis it appears likely that the highlands along the Continental Divide were no greater barriers to faunal migration then than they are now and that mammalian species representation was about equivalent in the intermontane valleys on both sides of, and adjacent to, the Divide.

Although the probability of complete species representation of a prehistoric fauna is a function of many variables, it increases with the numerical size of the fossil assemblage. A conservative estimate of the total number of specimens collected by professional and amateur paleontologists from the Canyon Ferry and Pipestone Springs localities would be on the order of several thousand. Two species of lizard; a snake; and 37 genera (including 43 species) of mammals are recorded. Twelve of the 13 Douglass Creek species of vertebrates, omitting the fish, are common to the Pipestone Springs-Canyon Ferry early Oligocene fauna, at least at their known levels of classification. It appears then, on the basis of analogies drawn from the modern ecological relationships, that the three ancient ecosystems were at least grossly similar, and that the combined fossil assemblages probably approach complete species representation of the ancient vertebrate fauna.

EARLY OLIGOCENE ECOSYSTEM

Numerical and specific inadequacies of the fossil record detract materially from the degree of accuracy and refinement of detail obtainable in the following description of the ancient Douglass Creek basin ecosystem. On the other hand, the validity (and value) of the description is greatly enhanced in that it is based on a variety of geological, biological, and ecological data.

The early Oligocene climate was temperate as shown by the flora and probably varied seasonally as indicated by the laminated bedding in the plant shale. The winters were quite mild compared to the present. Rainfall was approximately double the present amount with at least 30 inches annually and was distributed in both summer and winter.

The waters of ancient Lake Douglass lay over most of the area now incorporated in the floor of the basin. The inliers of early Tertiary volcanic rocks may have formed small islands in the northern part of the lake. The limestone facies shows that the water was relatively hard. The invertebrate fauna suggests that the climate was temperate and that the water averaged no more than 3 or 4 m deep. Aquatic life included fish, at least one species of pelecypod, an abundance of numerous species of gastropods, and myriads of ostracodes.

The terrestrial part of the ancient ecosystem was confined to the marshland adjacent to the lake as indicated by the cattails, and to the surrounding mountain slopes. The early Oligocene Pipestone Springs, and by inference Canyon Ferry, fossil assemblage has been described as representative of a montane woodland habitat in contrast to a savannah or open plains environment (Russell, 1952, p. 94; White, 1954, p. 429). In view of its proximity and similar biological composition, the Douglass Creek basin may be assumed to have had a grossly similar habitat. However, the fineness of the sediments indicates that cross-valley relief was relatively low, probably no greater than it is now. Because of this, erosion of the highlands marginal to Lake Douglass was relatively slow and was apparently a function of chemical as well as mechanical weathering.

The bulk of the lake sediments consisted of the finer grades of volcanic ejecta, clay, silt, and carbonates. Silt, bentonitic clay, and minor amounts of carbonate were deposited in the near-shore localities, marly lime in the offshore areas. Small amounts of silt and sand were deposited in areas of maximum current flow.

Floral distribution in the valley was then, as it is now, a function of water supply, topography, and substrate. The flora included both an upland coniferous forest and a lowland-lake border association. Because of the relatively low cross-valley relief and the shallowness of the lake, its marginal areas were probably comparable to the lowland, mesohydrophytic 19th century habitat zone. Mammalian-species representation was numerically similar to that of the 19th century fauna, *i.e.*, about 37+ genera including 43+ species, as contrasted to 40 genera and 49 modern species. Because of the likelihood of sample error, the discrepancy is perhaps less than indicated by these data, and may be a positive rather than a negative figure.

Many individuals of the ancient biota died near or along the lake margins, and their remains were preserved in near-shore deposits. A few were carried by currents into the central part of the lake and were buried there. The remains of those individuals that died on the marginal highlands were mostly destroyed by weathering and erosion.

REFERENCES CITED

Anthony, H. E., 1928, Field book of North American mammals: New York, G. P. Putnam's Sons, 625 p.

Burke, J. J., 1936, *Pseudocylindrodon*, a new rodent genus from the Pipestone Springs Oligocene of Montana: Carnegie Mus. Annals, v. 25, p. 1–4

Burt, W. H., *et al.*, 1952, A field guide to the mammals: New York, Houghton Mifflin Co., 200 p.

Donohoe, J. C., 1956, New Aplodontid rodent from Montana Oligocene: Jour. Mammalogy, v. 37, p. 264–279

Douglass, E., 1901, Fossil Mammalia of the White River beds of Montana: Am. Philos. Soc. Trans., new ser., v. 20, p. 237–279

—— 1903, New vertebrates from the Montana Tertiary: Carnegie Mus. Annals, v. 2, p. 141–199

—— 1908, Fossil horses from North Dakota and Montana: Carnegie Mus. Annals, v. 4, p. 267–277

MacGinitie, H. D., 1953, Fossil plants of the Florissant beds, Colorado: Carnegie Inst. Washington Pub. 599, 198 p.

Matthew, W. D., 1903, The fauna of the Titanotherium beds of Pipestone Springs, Montana: Am. Mus. Natl. History Bull., v. 19, p. 197–226

Pardee, J. T., 1913, Coal in the Tertiary lake beds of southwestern Montana: U. S. Geol. Survey Bull. 531, p. 229–244

Pennak, R. W., 1953, Fresh water invertebrates of the United States: New York, Ronald Press Co., p. 1–769

Reed, C. A., 1954, Some fossorial mammals from the Tertiary of western North America: Jour. Paleontology, v. 28, p. 102–111

Russell, L. S., 1952, Mammalian fauna of the Kishenehn Formation, southeastern British Columbia: Canada Natl. Mus. Bull. 132, p. 92–111

Stirton, R. A., 1940, Phylogeny of North American Equidae: Univ. Calif. Dept. Geol. Sci. Bull., v. 25, no. 4, p. 165–198

U. S. Dept. Agriculture, 1941, Climate and man: U. S. Govt. Printing Office, 1248 p.

Van Houten, F. B., 1952, Sedimentary record of Cenozoic orogenic and erosional events, Big Horn Basin, Wyoming: Wyo. Geol. Assoc. Guidebook 7th Ann. Field Conf., p. 74–79

White, T. E., 1954, Preliminary analysis of the fossil vertebrates of the Canyon Ferry Reservoir area: U. S. Natl. Mus. Proc., v. 103, no. 332, p. 395–438

Wright, P., 1951, Check list of the Recent mammals of Montana: Mont. Acad. Sci. Proc., v. 10, p. 47–50

MANUSCRIPT RECEIVED BY THE SECRETARY OF THE SOCIETY, JANUARY 11, 1960

JOHN W. HUDDLE *U. S. Geological Survey, Washington 25, D. C.*
SAM H. PATTERSON *U. S. Geological Survey, Beltsville, Md.*

Origin of Pennsylvanian Underclay and Related Seat Rocks

Abstract: Seat rocks, including underclay, underlie coal beds and show features such as roots, profiles similar to water-logged soils, lack of bedding, soil-like fracture, and gradation into normally bedded sedimentary rocks indicating that they were once soils. Coarse-grained seat rocks range from argillaceous to nearly pure quartz sandstone (ganister). Seat rocks composed of clay-sized particles (underclays) range from mixtures of illite, mixed-layer clay, and kaolinite to essentially pure kaolinite. Variations in the quartz or kaolinite content suggest that there are degrees of alteration in the formation of a seat rock and that all kinds of seat rock were formed by leaching of the substratum in a swamp. The increasing crystallinity of the clay minerals from plastic underclays to semiflint clay to flint clay and the corresponding increase in titanium support this conclusion. These two features suggest strongly that flint clays formed in place in an acidic swamp environment. The Olive Hill clay shows residual acidity. Seat rocks are affected by the chemical environments in the swamp before peat accumulation, during peat accumulation, and during coalification. Kaolinite is forming in present-day swamps and in wet acidic soils in Hawaii and probably formed in late Paleozoic swamps. The facts can be interpreted to show that all kinds of seat rocks could have formed in Pennsylvanian swamps and probably most did.

CONTENTS

Introduction 1643
Evidence relating to theories of origin 1645
General statement 1645
Association of coal beds with seat rocks . . . 1645
Time of formation of seat rock and partings and accumulation of peat 1646
Underclays and other seat rock as the geologic record of soils 1647
Nonbedding and slickensides 1649
Leaching 1650
Formation of kaolinite in a water-logged environment 1651
Plastic, flinty, and diaspore-bearing underclays as successive stages in the alteration of bedrock by the same process 1652
Concentration of high purity kaolin in Lower Pennsylvanian underclays. 1653
Similarity of plastic underclays to Pennsylvanian shales 1655
Leaching of quartz and feldspar in underclays . 1655
Titanium in underclays. 1656
Shapes of underclay deposits 1656
Formation of kaolinitic seat rocks 1658
Summary 1658
References cited 1658

Figure
1. Cross section of a petrified root of *Stigmaria ficoides* Brongniart from a Pennsylvanian coal bed, Leslie County, Kentucky . . . 1648
2. Slice cut from petrified peat (coal ball) from Pennsylvanian coal bed, Leslie County, Kentucky 1649
3. Thickness map of the Olive Hill bed, Haldeman quadrangle, Kentucky 1654
4. Diagrammatic representation of deposition in modern swamps 1656

Table Facing
1. Chemical analyses of underclay, Pennsylvanian shales, kaolinite, and diaspore 1656

INTRODUCTION

The origin of underclay has aroused considerable interest. Keller, Wescott, and Bledsoe (1954) worked on the Cheltenham underclay in Missouri; McMillan (1956) dealt with the plastic Nodaway underclay of Kansas; McConnell, Levinson, and de Pablo-Galan (1956) dealt with the mineralogy of several underclays in Ohio described by Stout (1923); Patterson and Hosterman (1960) investigated the Olive Hill bed of Kentucky; and Erickson (1958) studied the Mercer bed of Pennsylvania. Hoehne (1957) considered claystone partings

Geological Society of America Bulletin, v. 72, p. 1643–1660, 4 figs., November 1961

in coals from Germany, the United States, and other parts of the world. Schultz (1958) studied underclays of the Midcontinent, Illinois, and Appalachian basins and presented excellent mineralogical data; however, he concentrated on plastic underclays, dealing only briefly with the flint clays and semiflint clays that are of primary interest to those working in Missouri, Kentucky, and Pennsylvania. All these papers are important contributions to Pennsylvanian stratigraphy, ecology, and petrology. The differences of opinion expressed as to the origin of underclay result from slightly different definitions of terms, different emphasis on mineralogical and stratigraphic data, and different approaches because of experience and areas of field work. This paper presents an opinion on the origin of seat rock based principally upon field work in the Appalachian basin and a review of the literature.

Rocks similar in many respects to underclays but composed of silt- or sand-sized particles underlie coal beds in many places. Very little information is available regarding the geology, mineralogy, and petrology of these seat rocks composed of silt-sized and coarser grains. Underclay has received greater emphasis because it is more common, has economic value, and is more amenable to environmental interpretation. Coarser-grained seat rocks are closely associated with underclay, and any theory of origin that fails to consider important evidence in them is incomplete. The existence of seat rocks ranging in grain size from clay to coarse sand indicates that they developed from a wide variety of materials.

R. E. Grim, W. D. Keller, L. G. Schultz, E. S. Erickson, T. A. Hendricks, J. W. Hosterman, Linn Hoover, J. M. Schopf, H. A. Tourtelot, E. D. Patterson, W. V. Searight, and R. M. Foose have read the paper. We are grateful for their criticisms, which have improved the manuscript. We are responsible for the conclusions, and not all the readers agreed with them.

The following definitions are used in this paper.

Seat rock: a rock normally underlying a coal bed with physical characteristics suggesting that it served as a soil. It is generally composed of clay-, silt-, or sand-size particles but may be limestone, black shale, or some other rock type. Commonly it is nonbedded, slickensided, or irregularly fractured, and it may have traces of roots and an accumulation of iron or calcium compounds (generally siderite, pyrite, and calcite) near the base. Many seat rocks are bleached, but a few are dark gray or brown and show no bleaching, especially when fresh. The typical bleaching, characteristic weathering, and peculiar fracture of most seat rocks are commonly recognizable regardless of grain size or mineral composition and indicate that all seat rocks are related in origin. Seat rocks are generally thin, ranging from a few inches to a few feet in thickness, but exceptionally they are as much as 30 feet thick. Seat rocks commonly grade laterally or downward into other sedimentary rocks. For example, some underclays grade laterally and vertically into sandstone, siltstone, limestone, black shale, and coal, and in the Conemaugh and Monongahela formations of Pennsylvanian age seat rocks grade laterally into red beds (Waagé, 1950, p. 47–48).

Seat rocks vary from sandstones and siltstones consisting essentially of pure quartz (called ganister, especially in European literature) through sandy, silty, and argillaceous rocks to essentially pure kaolinite. A complete gradation in grain size and mineral composition exists between seat rocks composed of sandstone and those of plastic or flint clay. Most plastic underclays consist of mixtures of illite, kaolinite, and quartz with subordinate amounts of mixed-layer clays and chlorite. Most flint clays consist mainly of kaolinite with small amounts of illite and mixed-layer clays, but a few are essentially pure kaolinite. Feldspar locally is present in plastic underclays but seems to be absent in semiflint, flint, and diaspore clays. The kaolinite minerals in flinty underclays are well crystallized, those in plastic underclays show a lesser degree of crystallinity (Schultz, 1958, p. 367, 384; Keller, Wescott, and Bledsoe, 1954, p. 19; McConnell, Levinson, and de Pablo-Galan, 1956, p. 279), and those in semiflint clays show intermediate degrees of crystallinity (Patterson and Hosterman, 1960).

Underclay: a seat rock composed mainly of clay minerals that is generally nonbedded, slickensided, associated with a coal bed, fractures irregularly, and contains traces of plant roots and concentrations of iron or calcium compounds in the lower part.

Kaolin: a rock term; kaolinite is used as a mineral term.

Soil: an earth material so modified by physical, chemical, and biological agents that it will support rooted plants (Howell, 1957, p. 272).

ECONOMIC IMPORTANCE OF SEAT ROCKS: Underclays are used in a number of ceramic

products. They furnish all but a very small percentage of the fire clay and stoneware clay sold in Illinois, Indiana, Kentucky, Maryland, Missouri, Ohio, Pennsylvania, and West Virginia. Gunsallus and Blankenbaker (1956, p. 338) valued this clay in these states in 1953 at $40,314,640. In general, the value of an underclay depends on its purity and alumina content, which in turn, govern its refractory properties. Accordingly, boehmite- and diaspore-bearing clays and essentially pure kaolinite underclays are in demand by the refractory industry. Plastic underclays are used chiefly for ceramic products for which low or moderate refractory properties are needed. In a few places ganister has been used for silica brick and silica sand, but most of the medium- and coarse-grained seat rocks have little value.

EVIDENCE RELATING TO THEORIES OF ORIGIN

General Statement

Geologists have differed on whether underclays formed within or without the basin of deposition ever since Logan (1842, p. 275–276) concluded that stigmarian rootlets in underclays indicated a close relationship to the coals and that underclays represent ancient soils. McMillan (1956, p. 203–207) and Greaves-Walker (1939, p. 10–20) summarized the history of the controversy. Recent arguments, especially among clay mineralogists, have concentrated on whether kaolinite in underclays formed within or without the basin. Some investigators (Schultz, 1958; Erickson, 1958) interpret the information from clay-mineral studies to indicate that the clays were formed outside the basin of deposition and that certain characteristics of the clays result from sedimentary winnowing processes. Schultz (Written communication, 1959) considers this origin applicable to only the plastic clays. Erickson, following in general Stevenson's (1913, p. 396) idea for certain clay deposits, suggests that the material high in aluminum was brought into the basin in a "colloidal" or "nonmineral" state and precipitated as gel-like deposits in swamps. Other students of clay minerals in underclays (Keller, Wescott, and Bledsoe, 1954; Keller, 1956; McMillan, 1956; Patterson and Hosterman, 1960), following Stout (1923), believe that the clays underwent varying degrees of alteration in swamps and that there was nothing extraordinary about the sediment at the time it was introduced into the basin of deposition.

The principal arguments for or against the formation of minerals, physical characteristics, or seat rocks in a swamp rather than in an upland area are discussed in subsequent paragraphs.

Association of Coal Beds with Seat Rocks

Mammatt (1834) recognized the common association of coal beds with seat rocks, usually underclays. This association represents part of the well-known cyclic pattern of Upper Paleozoic sedimentation (Weller, 1930). Locally either seat rock or coal may be present without the other, but if one were to trace the unit laterally, he would almost invariably find the missing unit. Wheeler and Murray (1957, p. 2002; *in* Weller, Wheeler, and Murray, 1958, p. 445) cite the Dry Wood and Riverton coal beds in southeastern Kansas as examples of coal beds without underclays, but Weller (*in* Weller, Wheeler, and Murray, 1958, p. 442–446) and Searight (1955, p. 9, 11, 14, 18) disagree. Such differences of opinion may be due to different criteria for recognition of seat rocks and differences in the definition of underclay, especially the amount of admixed sand or silt allowed, and whether or not the presence of stigmarian rootlets is required. Coal beds formed from plant debris transported from the site of growth might lack a subjacent seat rock locally, but even these, if they are extensive, should be associated with ancient soils. Each local or regional absence of coal beds or seat rocks requires explanation. Such explanations include lack of formation, subsequent removal by erosion, sliding, flowage, or decay.

A common argument against the close genetic relationship of coal and seat rock is the lack of a consistent relationship between the thickness of a coal bed and the thickness and quality of the underclay. Stout (1923) regarded this as expectable, if peat accumulation immediately followed underclay formation in the same swamp. Stout argued convincingly against the ideas that all underclays were formed contemporaneously with the accumulation of peat and that the alteration was due to leaching by the same plants as those preserved in the coal and swamp-water acids. He pointed out that if underclay formed in this manner the purest clay should be at the top and should grade downward into shale, and that the thickest and most refractory deposits should be under the thickest coals. This is not the case. The highly kaolinitic Olive Hill fint clay of Kentucky (Crider, 1913; Patterson and Hosterman, 1960)

and the Sciotoville flint clay of Ohio (Stout, 1923), and the diaspore-bearing clay of the Mercer bed of Pennsylvania (Galpin, 1912, p. 314–315), all underlie thin coal beds generally less than 6 inches thick. Only very local and thin coals are associated with the Cheltenham clay bed of Missouri. However, most coals, especially thick coal beds, are associated with plastic underclays containing a large proportion of clay minerals other than kaolinite. This suggests that peat and kaolinite formation are partially exclusive processes, and that normally kaolinite forms before peat.

Time of Formation of Seat Rocks and Partings and Accumulation of Peat

Logically, peat rock could have formed long before, immediately preceding, or concurrently with peat. Weller (1931, p. 174–175; 1956, p. 31) and Schultz (1958) argue for formation by long-continued weathering before the accumulation of peat. Stout (1923, p. 545) argues for accumulation immediately preceding the accumulation of peat. Many geologists since Logan (1842) have argued for concurrent formation. Weller's (1931, p. 174–175) arguments were:

(1) No relationship exists between the thickness of underclay and the associated coal.

(2) Underclays at certain horizons are extensive without overlying coal beds.

(3) Coal beds are not invariably underlain by underclays.

(4) Underclays and coals are locally unconformable.

These are not convincing arguments for the formation of all underclays by long-continued weathering before peat accumulation. The normal superposition of coal beds over seat rocks suggests that generally seat rocks formed shortly before or occasionally contemporaneously with the accumulation of peat. Certainly seat rocks were deposited before the overlying coal, and the real problem is to determine when the peculiar characteristics of the seat rock were acquired and where the highly kaolinitic clays formed, within or without the basin. The association of highly kaolinitic clays with thin coals suggests that these clays formed mainly before any real accumulation of peat.

Local seat-rock partings in coal beds indicate that some seat rock formed contemporaneously with peat elsewhere in the same swamp area, but they do not indicate that the two formed at the same time in one place. Most partings are clay or shale; some partings are flint clay, siltstone, and sandstone. Many partings contain leaves or stigmarinan roots, and some contain both. The plant roots may have invaded the partings before or up to a short time after peat formation began again. These partings probably served as a soil for only a very short time, possibly supporting only a single generation of plants, as did the slightly altered seat rocks underlying coal beds. As Stout (1923, p. 547) pointed out, the formation of underclay and the accumulation of peat require opposite chemical conditions in the swamp, one oxidizing, the other reducing, but neither underclay nor peat is the product of only one chemical environment, and both show the effects of changing environments. Although locally these environments succeeded one another, regionally they may have been contemporaneous. Stout (1923, p. 535) and other authors have pointed out that even the most extensive coal beds, such as the Pittsburgh, Kittannings, Freeport, Cedar Grove, Fire Clay, Herrin, and Harrisburg coal beds, vary greatly in thickness. Either they were not deposited in a single swamp or there were local areas in the swamp where peat was not accumulating but seat rocks were forming (Stevenson, 1913, p. 379–385; Stout, 1923, p. 534–536). The pockety nature of the highly kaolinitic clays is even more apparent than that of the coals.

Most partings are local, but a few are widespread, such as the benches in the Pittsburgh coal in the main part of the Appalachian basin, the "blue band" of the Herrin coal of the Eastern Interior basin, and the flint-clay parting in the Fire Clay coal of Kentucky, Tennesee, Virginia, and West Virginia. The blue band and the partings in many other coal beds are best explained by assuming that peat deposition ceased long enough for several inches of clay to accumulate (perhaps a large flood) and to be somewhat altered by mildly oxidizing conditions and by plant growth. The flint-clay parting in the Fire Clay coal bed is more difficult to explain. This parting, while extensive, is not present everywhere, nor is it uniformly thick. Its position in the coal bed varies, but it is generally in the lower third, and in some areas the flint clay has no coal above or below it. Locally the parting is represented by plastic or semihard clay rather than the typical dark-brown or dark-gray flint clay with plant rootlets and locally well-preserved leaves. Similar partings occur in one bed above and one bed below the Fire Clay coal in Kentucky, but these are local. An unusual origin for the

flint-clay parting seems required because it is widespread, unique, and composed chiefly of kaolinite. If it is the ordinary product of weathering in a swamp such partings should be more common; if long-continued weathering is required for formation of the well-crystallized kaolinite in flint clay, the peat below the clay should have decayed. Ashley (1928, p. 63) suggested that the parting came into the basin of deposition as an ash fall, but petrographic and other convincing evidence for this idea is lacking.

Stout suggested (1923, p. 545, 568) that the insoluble inorganic portion of plant residue contributed slightly to the formation of underclay and underclay partings. This is undoubtedly true, but the material that formed the residue was collected by the plants from material in the swamp, the seat rock, the underlying peat, and the dissolved solids in swamp water. Nevertheless, an accumulation of inorganic plant residue may explain some very thin clays lying between ganisters and coal beds. Such clays must be older than the overlying coal beds.

The presence of a dark humuslike zone (Wanless, 1950, p. 26; 1955, p. 1805) between some underclays and the overlying coal bed also shows that peat formed immediately after the underclays. In other places, laminated or bony coal in the upper part of the seat rock or at the base of the coal bed also suggests a transition from seat-rock formation to peat accumulation (Stevenson, 1913, p. 397–398). Generally a sharp contact separates a seat rock and the overlying coal bed. This could be attributed to consolidation of the seat rock long before peat accumulation began. The sharp contact could also result from a relatively sudden change from seat-rock formation to peat accumulation. Certainly differential compaction of peat and underclay tends to make the contact more obvious, and the sharpness of the contact is not an indication of time lapse. The contact generally lacks scour and channel cuts suggesting that erosion has not been significant. A close examination of many apparently abrupt contacts reveals thin layers of bony (high ash) attrital coal, which represents the transition from seat-rock formation to peat accumulation.

Blocks of banded coal are common in the lower parts of channel sandstones (Stevenson, 1913, p. 266–268, 273), showing that Pennsylvanian peat was tough enough to hold together in mats several feet long and to survive turbulent transportation. These mats, probably formed by undercutting, and the coal "spars" they now form, differ from the vitrinized stems of trees in the log jams near the base of many channel sandstones. Undercut beds of modern peat, not strictly comparable with the Pennsylvanian examples because of the difference between Pennsylvanian and modern plants, can be seen along the Inland Waterway in South Carolina, where peat beds are undercut by wave action. The toughness of fibrous peat, which permits the undercutting and transportation of mats, can explain outcrops that seem to show post-underclay, pre-coal faulting and eliminates the need for two cycles of channel cutting in examples such as those Schultz (1958, p. 380–382, Figs. 13a, 13b) interpreted to indicate the elapse of some time between the formation of seat rock and accumulation of peat. It is not surprising that squeezing and faulting occurred at such widely scattered localities as those described by Schultz during the compaction of peat and water-logged underclays, or that some small faults stopped at the tough peat whereas others broke through. Reference to "The fairly common occurrence of shales, limestone, and in one case . . . a marine brachiopod-bearing shale between the underclays and their overlying coals" (Schultz, 1958, p. 382) as showing a difference in the time of formation of the coal and underclay is inconclusive. The Lehigh coal in Coal County, Oklahoma, includes a coquina of gastropods and pelecypods 4 inches thick (T. A. Hendricks, written communication, 1959). Marine fossils in coal beds and many coal balls indicate that marine waters invaded peat-forming swamps and interrupted plant growth. The example cited by Schultz could be similar in origin or due to the development of two soil zones, the younger one being thin and obscure.

Underclays and Other Seat Rocks as the Geologic Record of Soils

The distinguishing characters of seat rocks result primarily from the growth of plants. Gradation upward from bedded shale, siltstone, or sandstone into nonbedded deposits with abundant plant rootlets suggests that these rootlets destroyed bedding and modified the deposits. Such a modified substratum was a soil, however immature or incipient, because plants grew on it, and it is residual in that it was formed in place from the sediments that happened to be present, generally clay, silt, and sand. The modification varies from a slight physical disturbance of bedding and with-

drawal of elements by a single generation of plants to the cumulative effects of many generations of plants, including total destruction of bedding, deep leaching, and alteration of minerals.

Acceptable evidence for seat rock having served as soils includes the presence of fossil roots, the concentration of iron and calcium in concretions or cracks near the base, and a mineralogy resembling modern water-logged soils. Nonbedding and slickensides are suggestive but not conclusive evidence; the latter may be due to compaction resulting from various causes.

Many of the rootlike fossils in seat rocks of Pennsylvanian age can be identified with the most common species of the genus *Stigmaria*, *S. ficoides* Brongniart. Specimens assigned to this species show only long-ranging, conservative characteristics that were evidently common to a wide variety of late Paleozoic treelike lycopsids, such as *Lepidodendron*, *Sigillaria*, *Lepidophloios*, and *Bothrodendron*. Occasionally rootlike specimens are found in connection with more diagnostic features so that a more precise determination is possible, but the rootlike fossils of the seat rocks are characteristically incomplete. The best of the common fossils consist of a stout axis, usually now compressed as a thin, coaly sheet, on which the points of attachment of roots, or scars at the points of former attachment, are spirally arranged. Axes are not so abundant as roots. The roots are commonly compressed into very thin, filmy ribbons that cut the rock at all angles. Occasionally the coaly film has been lost and only more obscure impressions remain.

Other less diagnostic types of roots may also be present (fibrous forms identified as *Radicites* H. Potonie, or roots more difficult to identify, which can occasionally be referred generically to tree ferns of the *Psaronius* type), but the lycopsid treelike forms, which show features diagnostic of *Stigmaria*, were exceedingly widespread (J. M. Schopf, written communication, 1959).

Undoubtedly, subsequent plant growth, ground-water action, compaction, and weathering have destroyed many traces of roots. Some stigmarian rootlets are contorted, but many are compressed into straight straplike films similar to grass leaves. Their outline invites identification as leaves, and while leaves may be present in underclays, some references in geologic literature to abundant fossil leaves in underclays probably are based on faulty identifications (Mammatt, 1834, p. 73; Schultz, 1958, p. 391). Many geologists recognize only the large axial casts and attached compression films of rootlets as *Stigmaria* and fail to recognize the much more common small rootlets. In most cases the attachment of these abundant rootlets to an axis is missing, but enough specimens showing the attachment of stigmarian roots and axes are present in roof shales, partings, and sandy or silty seat rocks to demonstrate the normal relationship. Figures 1 and 2 show the spongy nature of stigmarian roots in uncompressed specimens. Stigmarian plants had very shallow root systems (White and Thiessen 1913, p. 56), which were commonly embedded entirely in peat as soon as 2–3 feet of peat accumulated. Stigmarian axes as much as 40 feet long and 4–10 cm in diameter have been reported (Walton, 1953, p. 44), and roots are known to extend as much as 18 inches and to have a diameter of 1 inch (Francis, 1954, p. 58).

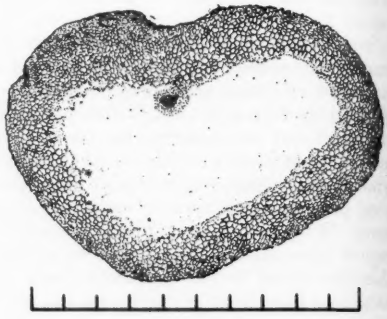

Figure 1. Cross section of a petrified root of *Stigmaria ficoides* Bgt. from a Pennsylvanian coal bed, Leslie County, Kentucky, showing delicate outer cortical tissue. The inner and middle cortex have broken down, leaving a large open cavity and a thin strand of wood conductive tissue. Shown about five times natural size. Identified and drawn by J. M. Schopf, U.S. Geological Survey Coal Geology Laboratory, Columbus, Ohio

Reports of stigmarian roots extending down from coal beds into seat rocks are common in older geologic literature (Stevenson, 1913, p. 232–241; 1921, p. 402–405; Ashley, 1928, p. 65), but the occurrences seem to be rare, possibly because of inherent difficulties in observation. Stumps with stigmarian roots extending

down into coal beds from roof shale are also known (Stevenson, 1913, p. 452–458; 1921, p. 339, 402–405). These occurrences show that at least some seat rocks served as substrata for plants which formed the overlying coal and that plants were rooted in peat during the closing stages of peat accumulation. Although these occurrences do not prove that this condition was true for all peat-forming swamps in the Pennsylvanian, there is a strong basis for inference that it was characteristic of many of them.

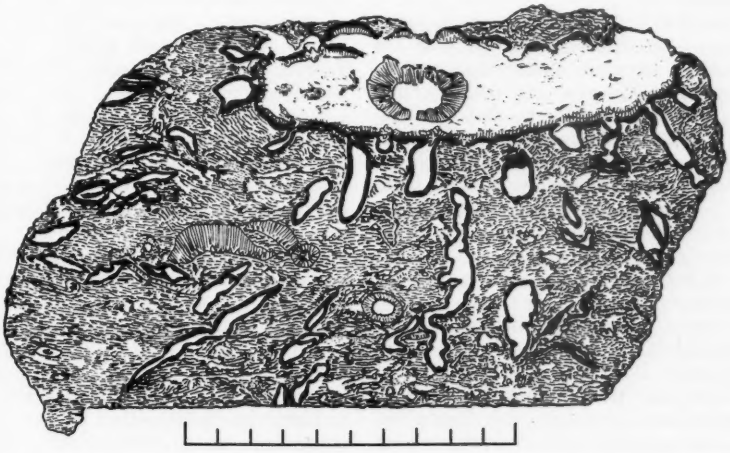

Figure 2. Slice cut from petrified peat (coal ball) from Pennsylvanian coal bed, Leslie County, Kentucky, showing a petrified stigmarian axis with appended roots (*Stigmaria ficoides* Bgt.). The outer cortex of roots, cut at various positions, is shown in black; the open interior cavities of both roots and axis are without shading. The roots and axis are embedded in peaty litter consisting of various sized vegetable fragments and debris shown diagrammatically. Shown one-half natural size. Identified and drawn by J. M. Schopf, U.S. Geological Survey Coal Geology Laboratory, Columbus, Ohio

Where preserved roots or rootlets are absent the structure of the seat rock may suggest their former presence (Stutzer and Noe, 1940, p. 145–146). The characteristic irregular blocky fracture seems, like that of modern soils, to be partly due to the former presence of roots. Stigmarian roots, as well as roots of other Carboniferous plants, could have caused the fracture systems.

A few highly kaolinitic claystones may never have served as soil. Some may have acquired characteristics not typical of underclays by transportation and redeposition or through alteration in place. In these groups fall the local flint clays that were transported or disturbed after some induration. They include bedded deposits, clay breccias, clay conglomerates, and clays that are highly involute and distorted owing to flowage. Also some sinkhole deposits in Missouri probably contain transported clays that never served as soils at their present locations.

Nonbedding and Slickensides

The lack of bedding in seat rocks is probably due chiefly to churning action of plant roots; other causes are important only locally. The growth and decay of several generations of spongy roots (Figs. 1, 2) results in a churning of the substratum, which could destroy any bedding in a seat rock. Compression of stigmarian roots results in a reduction in volume of more than 80 per cent. That this is at least a contributing factor to the nonbedded character of seat rocks is indicated by the gradation downward from nonbedded seat rock to bedded

rock. This gradation is commonly observed in sandstone and siltstone seat rock and less commonly in underclay in the Appalachian region. Flowage, sliding due to loading, and compaction due to dewatering locally erased traces of bedding. Conceivably some seat rocks could have been deposited without bedding, possibly from dewatered gels, but this hypothesis is difficult to prove or disprove with available evidence.

Slickensides in underclays are generally ascribed to compaction associated with the decay and compression of plant roots and dewatering of argillaceous seat rock. Schultz (1958, p. 363), however, states that "Slickensides and lack of bedding in underclay are attributed to the flocculation of clay combined with slipping when the hydrous mass was compacted." While flocculation undoubtedly accounts for some nonbedded slickensided clay, it is merely a contributing factor in others. Many slickensides in underclays occur along carbonaceous films of stigmarian rootlets, which, when compressed, determined the plane of sliding. Slickensides are common in bedded shales along compressed remains of pithy trunks and stems and must have formed by compression. Obviously, the dewatering, decay, and compaction of plant tissue can form slickensides.

Many of the semiflint clays of the Olive Hill bed, Kentucky, when fresh, break down with a hammer blow into a rubble of irregular polyhedra having each face formed by a slickenside surface. Where slickensides cut carbonaceous films of rootlets in partially broken masses of clay, displacement can often be observed. The displacement is mostly less than 1 mm and is commonly barely perceptible. Some slickenside surfaces show intense iron-oxide stain and encrustations of films of soluble salts precipitated from ground water, whereas others appear exceedingly fresh and shiny and are free from iron coloration and soluble salts. Inasmuch as these two types of slickenside surfaces occur in the same clay and were apparently subjected to the same ground-water action, two periods of slickenside formation are suggested. Perhaps the latest slickensides result from expansion accompanying the release of confining pressures during mining.

Leaching

Calcareous seat rocks and limestone beds in underclays are common where other rocks in the sequence are also calcareous, and they are rare or absent where the other rocks are noncalcareous. In the Appalachian coal basin the Pottsville Formation contains a few limestones, calcareous shales, or calcareous seat rocks, whereas the Conemaugh and Monongahela formations have proportionately more limestones and calcareous shales and also more calcareous seat rocks and limestone beds in underclays. In the Eastern Interior coal basin there is a strong correlation between the proportion of calcareous seat rocks and limestone and calcareous shale in the rock sequence. The association of calcareous seat rocks can result from a lack of leaching of originally calcareous rocks, a slight leaching of very calcareous rocks, or from secondary deposition of calcite that migrated from adjacent calcareous sediments. Calcareous matter in seat rocks is not a certain indication of the amount of leaching the seat rock has undergone.

In western Illinois calcareous underclays and limestone beds in underclays are common, but the upper part of most underclays, and all or some, are noncalcareous and contain stigmaria and slip fractures (Wanless, 1957, p. 56; Weller, 1931, p. 174–175). In many localities the number and size of the calcareous pisolites, spherules, and irregular masses in the calcareous zone increase downward to limestone beds. This probably results from original gradation upward from limestone to scattered smaller and smaller lumps and pellets of limestone. The noncalcareous zone above, however, seems to have been leached (Grim and Allen, 1938, p. 1503). Leaching is indicated by a lack of calcium and iron. The leached seat rock exhibits peculiar weathering properties in the current weathering cycle. These properties include a more abrupt change to plastic clay, as though it were preweathered, and a lighter color than mineralogically similar shales in the same sequence and a rusty zone that appears on weathering at the base of the noncalcareous zone. The rusty weathering seems to indicate a concentration of iron at the base of the noncalcareous zone. The noncalcareous zone of calcareous seat rocks seems to represent the depth of penetration of shallow root systems of the majority of plants that grew in the seat rock. Other calcareous seat rocks probably formed by precipitation in the calcareous zone (subsoil) of calcium and iron carbonates. These deposits are characterized by veins, irregular lumps, and pellets of calcite and siderite. Siderite is more common in the zone than calcite.

Some underclays are calcareous throughout,

and in places coal rests directly on limestone. Stigmarian roots may penetrate the limestone. In such places there was an excess of calcium after the needs of the plants were filled, and even after considerable leaching the underclay remained calcareous. Most calcareous seat rocks are no more kaolinitic than other claystones in the same areas, and deep leaching is not needed to explain the kaolinite. Other seat rocks, especially the silty and sandy ones, become calcareous during diagenesis or by secondary deposition of calcite. Secondary cementation of seat rocks by calcite is indicated by large reflecting "crystals" of some silty and sandy seat rocks and by calcite veins in seat rocks and along cleats in coal beds. Ground-water commonly moves along the cleats in coal beds, and the local deposition of calcite in coal beds and seat rocks is expectable.

Formation of Kaolinite in a Water-Logged Environment

The idea that kaolinite may have formed in a water-logged environment is not new: Ries (1911, p. 74) states ". . . all workable kaolin deposits of the United States, and probably many of those of Central Europe, are the work of surface waters, whether they entered direct from the surface or filtered first through a swamp or a bed of peat." Keller, Wescott, and Bledsoe (1954) and McMillan (1956) postulated the formation of kaolin in acid-swamp conditions, and Keller (1956, p. 2701–2702) described some chemical characteristics of environments and materials that lead to kaolinite formation.

Weller (1930, p. 122; 1956, p. 24, 31) argued that underclays must have formed under widespread emergent conditions, long before peat accumulation began. This assumes that emergent conditions are the only ones suitable for the formation of kaolinite, for widespread leaching, and for the concentration of iron compounds and calcium compounds in the lower part of the underclay, whereas Keller (1956) suggested that kaolinite forms under a much wider range of conditions. Most of the features which Weller considered to require a downward circulation of ground water can be explained by one or more of the following conditions:

(1) Alternate wet and dry periods.
(2) Circulation of swamp water before, after, and during peat accumulation.
(3) Leaching by plants, especially silicon- or aluminum-accumulator plants.
(4) Diffusion of iron compounds downward in a water-logged soil (McMillan, 1956, p. 241–242).
(5) Activity of micro-organisms in the seat rock during formation.

All these conditions do not require ground-water circulation or widespread emergent conditions.

That certain plants concentrate particular elements has been known for a number of years; Lovering (1958, p. 416–417; 1959) has suggested that silicon-accumulating plants might contribute greatly to the formation of laterite soils and that aluminum-accumulating plants might alter the aluminum-silicon ratio of soils greatly. Analyses given by Lovering (1959, p. 785) show 0.37 and 5.4 per cent silica in the ash of two dried *Equisetum* species. Closely related plants, *Calamites*, which were abundant in the Carboniferous swamps, may likewise have been silicon accumulators. Hutchinson (1943, p. 130–133) and Hutchinson and Wollach (1943) have shown that certain species of lycopods accumulate aluminum and silicon. Possibly their ancient relatives, *Lepidodendron* and *Sigillaria*, were also able to accumulate these elements. If so, such plants may have contributed to the formation of kaolinitic deposits; the full effects of accumulator plants are unknown. Local abundance of aluminum-accumulator plants may have contributed to the formation of ganister. Conceivably the same flora may have contributed to the formation of both ganisters and kaolinite-rich clays by removing scarce elements from the seat rock. The silicon-accumulator plants in a flora would have little effect on the siliceous or sandy seat rocks, but the aluminum-accumulator plants in the flora might aid in forming a ganister. The same flora on an argillaceous seat rock might have contributed to the formation of kaolinite by depletion of silicon by accumulator plants, while the aluminum-accumulator plants had little effect because of the abundance of aluminum in the seat rock.

The report of clayey matter in lycopods (Moore, 1940, p. 165) seemed questionable. We collected samples of *Lycopodium* from the grounds of the Agricultural Research Center at Beltsville, Maryland, washed the specimens, separated main stems and leaf-bearing stems, dried them at 160°C, weighed and ashed them at 375°C, and X-rayed the ash. No clay minerals were present.

Delicate wormlike crystals of kaolinite commonly found in coal and similar crystals in coal

partings show that kaolinite crystallized in peat and partings after these rocks were deposited. Such delicate crystals could not have been carried into the swamps by any agent without being destroyed and must have formed where they are found. Sprunk and O'Donnell (1942, p. 6–19, 58) report that kaolinite is common in coal-bed partings and as an impurity in coal and occurs as (1) tiny irregular masses, and (2) small to large vermiform crystals which impregnate or replace uncrushed plant tissues, surround "eyes" in coal, and fill cracks in the coal. They suggested that the kaolinite was brought into the swamp in solution and crystallized in cracks in the peat both during peat accumulation and after peat accumulation had ceased. Well-crystallized kaolinite within ironstone concretions and in coal "eyes" may have been precipitated from solution, but other occurrences probably resulted from leaching of existing materials in the coal and partings and washing of kaolinite into cracks. Hoehne (1957) not only reports kaolinite replacing plant tissues and wormlike crystals in coal-bed partings from various parts of the world, including the "blue band" in the Herrin coal of Illinois and the flint clay of the Fire Clay coal of Kentucky, but also reports pseudomorphs of kaolinite after feldspar in the flint-clay partings in Tennessee and a parting from Australia. Pseudomorphs clearly indicate formation of kaolinite from material existing in the swamp rather than precipitation from solution. The uncrushed nature of the large wormlike crystals of kaolinite suggests that they grew after some compaction of the peat or parting had taken place, but it does not seem probable that these crystals could have replaced coal after coalification had occurred.

Kaolinitic clay derived from basaltic lavas in acid swampy conditions in Hawaii is described by Wentworth, Wells, and Allen (1940, p. 1–33). No reason is apparent why kaolinite could not have formed in a similar manner from fine-grained sediments in acid Pennsylvanian swamps. Evidence for the acidity of Pennsylvanian swamps lies in: (1) coal beds overlying the clay, (2) vitrinized plant fragments scattered throughout the clay, and (3) small pyrite crystals and other sulfide minerals in the clay. Furthermore, pH measurements of 40 samples from the Olive Hill bed in Kentucky (Patterson and Hosterman, 1960) show two neutral samples and 38 acid samples ranging down to pH 3.9. Clearly the clay is acid now, and apparently this clay formed in an acid environment and remained acid throughout its entire history. There is no evidence regarding the disposition of silica and alkalies that were removed. Leached materials probably diffused upward in the acid water and were flushed away by sluggish movement of water through the swamps and periodic floods. Both the seat rock and the coal beds (Sprunk and O'Donnell, 1957, p. 3–4) are deficient in potassium and sodium compared to adjacent sediment and the inherent mineral matter of modern plants respectively.

Plastic, Flinty, and Diaspore-Bearing Underclays as Successive Stages in the Alteration of Bedrock by the Same Process

Flinty and diaspore-bearing underclays are generally thought to have been formed by *in situ* alteration of pre-existing material, although some of these clays contain evidence of transportation and redeposition. The processes that can form these highly aluminous clays seem to us to have been operative in the environments in which plastic underclays were deposited, and we prefer to interpret the plastic underclays as the first stage of a sequence of which the boehmite- and diaspore-bearing underclays are apparently the last stage.

Schultz (1958, p. 367) has shown the principal clay minerals in plastic underclays to be ". . . illite, a poorly crystallized type of kaolinite which varies somewhat in its degree of disorganization, and mixed-layer illite-montmorillonite or more rarely illite-montmorillonite-chlorite; about one-third of the samples also contain a 14Å chloritic mineral." The kaolinite in most plastic clays is subordinate to the other clay minerals. The kaolinite content of flint clay ranges from 75 to about 95 per cent, but nearly all flint clays contain at least traces of illite or mixed-layer clay. The kaolinite content of semiplastic clays ranges from subordinate amounts to roughly two-thirds. The clay composition of semiflint clays is in general intermediate between that in plastic and flint clays. Obviously, a complete gradation exists between the mineralogical composition of flint clay and plastic clay. Plastic clay, in turn, is very similar in mineral constituents to many Pennsylvanian shales. Chemical analyses of underclays (Table 1) show a complete gradation in composition between plastic and flint clay, and they also show that plastic clays have compositions similar to Pennsylvanian shales. Furthermore, there is a complete gradation in the crystallinity of the

kaolinite, from the poorly crystallized variety characteristic of the plastic clays described by Schultz to well-crystallized kaolinite in flint clays. This range of crystallinity is known to occur within the Olive Hill bed (Patterson and Hosterman, 1960) and has also been recognized in Ohio underclays by McConnell, and de Pablo-Galan (1956, p. 279). Keller, Wescott, and Bledsoe (1954, p. 19) have described the crystallinity of the kaolinite in the Cheltenham bed of Missouri as follows:

> "X-ray powder diffractograms of the clay show sharp and intense basal reflections, but those from pyramidal and some prismatic planes are diffuse or lacking. Hence, disorder is indicated in the stacking within the fire clay crystals, but orderliness appears to increase as the clay becomes 'harder' and approaches flint clay. The latter gives an X-ray pattern, . . . closely similar to one of well-crystallized kaolinite. The basal spacing of the semi-flint and semi-plastic fire clays is of the order of 7.2 to 7.3Å, which suggests the presence of some interlayer water."

Alteration of illite to kaolinite is strongly suggested by the close association of poorly crystalline kaolinite with illite in plastic clays and the increase in crystallinity of kaolinite accompanied by a decrease in the amount of illite present in semiflint and flint clays. Further leaching of the nearly pure kaolin to form the parent material of bauxite minerals is implied by the close association of these minerals in the Cheltenham bed of Missouri, the lower part of the Mercer of Pennsylvania, and at least two localities in the Olive Hill bed of Kentucky. Certainly some change took place in all clays between burial and the present, and it seems logical to conclude that diagenetic changes were greatest in those clays that were most thoroughly altered prior to burial. Patterson and Hosterman (1960), Bolger and Weitz (1952, p. 91–93), and others have noted evidence of recrystallization including vermicular kaolinite crystals in flint clays, and Foose (1944, p. 576) has noted two generations of diaspore formation. Some recrystallization of kaolinite in flint clays and some recrystallization or formation of diaspore probably took place after burial. Also, it seems probable that time or pressure or both are required for formation of boehmite and diaspore, as implied in comments by Bridge and Roy (1952, p. 212–213). Some sort of an aluminous hydroxide gel, however finely distributed, may have been the first alteration product of kaolinite. The trihydrate, gibbsite, or some related hydrous bauxite mineral probably existed as an intermediate stage and may have been the form of what is now diaspore until long after burial. Boehmite also appears to represent an intermediate stage before the formation of the stable diaspore.

Concentration of High-Purity Kaolin in Lower Pennsylvanian Underclays

Grim's (1935) conclusion that the purer kaolinitic underclay occurs in the lower part of the Pennsylvanian section and that illite and other clay minerals predominate in underclays in upper Pennsylvanian rocks is valid not only for Illinois but in a genera way, for much of the United States. The most important high-purity kaolin underclays, the Cheltenham bed of Missouri, Olive Hill bed of Kentucky, Sciotoville bed of Ohio, and Mercer bed of Pennsylvania, are of Pottsville age, and all except the Mercer occur within a few feet above the unconformity between the Pennsylvanian and Mississippian or older rocks. Schultz (1958) has fully demonstrated the predominance of illite and mixed-layer clays over kaolinite in post-Pottsville underclays.

The concentration of kaolin n underclays in the Lower Pennsylvanian rocks is equally difficult to explain by either the alteration in place or sedimentary winnowing theories of clay formation. Lower Pennsylvanian rocks contain high proportions of quartzose sandstone and other types of mature sediments, which are probably related to a long period of weathering beginning with the erosional cycle represented by the Mississippian-Pennsylvanian unconformity. This implies that more kaolinite was available in source areas in the Early Pennsylvanian than later; however, it does not account for the purity of the deposits. Pennsylvanian rocks enclosing the high-purity kaolin deposits in Missouri (Keller, Wescott, and Bledsoe, 1954) and in Kentucky (Patterson and Hosterman, written communication, 1959) are extremely variable and discontinuous and are characterized by both vertical and lateral gradations in grain size within short distances. An abrupt change from the environment responsible for these variable rocks to one in which very fine-grained kaolinite was essentially the only mineral deposited is unlikely. Furthermore, the shape of underclay deposits (Fig. 3) shows a lack of orientation and continuity that would be expected in clays deposited as sedimentary units.

Accordir.g to the theory of alteration in place

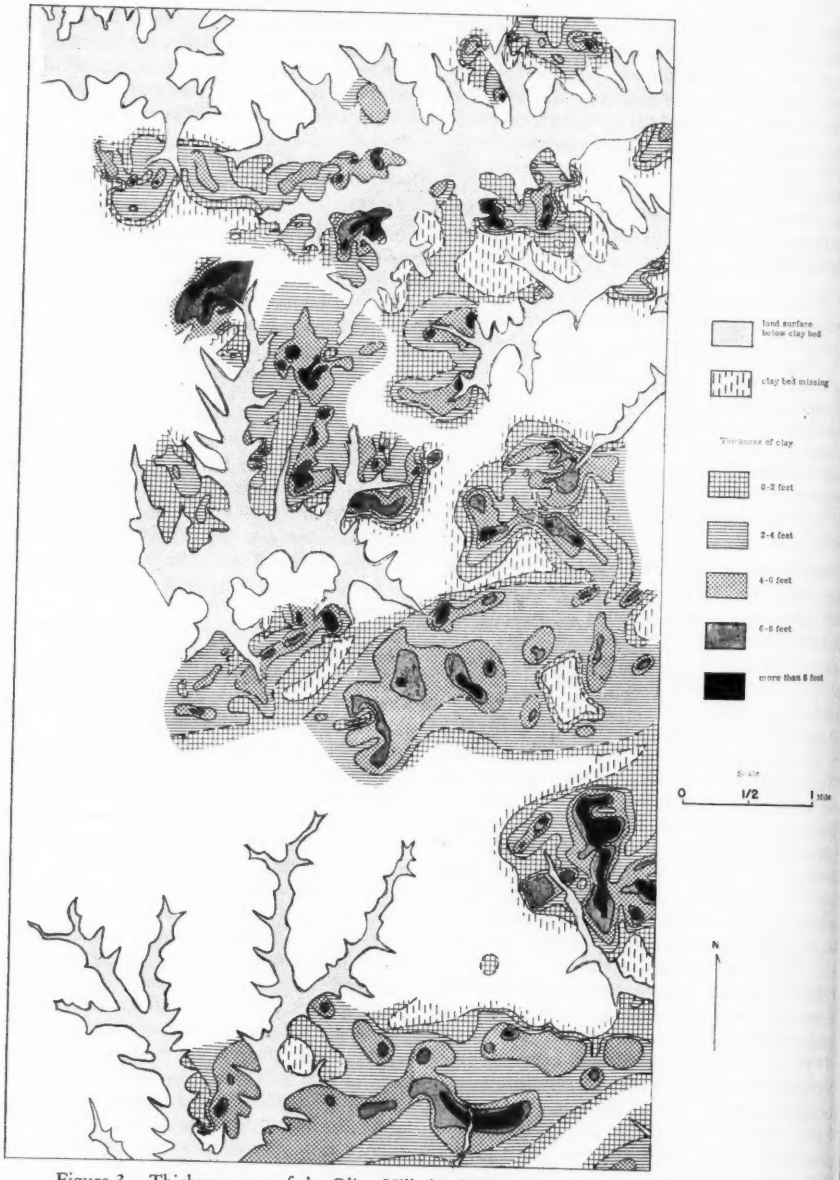

Figure 3. Thickness map of the Olive Hill clay bed, Haldeman quadrangle, Kentucky

advocated by the authors, the concentration of kaolin can be explained by alteration of ordinary fine-grained sediments in uncommonly long-lasting swamps, which developed under nearly stable crustal conditions along coastal lowlands. Although concrete evidence concerning the life of swamps is lacking, this theory would explain: (1) the high purity of kaolin deposits by the length of time available for leaching of normal Pennsylvanian sediments, (2) the irregular lens shape and lack of continuity of the deposits by the irregular shape and depth of the swamps, (3) the irregular distribution, interlensing, and lack of gradational contacts between flint, semiflint, and plastic clay masses in a single bed by variations in depth of water and other factors influencing alteration in swamps, and (4) the absence of thick coal beds above high kaolinitic underclay beds by the wasting of organic matter during long periods of leaching. Some support of this idea is given by Wanless (1931, p. 191; 1957, p. 64), who, using an entirely different approach, concluded that the highly kaolinitic Cheltenham bed in western Illinois is a composite bed representing all underclays of Pottsville cyclothems below the Liverpool, and, therefore, must represent a much longer period of time than any underclay of a single cyclothem.

Similarity of Plastic Underclays to Pennsylvanian Shales

Plastic underclays differ little in mineralogical and chemical composition from the fine-grained sedimentary rocks below coal beds. This is particularly well documented by Schultz (1958), who also shows that significant differences exist between underclays and the shales above the coals. Shales above coal beds tend to contain smaller amounts of kaolinite than the underclays, but shales below the coals contain about the same amount as underclays. The mineral composition of many of these plastic underclays is very similar to that of several shales of Pennsylvanian age reported by Grim, Bradley, and White (1957) and by Murray (1954). Chemical analyses (Table 1) clearly support this similarity in mineralogy. McMillan (1956, p. 211) observed that feldspars occur more commonly and in a less altered state in shale than in underclay, which suggests that underclays were developed from the shales. He also comments (p. 191) that the Nodaway underclay of Kansas is very similar mineralogically to the underlying shale where the underclay is poorly developed but that the shale and underclay show considerable mineralogical difference where the underclay is well developed.

Leaching of Quartz and Feldspar in Underclays

Patterson and Hosterman (1960) have presented evidence showing that quartz grains were leached in flint clay of the Olive Hill bed, Kentucky. They describe quartz grains with serrated grain boundaries and partial replacement of quartz by kaolinite. Clearly quartz grains replaced by clay could not have withstood transportation, and leaching in place is indicated.

Hoehne (1957, p. 114–119) reports kaolinite replacing quartz, the leaching of kaolinite crystals and partial replacement by quartz, and the growth of secondary quartz splinters. These mineralogical changes indicate a succession of chemical environments probably associated with the change from seat-rock formation to peat accumulation to coalification. Possibly the silicification occurred when acid, probably silica-rich waters were being squeezed out of the peat during coalification.

The degree of alteration or absence of detrital feldspar is one criterion for determining the amount of leaching a rock has undergone. Grim and Allen (1938, p. 1491, 1495), dealing primarily with plastic and semiflint underclays, observed that "White mica is very common, and feldspar (orthoclase, microcline, albite) is a common constituent . . . ." McMillan (1956, p. 211) states, "Plagioclase was noted more commonly than orthoclase. Only a few scattered grains of angular, fairly clear, slightly kaolinized orthoclase were identified on the basis of Carlsbad twinning or refractive index." Rubey (1952, p. 55) noted partly decomposed grains of orthoclase in a plastic underclay of Pottsville age in Illinois. In investigating the flint clays of Kentucky, however, Patterson and Hosterman (1958) found that the only detrital minerals present are those more resistant than feldspar. Furthermore, other thorough studies of flint clays (Keller, Wescott, and Bledsoe, 1954; Keller, 1956; Bolger and Weitz, 1952) mention only those detrital minerals that are more resistant than feldspar and indicate that feldspar is much more common in plastic underclays than in flinty underclays. To believe that plastic underclays originally contained feldspar but that flint clays did not seems illogical, inasmuch as both types of clay have similar suites of more resistant minerals. Available evidence

regarding the condition of detrital feldspar strongly suggests alteration in place, and suggests that flint clays are more highly altered than plastic clays.

Titanium in Underclays

Variations in titanium content of underclays are also in accord with theories of alteration in place and are difficult to explain by any method of sedimentary sorting, because heavy titanium-bearing minerals and light very fine-grained kaolinite would not be deposited under the same conditions. Titanium oxide content in most plastic underclays ranges from 0.5 to 1.5 per cent, which is of the same order of magnitude as in Pennsylvanian shales (Table 1). The high-alumina diaspore-bearing underclays contain 2.5–3 per cent titanium oxide, or more than twice as much titanium oxide as the average plastic underclay, and flint and semiflint clays have intermediate amounts. Such an increase in titanium in leaching and weathering products is a common phenomenon (Allen, 1952, p. 666–667). Rankama and Sahama (1950, p. 563) explain it as follows: "The soluble salts of titanium are readily hydrolyzed. During the weathering, titanium consequently remains largely in the resistates. The most important rock-making titanium minerals, particularly ilmenite and rutile, are stable against weathering, and consequently they remain unchanged in resistate sediments." Inasmuch as titanium-bearing minerals are of much higher specific gravity than kaolinite, the increase in titanium content with increasing purity of the kaolin cannot be explained by any sedimentary winnowing process.

The titanium-oxide content of underclays from Kentucky, as shown by chemical analyses, is greater than can be accounted for by the amount of titanium-bearing heavy minerals present identifiable by optical methods (Patterson and Hosterman, written communication, 1959). Nearly all this titanium is probably present in the form of finely divided anatase, which formed as a leaching product of heavy minerals. Unfortunately no real evidence exists as to whether or not fine-grained anatase can be transported and deposited with kaolinite. Grim (1953, p. 49) has suggested that titanium can occupy lattice positions in poorly crystallized kaolinite like the kaolinite in plastic underclays. However, there is no evidence that titanium in underclay is in the crystal structure of kaolinite, and furthermore its concentration in diaspore cannot be explained in this way.

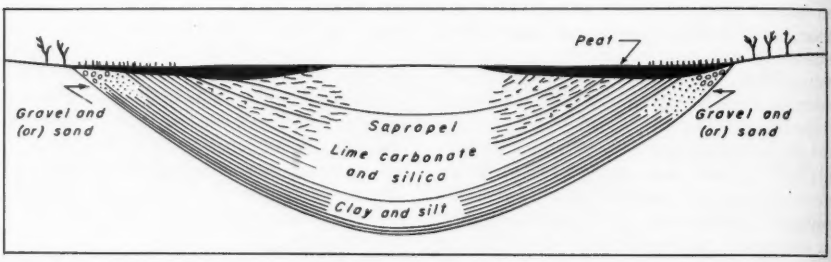

Figure 4. Diagrammatic representation of deposition in modern swamps. By permission from *Principles of Sedimentation*, by W. H. Twenhofel. Copyright 1950. McGraw-Hill Book Co., Inc.

Shapes of Underclay Deposits

Figure 3 shows that the Olive Hill bed in the Haldeman quadrangle, Kentucky, occurs in irregular lenses forming a discontinuous bed. Very similar irregularly shaped deposits make up the Mercer bed near Clearfield, Pennsylvania, as shown by unpublished isopach maps prepared by Spotts McDowell of the Harbinson-Walker Refractories Company (Oral communication, 1958) and by John M. Parker, III (Written communication, 1943). These deposits are definitely not channel accumulations, such as are known to form sedimentary kaolins of Cretaceous age in Mississippi (L. C. Conant, written communication, 1958), nor do they show any alignment that would be expected in dissected blanket deposits or in sediments accumulated in ponds formed by cutoff stream segments, as suggested for Georgia kaolins by

yses,
the
erals
tter-
tion,
ably
tase,
eavy
xists
n be
Grim
can
ized

iples

der-
that
ture
tion
y.

l in
curs
ed.
ake
syl-
aps
oin-
om-
III
sits
uch
of
nt,
ney
l in
nts
am
by

UN

Bed	State	Type of clay	SiO_2	Al_2O_3	Fe_2O_3
Clay fraction of 38 Pennsylvanian shales from Illinois*			49.67	26.7	3.1
Fithian illite			51.22	25.91	4.59
Nodaway	Kansas	Plastic	64.42	15.98	4.22
Nodaway	Kansas	Plastic	63.7	16.68	6.19
Nodaway	Kansas	Plastic	61.60	18.10	5.02
Middle Kittanning	Ohio	Plastic	50.02	21.73	7.93
Meigs Creek	Ohio	Plastic	48.36	22.36	3.61
Nodaway	Kansas	Plastic	58.66	22.50	4.86
Cheltenham	Missouri	Plastic	56.10	24.47	3.64
Lower Freeport	Ohio	Flint	59.71	24.58	2.26
Thomas	Maryland	Plastic	58.47	25.09	3.60
Bolivar	Maryland	Semiplastic and semiflint	54.54	29.63	2.80
Cheltenham	Missouri	Plastic	48.90	33.20	1.47
Lower Kittanning	Maryland	Semiflint	51.30	33.88	1.75
Olive Hill	Kentucky	Plastic	46.4	34.0	1.4
Cheltenham	Missouri	Semiflint	45.92	35.79	.75
Olive Hill	Kentucky	Semiflint	45.1	36.4	1.0
Sciotoville	Ohio	Flint	45.2	36.77	1.30
Mt. Savage	Maryland	Flint	46.51	37.15	.95
Olive Hill	Kentucky	Semiflint	44.7	37.6	.59
Olive Hill	Kentucky	Flint	44.7	38.0	.57
Mercer	Pennsylvania	Flint	43.74	38.37	1.29
Cheltenham	Missouri	Flint	44.42	38.63	.055
	Theoretical kaolinite		46.54	39.50	....
Olive Hill	Kentucky	"Aluminite" flint	39.01	42.01	4.04
Olive Hill	Kentucky	"Aluminite" flint	39.56	43.35	2.57
Olive Hill	Kentucky	"Aluminite" flint	37.21	43.76	3.53
Cheltenham	Missouri	"Burley" diaspore	32.48	46.53	.38
Cheltenham	Missouri	"Burley" diaspore	32.60	48.26	.49
Olive Hill	Kentucky	"Aluminite" flint	34.76	48.50	1.26
Mercer	Pennsylvania	"Green nodule" diaspore	26.76	54.50	.80
Cheltenham	Missouri	"Burley" flint and diaspore	22.96	58.51	.63
Mercer	Pennsylvania	Diaspore	....	61.52	....
Cheltenham	Missouri	Diaspore	15.60	64.46	.42
Cheltenham	Missouri	Diaspore	12.59	68.32	1.29
Mercer	Pennsylvania	Diaspore	4.00	75.72	2.17
Cheltenham	Missouri	Diaspore	3.89	76.21	.98
	Theoretical diaspore		....	85.00	....

*Clay fractions contain lower SiO_2 and slightly lower alkalies than whole samples; Al_2O_3 contents are accordin

HUDDLE AND PATTERSON, TABLE 1
Geological Society of America Bulletin, volume 72

TABLE 1. CHEMICAL ANALYSES OF U

SiO_2	Al_2O_3	Fe_2O_3	FeO	MgO	CaO	Na_2O
49.67	26.7	3.1	2.74	2.12	0.70	0.71
51.22	25.91	4.59	1.70	2.84	.16	.17
64.42	15.98	4.22	....	1.00	3.20	.48
63.7	16.68	6.19	....	1.37	1.63	1.25
61.60	18.10	5.02	....	2.01	.61	1.45
50.02	21.73	7.93	....	1.66	.56	.14
48.36	22.36	3.61	....	3.13	2.88	.33
58.66	22.50	4.86	....	1.29	.34	.60
56.10	24.47	3.64	....	1.11	.61	.17
59.71	24.58	2.26	....	.14	.33	.19
58.47	25.09	3.60	....	1.00	.65	....
54.54	29.63	2.80	1.02	.91	.63	....
48.90	33.20	1.47	....	.34	.56	.10
51.30	33.88	1.75	....	....	....	....
46.4	34.0	1.4	.41	.69	.11	.24
45.92	35.79	.75	....	.36	.06	.44
45.1	36.4	1.0	.23	.52	.10	.18
45.2	36.77	1.30	....	.08	.50	.00
46.51	37.15	.95	....	.09	.20	....
44.7	37.6	.59	.22	.16	.06	.09
44.7	38.0	.57	.09	.10	.06	.06
43.74	38.37	1.29	....	.28	.04	....
44.42	38.63	.055	....	.10	.04	.30
46.54	39.50	....	....	....	....	....
39.01	42.01	4.04	....	.45	.68	....
39.56	43.35	2.57	....	.50	.56	....
37.21	43.76	3.53	....	.06	.88	....
32.48	46.53	.38	....	.66	.69	2.08
32.60	48.26	.49	....	1.62	.28	.61
34.76	48.50	1.26	....	.11	.76	....
26.76	54.50	.80	....	.30	.18	....
22.96	58.51	.63	....	.98	.40	.65
....	61.52	....	....	....	....	....
15.60	64.46	.42	....	1.52	.92	.37
12.59	68.32	1.29	....	.15	1.85	1.34
4.00	75.72	2.17	....	.25	.10	....
3.89	76.21	.98	....	.06	.08	.79
....	85.00	....	....	....	....	....

mples; Al_2O_3 contents are accordingly somewhat higher than in whole samples.

NALYSES OF UNDERCLAY, PENNSYLVANIAN SHALES, KAOLINITE, AN

O	Na_2O	K_2O	TiO_2	P_2O_5	MnO	Ignit loss a or H
	0.71	4.32	1.44	Tr	....	16.
	.17	6.09	.53	....	....	7.
	.48	2.50	1.11	0.01	....	6.
	1.25	3.47	1.30	.27	....	5.
	1.45	3.69	1.10	.16	....	5.
	.14	3.90	.96	.11	0.07	8.
	.33	4.70	1.10	.07	.27	9.
	.60	4.28	.78	Tr	....	6.
	.17	2.89	1.58	....	....	8.
	.19	1.20	1.4	.02	Tr	9.
	....	....	1.11	....	....	8.
	....	....	1.02	....	....	9.
	.10	1.53	1.58	....	....	11
	....	....	1.47	....	....	9.
	.24	3.1	1.4	.02	.00	11.
	.44	.41	2.28	....	....	13.
	.18	1.2	2.4	.05	.01	12.
	.00	.52	1.80	.02	Tr	12.
	....	....	1.55	....	....	12.
	.09	.41	1.5	.03	.00	14.
	.06	.36	2.0	.01	.00	13.
	....	....	1.72	....	....	13.
	.30	.12	2.12	....	....	13.
	....	....	....	....	....	13.
	....	....	....	....	....	14.
	....	....	....	....	....	13.
	....	....	....	....	....	14.
	2.08	1.39	2.38	....	....	13.
	.61	.54	2.25	....	....	14.
	....	....	....	....	....	14.
	....	....	....	....	....	13.
	.65	1.67	2.10	....	....	13.
	....	....	....	....	....	13.
	.37	.81	2.60	....	....	14.
	1.34	.19	2.04	....	....	13.
	....	....	2.75	....	....	14.
	.79	.24	3.52	....	....	14.
	....	....	....	....	....	15.

whole samples.

Kesler (1956, p. 553). The shape of these clay deposits seems indicative of swamp accumulation.

Further evidence for swamp accumulation rests in the relation of lithologic units within underclay beds and of the underclays to the overlying coal. These relations are remarkably in accord with the diagrammatic illustration of recent swamp deposits given by Twenhofel (1950, p. 83), reproduced herein as Figure 4. The lateral gradation in seat earths from essentially pure clay through sandy clay to sandstone is very similar to that shown in the figure. The authors believe this is the explanation for the close lateral association of underclays with coarse-grained seat earths. The invasion of swamps by plants and the accumulation of peat seems to be a direct parallel to the roots of stigmarians in seat earths and overlying coal beds. The calcium carbonate in Twenhofel's diagram is present in many plastic underclays (Grim and Allen, 1938, p. 1487), but it is missing in flinty underclays, which we believe have undergone extreme leaching in place.

A tendency for the refractory properties of flint clays in the Olive Hill district to be greater in the middle part of the bed than near the top and the bottom was noticed by Patterson during the examination of several hundred drill logs and the results of firing tests, made available by Mr. Fred Gesling, consulting engineer, Ashland, Kentucky. Commonly, the decrease in refractory properties in the upper part of the clay is caused by less than 1 per cent increase in potassium and even less of sodium, and the refractory decrease near the base by an increase in the amount of admixed sand and illitic clay. Similar observations of a decrease in ceramic properties in the upper parts of underclay beds have been made in Illinois by Grim and Allen (1938, p. 1504) and in Ohio by Stout (1923, p. 552–553). Grim and Allen (1938, p. 1502, 1508) argue that kaolinitic clays could not have formed from illite because that change requires the removal of potassium and magnesium, as in weathering processes, and they state that such alteration did not occur. Alkalies gradually supplied by decaying peat in swamps might be fixed by leached illitic minerals in the upper part of sub-peat swamp muds. Possibly this fixing could be sufficient to preserve illitic minerals in the upper part of swamp muds while deeper zones were actively leached. The feasibility of this idea is supported by Sprunk and O'Donnell (1942, p. 3–4), and by Stutzer and Noe (1940, p. 12) who state that "The alkalies, which are the main constituents of the ashes of living plants, are found in only small quantities in coal ashes. The alkalies either are leached out or are used again and again by succeeding generations of plants. The small quantities of alkalies which are found in coal ash are usually contained in the coal as aluminum silicates . . . ." Accordingly, the presence of poor refractory material in the upper parts of underclay beds does not seem to be in opposition to alteration in place.

A second explanation for the occurrence of high-quality clay in the middle part of underclay beds may lie in little-understood bauxitization processes. Allen (1952, p. 665) has found that the highest alumina contents in Georgia bauxite deposits are in the middle parts of the deposits. Bridge (1950, p. 185) has described kernels of bauxite enclosed by bauxitic clay in similar deposits which, in turn, are enveloped by kaolin. Furthermore, in these deposits the bauxite is restricted to the thicker portions of the bauxite-kaolin deposits. Similarly the uncommonly high-alumina flint clay in the Olive Hill bed described by Greaves-Walker (1907, p. 469–470) as "aluminite" and by Galpin (1912, p. 327) as gibbsite has been found only where a bed is exceptionally thick and is not present where the bed is of average thickness or less (Patterson and Hosterman, written communication, 1959). Also, the diaspore- and boehmite-bearing clays in the Mercer bed in Pennsylvania are restricted to the thicker portions of the bed, where they occur in irregular masses surrounded by clay of lower alumina content. Foose (1944, p. 568) describing this occurrence, noted that "Nodule clay, when present, usually lies near the middle of the flint clay, into which it often grades through spotted flint clay."

The restriction of high-alumina material to the thicker portions of the deposits, together with its envelopment by lower-alumina clays in both Pennsylvanian underclays and Coastal Plain bauxite, suggests that related processes operated in the formation of both. Apparently the processes were effective in moving all constituents but aluminum and water outward from centers. Regarding the nature of these processes, Bridge (1950, p. 186) states: "Probably most students of this problem accept the origin of gibbsite from kaolinite by the leaching of silica from the clay minerals; others believe that some of the kaolin has been formed by the

resilication of bauxite, and a few advocate other less plausible origins." When adequate facts can be presented to explain these phenomena, light will probably also be shed on the oölites and pellets in underclays, whose origin has been uncertain for a long time (McMillan, 1956, p. 235).

FORMATION OF KAOLINITIC SEAT ROCKS

The following sequence of environments seems to explain the mineralogy and the origin of kaolinitic underclays at least as well as the theory that they were transported.

Probably many underclays and other seat rocks formed under three different water-logged micro-environments from the parent material present in the substratum. A similarity in the mineral composition of the many plastic underclays and the enclosing strata strongly suggests that the plastic clays were derived from the same kind of sediments. At first considerable leaching took place because the water was not stagnant, and large plants, possibly silicon- or aluminum-accumulator plants, removed some materials from the substratum. In places iron compounds accumulated at the base of the bed; peat did not accumulate because of the activity of micro-organisms. Later the water was partially stagnant, decay was slowed, peat accumulated, withdrawal of compounds by large plants continued (which degraded some clay minerals), and sulfides formed in the seat rock. When a thick layer of peat had accumulated, deep leaching stopped and the shallow root systems of the plants were largely confined to the peat itself. After the peat was buried and during coalification, decay continued and various ions were transferred from the decaying plants back into the seat rock. Keller (1956, p. 2703) and Schultz (1958, p. 391) have suggested that during coalification degraded clay minerals may have been altered and even formed chlorite. Schultz (1958, p. 374, 391) regards chlorite as strong evidence of no leaching during the formation of underclays but does not eliminate the possibility of chlorite development in place. Primary and secondary clay minerals, and perhaps even feldspar, probably existed under the conditions which must have predominated. The length of time involved in each of the stages varied considerably, and this explains why there is not and should not be any direct relation between the amount of leaching, the thickness of the underclay, and the thickness of the coal.

SUMMARY

Most seat rocks formed in a water-logged environment and acquired peculiar characters from plant roots, and continued leaching by acid swamp water. The plants which grew in the available substratum (any previously deposited sediment) were the same kind, but not necessarily the same ones, that contributed to the formation of the overlying coal. Sediments brought into the swamp and the mineral residue of decayed plants sometimes were added to the pre-existing sediment and contributed to the formation of seat rocks. Seat-rock formation was a stage in the development of coal swamps which lasted for a variable period of time, as is indicated by the complete gradation from sandstone to ganister, and illitic shale to kaolin. Some seat rocks were only slightly leached, others deeply leached. Some seat rocks, including high-purity kaolin, may have been eroded, transported, and redeposited, but most formed in place in a swamp, and their development was generally followed immediately by the accumulation of peat. Long-continued subaerial weathering in a well-drained area under stable conditions is not necessary for formation of all the kaolinite found in seat rock.

REFERENCES CITED

Allen, V. T., 1952, Petrographic relations in some typical bauxite and diaspore deposits: Geol. Soc. America Bull., v. 63, p. 649–688

Ashley, G. H., 1928, Bituminous coal fields of Pennsylvania, pt. I: Pennsylvania Topographic and Geol. Survey, ser. 4, Bull. M-6, 241 p.

Bolger, R. C., and Weitz, J. H., 1952, Mineralogy and origin of the Mercer fire clay of north central Pennsylvania, p. 81–93 *in* Problems of clay and laterite genesis: Am. Inst. Min. Metall. Engineers St. Louis meeting (1951) Symposium

Bridge, Josiah, 1950, Bauxite deposits of the southeastern United States, p. 170–201 *in* Snyder, F. G., *Editor*, Symposium on mineral resources of the southeastern United States: Knoxville, Tenn., Univ. Tennessee Press

Bridge, Josiah, and Roy, Rustum, 1952, Discussion remarks, p. 212–214 *in* Problems of clay and laterite genesis: Am. Inst. Min. Metall. Engineers St. Louis meeting (1951) Symposium

Crider, A. F., 1913, The fire clays and the fire clay industry of the Olive Hill and Ashland districts of northeastern Kentucky: Kentucky Geol. Survey, ser. 4, v. I, pt. II, p. 592–711

Erickson, E. S., Jr., 1958, Mineralogical, petrographic and geochemical relationships in some high-alumina and associated claystones from Pennsylvania [Abstract]: Seventh Natl. Conf. Clays and Clay Minerals Proc. Washington, D. C.

Foose, R. M., 1944, High-alumina clays of Pennsylvania: Econ. Geology, v. 39, p. 557–577

Francis, Wilfrid, 1954, Coal; its formation and composition: London, Edward Arnold Ltd., 567 p.

Galpin, S. L., 1912, Studies of flint clays and their associates: Am. Ceramic Soc. Trans., v. 14, p. 301–346

Greaves-Walker, A. F., 1907, The flint fire clay deposits of northeastern Kentucky: Am. Ceramic Soc. Trans., v. 9, p. 461–472

—— 1939, The origin, mineralogy and distribution of the refractory clays of the United States: North Carolina Univ. Eng. Exper. Sta. Bull. 19, 87 p.

Grim, R. E., 1935, Petrology of the Pennsylvanian shales and noncalcareous underclays associated with Illinois coals: Am. Ceramic Soc. Bull., v. 14, p. 113–119, 129–134, 170–176

—— 1953, Clay mineralogy: New York, McGraw-Hill Book Co., Inc., 384 p.

Grim, R. E., and Allen, V. T., 1938, Petrology of the Pennsylvanian underclays of Illinois: Geol. Soc. America Bull., v. 49, p. 1485–1513

Grim, R. E., Bradley, W. F., and White, W. A., 1957, Petrology of the Paleozoic shales of Illinois: Illinois State Geol. Survey Rept. Inv. 203, 35 p.

Gunsallus, B. L., and Blankenbaker, E. V., 1956, Clays: U. S. Bur. Mines 1953 Minerals Yearbook, Metals and Minerals (except fuels), v. 1, p. 331–351

Hoehne, K., 1957, Tonsteine in Kohlenflözen der Oststaaten von Nordamerika und Ostaustralien: Chemie d. Erde, Bd. 19, H. 2, p. 111–129

Howell, J. V., Chairman, 1957, Glossary of geology and related sciences: Am. Geol. Inst., Natl. Acad. Sci.-Natl. Research Council Pub. 501, 325 p.

Hutchinson, G. E., 1943, The biochemistry of aluminum and of certain related elements: Quart. Rev. Biology, v. 18, p. 128–153

Hutchinson, G. E., and Wollach, Anne, 1943, Biological accumulators of aluminum: Conn. Acad. Arts and Sci. Trans., v. 35, p. 73–127

Keller, W. D., 1956, Clay minerals as influenced by environments of their formation: Am. Assoc. Petroleum Geologists Bull., v. 40, p. 2689–2710

Keller, W. D., Wescott, J. F., and Bledsoe, A. O., 1954, The origin of Missouri fire clays, p. 7–46, *in* Swineford, Ada, *Editor*, Clays and clay minerals: Second Natl. Conf. Clays and Clay Minerals Proc., Natl. Acad. Sci.-Natl. Research Council Pub. 327

Kesler, T. L., 1956, Environment and origin of the Cretaceous kaolin deposits of Georgia and South Carolina: Econ. Geology, v. 51, p. 541–554

Logan, W. E., 1842, On the character of the beds of clay lying immediately below the coal seams of South Wales: Geol. Soc. London Proc., v. 3, p. 275–277

Lovering, T. S., 1958, Accumulator plants and rock weathering: Science, v. 128, p. 416–417

—— 1959, Significance of accumulator plants in rock weathering: Geol. Soc. America Bull., v. 70, p. 781–800

Mammatt, Edward, 1834, A collection of geologic facts and practical observations of the Ashby coal-field: London, W. Hextall, 101 p.

McConnell, Duncan, Levinson, A. A., and de Pablo-Galan, Liberto, 1956, Study of some chemically analyzed Ohio clays by X-ray diffraction and differential thermal analysis: Ohio Jour. Sci., v. 56, p. 275–284

McMillan, N. J., 1956, Petrology of the Nodaway underclay (Pennsylvanian), Kansas: Kansas Geol. Survey Bull. 119, pt. 6, p. 187–249

McQueen, H. S., 1943, Geology of the fire clay districts of east-central Missouri: Mo. Geol. Survey and Water Res. ser. 2, v. 28, 250 p.

Mitchell, W. A., 1955, A review of the mineralogy of Scottish soil clays: Jour. Soil Sci., v. 6, p. 94–98

Moore, E. S., 1940, Coal; its properties, analysis, classification, geology, extraction uses and distribution, 2d ed.: New York, John Wiley and Sons, Inc., 473 p.

Murray, H. H., 1954, Genesis of clay minerals in some Pennsylvanian shales of Indiana and Illinois, p. 47–67 *in* Swineford, Ada, *Editor*, Clays and clay minerals: Second Natl. Conf. Clays and Clay Minerals Proc., Natl. Acad. Sci.-Natl. Research Council Pub. 327

Patterson, S. H., and Hosterman, J. W., 1960, Geology of the clay deposits in the Olive Hill district, Kentucky, p. 178–194 *in* Swineford, Ada, *Editor*: Seventh Natl. Conf. Clays and Clay Minerals, Washington, D. C.

Rankama, Kalervo, and Sahama, T. G., 1950, Geochemistry: Chicago, Univ. Chicago Press, 912 p.

Ries, Heinrich, 1911, A review of the theories of origin of white residual kaolin: Am. Ceramic Soc. Trans., v. 13, p. 51–74

Rubey, W. W., 1952, Geology and mineral resources of the Hardin and Brussels quadrangles (in Illinois): U. S. Geol. Survey Prof. Paper 218, 179 p.

Schultz, L. G., 1958, Petrology of underclays: Geol. Soc. America Bull., v. 69, p. 363–402

Searight, W. V., 1955, Guidebook, field trip, 2d annual meeting, Association of Missouri Geologists: Mo. Geol. Survey Water Res. Rept. Inv. 20, 44 p.

Sprunk, G. C., and O'Donnell, H. J., 1942, Mineral matter in coal: U. S. Bur. Mines Tech. Paper 648, 67 p.

Stevenson, J. J., 1911–1913, The formation of coal beds: Lancaster, Pa., New Era Printing Co., 530 p.

—— 1916–1921, Interrelations of fossil fuels: Lancaster, Pa., New Era Printing Co., 458 p.

Stout, Wilber, 1923, Origin of coal formation clays: Ohio Geol. Survey Bull. 26, ser. 4, p. 533–568

Stout, W., Stull, R. T., McCaughey, W. J., and Demorest, D. J., 1923, Coal formation clays of Ohio: Ohio Geol. Survey Bull. 26, ser. 4, p. 103–492

Stutzer, Otto, and Noe, A. C., 1940, Geology of coal: Chicago, Univ. Chicago Press, 461 p.

Twenhofel, W. H., 1950, Principles of sedimentation, 2d edition: New York, McGraw-Hill Book Co., 673 p.

Waagé, Karl, 1950, Refractory clays of the Maryland coal measures: Maryland Dept. Geology, Mines, and Water Resources Bull. 9, 182 p.

Walton, John, 1953, An introduction to the study of fossil plants: London, Adam and Charles Black, 201 p.

Wanless, H. R., 1931, Pennsylvanian cycles in western Illinois: Ill. State Geol. Survey Bull. 60, p. 179–193

—— 1950, Late Paleozoic cycles of sedimentation in the United States: 18th Internat. Geol. Cong., Great Britain, Rpt., pt. 4, p. 17–28

—— 1955, Pennsylvanian rocks of Eastern Interior basin: Am. Assoc. Petroleum Geologists Bull., v. 39, p. 1753–1820

—— 1957, Geology and mineral resources of the Beardstown, Glasford, Havana, and Vermont quadrangles: Ill. State Geol. Survey Bull. 82, 233 p.

Weller, J. M., 1930, Cyclical sedimentation of the Pennsylvanian period and its significance: Jour. Geology, v. 38, p. 97–135

—— 1931, The conception of cyclical sedimentation during the Pennsylvanian period: Ill. State Geol. Survey Bull. 60, p. 163–177

—— 1956, Argument for diastrophic control of Late Paleozoic cyclothems: Am. Assoc. Petroleum Geologists Bull., v. 40, p. 17–50

Weller, J. M., Wheeler, H. E., and Murray, H. H., 1958, Cyclothems: Am. Assoc. Petroleum Geologists Bull., v. 42, p. 442–447

Wentworth, C. K., Wells, R. C., and Allen, V. T., 1940, Ceramic clay in Hawaii: Am. Mineralogist, v. 25, p. 1–33

Wheeler, H. E., and Murray, H. H., 1957, Base-level control patterns in cyclothemic sedimentation: Am. Assoc. Petroleum Geologists Bull., v. 41, p. 1985–2011

White, David, and Thiessen, Reinhardt, 1913, The origin of coal: U. S. Bur. Mines Bull. 38, 390 p.

Manuscript Received by the Secretary of the Society, January 27, 1960
Publication Authorized by the Director, U. S. Geological Survey

JONATHAN BARRINGTON *E. I. duPont deNemours and Company, Gibbstown, N. J.*
PAUL F. KERR *Dept. Geology, Columbia University, New York, N. Y.*

Breccia Pipe near Cameron, Arizona

Abstract: Black Peak protrudes above a tableland of Navajo Sandstone on the Colorado Plateau just east of Echo Cliffs and 30 miles north of Cameron, Arizona. A breccia pipe on the west slope of the butte locally contains breccia fragments of sandstone, mudstone, shale, and altered dike rock believed to have been plucked from wall rocks and transported upward. Sources of uranium mineralization in the Cameron area may be inferred from the origin of the pipe.

A vesicular, silicified collar several feet thick encloses the pipe on three sides. Minute microacicular quartz overgrowths on quartz crystals in the wall rock suggest that explosive penetration of superheated steam formed the pipe. Irregularly distributed argillic alteration, silicification, and mineralization suggest subsequent hydrothermal activity.

Associated with the pipe are carbonates, alunite, gold, silver, iron, manganese, and possibly uranium and copper. Silica has been introduced in the largest quantities.

The butte was probably formed by vertical penetration by fluids of magmatic origin from below; this suggests a possible original source and one phase in the mechanism of introduction of mineralization in the Cameron area.

CONTENTS

Introduction 1661
Acknowledgments 1662
Regional structure 1663
Stratigraphy 1663
Intrusive dikes 1664
Breccia pipe 1667
General description 1667
Mode of formation 1670
Conclusions 1673
References cited 1674

Figure
1. Index map of the Cameron area, Arizona, showing the position of Black Peak 1662
2. Breccia pipe and quartzite outcrop on the south side of Black Peak 1663
3. Outcrop map of Black Peak 1665
4. Relationship of Black Peak to the truncated Echo Cliffs monocline 1666
5. Exposure of the stratigraphic section in the Echo Cliffs monocline 1668
6. Columnar quartzite in outcrop northeast of the breccia pipe 1670
7. Plan and sections of the breccia pipe 1671

Plate — Facing
1. Black Peak, Arizona 1672
2. Vesicular collar material from breccia pipe, Black Peak, Arizona 1673

INTRODUCTION

Black Peak lies approximately 30 miles north of Cameron, Arizona, and is about 4 miles southeast of The Gap (Fig. 1). The peak forms a conical butte that rises 300 feet above the generally flat-lying adjacent terrain of the Colorado Plateau (Pl. 1, figs. 1, 2). It contrasts with the light-buff sedimentary rocks on which it rests.

A cursory examination in the summer of 1958 suggested that the butte might contain a breccia pipe. Subsequently an aerial scintillometer survey indicated a radioactive anomaly, and the Cameron Mining Company and the Rare Metals Corporation of America initiated a drilling program. Seven holes were drilled, but no ore-grade mineralization was found. Chemical analyses showed traces of gold and silver, but no uranium, thorium, or copper.

The breccia pipe (Fig. 2) crops out about midway on the southern slope of the butte; it is partly obscured by wind-blown sand and float. The pipe core forms a shallow depression about 10 feet deep surrounded on all sides but the southern by a resistant collar of vesicular silicified breccia with a sandstone matrix. An altered monchiquite dike occurs on the butte below the pipe, whereas a thin fresh monchiquite dike occurs on the north side of the

Geological Society of America Bulletin, v. 72, p. 1661–1674, 7 figs., 2 pls., November 1961

butte. Navajo Sandstone near the pipe has been bleached and in places stained with iron oxide. Resistant quartzite crops out on the southern slope of the butte, and partially silicified and altered sandstone covers a large area. Figure 3 indicates the distribution of the normal and altered Navajo Sandstone with reference to the surface exposure of the breccia pipe.

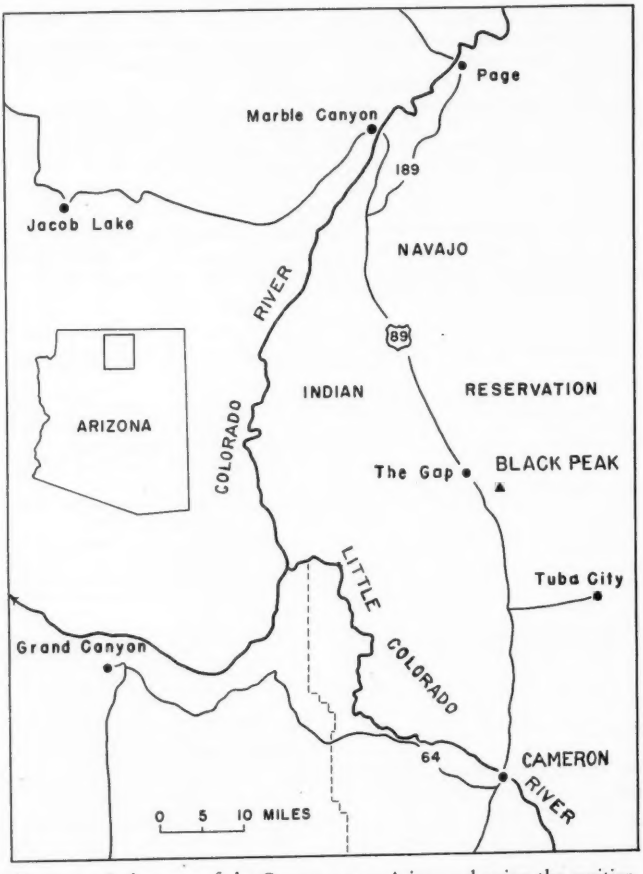

Figure 1. Index map of the Cameron area, Arizona, showing the position of Black Peak

ACKNOWLEDGMENTS

The authors express their appreciation to Mr. Page Blakemore, Jr., of the Cameron Mining Company, Cameron, Arizona, for his interest and generous donation of both time and effort in association with this study. The Rare Metals Corporation granted access to the drilling logs, which was most helpful. The sponsorship of the Division of Research and the Division of Raw Materials of the U. S. Atomic Energy Commission made this study possible. Discussions with Mr. E. M. Bollin of the Department of Geology, Columbia University, concerning the geology and the mineralization in the Cameron area were of great assistance.

REGIONAL STRUCTURE

Black Peak rises a few thousand feet east of the Echo Cliffs monocline at the western edge of the Preston bench, a structural feature of the Black Mesa basin of northeastern Arizona. The Preston bench has an over-all structural relief of not more than a few hundred feet. It is moderately folded with north-trending structures. To the east the bench grades into the Red Lake monocline, which separates it from the Kaibito saddle and the Black Mesa basin; on the south it grades into the Cameron bench; and on the north it inclines into the Kaiparowits basin (Kelley, 1958). Numerous local small faults and fractures trend northerly and northeasterly and form a prominent fracture pattern in the Navajo Sandstone, the generally exposed formation in the vicinity of the butte.

The Echo Cliffs monocline represents the most prominent part of the Echo Cliffs uplift, a long, narrow, northward-trending structure that is concavely arcuate and asymmetrical (Gregory, 1917). According to Kelley (1958), the Echo Cliffs uplift represents an intermediate step between the lower Preston bench to the east and the Kaibab uplift to the west.

Figure 4 shows the position of the butte relative to the Echo Cliffs monocline and the trend of the fracture pattern.

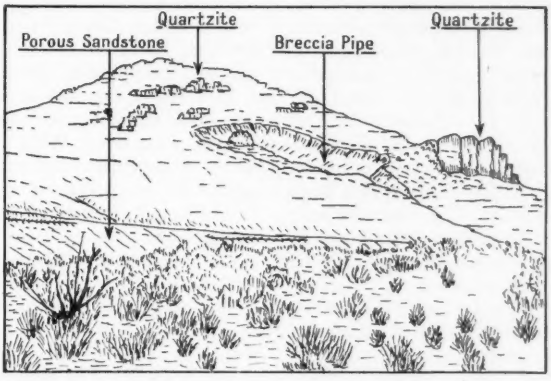

Figure 2. Breccia pipe and quartzite outcrop on the south side of Black Peak

STRATIGRAPHY

Black Peak originated in Navajo Sandstone and forms an isolated erosional remnant because of the cementation that accompanied the mineralization associated with the formation of the pipe. The Navajo Sandstone constitutes the uppermost formation of the Glen Canyon Group. This group overlies the Chinle Formation and underlies the Carmel Formation (Middle and Late Jurassic). The Glen Canyon Group and the upper portion of the Owl Rock Member of the Chinle crop out along Echo Cliffs about 1 mile west of Black Peak where a fairly complete section is exposed (Fig. 5). Harshbarger, Repenning, and Irwin (1957) have described the Glen Canyon Group in this area in detail; and Akers, Cooley, and Repenning (1958) have described the Chinle.

The Navajo Sandstone ranges from buff tan to orange red, being predominantly buff in the vicinity of the butte. It pronouncedly shows large-scale, relatively high-angle cross-bedding, and Baker, Dane, and Reeside (1936) interpret it as an eolian sandstone. The rock is composed of medium- to fine-grained subangular to rounded quartz grains with small amounts of microcline. Thin sections show occasional grains of tourmaline and biotite. The sandstone is friable and disintegrates easily when rubbed by hand. Numerous sand dunes derived from the Navajo have formed on the Preston bench around the butte.

The writers estimate the depth from below the surface exposure of the pipe to the underlying Kayenta Formation of the Glen Canyon Group, or the base of the Navajo, as 700 feet. In the vicinity of Black Peak along Echo Cliffs the Kayenta is 470 feet thick. Along the

many miles of the cliffs it grades from a sandy facies on the northeast to a thicker silty facies on the southwest. Along the cliffs here and farther south near Tuba City the silty facies predominates with thin interbedded layers of red sandstone.

The Moenave Formation, the lowest formation of the Glen Canyon Group in this area as defined by Harshbarger, Repenning, and Irwin (1957), underlies the Kayenta Formation. It comprises the upper Springdale Sandstone Member and the lower Dinosaur Canyon Sandstone Member. The Springdale is a red, resistant unit that forms a conspicuous shoulder along the Echo Cliffs. The rock is composed of fine- to medium-grained, subangular to angular grains and displays both claystone lenses and conglomeratic zones. The Dinosaur Canyon Member is a fluvial sandstone with a considerable proportion of associated eolian sandstone. The rock is coarse- to fine-grained with large amounts of silty material. The Moenave near Black Butte is 460 feet thick and consists of 160 feet of Springdale Sandstone with 300 feet of Dinosaur Canyon Sandstone.

Below the Moenave is the Chinle Formation, which, in the region of Black Butte, displays a total thickness of approximately 1200 feet (270 feet of the Owl Rock, 850 feet of the Petrified Forest and about 100 feet of the Shinarump). The Owl Rock Member is separated from the Moenave by an unconformity and consists of interbedded limestones and calcareous siltstones. The limestone contains chert nodules and mud pellets; bedding in the siltstone is irregular and lenticular (Akers, Cooley, and Repenning, 1958). The Petrified Forest Member, consisting of various zones of mudstone and associated sandy or conglomeratic facies, underlies the Owl Rock. The base of the Chinle is the conglomeratic Shinarump.

The Moenkopi Formation, a red silty sandstone with local variations to mudstone and to coarser sandstones, represents the base of the Triassic in the area. Unconformities separate the Moenkopi from the Shinarump above and from the Permian Kaibab Limestone below. Near Black Peak the Moenkopi is 300 feet thick. Beneath the Triassic strata are formations characteristic of the Paleozoic section at the eastern end of the Grand Canyon, probably extending down to the Precambrian.

INTRUSIVE DIKES

Mafic dikes are associated with the breccia pipe at Black Peak (Fig. 3). Altered dike rock is found near the pipe on the south side of the butte, whereas a thin unaltered dike crops out on the north.

UNALTERED DIKE ROCK: The unaltered dike occupies a narrow, vertical fracture that strikes N. 15° W. and approximately parallels the regional fracture direction in the Navajo Sandstone. This fracture and two that lie parallel on the north side of the butte extend from the base almost to the summit of the cone. A similar large fracture occurs on the south side of the butte about 300 feet east of the pipe. The altered dike strikes roughly parallel to these fractures. No dike rock was observed in the other fractures.

The unaltered dike ranges in width from 1 to 3 feet and is exposed for approximately 170 feet. Hand specimens are black to black green with limonitic stains. White centers of carbonate are common, and carbonate-filled fractures parallel and perpendicular to the strike cut the rock, forming a symmetrical rectangular fracture pattern.

The rock appears aphanitic, and both biotite and magnetite may be seen with a hand lens. In thin section, it is porphyritic, showing replaced olivine crystals averaging 0.5 mm in diameter in a matrix of fine-grained augite and opaque minerals. The writers estimate of the mineral content, on the basis of thin-section examination, is: dolomite (after olivine), 25 per cent; augite, 45 per cent; biotite, 14 per cent; magnetite, 10 per cent; and nepheline 4 per cent, with accessory apatite, quartz, chabazite, and limonite. X-ray diffraction studies show that the dolomite has completely replaced olivine: the euhedral, prismatic outlines of the original mineral remain. Dolomite also occurs as small veins cutting the rock and represents the carbonate observed in hand specimens. Chabazite occurs at the center of a few of the replacement masses. X-ray fluorescent spectrometry indicates that the magnetite is titaniferous. It is present as small euhedral cubes not more than 0.05 mm in diameter and is contained in crystals of other minerals, including the replaced olivine, indicating that it was probably the first mineral to crystallize. The augite occurs as pale-green slightly pleochroic blades elongated along the *b* and *c* axes. Crystals are euhedral and fine-grained, averaging 0.01 mm in width and 0.03 mm in length.

Biotite occurs as large crystals, which average 0.03 mm in diameter, in a fine groundmass. It is subhedral, brown, and strongly absorptive

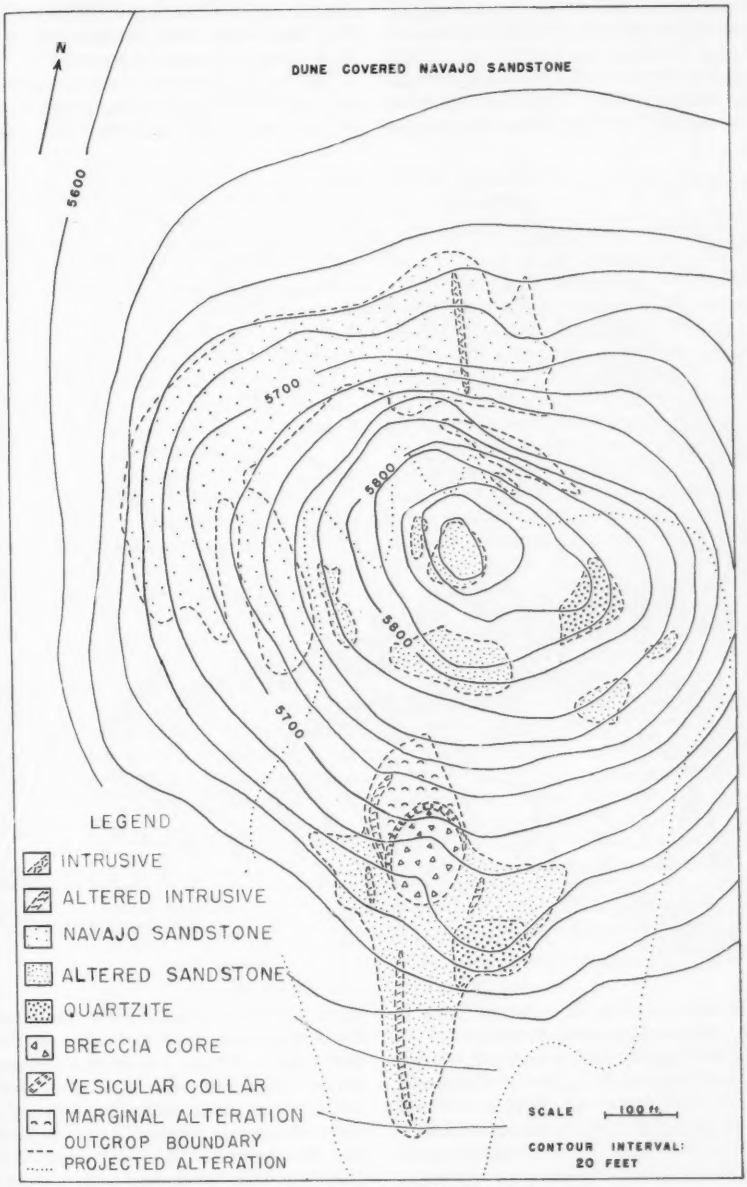

Figure 3. Outcrop map of Black Peak

with inclusions of euhedral magnetite, augite, and apatite. Much of the biotite has formed at the edge of olivine crystals and may represent a reaction between the early formed olivine and the modified melt. Nepheline represents the last mineral to form from the igneous deuteric effects associated with an excess of CO_2 and water. The presence of chabazite further suggests such a process.

The Navajo Sandstone within 1 foot of the dike is an unusual red, owing to small amounts of introduced iron oxide that coat the sand

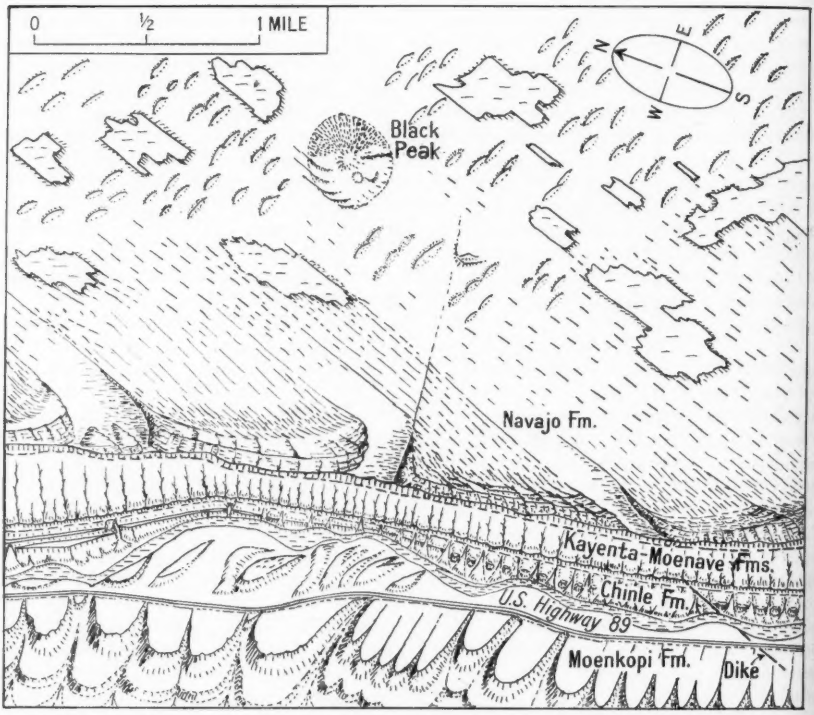

Figure 4. Relationship of Black Peak to the truncated Echo Cliffs monocline. Note prominent regional fracture in the Navajo Sandstone; outcrop of stratigraphic section in the Echo Cliffs sketch of a vertical aerial photograph.

phase. It occurs as small anhedral crystals filling the interstices in the augite matrix.

On the basis of mineral content and texture the rock is a monchiquite, a subtype of lamprophyre rich in Na_2O. As Williams (1936) showed, monchiquite is the common dike rock of the western portion of the Navajo country and contains unusual amounts of titanium. Excess phosphorus in the form of apatite is also common.

Turner and Verhoogen (1951) hold that dolomitic alteration is common for this rock type: they believe it represents late-stage grains. No alteration effects produced by raised temperatures are observed in thin sections from specimens collected at or near the contact with the dike, indicating that the emplacement of the intrusive mass had little effect on the sandstone. The writers believe that the dike was emplaced within a short time, had only moderate heat content, and cooled rapidly.

An aqueous phase became prominent subsequent to emplacement or, perhaps, during the last stage of crystallization. This phase presumably contained mineralizers such as CO_2

and sulfate, as indicated by dolomitization and traces of alunite in the sandstone adjacent to the dike. Samples of sandstone from the fracture openings parallel to the dike display traces of alunite as well as calcite, indicating that aqueous solutions were distributed over a large part of the butte.

Bowen and Tuttle (1949) suggest that the alteration of olivine in lamprophyres to a talc-carbonate phase without the development of serpentine indicates a rather high temperature of replacement, somewhat above 500°C. This may imply that the aqueous solutions originated with the dike rock either from a common source or as a differentiate from the cooling dike rock. These apparently high-temperature solutions must have been active for only a short period of time as indicated by the lack of alteration and appreciable mineralization in the adjacent sedimentary rocks.

HYDROTHERMAL ALTERATION: The dike rock on the south side of the butte, in the vicinity of the breccia pipe, has been altered almost completely to montmorillonite of the 14.6A basal spacing type. The only other alteration mineral found in appreciable amounts, as indicated by X-ray diffraction, is actinolite. However, small amounts of calcite, quartz, illite, and limonite occur. The rock crumbles easily in the hand and is gray brown to gray green. It displays white specks on the surface corresponding to the carbonate-replaced olivine phenocrysts. Such modifications suggest extensive, moderate- to high-temperature hydrothermal alteration of the dike rock. The alteration is not believed to be a weathering phenomenon or a deuteric effect because of the comparatively fresh nature of the dike rock on the north side of the butte.

BLACK PEAK DIKE: A dike of mafic igneous material occurs slightly more than 2 miles south of Black Peak and strikes generally parallel to the regional fracture. This dike appears along the face of the Echo Cliffs (Figs. 4, 5). Thin sections show it is similar to the dike rock at Black Butte, the only major difference being in the nature of the deuteric alteration. Mineralogically and texturally it is almost identical to the fresh rock on the north side of the butte. The rock may also be classified as a monchiquite. The olivine phenocrysts in this dike, named, for convenience, the Black Peak dike, have been largely altered to serpentine, with little dolomite. Bowen and Tuttle (1949) interpret such an occurrence as indicating a lower temperature of deuteric alteration than that indicated by the carbonate-rich phase observed at the butte itself. In general, this dike rock, while relatively near the butte, was subjected to lower temperature and less intense hydrothermal alteration than the igneous material at Black Peak.

BRECCIA PIPE

General Description

The breccia pipe at Black Peak is not prominent, but it is clearly outlined on close examination. In places wind-blown sand and float partly conceal the circular pipe exposure. An absence of extensive slumping within the pipe has also retarded the development of pronounced topographic expression in the pipe itself, although associated silicification is largely responsible for the residual cone of Black Peak.

Figure 3 shows the position of the pipe with its relationship to alteration zones and the dike rock. A vesicular, silicified collar several feet thick borders the pipe, and a zone of intense marginal alteration lies immediately uphill.

BRECCIA CORE: The central part of the pipe is approximately 100 feet in diameter and slightly ellipsoidal with the longer horizontal axis oriented about north-south. The core is breccia embedded in a loosely cemented sandstone matrix. The breccia consists chiefly of subangular to rounded pieces of sandstone, mudstone, black shale, and highly altered dike rock ranging from 1 inch to several inches in diameter. A few pieces of cemented sandstone approach 2 feet in diameter. The sandstone matrix shows no bedding and, in general, exhibits a random distribution suggestive of turbulent emplacement. Within the pipe a few small veins of black manganese oxide material cut through the matrix and fragments. X-ray diffraction shows the mineral to be psilomelane. The veins apparently formed after the brecciation.

VESICULAR COLLAR: A highly resistant collar displaying numerous small vesicles encloses the breccia core on all sides but the southern. The collar is about 10 feet thick and shows red hematite staining and lesser black manganese oxide staining. Its composition is much the same as the material in the pipe, but the breccia fragments are smaller, rarely exceeding 2–3 inches in diameter, and no pieces of altered dike rock may be observed. Its resistance to erosion, resulting from the silicification of the sandy matrix, makes it the most prominent topographic feature of the pipe area. In thin

section the grains of the matrix exhibit an unusual and interesting habit. Several of the original rounded grains, derived from the Navajo Sandstone, are encircled radially with acicular cyrstals of quartz (Pl. 2, fig. 1) that grow out from granular surfaces approximately at right angles. The interlocking needles provide strength for the collar since the intergranular spaces are not completely filled with silica. The quartz needles have the same optical orientation as the grains from which they protrude. The minute crystals are well crystallized.

X-ray examination shows the filling of the vesicles to be principally illite and calcite with a little accessory quartz. These materials weather away, leaving open vesicles or cavities. Many vesicles within the rock are partially open, indicating incomplete filling. Figure 2 of Plate 2 indicates the vesicular texture and its relationship to the pieces of breccia in the collar. Dark iron oxide stain rings many vesicles, indicating that the vesicles may form an extensive system through which solutions might travel. Most of the vesicles are on the order of half an inch to 1 inch in diameter, but some have diameters of up to 2 inches.

The vesicular nature of the collar indicates gas action and suggests the mechanism of formation of the pipe. The peculiar habit of the acicular quartz crystals may also imply the action of a gaseous phase. A high-temperature steam phase would foster the growth of quartz crystals, whereas low-temperature or colloidal systems would foster the growth of concentric layers of cryptocrystalline quartz. The low viscosity of a steam system would be expected to have the same effect as a high concentration of dissolved silica in a lower-temperature, aqueous phase. Morey and Hesselgesser (1951) have shown that the solubility of silica increases noticeably in a steam phase under pressure over that in an aqueous phase. A gaseous phase might be expected to provide more silica in a shorter period of time than a liquid phase, thus permitting a more rapid rate of crystal growth; hence it would provide

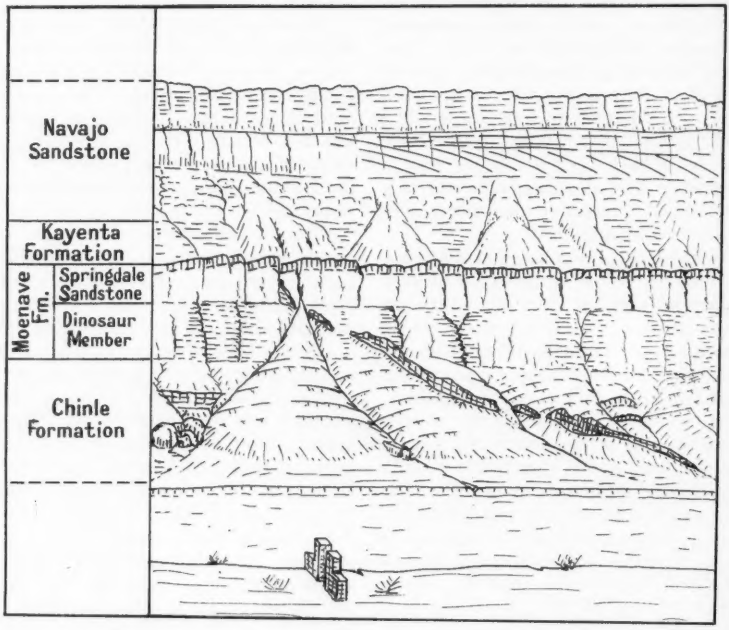

Figure 5. Exposure of the stratigraphic section in the Echo Cliffs monocline. Black Peak dike crosses the face of the cliff from lower right to upper left (old highway sign in foreground).

a more suitable environment in which minute, well-developed, individual crystals might form. The acicular clusters resemble crystals occasionally pictured as formed by gaseous transport in a furnace.

MARGINAL ALTERATION ZONE: A wedgelike area of intense marginal alteration approximately 50 feet across extends northward from the vesicular collar. Intense iron oxide staining and a poorly cemented matrix containing small areas of well-cemented material give the area the appearance of an extension of the breccia core. However, close examination of hand specimens and thin-section study indicate that the region is one of intense alteration and partial silicification. Apparent vesicles prove to be centers of clay alteration and solution activity. This marginal-alteration zone grades into the altered sandstone zone that surrounds the pipe area.

The alteration in this zone consisted of the formation of illite from kaolinite and microcline feldspar of the Navajo; bleaching of the original Navajo Sandstone; cementation of the sandstone by means of the filling of intergranular spaces; partial recrystallization of the rims of the sedimentary grains; and the introduction of iron oxide.

ALTERATION OF THE NAVAJO SANDSTONE: Alteration of the Navajo in the outer zone (Fig. 3) was not intense. The principal effect was the development of illite in place of kaolinite as an alteration of the microcline feldspar in the sandstone. The rock has become deep buff because of the extensive introduction of small amounts of iron oxide, presumably by circulating solutions associated with later phases of the breccia-pipe formation.

ALTERATION OF THE DIKE ROCK: As previously mentioned, the dike rock in the vicinity of the pipe has been highly altered to montmorillonitic clay with small amounts of actinolite, illite, quartz, and calcite. Such a mineral assemblage is indicative of intense hydrothermal alteration of the rock type observed as dike material on the north side of the butte. The close association of such intensely altered dike rock with the pipe, both as breccia fragments within the pipe and as altered dikes near the pipe, and the confinement of such alteration to the immediate vicinity of the pipe indicate that the formation of the breccia pipe involved a high-temperature aqueous phase.

MINERALIZATION: A small amount of mineralization occurs associated with the pipe. The introduction of silica is most noticeable, and at certain points a dense, white quartzite has been formed. Thin sections show that this quartzite is composed of grains of Navajo Sandstone cemented with introduced silica. The edges of grains are serrated, indicating partial recrystallization, and the rock may contain small amounts of calcite and illite formed by the replacement of feldspar. Figure 3 indicates the position of the prominent outcrops of this quartzite, but small amounts of quartzitic material occur throughout the altered zone of the Navajo Sandstone.

Outcrop surfaces of quartzite are dark as a result of manganese-stained desert varnish. Fresh surfaces are brilliantly white. Examination indicates that the silica has been introduced along minute vertical fractures within the Navajo, and that silicification spread out from these small fractures. In the intensely silicified quartzite outcrops these fractures are numerous, and the intersection of two and commonly three localized fracture patterns has led to the development of columnar-appearing quartzite (Fig. 6).

Calcite is widely distributed in the rocks at Black Peak, extending roughly north-south along the trace of the dikes and fractures. It occurs in interstices of the Navajo Sandstone and as fracture fillings in the various dike materials. Near the pipe but outside the intense marginal alteration zone it is closely associated with small prismatic crystals of alunite. Since neither of these minerals occur in the Navajo Sandstone examined outside the region influenced by the introduction of the pipe, the writers assume that they have been precipitated from fluids associated with the formation of the pipe. Calcite occurs to a certain degree outside the immediate area of the pipe, and certain points on the surface of the Preston bench adjacent to Black Peak show heavily iron-stained portions of the Navajo Sandstone. The iron staining appears to be confined to certain zones within the Navajo, and cross-bedding guided the transporting medium. These zones display dark-brown nodules composed of sand grains cemented by large amounts of calcite. The writers interpret the iron-stained zones with their nodules of calcite as evidence of the movement of solutions through the Navajo.

The writers examined Black Peak in detail as a result of the radioactive anomaly observed during an airborn scintillometer survey. However, little or no gamma radiation has been detected on the ground. The pipe was drilled in 1958 with a view to the development of

uranium, but chemical analyses failed to indicate either uranium or thorium, although traces of both silver and gold were reported. Analyses of drill cuttings from the breccia pipe showed small amounts of pyrite in an altered dike rock at a depth of 450 feet.

The principal mineralization at Black Peak has been the introduction of silica, iron oxide, and manganese oxide. The Navajo is so porous that soluble metal salts such as those commonly occurring with copper and uranium mineralization could have been removed.

uranium mineralization is associated with the copper minerals. Copper mineralization has been observed at other places in the Navajo, as for example along the top of the Echo Cliffs.

Black Peak provides an indication as to possible sources of mineralization. The cross-bedding control, mineralization centers, joint-pattern control, and presence of associated silicification suggest a close similarity between the features of the Black Peak mineralization and White Mesa deposits. The White Mesa copper and uranium could represent a point

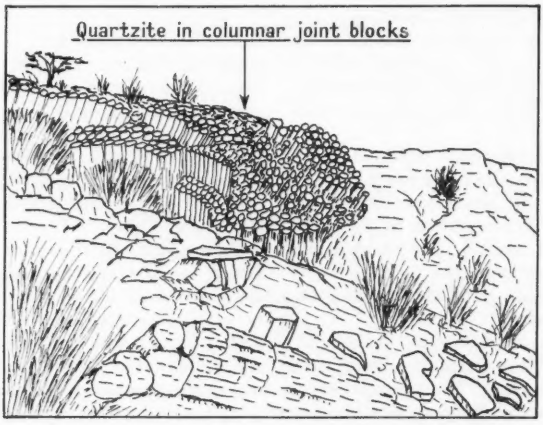

Figure 6. Columnar quartzite in outcrop northeast of the breccia pipe

Important metallic mineralization does occur elsewhere in the Navajo. The White Mesa copper deposit, for example, lies 30 miles northeast of Black Butte. Mayo (1955) reports that the mineralization there consists of malachite and chrysocolla with traces of azurite and copper pitch. Thin sections show that the copper minerals occupy the interstices between the rounded sand grains of the Navajo Sandstone. The area shows jointing and faulting trending northerly and northwesterly. Mineralization is associated with the jointing, and many joints show extensive silicification. Mayo refers to centers of mineralization with copper content decreasing with distance as "feeders." These feeders apparently represent original centers of rising solutions whose distribution was closely controlled by the prominent cross-bedding in the Navajo.

Some small chalcocite veins have been observed at White Mesa, and locally considerable higher up in the structure or mineralization similar in original source to the breccia pipe at the butte.

Mode of Formation

BRECCIA-PIPE STRUCTURE: Examination of the outcrop and consideration of the drilling logs suggest structure sections as illustrated in Figure 7. Drill holes put down adjacent to the pipe in the altered Navajo Sandstone met only the altered sandstone, which indicates that the pipe does not deviate to any great extent from the vertical. A drill hole put down in the marginal alteration zone emerged from this zone at a depth of 180 feet, suggesting that the zone may form a smaller circle at depth. The core log of a drill hole put down near the center of the breccia pipe shows that only breccia material was met to a depth of 450 feet. At this depth a small amount of altered dike rock bearing pyrite was met. At a depth of a little

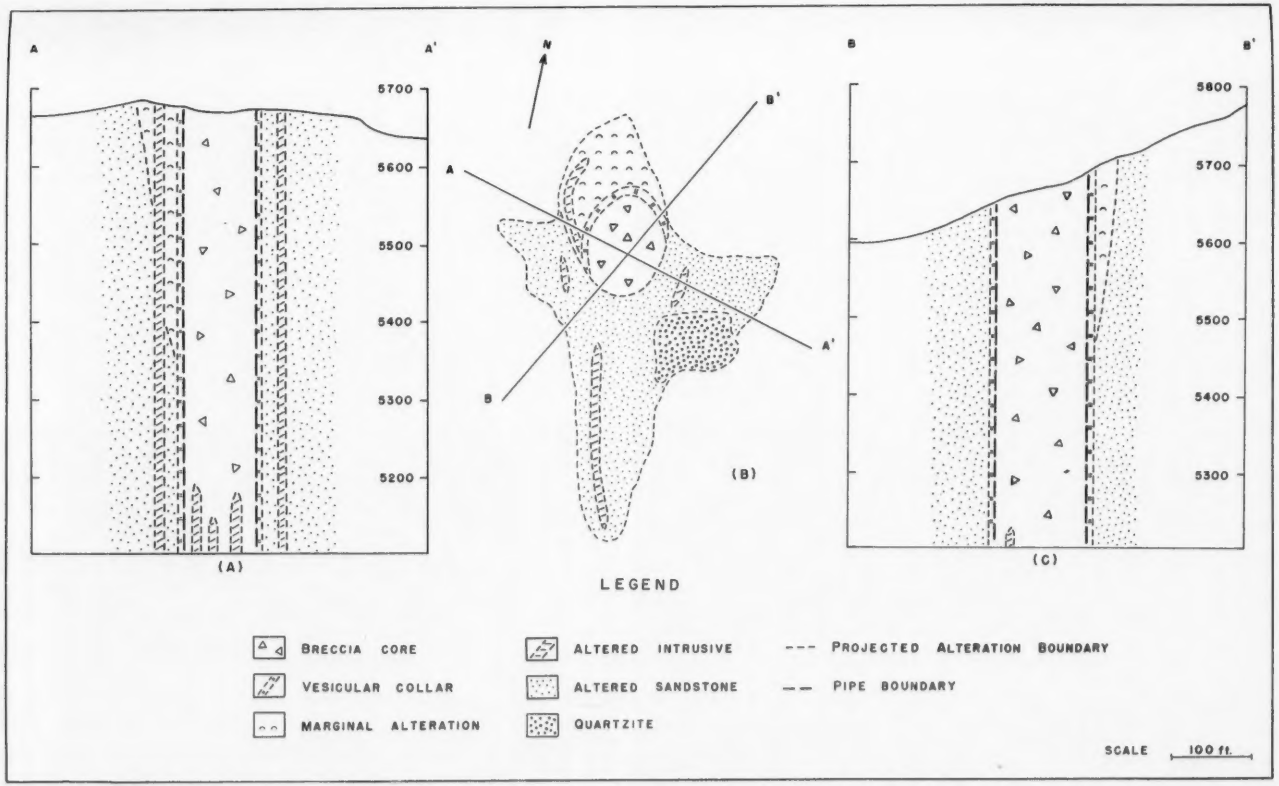

Figure 7. Plan and sections of the breccia pipe. A, cross section of the breccia pipe showing the relationship of monchiquite dikes; B, outcrop map of the pipe area indicating the position of the cross sections; C, portion of the breccia pipe where dike rock is absent

more than 500 feet, more breccia and dike rock were met. Figure 7A indicates schematically the position of this dike rock. The postulated relationship of dike rock to the pipe at depth shown is based on the proximity of the dikes to the pipe at the surface, on the vertical nature of the regional fractures, and the observed vertical orientation of dikes in the area. Figure 7C indicates the nature of the pipe in a section where the dike rock was not observed. The dikes are pictured as having a common origin with the pipe, but the writers have not established that their position or proximity were necessarily the primary controlling factors in determining the position or the structure of the breccia pipe. Gas action and hydrothermal alteration were probably more influential.

GAS ACTION: Several features at Black Peak indicate that the main mechanism of formation was gas action. The vesicular nature of the collar around the pipe suggests a vapor phase. The subangular nature of the breccia and the well-defined limits of the pipe proper negate the possibility of long-term passage of water, and small amounts of water probably would not have provided sufficient force or energy to create the pipe. The only indication of slumping in the pipe is a slight depression of not more than 10 feet within the silicified collar, which could have resulted from erosion. The surrounding sandstones show no warping either upward or downward to furnish evidence of solution stoping. The general picture is one of rapid penetration confined to a relatively small area—the pipe. The writers did not observe pyroclastics or lava at Black Peak, and it does not appear to be a volcanic explosion vent such as the Hopi diatremes (Hack, 1942). The most likely interpretation seems to be that the pipe was formed by the rapid passage of steam derived from the crystallizing dike rock or from a common parent magma, perhaps a sill-like mass at the base of the Paleozoic rocks as suggested by Williams (1936).

BRECCIA TRANSPORT: Several zones may have provided the source for the sandstone, mudstone, dike-rock, and black-shale fragments within the pipe, the most likely source of the black shale being the base of the Petrified Forest Member of the Chinle. If this source is accepted, the pipe-forming mechanism must have been capable of carrying a fragment approximately 6 inches in diameter a vertical distance of 2800 feet. Assuming a density of 2.3 for the black shale and applying Stoke's Law, a stream of water moving at a highly abnormal velocity would be required to transport such a fragment. Considering the size of the pipe and the velocity apparently required, one may calculate the rate of flow of water that would have occurred and, in turn, the amount of magma required as a source for this water. Goranson (1931) determined that a granitic magma could hold a maximum of 9 per cent dissolved H_2O at a temperature of 900°C and at a depth of 15 km, or 4 per cent at a depth of 2 km. Under these most favorable conditions, the amount of water required could have been obtained only if several thousand cubic feet of magma crystallized per day. Williams (1936) felt that any underlying igneous bodies must be mafic and would, therefore, have contained a very small per cent of water in the magmatic state, implying that even larger quantities of magma would have been necessary to supply the amount of water indicated. The presence of large mafic bodies underlying the region is not indicated at present.

It is unlikely that the black shale in the pipe descended from above or that the material within the pipe represents infilling. The monchiquite of the dikes resembles the monchiquite dike rock at other places in the region, and Williams (1936) relates these rocks both in age and origin to the Pliocene volcanic rocks of the district. He states that at the time of the formation of the dikes and necks of the Navajo country, the overlying Jurassic strata had been eroded away. This would indicate that the original upper extent of the pipe in Black Peak was either the same as it is today or slightly higher; the pipe probably never extended above the Navajo Sandstone. Further evidence of this is the nature of Tuba Butte, which also crops out in the Navajo Sandstone of the Preston bench. Tuba Butte is an explosion pipe displaying monchiquite lapilli and thin curved sheets of lava. Black Peak and Tuba Butte probably formed contemporaneously, with Black Peak representing somewhat more docile activity, either as a result of the magma not having penetrated quite as near the surface as at Tuba Butte, or as a result of the presence of smaller amounts of igneous material.

The black shale must have been introduced from below, and rapidly moving steam appears to have been the most probable transporting medium.

ORIGIN OF THE STEAM: The nature of the deuteric alteration in the dike rock on the north side of Black Butte points to the activity of aqueous phases at temperatures above 500°C.

Figure 1. Black Peak from the southwest. Aerial oblique view. Breccia pipe occupies area near end of drilling road.

Figure 2. Black Peak from the west

BLACK PEAK, ARIZONA

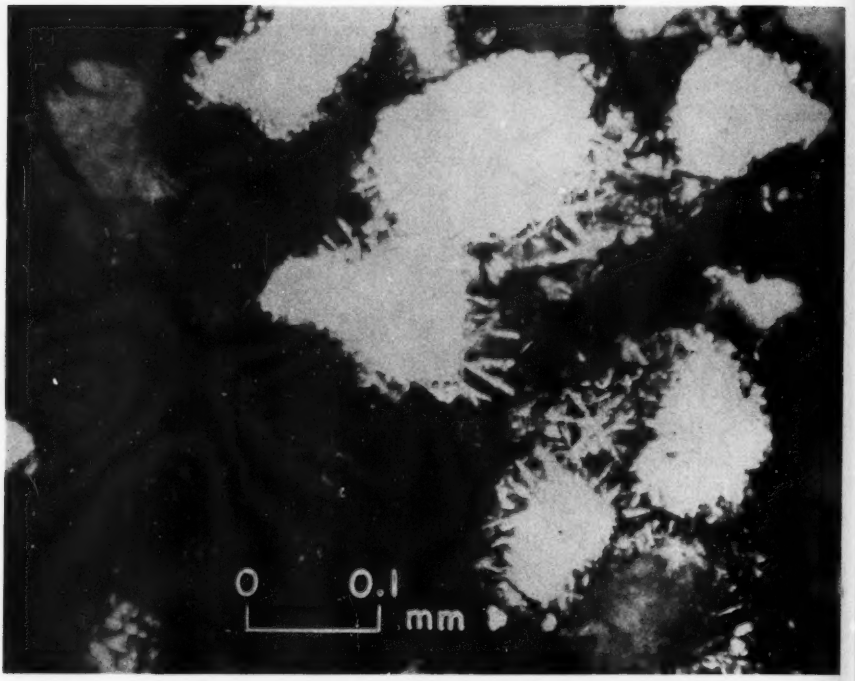

Figure 1. Acicular quartz growth. Needlelike crystals have grown normal to surfaces of quartz grains making up matrix in vesicular rock.

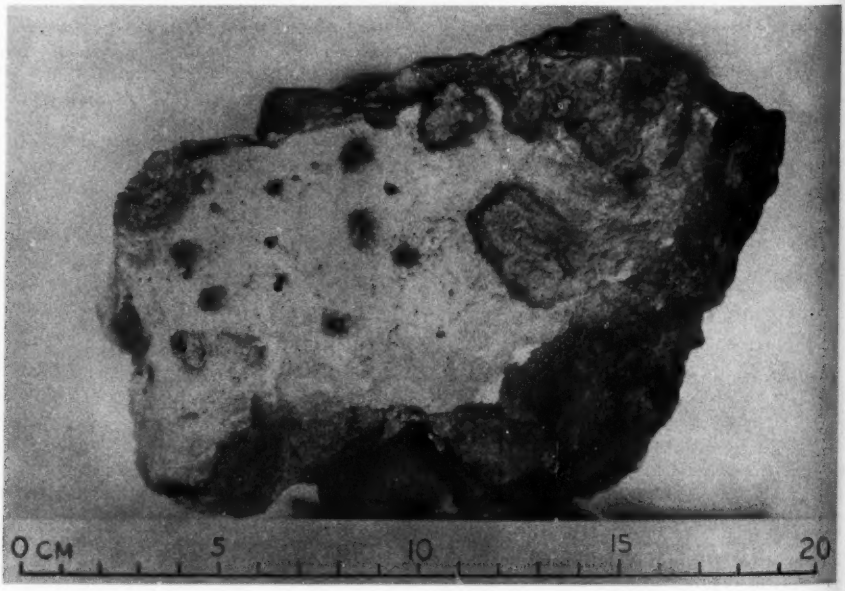

Figure 2. Unweathered vesicular collar rock with small breccia fragments, and silica-cemented sandstone matrix

VESICULAR COLLAR MATERIAL FROM BRECCIA PIPE, BLACK PEAK, ARIZONA

BARRINGTON AND KERR, PLATE 2

Geological Society of America Bulletin, volume 72

This is, of course, well above the critical temperature of water, 374°C, and further confirms the presence of steam. It seems probable that the steam was produced either during the crystallization of the dike-rock material at the butte or as a residual product of the crystallization of the underlying magma. Morey (1922) has pointed out that even in silicate systems where there is a very small amount of water in solution, tremendous pressures, resulting from large increases in the partial pressure of the water, are produced extremely rapidly as soon as crystallization of the melt begins. If the monchiquite magma penetrated almost to the surface before crystallization began, rapid cooling of this magma would have produced steam. The steam would have been produced so rapidly that large pressures would have built up, and eventually explosive penetration of the thin covering of Navajo Sandstone would have occurred, probably along lines of weakness represented by the regional fracture system.

FLUIDIZATION: In industry, a process called fluidization is used when accelerated mixing and chemical reaction are desired in a bed of fine-grained particles. The process involves passing a gas through the fine-grained bed. At a particular rate of gas flow the bed expands, and the individual particles become free to move. As the rate of gas flow is increased, bubbles form and travel upward through the expanded bed, agitating the solid particles. Under these conditions the bed is said to be fluidized. Continued increase in the rate of gas flow creates a greater number of bubbles until a large part of the gas travels as bubbles carrying suspended particles. The final result is the entrainment and transportation of the solid particles. Reynolds (1954) indicated that such a process could explain the origin of certain geological features. In particular, Reynolds discussed Cloos' (1941) investigation of the Swabian tuff pipes, considering these to be examples of large-scale intrusive fluidized systems. According to Cloos (1941) one pipe displays sharply defined inner and outer zones. The inner zone is composed of a higher proportion of material from deeper levels, indicating that this was the region of the most rapid flowage of the gas-tuff stream; the outer zone contains material from the adjacent wall rock, suggesting that the outer zone was a "stagnant" zone where little movement occurred. It is interesting to compare this zoning with the breccia pipe at Black Peak where a vesicular, silicified breccia collar surrounds a perhaps more highly disturbed central breccia core.

The writers suggest that the pipe at Black Peak was formed by the rapid passage of steam up through the Navajo Sandstone with perhaps less than explosive force but with a sufficient rate of flow to transport material upward from deep in the stratigraphic section. Brecciation of entrained fragments and homogenation of the matrix through a mechanism comparable with the industrial process of fluidization may have taken place. The activity represented probably occurred within a relatively short time, as there is no evidence of sufficient igneous material to have acted as a source of large quantities of steam. The small amount of mineralization associated with the pipe indicates a lack of any solvent in large amounts, especially when the increased solubility of materials in steam is considered. In a steam phase, much smaller quantities of solvent would be required to introduce the same amount of dissolved material as might be emplaced by a liquid phase. If formation of the pipe and associated features did occur within a short time interval, the alteration of the dike rock almost completely to montmorillonite may be interpreted as further evidence of the intensity of solvent action prevailing during the short duration of activity.

CONCLUSIONS

The breccia pipe at Black Peak was probably formed by the turbulent penetration of steam originating as an end-stage effect from the crystallization of underlying igneous material. Rapid passage of the steam through the stratigraphic column developed a fluidized, gas-solid system.

Silica was introduced both by the initial gas phase and by associated or later liquid phases. In the wall of the pipe, minute acicular crystals of quartz are formed on sedimentary quartz grains. Quartzite developed in altered sandstone nearby suggests that solutions penetrated into the border area. Calcite and alunite occur as interstitial crystals in the altered zone in the surrounding Navajo Sandstone.

Scintillometer surveys indicate small amounts of radioactive material, but uranium and thorium have not been reported in routine chemical analyses. This may mean that uranium or thorium have been largely absent, but the porosity of the Navajo Sandstone lends itself to the rapid removal of soluble salts, hence the metal content may have been greater than at present. The radioactivity indicated may be the

mass effect of small amounts of residual material. The iron oxide and psilomelane and the widespread occurrence of copper minerals nearby at White Mesa in the Navajo strata indicate that metallic mineralization is not foreign to this formation. Traces of silver and gold in and near the breccia pipe further suggest that metallic mineralization was associated with the formation of the pipe.

Black Peak contributes significant evidence pointing to (1) the upward transport of rock fragments, and (2) hydrothermal activity. Mudstone and black shale are found in the breccia pipe high above their stratigraphic position. Highly altered dike rock and induration of the Navajo Sandstone point to the action of ascending solutions. The butte represents a hardened remnant remaining as a cone after erosion of the surrounding and overlying strata. The alteration of mudstone to sericite and illite, the bleaching of the sandstone and black shale, and the intense alteration of dike rock to montmorillonitic clays further suggest hydrothermal activity.

REFERENCES CITED

Akers, J. P., Cooley, M. E., and Repenning, C. A., 1958, Moenkopi and Chinle formations of the Black Mesa and adjacent areas: N. Mex. Geol. Soc. Guidebook, 9th Field Conf., p. 88–94

Baker, A. A., Dane, C. H., and Reeside, J. B., Jr., 1936, Correlation of the Jurassic formations of parts of Utah, Arizona, New Mexico and Colorado: U. S. Geol. Survey Prof. Paper 183

Bowen, N. L., and Tuttle, O. F., 1949, The system MgO–SiO_2–H_2O: Geol. Soc. America Bull., v. 60, p. 439–460

Cloos, H., 1941, Bau und tatigkeit von tuffschloten. Untersuchungen an dem Schwabischen vulkan: Geol. Rundschau, v. 32, p. 709–800

Goranson, R. W., 1931, The solubility of water in granite magmas: Am. Jour. Sci., v. 22, p. 481–502

Gregory, H. E., 1917, Geology of the Navajo country: U. S. Geol. Survey Prof. Paper 93

Hack, J. T., 1942, Sedimentation and volcanism in the Hopi buttes, Arizona: Geol. Soc. America Bull., v. 53, p. 335–372

Harshbarger, J. W., Repenning, C. A., and Irwin, J. H., 1957, Stratigraphy of the Uppermost Triassic and Jurassic rocks of the Navajo country: U. S. Geol. Survey Prof. Paper 291

Kelley, V. C., 1958, Tectonics of the Black Mesa basin region, Arizona: N. Mex. Geol. Survey Guidebook, 9th Field Conf., p. 137–144

Mayo, E. B., 1955, Copper, *in* Mineral Resources, Navajo-Hopi Indian reservations, Arizona-Utah; v. 1—Metalliferous minerals and mineral fuels: Tucson, Univ. Ariz. Press, p. 19–32

Morey, G. W., 1922, The development of pressures in magmas as a result of crystallization: Wash. Acad. Sci. Jour., v. 12, p. 219–230

Morey, G. W., and Hesselgesser, J. M., 1951, The solubility of some minerals in superheated steam at high pressures: Econ. Geology, v. 46, p. 821–835

Reynolds, D. L., 1954, Fluidization as a geological process, and its bearing on the problem of intrusive granites: Am. Jour. Sci., v. 252, p. 577–614

Turner, F. J., and Verhoogen, J., 1951, Igneous and metamorphic petrology: New York, McGraw-Hill Book Co., Inc., 580 p.

Williams, H., 1936, Pliocene volcanoes of the Navajo-Hopi country: Geol. Soc. America Bull., v. 47, p. 111–172

Manuscript Received by the Secretary of the Society, March 8, 1960

BAHNGRELL W. BROWN *Mississippi Southern College, Hattiesburg, Miss.*

Stochastic Variables of Geologic Search and Decision

Abstract: Certain problems of geological search and decision can be treated stochastically. The basic equation for search and decision problems is

$$p = r_t^2/r_s^2 ,$$

where p is the probability of a success and r_t and r_s are radii of circles inscribed in the respective target and search areas. Completely blind search, or "wildcatting" involves contingent probability. The equation for successful wildcatting of a linear target in a linear belt is

$$P_{kit} = p_v p_x = \left[\frac{(1)! \left(\frac{b}{a} - 1\right)!}{\left(\frac{b}{a}\right)!} \left(\frac{c}{d}\right) \right],$$

where ca is the area of a random target and bd is the area of a randomly searched belt.

All geologic decisions, however insignificant, have economic implications when integrated into the search effort. The economic aspect of the search game may be expressed by the equation

$$XB = n \left[\frac{T}{S} \sum a - \left(1 - \frac{r_t^2}{r_s^2}\right) \sum_{1}^{B-1} b \right] = K,$$

where X is the interest on investment B, n is the number of trials, T/S is the probability of success, a is net value of a discovery, r_t and r_s are radii of target and search areas, b is the exploration cost, and K represents the total gain of the game.

CONTENTS

Introduction 1675
Decision 1676
The covered-interval decision 1676
Sampling decisions 1678
Choice of hypothesis 1679
Search 1680
Random search for random targets 1680
Random search for aligned targets 1682
Patterned search 1683
Game decisions and search economics 1684
Summary and conclusions 1685
References cited 1685

Figure
1. Covered interval separating vein segments *a* and *b* 1676
2. Fault interpretation for Figure 1 situation . . 1676
3. Two-vein interpretation for Figure 1 situation 1676
4. Continuous vein interpretation for Figure 1 situation 1676
5. Figure 2 interpretation supported by extant fault in adjunct area 1677
6. Quandary in a *universe* of random facts . . . 1677
7. Inscribed target area (T) and search area (S) . 1681
8. Diagrammatic illustration of parameters of search of point Y for area I, or area I for point Y, in a field of nine equally probable areas 1682
9. Search in an alignment situation 1683

INTRODUCTION

Kneale (1949, p. 19) stated

"When a geologist says that certain marks on a mountain-side were probably caused by a glacier during the Ice Age, it may seem that the question at issue has no relevance at all, or only the most remote, to any practical decision, but it should be remembered that intellectual inquiry is itself a kind of practice which requires decisions from time to time. If the marks were probably caused by a glacier, it is reasonable to proceed with the construction of a theory according to which the whole region was once much colder than it is now, and a decision to work this hypothesis out in detail is practical in the sense that it commits the geologist to a great deal of activity. At the least he will have to direct his attention to other consequences of the hypothesis, but there may be need also for physical actions, such as travelling to places where he can make new observations or consult the books of other scientists. Whenever we choose to pursue one line rather than another in our theorizing, we make

Geological Society of America Bulletin, v. 72, p. 1675–1686, 9 figs., November 1961

a practical decision; and it often happens that such decisions can be justified only by consideration of probability."

If Kneale were a geologist rather than a mathematician, he might also have recognized that geology is an integrated science, and that in the indisputably practical effort of economic production the exploration geologist cannot ignore even so seemingly insignificant a fact as glacial scour.

The writer (1959, p. 651) has similarly pointed out that geology is very much a probabilistic science, even where the stochastic operations may have been more implied than quantitatively treated. Considering the integrated nature of our geological science we should, perhaps, concede the need for a more qualitative approach than that of the strictly laboratory sciences. Nevertheless, certain aspects of earth science can be studied quantitatively by means of the probability calculus. This paper examines in an introductory stochastic way some of the quantitative aspects of decision and search.

The writer is grateful to Claude Albritton for his critical review of this paper.

DECISION

The Covered-Interval Decision

Almost every field geologist has at some time faced the covered-interval problem. Even in areas of reasonably good exposure one will find an occasional slide or scree slope that more or less obscures the vision. When a geological decision must be made, and where it is impractical to strip away the overburden, as is most often the case, the geologist has only his art to rely on and a nebulous judgment principle called, for want of better name, field experience.

Some geological decisions do involve high probability or even certainty, but many decisions must be made in spite of limits placed on evidence. The "doubting Thomas" sort of field worker who recognizes no faults except those which have slickensides that he can feel will undoubtedly miss the over-all structural picture of any problem.

One of the simpler decision problems, that of the covered interval separating and obscuring two vein segments (Fig. 1, *a* and *b*), harassed the writer during a study of huebnerite veins in the Tobacco Root Mountains of Montana. Scree slopes obscured structurally critical areas. Repeatedly the same question arose: what happens to the vein segments beneath the covered interval?

Figures 2, 3, and 4 show the three possibilities: (1) a vein is faulted, (2) there are two veins terminating somewhere in the covered area, and (3) the segments swing to join in one continuous vein. As the writer has drawn the

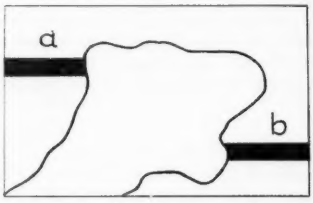

Figure 1. Covered interval separating vein segments *a* and *b*

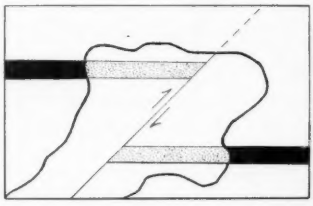

Figure 2. Fault interpretation for Figure 1 situation

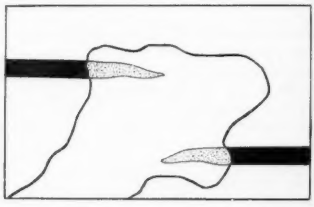

Figure 3. Two-vein interpretation for Figure 1 situation

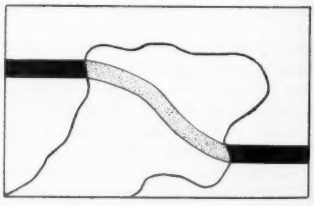

Figure 4. Continuous vein interpretation for Figure 1 situation

figure, purposely limiting the perspective, there can be no other basis for decision than a random choice between the three equally probable solutions illustrated. Therefore, the *a priori* probability that any one of the solutions presented is correct is 0.33. Such a low probability value is inadequate basis for economic work.

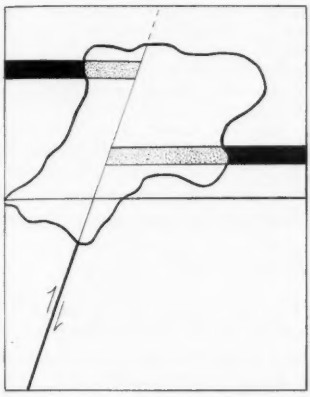

Figure 5. Figure 2 interpretation supported by extant fault in adjunct area

No competent field geologist would attempt a decision without referring to adjacent areas or considering the vein in its structural setting. As a qualitative decision, a geologist would, perhaps, favor a fault interpretation if faulting of veins were common in the neighborhood. In following this course of action he would be assigning to the set the equivalent parameters of the group of which the set appeared to him to be a member. The writer feels reasonably certain that where a fault trend could be established in the adjunct areas, as illustrated in Figure 5, one's confidence in a fault interpretation would soar.

If each covered-interval decision is studied in its own *universe*, it is consistent with qualitative geological practice to equate the decision probabilities with statistically determined probabilities of known events in the *universe*. Let us for our example assume a *universe* of one township and place in its section 16 a covered-interval situation (Fig. 6). Let us further postulate that all sections but number 16 are knowable and known, and that in the 35 knowable sections 15 of 19 similar situations involve faults. In all, there are 20 similar vein-segment pairs in the total *universe* (section 16 included). The probability of a fault within this *universe* is as high as 15/20 or 0.75, and this would at first inspection also seem a reasonable probability for a fault in the covered interval.

There is still another approach to this problem, one which, because it yields a probability value closer to the *a priori* value, is, perhaps, the more conservative. We may state that it is not known that section 16 has the parameters of the group in question, or that the group is in the same *universe* occupied by section 16. It is always possible that the phenomenon represented in section 16 is not contemporaneous with the others. We may equally state that it is not known it *isn't*. Because the probability of group membership for this decision subject is one of equal likelihood, the general probability equation can be written as follows:

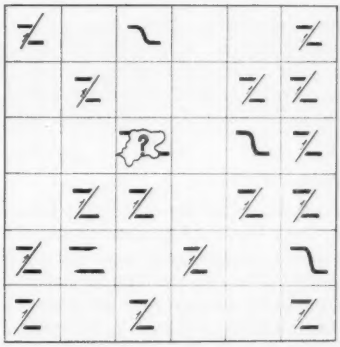

Figure 6. Quandary in a *universe* of random facts. (A diagrammatic township representing the *universe* for a covered-interval decision problem situated in section 16, indicated by (?). This township is known to contain 15 faulted veins, 3 continuous veins, and 1 double vein; all situations are possible solutions.)

$$P = \frac{p_i + (p_e\, p_c)}{2}$$

where p_i is the intrinsic or *a priori* probability that the event is as stated, p_e is the external or *statistical* probability of the event as determined in the study area or *universe*, and p_c is the contingent probability of confidence that the known *universe* parameters and the group parameters are identical.

In the township problem set up for an illustration p_i is 1/3 (because there are three equally probable events), p_e is 3/4 (because the indicated *universe* probability is 15/20), and p_c is 35/36 (because 1/36 of the *universe* remains unknown). For the problem,

$$P = \frac{\left(\frac{1}{3}\right) + \left(\frac{3}{4}\right)\left(\frac{35}{36}\right)}{2} = 0.53 .$$

Because this value is larger than 0.5, a fault decision would be acceptable for economic work. (The significance and limitation of 0.5 in the economic aspect of decision will be explained under *Game Decisions and Search Economics*.)

Sampling Decisions

Krumbein and Miller (1953) and Krumbein (1955; 1960) have adequately considered the more important aspects of statistical sampling. This study does not attempt to elaborate on the criteria for decision in a statistically valid sampling program but merely to reaffirm the fact that a statistically valid sample can itself become a sound basis for decision. To introduce this concept the writer quotes from Fisher (1954, p. 278–279):

"With the aid of the eminent French conchologist M. Deshayes, Lyell proceeded to list the identified fossils occurring in one or more strata, and to ascertain the proportions now living. To a Sicilian group with 96 per cent surviving he gave, later, the name of Pleistocene (mostly recent). Some sub-appenine Italian rocks, and the English Crag with about 40 per cent of survivors, were called Pliocene (majority recent). Forty per cent may seem to be a poor sort of majority, but no doubt scrutiny of the identifications continued after the name was first bestowed, and the separation of the Pleistocene must have further lowered the proportion of the remainder. The Miocene, meaning 'minority recent,' had 18 per cent, and the Eocene, 'the dawn of the recent,' only 3 or 4 per cent of living species. Not only did Lyell immortalize these statistical estimates in the names still used for the great divisions of the Tertiary Series, but in an Appendix in his third volume he fills no less than 56 pages with details of the classification of each particular form, and of the calculations based on the numbers counted. There can be no doubt that, at the time, the whole process, and its results, gave to Lyell the keenest intellectual satisfaction.

"Now the point of this little history, its point for statisticians, is that the statistical argument by which this revolution in geological science was affected was almost immediately forgotten. In later editions of the *Principles* this great Appendix, on which so much labour had been expended, has disappeared; it survived indeed only two years. It had served its purpose; the ladder by which the height had been scaled could be kicked down. Geologists could quickly recognize a fossiliferous stratum by a few characteristic forms with clear morphological peculiarities. There was no need to wait for extensive collection, or statistical tabulation. Nor does it seem to have been thought that future geologists had anything to learn from the example, or the particular method, of Lyell's discovery. His designations of the Tertiary formations remain as records of a forgotten past, like fossils themselves, less intelligible to the geological students than the casts of sea shells they extract from the rocks."

In general, samples are substitutes for the whole. In the Lyell example, this is true. The probability that any sample is representative of the whole may be expressed by the formula:

$$P = \frac{V_S}{V_T}$$

where V_S is the volume of the sample and V_T is the volume of the whole. The properties of the whole volume are the parameters sought in the sample. Conversely, any inferences based on the properties of the sample will have the probability of exactitude only in so far as the premises fit the parameters of the whole. In this respect, geologic sampling is no different from a mathematician's urn problem, or a coin-tossing problem.

Let us take a set of results of a series of coin tosses. Say that in 499 consecutive throws a *head* appeared as the result of each throw. The volume of the sample is 499. The volume of the *universe* or whole is an infinite number of tosses. On a more pragmatic level the whole volume would be some "statistically valid" quantity that is in a practical sense obtainable.

Now let us base a decision on the coin experiment. Either (1) the coin has two heads, or, (2) it has a tail but is biased, or, (3) it is an unbiased coin uniquely tossed. If, as the result of toss 500, a tail is observed, we will know for certain that the first hypothesis is 100 per cent in error. However, let us assume a tail does not appear on the 500th trial, nor even after a "statistically valid" number of tries. We can never be 100 per cent certain about the true status of the coin until the nth trial is made. The element of doubt will of course decrease with an increase in the number of trials, but certainty can never be reached. In other words, we have presented a case in which no amount

of sampling effort except the taking of the whole can give a certainty answer.

An analysis of the example has convinced the writer that decisions based on sampling usually involve at least four sorts of probability viewpoints, as follows:

(1) The *a priori* probability of equal likelihood before the sampling effort, with no basis for a prior judgement.

(2) The statistical probability determined by experimentation (sampling) expressed as the fraction of total events favorable (in the sample) divided by total number of events (also in the sample).

(3) The ultimate probability expressed as the fraction of total events favorable (in the whole) divided by the absolute number of events (of finite magnitude).

(4) A judgement probability, which is to say an *a priori* probability that has been modified by experience of nonstatistical sampling.

In most geological examples the ultimate probability is unknowable.

Choice of Hypothesis

Sampling as a basis for decision is also a basis for choice of hypothesis. There is one significant difference, however, in the stochastic model for the choice of a hypothesis; there is no restrictive limit for the number of conceivable hypotheses from which to choose. The only conceptual limitation on the number of hypotheses is the imaginative fertility of the geologically trained mind.

As Good (1959, p. 445) has said, any hypothesis will have two probabilities; the initial or "prior" probability before some experiment is performed, and the "final" probability after the experiment is performed. Because the *a priori* likelihood of a hypothesis equals $1/n$ (where n is the total number of hypotheses), and because n is by the nature of its very development frequently a large number, the *a priori* probability of any given geologic hypothesis can be quite low. However, the lack of conceivable limitation does not mean n in this case is an infinite number. There are certain desiderata required of every valid geological hypothesis for its acceptance. First, it must be logically consistent within itself, and secondly, it must have been suggested by facts. These two acceptability requirements rule out a vast number of conceptual hypotheses that might be entertained by laymen.

Let us imagine a problem in which 10 discrete hypotheses have acceptance. We may presume that the hypotheses are mutually exclusive. In reality we could have two or more hypotheses that are equally correct in that some larger more inclusive concept was not developed at the outset. Let us further assume that at the start an equal number of facts suggested each idea, all of equal weight. Then, for any hypothesis A,

$$P_iA = 1/10 .$$

As additional experimentally determined facts either favor or disfavor hypothesis A over any other hypothesis, the initial probability of A is changed accordingly to become P_fA at the close of the experimentation; by LaPlace's law of succession,

$$P_fA = \frac{(r + 1)}{(n + 2)} ,$$

where r is the number of "successes", or facts in support of the hypothesis, and n is the number of trials, or facts gathered, inclusive of those that support other hypotheses or that support no hypothesis.

Referring now back to the covered-interval decision, we may wish to find our final probability in this choice decision in the same manner, finding it midway between the initial probability and the *a posteriori* probability. This can be calculated as follows:

$$P = \frac{(P_iA) + (P_fA)}{2} .$$

Indeed, we might have calculated the fault hypothesis in this way, also, with the following results based on $r = 15$ faults, $n = 20$ events;

$$P = \frac{(1/3) + (16/22)}{2} = 0.53 .$$

One may argue that, as more and more experimentation is done, the finalized probability should get farther from P_iA and closer to P_fA, and, ultimately, closely approximate either 1 or 0. The writer does not feel this objection is valid because we never know when n is at its greatest value or when geological experimentation is finished. Besides, it is not necessary to be certain of a hypothesis to prefer it. Any probability value larger than 0.5 would constitute automatic preference. The whole purpose of probability calculations is to conservatively predict a real state of being and is not to establish a fact as such.

SEARCH

Random Search for Random Targets

The economic search for blind or hidden fields of mineral and petroleum resources offers one of the most intriguing problems for stochastic construction. Nolan (1950, p. 601–608) has suggested that important ore districts may be hidden beneath the Columbia and Snake River volcanic rocks that might compare with those revealed within a 200 mile radius of Boulder dam. What an intriguing thought!

Lasky (1948) has questioned whether or not new mining districts could be found by the probability approach and doubts that the geologist has the ability to handle the complex probability factors in a realistic or successful way. He would substitute *permissibility* for probability. His statement (1948, p. 85) that this ". . . idea of geologic permissibility is not completely new, for the oil industry acts upon it as a matter of habit, requiring only permissive structure and some indication of source rocks", is really a stochastic point of view. In a discussion of Lasky's paper (Lasky, p. 89–90) T. M. Broderick pointedly remarked that without the geologist's rating of chances according to an implied geologic probability all search permissibility becomes as wild as blue-sky promotion.

The writer does not aim to defend or dispute Nolan's theorem, or to comment further on Lasky's contribution. Nolan's example is only one of the many that might illustrate the vast expanses of earth that, because of water, sand, or volcanic obscurement, are difficult to interpret structurally. For such areas there would seem to be, for the present at least, no methods of exploration except geophysics and blind search. Should geophysics for some cause fail, blind search alone remains.

Many questions might arise concerning blind-search areas. What would be the probability of success under various drilling programs? Would a target be more readily found within random-search or within patterned drilling? What would be the best pattern in a given search problem? And, furthermore, would the anticipated value of the target field justify the expected exploration expense?

The stochastic geologist can approach any problem with one of two states of mind; either he will have some little knowledge, or he will have no knowledge of it. We will consider blind search as meaning that there is no knowledge of the sought-after value other than the positive predilection that it exists as target area T, randomly placed in search area S at some unspecified but attainable drilling depth H.

Target area T may be one of a number of similar but hidden areas, and these may be arranged in some definite pattern, but this is not known, and the search would proceed as if the target existed alone. Some lineation may be suggested from the moment a second or third target is revealed, but to that extent the search is no longer blind but is pattern-controlled. As more and more targets of a structural pattern are revealed, the reality of the pattern would dominate the exploration thinking to the exclusion of other probability considerations, and the search would no longer be a blindly random effort.

The probability that a randomly selected point (drill hole) will fall in a target area, or a given point will fall in a random target area, is proportional to the respective areas of target and search fields:

$$p = \frac{T}{S}.$$

Levy and Roth (1947, p. 78–79) have shown that for simple curves, S for the curve bounding the search area and S' for a similar target area bounding curve, the basic probability relationship is given by the proportion;

$$\iint_{S'} dx\, dy \Big/ \iint_{S} dx\, dy,$$

which can be simplified as was done in the preceding formula.

From the standpoint of any practical drilling program, it may appear that a drill hole is not a point, but an area that has been known at times to miss real values when superposed on an ore body.

The first objection can be met with reference to the classic tile problem (Levy and Roth, 1947, p. 90) in which it can be demonstrated that if a circle (here the drill-hole section) of diameter d is thrown on a tile floor (here any gridded search area), the probability that it will lie on *one* tile (some specific area of the search area) is $(1 - d/a)(1 - d/b)$ when a and b are the two dimensions of the tile. In other words, the smaller d becomes and the larger the target area, the more likely will the *entire* circle fall within the target, which is to say that a small drill hole in search of a large

target acts as would a point in search of an area.

The second objection is a more serious one. We can only assume in each case that the penetration of the target area is tantamount to interception and sampling of the value. Massive ore bodies and finely disseminated deposits would probably satisfy the practical requirements of interception.

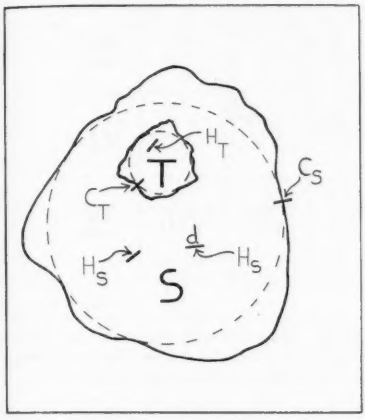

Figure 7. Inscribed target area T and search area S. (C_T, C_S, and H_T, H_S represent cuts and hits of a line of length d falling randomly in the respective target and search areas.)

A reasonable approximation for search and target areas of irregular shape would be the largest circles that could be inscribed in those areas (Fig. 7). If we let r_T equal the radius of the inscribed target circle and r_S equal that of the inscribed search circle, then because

$$p = \frac{T}{S},$$

$$p \cong \frac{r_T^2}{r_S^2}.$$

This relationship can be verified by using the Chalkley equation (Chalkley *et al.*, 1949, p. 295–297):

$$d\,\frac{H}{C} = \frac{\pi \text{ area}}{\text{perimeter}}$$

which for a circular area is,

$$d\,\frac{H}{C} = \frac{\pi r}{2},$$

where H is the number of hits in the area and C is the number of cuts on the perimeter of a circle of radius r by a line of length d randomly tossed on the circle.

Let us now assume that d is the diameter of a drill hole searching randomly for a target. All hits in the target area, H_T, can be counted successes. All cuts on the target perimeter, C_T, cuts on the search perimeter, C_S, and hits in the search area that avoid the target, $H_S - H_T$, will, because they are either misses or nearly so, be counted failures. For target circle T

$$\frac{H_T}{C_T} = \frac{\pi r_T}{2d}.$$

For search circle S

$$\frac{H_S}{C_S} = \frac{\pi r_S}{2d},$$

and,

$$\frac{\dfrac{H_T}{C_T}}{\dfrac{H_S}{C_S}} = \frac{r_T}{r_S}.$$

Because

$$p\,H_T = \frac{H_T}{H_S},$$

and

$$\left(\frac{H_T}{H_S}\right)\left(\frac{C_S}{C_T}\right) = \frac{r_T}{r_S},$$

$$p\,H_T = \left(\frac{r_T}{r_S}\right)\left(\frac{C_T}{C_S}\right).$$

As the probability of a cut on either the target circle or the search circle is proportional to their respective lengths,

$$\frac{C_T}{C_S} = \frac{r_T}{r_S},$$

and it follows that

$$p\,H_T = \frac{r_T^2}{r_S^2}.$$

Still another approach to proving the basic probability equation for blind search is from the viewpoint of degrees of freedom. In the classic coin-tossing game any coin with two unbiased throw chances has but one degree of freedom: the choice between a head and a tail.

Where F is the number of degrees of freedom and n the number of trials,

$$p = \frac{n}{n(1 + F)},$$

which for the unbiased coin equals one half.

A point searching for an area has the same freedom as an area searching for a point. In Figure 8 the point Y is in search of the randomly excluded area designated I. The parameters of Y are $(a,2)$ and of the area I, $(a,3)$. There are in all nine sets of parameters that designate some area equivalent to I. Because I corresponds to one of these, it has only eight degrees of freedom in its search for Y. The general freedom formulae for area search are given as:

$$F_A = \frac{A - not\ A}{not\ A}$$

and

$$p = \frac{n}{n(1 + F)}.$$

In the search problem illustrated in Figure 7 the freedom of search would be

$$F_S = \frac{S - not\ S}{not\ S},$$

and because

$$not\ S = T,$$

$$F_S = \frac{S - T}{T}.$$

The parameters of area are πr^2. Therefore,

$$F_S = \frac{\pi r_S^2 - \pi r_T^2}{\pi r_T^2} = \left(\frac{r_S^2}{r_T^2} - 1\right),$$

$$pH_T = \frac{n}{n\left(1 + \frac{r_S^2}{r_T^2} - 1\right)} = \frac{r_T^2}{r_S^2}.$$

This relationship, demonstrable in the several ways we have shown, is the probability that a given point will fall on a random area, or the probability that a random point will fall on a given area. It is not, however, the most reliable solution to a completely blind search wherein a random point is searching for a random area.

The probability that a randomly selected point will fall in a randomly located area is a contingent probability in which both point and area have their respective and independent degrees of freedom. Referring once more to Figure 8, the probability that target area I will be located at I is 1/9, and the probability that a randomly selected well point Y will also fall in I is 1/9. Therefore, the

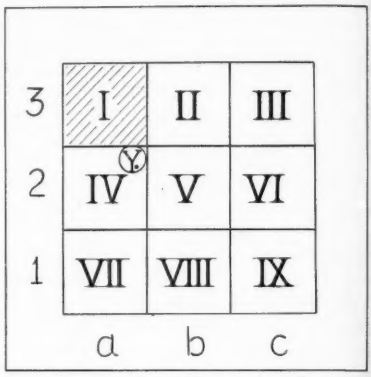

Figure 8. Diagrammatic illustration of parameters of search of point Y for area I, or area I for point Y, in a field of nine equally probable areas

probability that a random hole will penetrate the blind target area,

$$pH_T = p_I p_Y = \frac{1}{81} = 0.012.$$

As a general principle we can state that random search (wildcatting) for a random target has the lowest possible chance for success. On the other hand, a simple search pattern involving only 13 holes would guarantee penetration of the blind target in this illustration.

Slichter (1955, p. 885–915) has given considerable treatment to the application of probability theory in prospecting, especially for the function of target size and shape in the blind drilling of random targets.

Random Search for Aligned Targets

It can be shown that there is no increase in the search probability for blind search for a lineated target. The shape of the target and the mere fact that it will be found to be consistently elongate in one direction does not in the least affect the probabilities involved in random search, nor does the fact that the search area may be elongate in its shape alter the results.

Let us consider the problem of randomness of a linear target oriented in a linear search area (possible schist belt). In Figure 9 the search area (S') is bounded by (X,X') and (Y,Y'), and the target area (T) is bounded by (X,X_1) and (Y,Y_1). The probability of a random hit in the target area is

$$p = \left[1 - \left(\frac{b-a}{b}\right)\right]\left[1 - \left(\frac{d-c}{d}\right)\right]$$

with a, b, c, and d lengths indicated in the figure. The same value for P could also have been computed from the equation

$$p = \frac{T}{S'}.$$

If the target is now allowed freedom, as in blind random search, then there will be freedom not only in the point-seeking but in the possible motion of the target itself as it randomly seeks its position in the schist belt. As we have previously observed, such complete randomization makes the probability contingent. There are two degrees of freedom for a roving target; movement in the X direction and movement in the Y direction. If we first limit movement in the Y direction, the area of search (S) is bounded by cb and,

$$T = \frac{a}{b}S,$$

$$p = \frac{1}{C(n)r}, \text{ and}$$

$$p = \frac{r!(n-r)!}{n!} = \frac{(1)!\left(\frac{b}{a}-1\right)!}{\left(\frac{b}{a}\right)!} = p_Y,$$

where r is the number of successes and n the number of trials, which is also the probability of a point falling in the target as the target exercises its freedom in the Y direction. If the target is now fixed in the Y direction and given

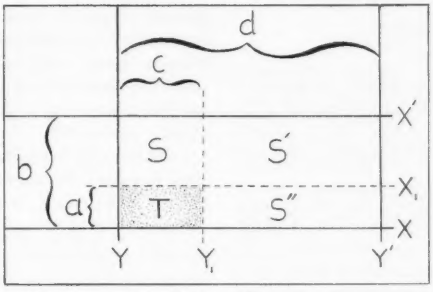

Figure 9. Search in an alignment situation

freedom in the X direction, $T = ac$ and $S'' = ad$,

$$p_X = \frac{ac}{ad} = \frac{c}{d}.$$

The contingent probability of a random point falling on a blind linear target of a schist field can, therefore, be expressed as

$$P_{hit} = p_Y p_X = \left[\frac{(1)!\left(\frac{b}{a}-1\right)!}{\left(\frac{b}{a}\right)!}\left(\frac{c}{d}\right)\right].$$

Patterned Search

Mickey and Jespersen (1954) have considered the calculation of search patterns in a drilling operation for well locations based on probability of a target hit. In general their results indicate that the minimum well density that can achieve a maximum hit probability is through patterns generated by diamond-shaped parallelograms. They assumed the target to be an ellipse.

The writer concluded on the basis of the low probability of random search that some form of formalized pattern search for the random target is better than wildcat search, and some form of parallelogram based on the anticipated shape of the target will yield a minimum point density for maximization of success.

In selection of a pattern for either a random or an aligned target search, the basic geometry

of each problem should be considered on its own merit. A probability acceptance level for each case can be established, and if the pattern chosen meets this level with the minimum of points it is the most efficient pattern. The shape and size of the anticipated target is the controlling factor in efficient pattern design.

GAME DECISIONS AND SEARCH ECONOMICS

Earlier in this paper the writer promised to elaborate on the economic significance of a decision probability and explain why a success probability greater than 0.5 would be adequate for economic work.

The writer has no doubt but that all geologic decisions, whether of hypothesis or drilling, have an economic influence. If the successes of decision can be kept *consistently* at some level above 50 per cent the business cannot help but succeed. To insure financial success a venture need not be perfect. If 49 dollar losses are matched by 51 dollar gains, the bank will grow. The rub comes in the word *consistently*. It is because of this word that staying power becomes so important. Even where 51 dollar gains are indicated, a player cannot win if he starts the game with only 97 dollars in his pocket and loses 49. He cannot stay to reach his gain.

There is no guarantee in a probability of 0.51 that there will be 51 successes out of every hundred. There may instead be 510 successes out of a thousand and the first 51 trials may fail (although this is not likely). It cannot be denied that what the gambler terms "staying power" is an important aspect of any economic game involving chance. The higher the level of probability acceptance the less critical is staying power or ability to absorb loss (because the indicated loss is small enough that it can mostly be covered with playing the game). The writer has often thought that he would be foolish not to wager on any proposition with a success probability higher than 0.99; he has no staying power for any game of chance.

Callaway (1954, p. 328–330) has offered the relationship $C = NR$ as the exploration stochastic model, where C is the maximum dollars that can be economically spent on a given exploration project, R is the estimated chance of making a discovery by wise spending of C dollars, and N is the net dollar value that can reasonably be expected from the discovery. Although this formula has academic appeal, there are many complexities in the economics of exploration, and it is probably oversimplified. For one thing, there are certain tax benefits from exploration expenditures. The usefulness is further limited because the "net dollar value" cannot be anticipated with any degree of certainty prior to the discovery.

The factor in the Callaway equation of special interest to us is the R factor, or success probability. As written, the equation represents a static condition of neither profit nor loss. The term R is a probability expectation and in that sense differs from a decision or search probability. Expectation is improved by a larger number of tries, whereas probability does not vary. Weaver (1950, p. 45) has shown that

> ". . . the same law that tells us that the *ratio* of successes tends to match the probability of success better and better as the trials increase also tells us that as we increase the number of trials the *absolute number* of successes tends to deviate more from the expected number."

The expectation of success is improved when it can be better assured performance will match anticipation. Probability estimates *per se* are pure anticipation. If we are to gain profit, R must be based on something more tangible than mere anticipation. The anticipation must also be reliable within the confines of the game as it is played. Its reliability increases with an increase in the number of trials.

An exploration program based on random or patterned search or probability decision of any sort can be likened to a "game of chance", which Uspensky (1937, p. 107) has defined as "any enterprise which may give us profit or may cause us loss, depending on chance, the probabilities of gain or loss being known." In this game Uspensky uses the following formula for expressing expected gain:

$$K = ma - (n - m)b$$

where K is the expected gain, a is the money player can win, b is the money player can lose, m is the number of successes, and n is the number of trials.

Because of the limiting aspect of "staying power", b must always be some sum smaller than the bank B. If X is the per cent of the bank capital that is required by the player for the risk of playing the game, then

$$XB = m \sum a - (n - m) \sum_{1}^{B-1} b = K.$$

In an area search problem where m/n equals P equals T/S the formula may be recast in the more usable form

$$XB = n\left[\frac{T}{S}\sum a - \left(1 - \frac{T}{S}\right)\sum_{1}^{B-1} b = K,\right.$$

where n is the number of drill holes, b is the cost of drilling each project, B is the net value of the exploration bank, a is the net value of each discovery, T is the area of target, S is the area of search, and X is the per cent return on investment.

In all likelihood b will be large and a relatively small. If S is small and T and n large there is some chance that X can be a positive integer. In any event, B will have to be larger than b by 1 dollar if the playing is not to break the bank.

SUMMARY AND CONCLUSIONS

Certain problems of geological search and decision can be treated stochastically. Where there is no prior knowledge, as in blind random search, an *a priori* probability can be assigned. Where there is prior knowledge, or where knowledge is gained through experimentation later, the *a priori* probability should be revised in the light of the experience. The basic equation that is most helpful in search and decision problems is

$$P = r_T^2/r_S^2,$$

where P is the probability of a success and r_T and r_S are radii of circles inscribed in the target and search areas respectively.

All geologic decisions, even those of strictly academic nature, because they are used in economic work, have economic implications. The economic game of search is expressed by the equation

$$XB = n\left[\frac{T}{S}\sum a - \left(1 - \frac{r_T^2}{r_S^2}\right)\sum_{1}^{B-1} b\right] = K,$$

which has been explained in the body of this paper.

REFERENCES CITED

Brown, B. W., 1959, Preliminary study of stochastic terms used in geology: Geol. Soc. America Bull., v. 70, p. 651–654

Callaway, H., 1954, Expense of exploration: Econ. Geology, v. 49, p. 328–330

Chalkley, H. W., *et al.*, 1949, A method for estimating volume-surface ratios: Science, n. s., v. 110, p. 295–297

Fisher, R., 1954, The expansion of statistics: Am. Scientist, v. 42, p. 275–293

Good, I. J., 1959, Kinds of probability: Science, v. 129, no. 3347, p. 443–447

Kneale, W., 1949, Probability and induction: London, Oxford Univ. Press, 259 p.

Krumbein, W. C., 1955, Experimental design in the earth sciences: Am. Geophys. Union Trans., v. 36, p. 1–11

—— 1960, The geological population as a framework for analysing numerical data in geology: Liverpool and Manchester Geol. Jour., v. 2, pt. 3, p. 341–368

Krumbein, W. C., and Miller, R. L., 1953, Design of experiments for statistical analysis of geologic data: Jour. Geology, v. 61, p. 510–532

Lasky, Samuel G., 1948, The search for concealed deposits—a reorientation of philosophy: Am. Inst. Min. Engineers Trans., v. 178, p. 82–90

Levy, H., and Roth, L., 1947, Elements of probability: London, Oxford Univ. Press, 197 p.

Mickey, M. R., and Jespersen, H. W., 1954, Some statistical problems of uranium exploration: U. S. Atomic Energy Comm., RME-3105, p. 1–78

Nolan, T. B., 1950, The search for new mining districts: Econ. Geology, v. 45, p. 601–608

Slichter, L. B., 1955, Geophysics applied to prospecting for ores: Econ. Geology, 50th Anniv. Volume, p. 885–969

Uspensky, J. V., 1937, Introduction to mathematical probability: New York, McGraw Hill Book Co.

Weaver, W., 1950, Probability: Scientific American, v. 183, p. 44–47

Manuscript Received by the Secretary of the Society, January 3, 1961

Short Notes

RICHARD FOSTER FLINT

TWO TILLS IN SOUTHERN CONNECTICUT

Abstract: A large borrow pit excavated at Lake Chamberlain, northwest of New Haven, Connecticut, exposed two tills in direct superposition. The younger till represents the last glaciation of the district. Measurement of three directional parameters on each till, coupled with observation of the contact between the two tills, strongly supports the assumption of glacial movement from north or northwest, later followed by movement from the northeast. An intervening episode of oxidation and valley cutting is likely but is not firmly established.

This paper reports an occurrence, in southern Connecticut, of two tills in stratigraphic sequence. The two tills were deposited by successive movements of glacier ice, each in a different direction. This inference can be established through more than one kind of evidence; hence the degree of probability is high. This kind of occurrence is sufficiently rare in the region to justify recording it.

Courtesies extended by Roald J. Haestad of Malcolm Pirnie Engineers, Resident Engineer at the Lake Chamberlain dam site during reconstruction, are acknowledged. The generous help of C. E. Fritts, U. S. Geological Survey, in checking lithologic identifications of till stones is much appreciated. An unpublished detailed map of the bedrock geology of the Mount Carmel and Southington quadrangles was kindly furnished by Mr. Fritts; a similar map of the adjacent Naugatuck quadrangle was supplied by M. H. Carr. The oriented sample of Lake Chamberlain Till was collected by K. L. Pierce.

The locality is Lake Chamberlain, a reservoir in the valley of Sargent River in Bethany, Connecticut, 1.9 miles south-southeast of Bethany (Center). The locality is near the southwest corner of the Mount Carmel 7½-minute quadrangle (Fig. 1).

In the summer of 1959 the reservoir was dry, and the dam at its downstream end was being reconstructed. A series of borrow pits was opened immediately north of the west abutment of the dam, at altitudes between about 360 feet and about 420 feet. The pits (essentially bays of a single pit) had a combined north-south length of about 350 feet and a maximum width of about 125 feet. They were cut into the west slope (4°) of a broad north-south valley. The continuous exposure free of sliderock was at no time greater than about 30 feet in height, although the maximum height of the pit walls exceeded 30 feet at times.

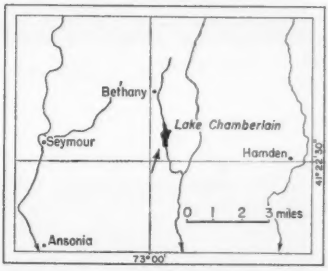

Figure 1. Index map showing location of Lake Chamberlain. Arrow points to exposure of two tills.

Throughout the exposure the sequence was the same, varying only in the exposed thicknesses of the units:

3. Loam, brown, containing stones; probably a mixture of colluvium and wind-blown sand and silt; contains a thin Brown-Podzolic soil profile; thickness 2–3 feet
2. Till, thickening from as little as 3 feet in the upslope direction to as much as 20 feet downslope (Hamden Till)

—Sharp contact with local drag effects—

1. Till, exposed thickness 12–20 feet (Lake Chamberlain Till)

—Striated surface—

Bedrock (Orange Phyllite)

Geological Society of America Bulletin, v. 72, p. 1687–1692, 5 figs., 2 pls., November 1961

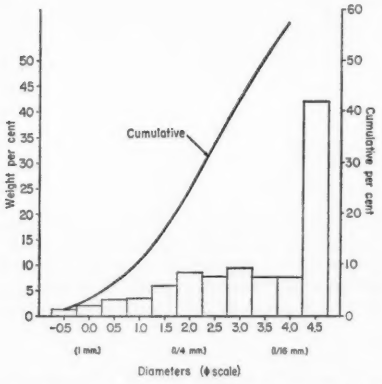

Figure 2. Grain-size data on fine fraction of Lake Chamberlain Till at the type locality. Histogram shows individual percentages of the various size fractions; curve shows cumulative percentages of the same fractions. Mechanical analysis by Whitman Cross 2d

The lower till is named the Lake Chamberlain Till; it is yellowish gray (5Y 7/2) when dry, very compact, and rather uniform in texture; it has a few irregular pods and pockets that differ in texture from the main mass. Pebbles, cobbles, and boulders constitute about 25 per cent of total mass. These coarse clasts are mostly pebbles and cobbles, but include boulders as much as 10 feet in diameter, of which most occur in the lower part of the exposure; they range from freshly fractured to fully glaciated shapes. The fraction smaller than pebble size comprises about 60 per cent sand sizes and about 40 per cent silt and clay (Fig. 2). A thin section cut from a sample of the till after hardening treatment showed a high proportion of quartz and feldspar in the sand and silt sizes, and outstandingly angular grain shapes, presumably the result of crushing while in transport.

The till possesses fissility clearly apparent in some parts of the exposure but indistinct in others. The laminae of fissility range from less than 1 inch to 4 inches in thickness and are weakly lenticular. In addition there are, in places, lenticular partings at intervals of 10 inches to 30 inches, parallel with and possibly a part of the pattern of fissility. The laminae of

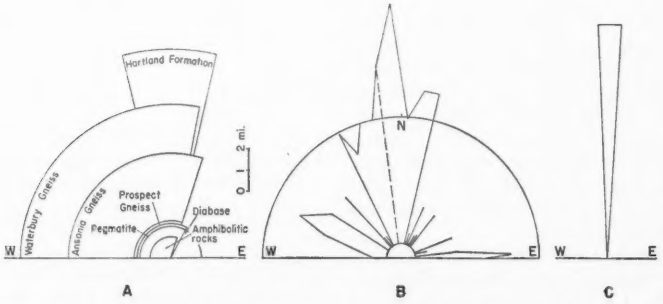

Figure 3. Directional data on the Lake Chamberlain glaciation; azimuths of three parameters

A. Probable directions of transport of rock types in the Lake Chamberlain Till. Data derived from 103 of 108 pebbles and cobbles collected from the till at the type locality (5 were eliminated as not diagnostic of direction of transport). In plotting the diagram only the area north of the collection locality was considered. Radial lines drawn from locality of collection embrace limits of outcrop area of each rock type; length of line indicates distance to nearest outcrop, regardless of size.

B. Fabric diagram, Lake Chamberlain Till, type locality. Of 107 pebbles and cobbles collected, 20 were first eliminated by inspection, because they are essentially equidimensional or have vertical long axes. Dashed line shows median orientation of the principal mode.

C. Directions of striations on bedrock immediately underlying Lake Chamberlain Till at the type locality. All lie within a range of 6°. Lengths of lines have no significance.

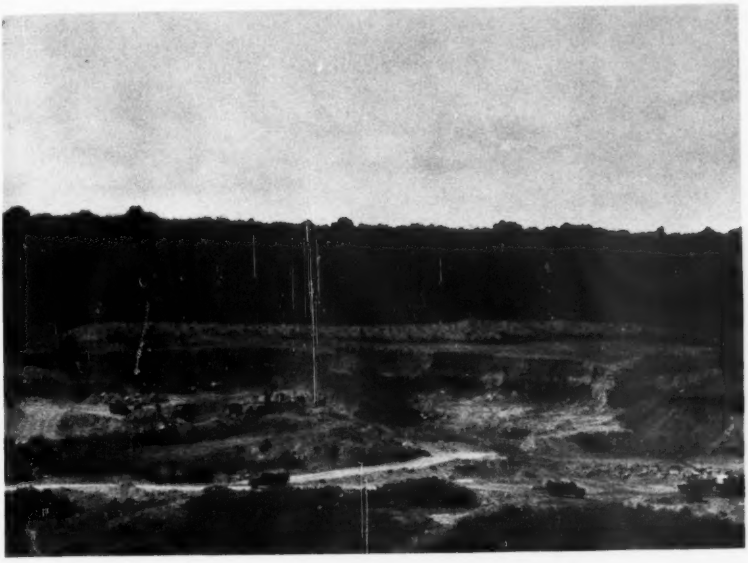

Figure 1. General view of borrow pit, looking west

Figure 2. Lake Chamberlain Till, showing flat-lying fissility. Top of exposure is a berm, from which Hamden Till has been stripped away.

TILLS AT LAKE CHAMBERLAIN DAM

Figure 1. Stony Hamden Till overlying Lake Chamberlain Till, fissile in lower part. Point of digging tool (20 inches long) marks contact. Dark band above contact is moisture seeping from Hamden Till just above contact. Surface of Hamden Till has been stripped away.

Figure 2. Detail of contact. Pick point of hammer is at interface, which slopes away from observer as well as from left to right. Boulder at left, a biotite gneiss, projects through the contact.

INTER-TILL CONTACT

fissility appear to be more nearly horizontal than the present land surface. A thin section cut from an oriented sample between two partings 2 inches apart showed a crude subhorizontal arrangement of long axes of sand-sized quartz grains, with no obvious orientation of the finer grain sizes. As no systematic measurement of microfabric was made, it is not known whether the arrangement is significantly related to fissility.

TABLE 1. LITHOLOGY OF STONES FROM TWO TILL SHEETS AT LAKE CHAMBERLAIN DAM

Lithology	Number of stones	
	Lake Chamberlain Till	Hamden Till
Waterbury Gneiss (probable)	56	55
Prospect Gneiss	25	10
Hartland Formation	2	0
Ansonia Gneiss	2	2
Amphibolitic rocks, miscellaneous	8	0
Pegmatites	9	3
Diabase (intrusive) and basalt (extrusive)	1	14
Vein quartz	5	7
Phyllite, nongarnetiferous	0	10
Arkosic sandstone of New Haven Arkose	0	1
Unidentified	0	1
Total	108	103

Notes: 1. A rectangular area was marked on the clifflike exposure of each till; all the pebbles and cobbles exposed within each area were collected.

2. The formal names of bedrock units used here are those being used by geologists currently mapping bedrock and are subject to revision as the mapping progresses.

The till appears to be fresh and unaltered throughout its exposure, except for local oxidation in a few sand-rich, relatively permeable pods near the top of the unit. It is inferred that, if any soil or weathering zone were present formerly in the top of the till, it was subsequently removed by erosion.

Three kinds of measurements yielded data on the local direction of movement of the glacier that deposited the Lake Chamberlain Till: fabric, provenance of pebbles and cobbles (Table 1), and striations. The results of the measurements are shown in Figure 3, in which *B* and *C* combine to indicate glacier movement from the north or slightly west of north; the data in *A* are permissive of such movement.

The till overlying the Lake Chamberlain Till is here referred to as the Hamden Till, because it occurs extensively at the surface throughout the Town of Hamden, east of Bethany. The Hamden Till (dry) is dusky yellow (5Y 6/4). The more strongly yellowish color, as compared with that of the underlying till, may have resulted from oxidation. Any oxidation probably would have developed prior to transport by the Hamden glacier, because the color is fairly uniform throughout the entire thickness of the Hamden Till. Apart from minor oxidation the till appears to be little altered even in its top, as the surface soil is almost entirely in the overlying stony loam.

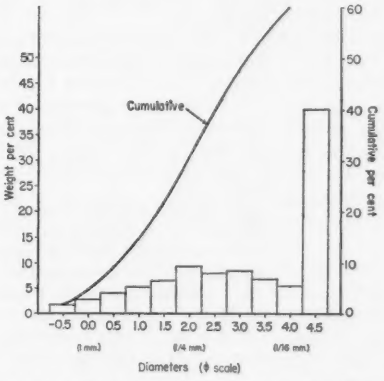

Figure 4. Grain-size data on fine fraction of Hamden Till at the Lake Chamberlain dam. Conventions as in Figure 2. Mechanical analysis by Whitman Cross 2d

Even at depths approaching 20 feet the Hamden Till is not fissile. It also is less compact and when dry is more friable than the underlying till. It is more permeable as well, for in wet weather seepage was observed along the trace of the contact between the two tills.

Pebbles, cobbles, and boulders are more numerous in it; these sizes constitute about 35 per cent (estimated) of total mass. The finer fraction consists of 58 per cent sand sizes and about 42 per cent silt and clay (Fig. 4), and hence is much like that in the Lake Chamberlain Till. The greater friability of the Hamden Till therefore is not the result of a larger

proportion of sand to finer sizes but probably is due to the less thorough compaction. If so, this property may be related to the absence of fissility already noted. Conceivably it might indicate glaciation by relatively thin ice, or of short duration, or both.

Although total boulders are more numerous, there are fewer large boulders than in the underlying till; shapes of stones lie within the same range as in that till; but texture is less uniform, with more pods and pockets of relatively coarser texture.

The Hamden Till, the surface till at this locality, is believed to be the till exposed at the surface throughout the New Haven district. This belief is based on physical character and on related direction of glacier movement as inferred from lithology and from striations on bedrock beneath the till.

Local direction of movement of glacier ice in Hamden time is inferred from the data in Figure 5. Both fabric (*B*) and provenance (*A*) indicate northeast-southwest movement. The diabases and basalts were considered significant, despite possible derivation from either northeast or northwest, because of their number (14) and because of nearness (1.75 miles) of a large area of source rocks to the east. Western sources are scattered and small.

As the Hamden Till was not exposed in contact with bedrock in the borrow pit, diagram (*C*) was constructed by plotting all the striations found in the western third of the Mount Carmel quadrangle. All the striations are northeast-southwest.

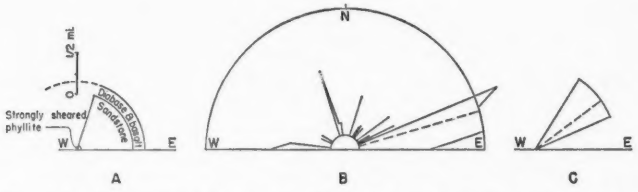

Figure 5. Directional data on the Hamden glaciation; azimuths of three parameters

A. Probable directions of transport of rock types in the Hamden Till. Data derived from 15 of 103 pebbles and cobbles collected from the till immediately overlying the Lake Chamberlain Till at the borrow pit near Lake Chamberlain dam site. (Eighteen were eliminated as not diagnostic of direction of transport; 70 others were eliminated because their sources lie northwest of the locality. Some of these are obviously reworked Lake Chamberlain Till, and all of them could be.) Conventions same as for Figure 3 (A)

B. Fabric diagram, Hamden Till, borrow pit near Lake Chamberlain dam site. Of 51 pebbles and cobbles collected, 10 were first eliminated by inspection, because they are essentially equidimensional or have vertical long axes. Dashed line shows median orientation of the principal mode.

C. Direction of all the striations on bedrock observed (10 localities) in the Mount Carmel quadrangle west of the West Rock Ridge diabase sheet. The striation locality nearest the borrow pit lies 1000 feet east of the pit, close to the east abutment of the dam. Lengths of lines have no significance.

At the 10 striation localities, including one close to the east abutment of the Lake Chamberlain dam, the till is believed to be the Hamden Till. The striations therefore are compatible with the other directional data, but until the till at all 10 localities is proved to be Hamden Till the striations as a group do not constitute fully independent evidence of the direction of Hamden ice movement. However, even if these striations are neglected, the other data indicate the probability of two successive glacial movements, differing in azimuth by an undetermined angle, possibly as much as 45° to 70°.

Striations in south-central Connecticut shown on general maps (Flint, Colton, Goldthwait, and Willman, 1959) include both the

trends that occur in the Mount Carmel quadrangle; this suggests that both trends may be part of a broad regional pattern.

The contact between the two tills slopes eastward more steeply than does the surface of the ground (4°) and more steeply than the fissility in the Lake Chamberlain Till; in the eastern part of the pit area the slope of the contact approached 25°. The contact was generally smooth, with local relief generally less than 1 foot. In places this relief consisted of features produced apparently by squeezing and dragging the underlying till while it was plastic. The features included one long, finger-like stringer of the lower till pointing upslope—that is, with a westerly component. Small gobs and squeezed lenticular masses of the lower till were incorporated in the basal part of the upper till, and in places as many as 25 per cent of the stones in the lower half of the upper till showed, adhering to them, the yellowish-gray matrix characteristic of the lower till.

These observations support the directional data in indicating two episodes of till deposition, with erosion of the lower till by the later glacier ice. Whether there was deglaciation of the Lake Chamberlain locality between the two episodes, and if so whether the interval was long or short, are inferences not fully evident from the data. Possibly the Hamden Till represents merely the response of an ice sheet to a radical change in local direction of movement, without deglaciation, as by change in center of glacial outflow or increasing effect of subglacial topography on flow directions.

The following facts, however, seem to be explained more satisfactorily on the assumption of an interval of deglaciation: (1) The relatively steep slope of the intertill contact, apparently cutting the structure of the Lake Chamberlain Till, suggests that the contact may represent one side of a former valley beneath the site of the present valley. (2) The more yellowish, disseminated color of the Hamden Till suggests erosion, by Hamden ice, of an oxidized zone in older till of similar texture. (3) The larger proportion of pebbles, cobbles, and boulders in the Hamden Till suggests derivation from a surface of erosion, from which fines had been selectively washed away, leaving a lag concentrate of the relatively coarse clasts. (4) The directional features show trends either northeast or north to northwest, with little indication of intermediate directions. As this combination of inferences is suggestive only, the question of an interval remains open. If there was an interval, probably it was long enough to permit at least some oxidation of the Lake Chamberlain Till and possibly some excavation in the valley now occupied by the reservoir.

Despite intensive search, the Lake Chamberlain Till has not been identified elsewhere in the Mount Carmel quadrangle nor in the adjacent Southington, Wallingford, and New Haven quadrangles. Very likely it is present in places, but is not exposed in the rather shallow cuts that are characteristic of the area. Its recognition at the Lake Chamberlain dam resulted from a temporary artificial exposure of extraordinary depth and lateral extent. Most if not all of the till now exposed at the surface in the quadrangles named is believed to be the Hamden Till.

In the Stafford Springs district, in northeastern Connecticut, S. E. White (1947) described a sequence of two tills consisting of a thick, compact, fissile, locally oxidized unit overlain unconformably by a sandy, friable unit also having considerable thickness. Nothing in the descriptions of those tills precludes their correlation with the tills at Lake Chamberlain, but nothing compels correlation either; the occurrence is mentioned only for possible future reference.

References Cited

Flint, R. F., Colton, R. B., Goldthwait, R. P., and Willman, H. B., 1959, Glacial map of the United States east of the Rocky Mountains. Scale 1:1,750,000: New York, Geol. Soc. America, 2 sheets

White, S. E., 1947, Two tills and the development of glacial drainage in the vicinity of Stafford Springs, Connecticut: Am. Jour. Sci., v. 245, p. 754–778

Box 2161, Yale Station, New Haven, Conn.

Manuscript Received by the Secretary of the Society, August 5, 1960

Published with Permission of the Director, Connecticut Geological and Natural History Survey

M. V. BROWN
JOHN NORTHROP
ROBERTO FRASSETTO
L. H. GRABNER

SEISMIC REFRACTION PROFILES ON THE CONTINENTAL SHELF SOUTH OF BELLPORT, LONG ISLAND, NEW YORK

Abstract: Seven reversed seismic refraction profiles were made extending from the Bellport Coast Guard Station, off Long Island, New York, to 45 miles offshore. The profiles show a thin layer of mud above the sedimentary wedge that covers the basement. The mud layer was found to have a compressional velocity of 5030–5260 ft/sec, the unconsolidated sediments, 5700–6040 ft/sec, the semiconsolidated sediments, 6370–6770 ft/sec, and the consolidated sediments, 7470–10,700 ft/sec. Consolidated sediment was found only in the profile farthest offshore. Basement velocities ranged from 16,300 to 18,300 ft/sec. The thickness of the sedimentary column in a section extending 45 miles offshore was found to increase from 1927 feet to 7598 feet, the greatest increase coinciding with the appearance of the consolidated layer. Comparison of the seismic profiles with well logs obtained in the area indicates that the unconsolidated sedimentary layer can be correlated with the Upper Cretaceous Magothy Formation of Long Island and the semiconsolidated sedimentary layer can be correlated with the Upper Cretaceous Raritan Formation which overlies the gneisses and schists that constitute the basement beneath Long Island. Strong evidence for a fault was found 8 miles offshore and again 19 miles offshore.

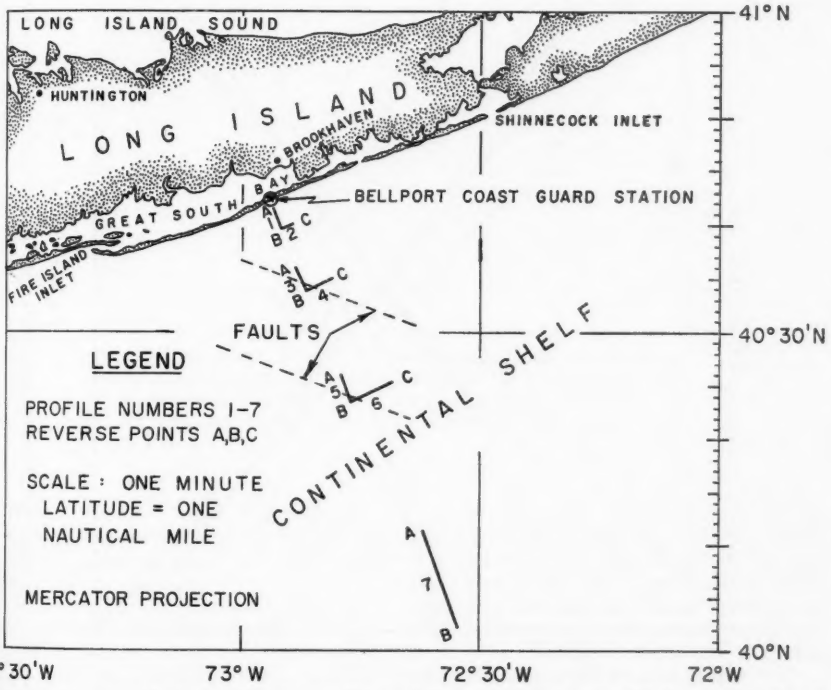

Figure 1. Location of seismic refraction profiles, well site, and faults south of Bellport Coast Guard Station, Fire Island, New York

Geological Society of America Bulletin, v. 72, p. 1693–1706, 10 figs., November 1961

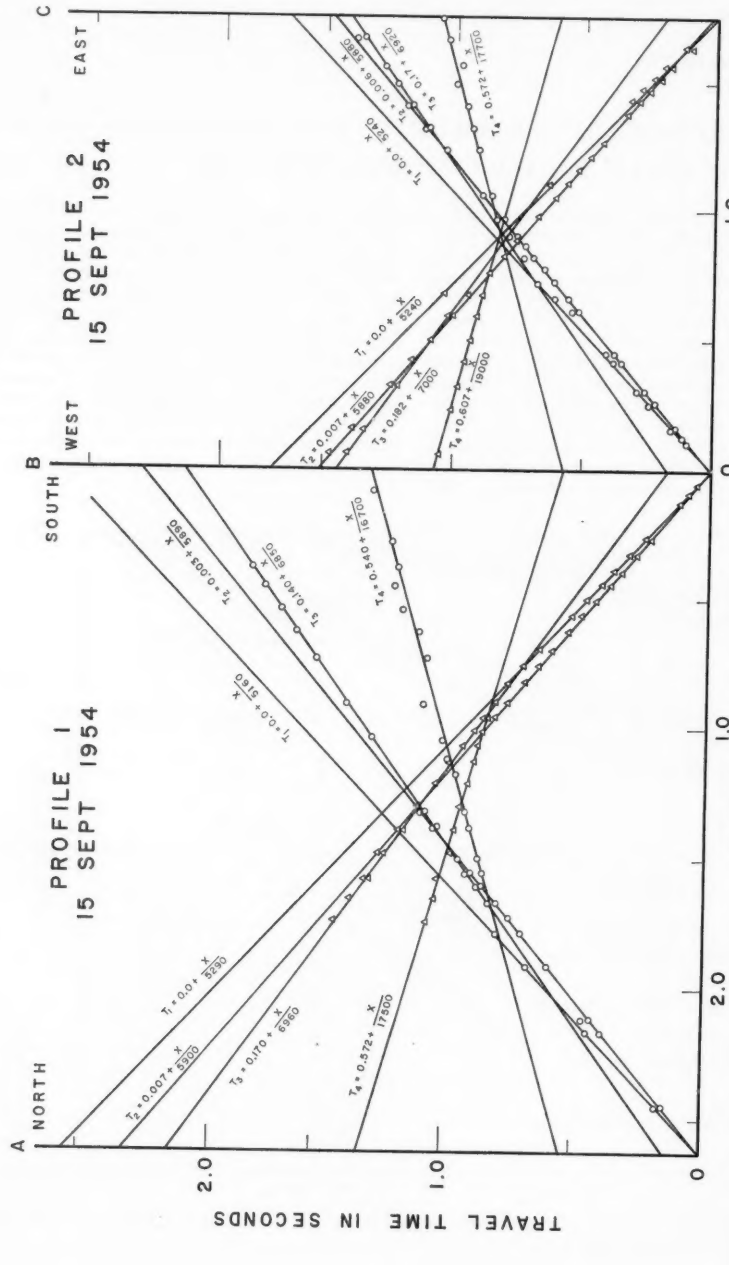

Figure 2. Travel-time curves for profiles 1 and 2. Center line common to both profiles, as at point B on Figure 3

Introduction

The thickness and acoustic characteristics of the sedimentary wedge and the slope of the basement for the area southeast of the Bellport Coast Guard Station, Fire Island, New York, have been determined through a series of seismic-refraction profiles. The region surveyed lies between the area off Fire Island Inlet surveyed by Ewing *et al.* (1950) and the area off Shinnecock Inlet surveyed by Oliver and Drake (1951).

Additional refraction studies have been published by Woods Hole Oceanographic Institution (1954) and by the Hudson Laboratories (Blaik, Northrop, and Clay, 1959). A reflection profile has also been made, extending 23 miles southeast of the station, paralleling the profiles shown in Figure 1 of this paper (Brown, Northrop, and Blaik, 1960).

Method

The USS ALLEGHENY (ATA-179) was the listening ship, the R/V ALPHA the shooting ship. The shots, fused to detonate at the bottom, ranged from half a pound to 75 pounds of TNT. The hydrophones (barium titanate) were also on the bottom.

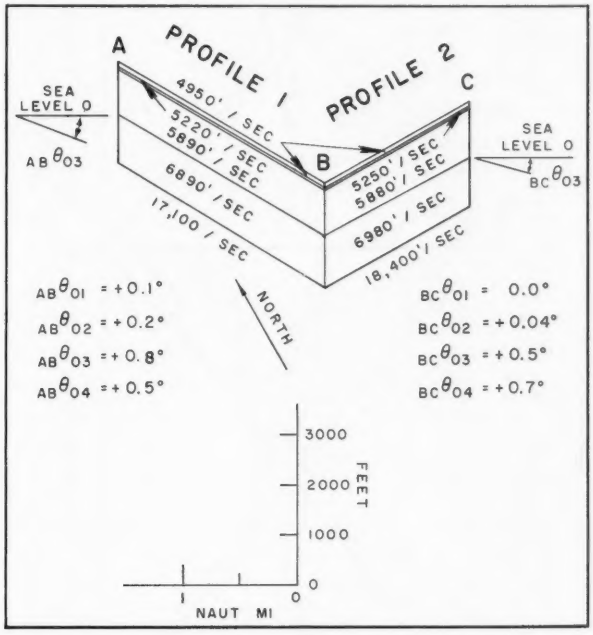

Figure 3. Structure section for profiles 1 and 2. Theta is the dip of the horizon referred to the horizontal. In the key A refers to the A end of the profile, B to the B end of the profile; 01, 02, and 03 refer to the horizon between the horizontal (sea level) and layers V_1, V_2, and V_3

At the end of each run, the position of the last shot was marked by a buoy. The ALLEGHENY then anchored at this point for the reverse profile. Three profiles were made parallel to the coast line, and four were made normal to it (Fig. 1). They were made in intersecting sets so that the true dip of the sedimentary and basement layers could be determined.

The signals were filtered through bandpass filters set at 5 to 30 cps, 30 to 100 cps, and 175 to 250 cps and also through a high pass filter set at 500 cps. An additional unfiltered trace

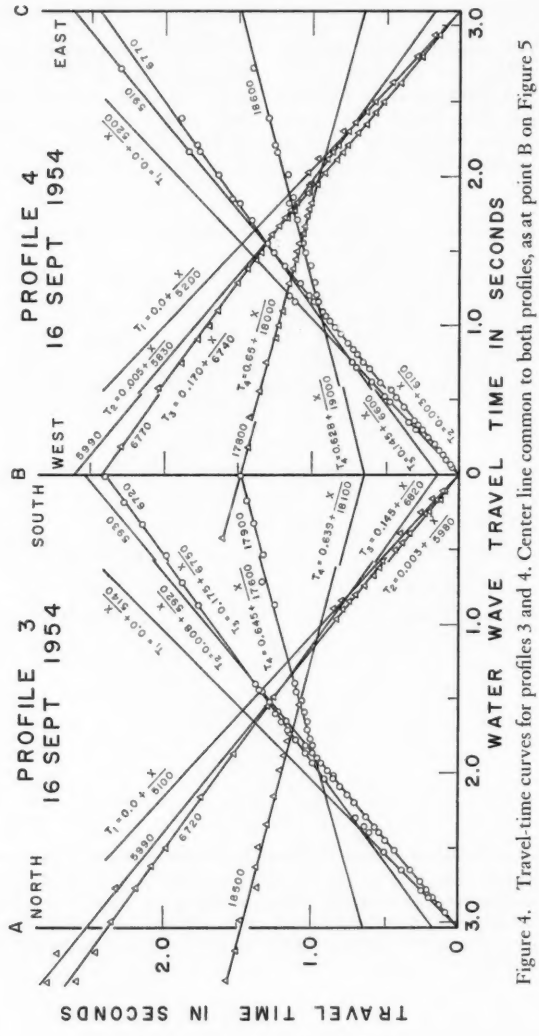

Figure 4. Travel-time curves for profiles 3 and 4. Center line common to both profiles, as at point B on Figure 5

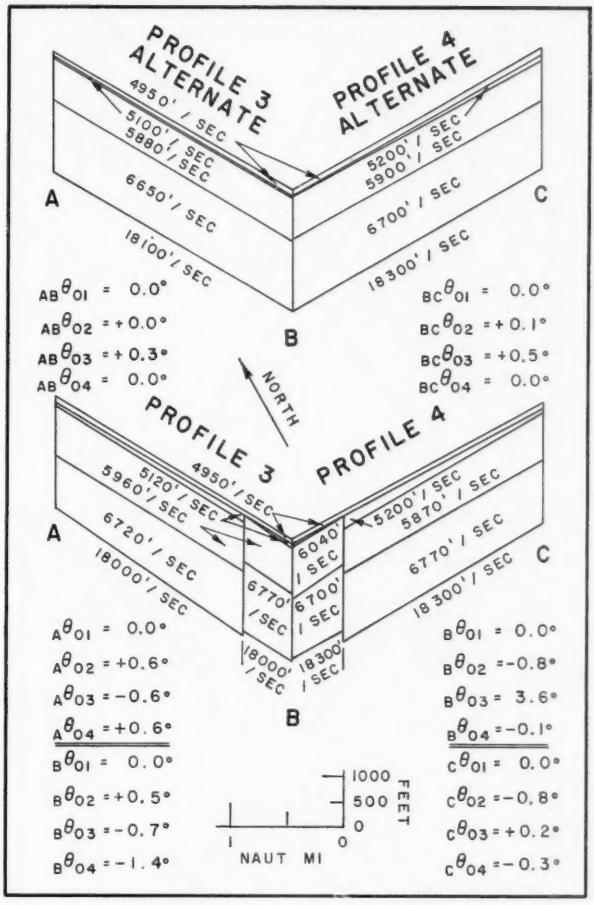

Figure 5. Structure section for profiles 3 and 4. The top section is an alternate solution disregarding the faults. In the alternate solution, there is considerable scatter of the points about the travel-time curves. *See* subcaption of Figure 3 for explanation of key.

was taken for the last three profiles; this trace indicated corrections for the arrival times read from the filtered traces of the first four profiles. Oscillograph records were obtained photographically. A pen recorder monitored the first arrivals.

Using temperature and salinity measurements made at each station, the writers interpolated the velocity of sound in water from the tables of Del Grosso (1952). The travel-time curves (Figs. 2, 4, 6, 8) were plotted using the travel time of the direct water wave as a measure of distance. Computations were made according to the method described in earlier papers (Ewing, Crary, and Rutherford, 1937; Carlson and Brown, 1955). The travel-time curves were fitted to the data by eye. By comparing the fit of the lines drawn to the plotted points, one can evaluate the correctness and accuracy of the interpretation (Woollard, Bonini, and Meyer, 1957).

Results

Profile 1 starts half a mile offshore and ex-

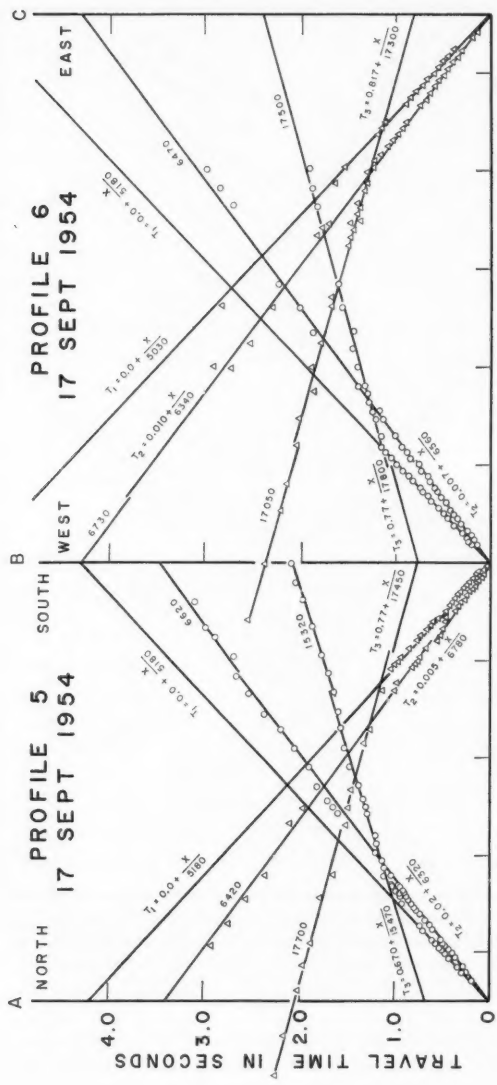

Figure 6. Travel-time curves for profiles 5 and 6. Center line common to both profiles, as at point B on Figure 7

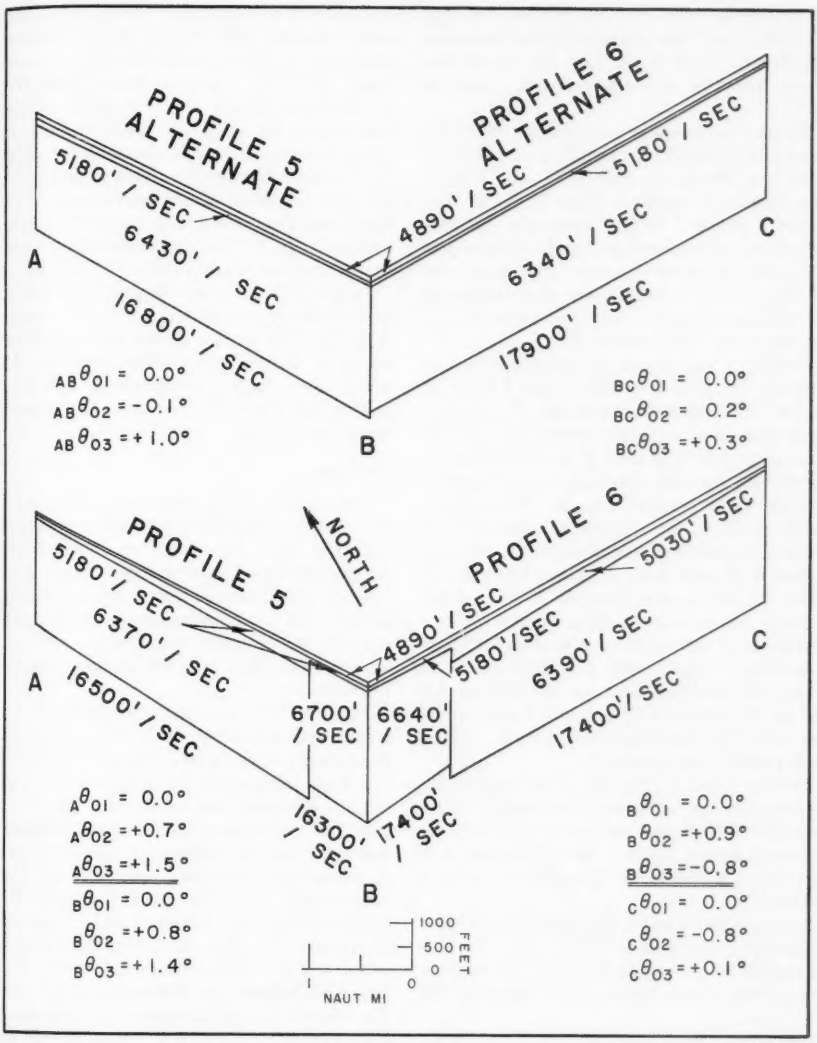

Figure 7. Structure sections for profiles 5 and 6. The top section is an alternate solution disregarding the breaks in the travel-time curves. *See* subcaption of Figure 3 for explanation of key.

tends 2 miles seaward on a bearing of 160° *T* from the Bellport Coast Guard Station (Fig. 1) into 60 feet of water. A mud layer with a velocity of 5220 ft/sec was found to be 17 feet thick on the inshore end of the profile and 39 feet thick on the offshore end (Figs. 2, 3; Table 1). This mud layer overlies an unconsolidated sedimentary layer having a velocity of 5890 ft/sec, 770 feet thick on the inshore end of the profile and 900 feet thick on the offshore end. Between this unconsolidated layer and the basement, a semiconsolidated sedimentary

layer 1000 feet thick, having a seismic velocity of 6890 ft/sec, was detected.[1] The basement velocity is 17,100 ft/sec, and the top surface of the basement dips offshore with a slope of 0.5°.

Profile 2 was made at a right angle to the offshore end of profile 1, extending eastward 1½ miles into 80 feet of water (Fig. 1). The results agree with profile 1 (Figs. 2, 3), the four layers in profile 2 having essentially the same velocities and thicknesses (Table 1). As in profile 1, the points on the travel-time curves are all first arrivals except those that determine the semiconsolidated layer. The top surface of the basement dips eastward 0.7°.

Profiles 3 and 4 can be interpreted as essentially the same as profiles 1 and 2 (Figs. 4, 5), but it is impossible to satisfy the requirement that the travel times reverse (*i.e.*, are the same from A to B as from B to A) without reconsidering the data, especially with respect to arrivals from points near B. Well-defined breaks occur in the travel-time curve for the unconsolidated layer near B when the listening is done at B, and in the basement layer near B when the listening is done at A or C. Only through recognition of these breaks can one choose travel times that reverse (Fig. 4). There is evidently a fault with a vertical throw of about 180 feet (indicated as 160 feet on AB and as 200 feet on BC) about 0.3 mile northeast of B. The fault plane strikes ESE., cutting both profile 3 and profile 4.

Profiles 5 and 6 (Figs. 6, 7) can also be interpreted as similar to profiles 1 and 2. However, the 5880 ft/sec layer is marked only by scattered second arrivals, and if it exists, it is very thin (< 100 feet). Therefore it has been omitted.

As in profiles 3 and 4, the travel-time curves of profiles 5 and 6 show breaks (Fig. 6). It is impossible to get satisfactory reverses without recognizing these breaks and assuming the existence of another fault.[2] Even then a difficulty remains: the velocity of the semiconsolidated layer is greater in the upthrown block than it is in the downthrown block (Fig. 7), and it is possible that the higher velocity observed in the upthrown block masks a low-velocity layer. If this is assumed, the depths can be made to correlate. This second fault is 0.5 mile northeast of the intersection of profiles 5 and 6 and has a strike parallel to that in profiles 3 and 4. The upthrown block is again near B, and the throw is about 270 feet (Fig. 7).

Profile 7 (Fig. 8) was begun at 34 nautical miles offshore, continuing 10 miles seaward (Fig. 9). This profile shows the three layers found in the inshore profiles and two additional layers having velocities of 7500 ft/sec and 10,700 ft/sec. All five layers are identified from first arrivals.

Discussion

The present survey correlates well with profiles already established east and west of Bellport (Fig. 10). A mud layer was detected above the previously established sedimentary layers. Tolstoy (1958) also measured this low-velocity layer, using a continuous wave method. The velocity he obtained was about 8 per cent higher than the writers' seismic-refraction velocity.

The four sets of profiles are generally consistent with respect to both the thickness and the velocity of the layers. The north-south and east-west pairs agree extremely well. Least-squares solutions (not containing the restriction that travel times reverse) gave thicknesses and velocities that differed at the intersection of profile 5 by less than 7 per cent and 5 per cent respectively. The eye fits reported here agree to 3 per cent in depth and 1.5 per cent in velocity (except in the case of the basement, where one pair of velocities differed by 5 per cent and another pair differed by 7 per cent). The depth of the basement increases slowly with an average dip of 0.5° out to 20 miles offshore. The depth then doubles with an average slope of 2.8° between 20 and 34 nautical miles offshore. At the same time two new strata appear. The dip levels off to only 0.35° between 34 and 44 miles offshore.

This rapid increase in depth and appearance

[1] The points on the travel-time curve that define this deeper sedimentary layer are all second arrivals; however it is included as a definite layer because (1) the arrivals are strong and persistent, (2) the layer correlates with the Magothy-Raritan interface (Suter, De Laguna, and Perlmutter, 1949) projected from Long Island, and (3) the layer correlates with a layer of similar seismic velocity found from first arrivals on profiles 5, 6, and 7. Moreover a similar second-arrival line was found on the adjacent profiles 2, 3, and 4, as well as at the Shinnecock Inlet (Oliver and Drake, 1951), at Ambrose Lightship (Carlson and Brown, 1955), and at Fire Island (Blaik, Northrop, and Clay, 1959).

[2] Figure 7 shows the alternate result obtained by neglecting points near B. This figure of course eliminates the 6700 ft/sec layer, since this layer shows only at ranges less than 1 mile from B.

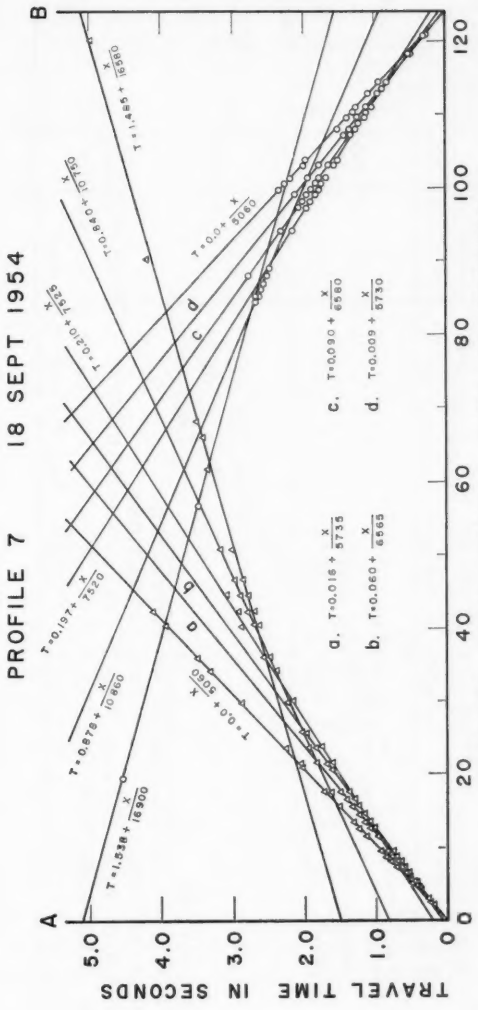

Figure 8. Travel-time curves for profile 7. Structure section for this profile in Figure 9

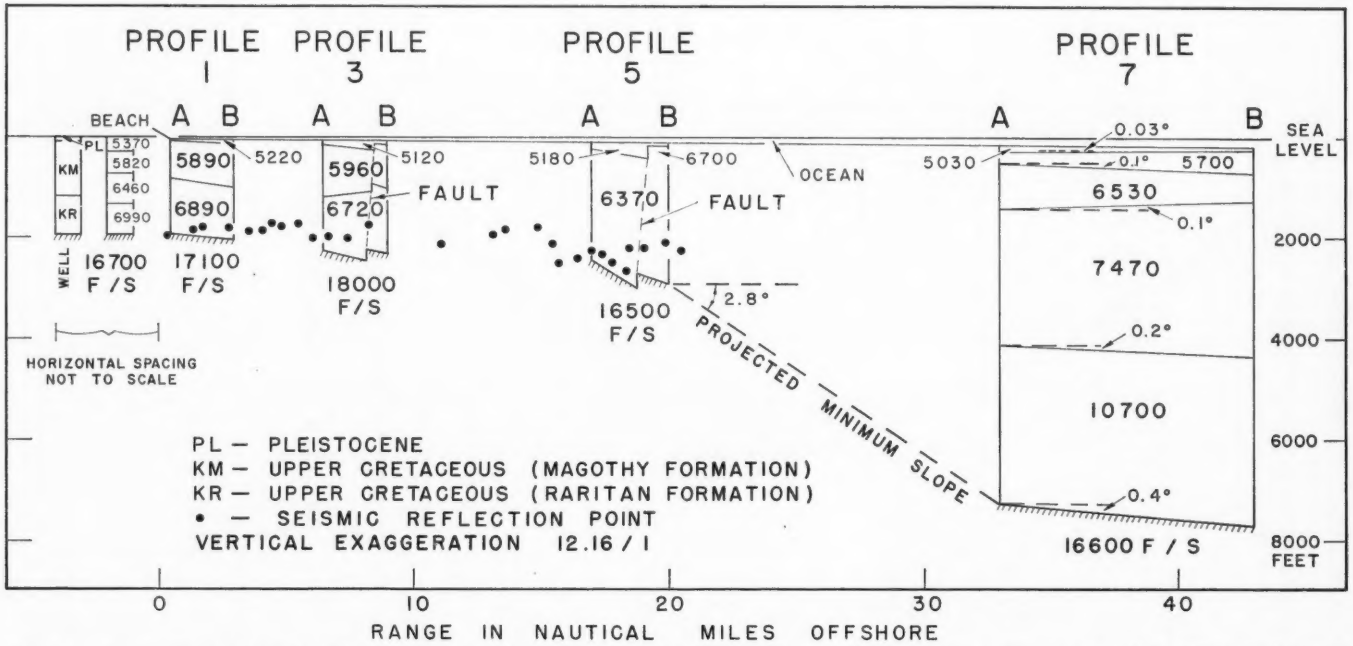

Figure 9. Structure section from Fire Island, New York, offshore to profile 7. Well data from the U.S. Geological Survey interpretation of the driller's log (through the kindness of N. M. Perlmutter). Beach-refraction data from Blaik, Northrop, and Clay (1959). Reflection points taken from Brown, Northrop, and Blaik (1960) and refer to strong reflections that appear to correlate (corrected for normal moveout)

of a thick consolidated layer indicate that the pre-Upper Cretaceous basin found by Ewing *et al.* (1950) extends at least as far east as profile 7.

Two fault areas 8 miles offshore and 18 miles offshore appear in profiles 3 and 4 and profiles 5 and 6 respectively. The first of these areas appears to be a simple normal fault.

Profiles 5 and 6 are difficult to interpret. A detailed reinvestigation of the region would probably show a more complex structure than has been assumed.

A reflection profile run along the same track from the Bellport Coast Guard Station by Brown, Northrop, and Blaik (1960) shows upthrown blocks in the basement coinciding with those reported in the present paper (Fig. 9). Since no comparison was made until after the analysis was complete, this coincidence can be given considerable weight.

A test borehole to basement[3] was made 0.8 nautical mile north of the inshore hydrophone location (point A of profile 1). Comparison of the well logs with the seismic sections provides an identification of the seismic horizons with geologic formations.

The Upper Cretaceous Magothy Formation of Long Island corresponds in depth to the unconsolidated sedimentary layer (approximately 5900 ft/sec), and the Upper Cretaceous Raritan Formation corresponds to the semiconsolidated sedimentary layer (6900 ft/sec). However, the interface between the Magothy and Raritan deposits is difficult to determine with pre-

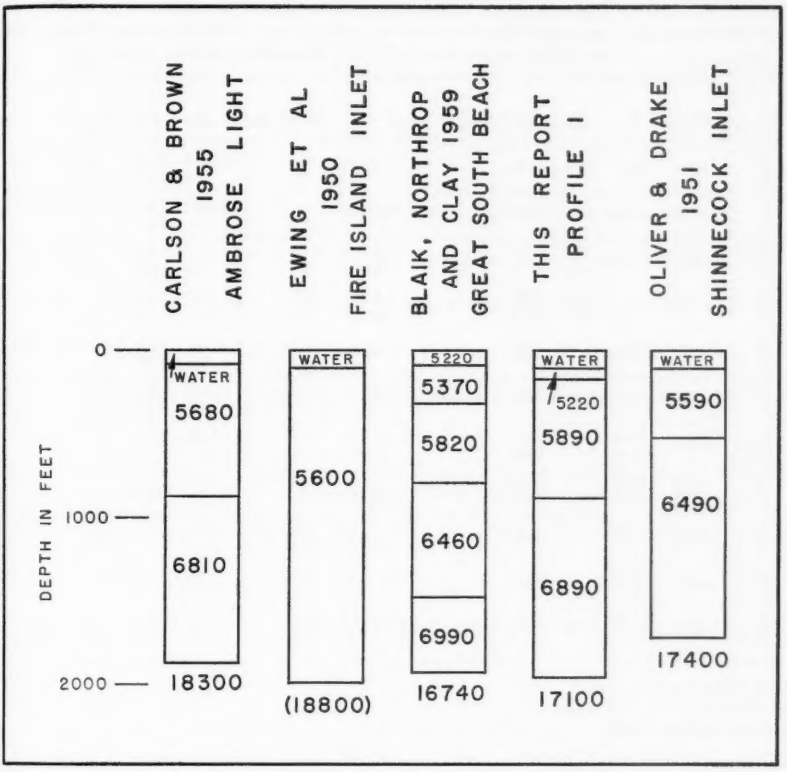

Figure 10. Comparison of data in this report with those of other published profiles off Long Island

[3] USGS # S-15106T

cision since in the Long Island area the dominantly terrestrial sands and sandy clays of the Magothy and the clays of the Raritan interfinger.

There is excellent agreement between the 1915 feet to basement obtained from the well log[4] and the 1927 feet calculated from the seismic data.

Table 1. True Velocities and Thicknesses of Layers

Thicknesses correspond to end points AB and BC on the profiles (Fig. 1). Velocities different at the end points because of the fault are also tabulated corresponding to AB and BC.

Profile		Water	V_1	V_2	V_3	V_4	V_5	V_6	Water	h_1*	h_2	h_3	h_4	h_5	Total depth†
1	A	4950	5220	5890	6890	..	..	17,100	60	17	770	1080	..	..	1927
	B					..	..		82	39	904	1020	..	..	2045
2	B	4950	5250	5880	6980	..	..	18,400	82	35	879	1044	..	..	2039
	C					..	..		82	41	944	1085	..	..	2152
3	A	4950	5120	5960	6720	..	..	18,000	115	40	1068	1055	..	..	2278
	B			5960	6770	..	..	18,000	120	15	840	1284	..	..	2309
4	B	4950	5200	6040	6700	..	..	18,300	120	15	987	1130	..	..	2252
	C			5870	6770	..	..	18,300	120	28	962	1140	..	..	2350
3**	A	4950	5100	5880	6650	..	..	18,100	115	26	777	1400	..	..	2318
	B					..	..		120	26	842	1320	..	..	2308
4**	B	4950	5200	5900	6700	..	..	18,300	120	28	820	1353	..	.	2321
	C					..	..		120	65	912	1230	..	..	2317
5	A	4890	5180	..	6370	..	..	16,500	145	89	2200	..	..	..	2434
	B		5130	..	6700	..	..	16,300	160	20	2580	..	..	..	2760
6	B	4890	5180	..	6640	..	..	17,400	160	29	2700	..	..	.	2889
	C		5030	..	6390	..	..	17,400	150	41	2750	..	..	..	2941
5**	A	4890	5180	..	6430	..	..	16,800	145	131	2200	..	..	..	2476
	B					..	..		160	44	2760	..	..	..	2964
6**	B	4890	5180	..	6340	..	..	17,900	160	45	2660	..	..	..	2865
	C					..	..		150	90	2770	..	..	..	3010
7	A	4855	5030	5700	6530	7470	10,700	16,600	195	86	220	907	2725	3180	7313
	B								200	48	454	537	3099	3360	7698

*h_1 = Thickness of V_1 layer
†With respect to sea level in feet
**Alternate, without faults

Acknowledgments

The authors wish to acknowledge the help and assistance of V. Lewis, H. Raff, W. Shuluk, J. Smith, and the late O. Manning, who took part in the field work, as well as LCDR Watson, captain of the Allegheny, and J. Kennedy, master of the Alpha. C. S. Clay, Maurice Blaik, and Ivan Tolstoy gave valuable advice on the interpretation of the data and were kind enough to read the manuscript critically prior to publication. The final drafts of the illustrations are by Irene Mayo Fiore.

All the authors participated in the field work and contributed to the reduction of the data. Northrop is responsible for the geological sections. Brown analyzed the faults.

The Office of Naval Research supported this work. Reproduction in whole or in part for any purpose of the U.S. Government is permitted.

[4] Well drilled and logged by Layne—New York, 1250 West Elizabeth Ave., Linden, New Jersey

References Cited

Blaik, M., Northrop, J., and Clay, C. S., 1959, Some seismic profiles onshore and offshore Long Island, New York: Jour. Geophys. Res., v. 64, p. 231–239

Brown, M. V., Northrop, J., and Blaik, M., 1960, Seismic evidence for post-Cretaceous faulting offshore, Long Island, New York (Abstract): Jour. Geophys. Res., v. 65, p. 2478

Carlson, R. O., and Brown, M. V., 1955, Seismic refraction profiles in the submerged Atlantic Coastal Plain near Ambrose Lightship: Geol. Soc. America Bull., v. 66, p. 969–976

Del Grosso, V. A., 1952, The velocity of sound in seawater at zero depth: Naval Research Lab. Rept. 4002, p. 1–40

Ewing, M., Crary, A. P., and Rutherford, H. M., 1937, Geophysical investigations in the emerged and submerged Atlantic Coastal Plain, Part 1: Methods and results: Geol. Soc. America Bull., v. 50, p. 753–802

Ewing, M., Worzel, J. L., Steenland, N. C., and Press, F., 1950, Geophysical investigations in the emerged and submerged Atlantic Coastal Plain, Part V: Woods Hole, New York, and Cape May sections: Geol. Soc. America Bull., v. 61, p. 877–892

Oliver, J. E., and Drake, C. L., 1951, Geophysical investigations in the emerged and submerged Atlantic Coastal Plain, Part VI; The Long Island area: Geol. Soc. America Bull., v. 62, p. 1287–1296

Suter, R., De Laguna, W., and Perlmutter, N. M., 1949, Mapping of geologic formations and aquifers of Long Island, New York: State of N. Y. Dept. Conservation, Water Power and Control Comm., Bull. G. W. 18, p. 1–212

Tolstoy, I., 1958, Shallow water test of the theory of layered waveguides: Jour. Acoust. Soc. America, v. 30, p. 348–361

Woods Hole Oceanographic Institution, 1954, Quarterly progress report, Reference No. 54-40, p. 4

Woollard, G. P., Bonini, W. E., and Meyer, R. R., 1957, A seismic refraction study of the subsurface geology of the Atlantic Coastal Plain and Continental Shelf between Virginia and Florida: Univ. Wisconsin Dept. Geology and Geophysics, Tech. Rept., p. 13–18

Columbia University Hudson Laboratories, Dobbs Ferry, N.Y. (Brown, Northrop, and Frassetto): International Business Machines Corp., Poughkeepsie, N.Y. (Grabner)

Manuscript Received by the Secretary of the Society, March 10, 1960
Hudson Laboratories Contribution No. 137

JOSEPH R. CURRAY

LATE QUATERNARY SEA LEVEL: A DISCUSSION

Abstract: Recent literature and new evidence on the position of sea level during the late Quaternary are reviewed critically. Some evidence suggests a glacial interstadial and stand of sea level at about −8 fathoms 30,000 years ago. Sea level then dropped to perhaps −65 fathoms. The rapid rise of sea level and warming of climate covered a period of time from 15,000 to 7,000 B.P. (Before Present) and consisted of a period of climatic and sea-level fluctuations rather than a single abrupt warming as proposed for 11,000 B.P.

McFarlan (1961) has presented a stimulating and extremely well-documented study of the position of sea level relative to the late Quaternary alluvial deposits of the Mississippi River. Broecker (1961, p. 159) has debated McFarlan's conclusions. It seems appropriate to test the hypotheses of these writers with data from the continental shelf off Texas (Curray, 1960) and with other pertinent new evidence.

McFarlan has attempted to date the position of sea level during the late Quaternary by means of radiocarbon dates of material from known environments of deposition. His task has been greatly complicated by the rapid deposition and subsidence in the Mississippi delta, thereby necessitating the application of corrections to most of the dates lying outside the "hinge-line" area of the delta. Despite the obvious difficulties and dangers of the determination of sea level from an unstable area, the general trend of dates from 6000 to 17,000 years B.P. reported by McFarlan is remarkably similar to the trends reported by other investigators (Bennema, 1954; van Straaten, 1954; Shepard and Suess, 1956; Godwin *et al.*, 1958; Fairbridge, 1958; 1960; Curray, 1960; Shepard, 1960; Jelgersma and Pannekoek, 1960). The agreement of the general trend of the dates from many parts of the world suggests that McFarlan has been essentially correct in the difficult task of applying corrections to dates from the rapidly subsiding Mississippi delta.

7000 B.P. to 15,000 B.P.

Broecker (1961) suggests that we should observe an acceleration in the rise of sea level correlating with an abrupt warming of climate about 11,000 years ago. This appears to be based on the assumption that the rise of sea level is a simple, one-way event, without allowing for the probable complexity of events around this general period of time. Broecker and Orr (1958) have shown the rapid climatic fluctuations affecting lake level in the Great Basin of western United States (Fig. 1). The levels of Lakes Lahontan and Bonneville lowered until approximately 12,000 to 13,000 years B.P., rose sharply at 11,000 to 12,000 years B.P., dropped, possibly rose again at about 10,000 years, and dropped immediately afterward to remain low until the present day. Meteorological events must certainly have been complex during the period of time from about 13,000 B.P. to 9000 B.P., so let us not assume simplicity in the position of sea level. Lake level presumably responds rather rapidly to local climatic events, while sea level responds more slowly to the net integrated effects of climate in all glaciated areas.

A comparison is made (Fig. 1) between the standard European pollen profile (Barendson *et al.*, 1957, as modified by Broecker, *et al.*, 1960), the levels of Lakes Lahontan and Bonneville (Broecker and Orr, 1958), and the position of sea level (Curray, 1960). The coincidence of peaks is striking. The pollen represents a very quick reaction to climatic changes. Lake levels were high during cold periods and low during warm periods, showing possibly a very slight time lag behind the pollen profile. Sea level, on the other hand, rises during warm periods and falls during cold periods, very probably showing considerably more time lag as a second-order effect caused by the growth and shrinkage of glaciers. The general trend of the sea-level curve of Figure 1 was postulated on the basis of radiocarbon dates; the fluctuations in the curve were postulated on the basis of distribution of sediment characteristics reflecting current directions and the morphology

Geological Society of America Bulletin, v. 72, p. 1707–1712, 2 figs., November 1961

of the areas of the Texas shelf covered with the basal sands of the Holocene transgression. Assuming that the interpretation is correct (Curray, 1960, p. 256–258), the relict shoreline deposits can determine fairly precisely the heights of sea level at the beginnings and ends of the brief regressions, but the dates are much less certain. The comparisons of Figure 1 cannot, therefore, be used to estimate the amount of time lag of sea level behind the causative climatic changes. The comparison is made only to demonstrate that a correlation may exist between climatic fluctuations and sea-level fluctuations.

Broecker *et al.* (1960) have attempted to demonstrate evidence for an abrupt change in climate about 11,000 years ago. Examination of their evidence shows two things: (1) A rather abrupt change in climate (*i.e.*, Atlantic surface-water temperature) occurred between about 15,000 B.P. and 7000 B.P. It is perhaps an unnecessary oversimplification to average the occurrence of this change to a single date such as 11,000 years. (2) The details of this

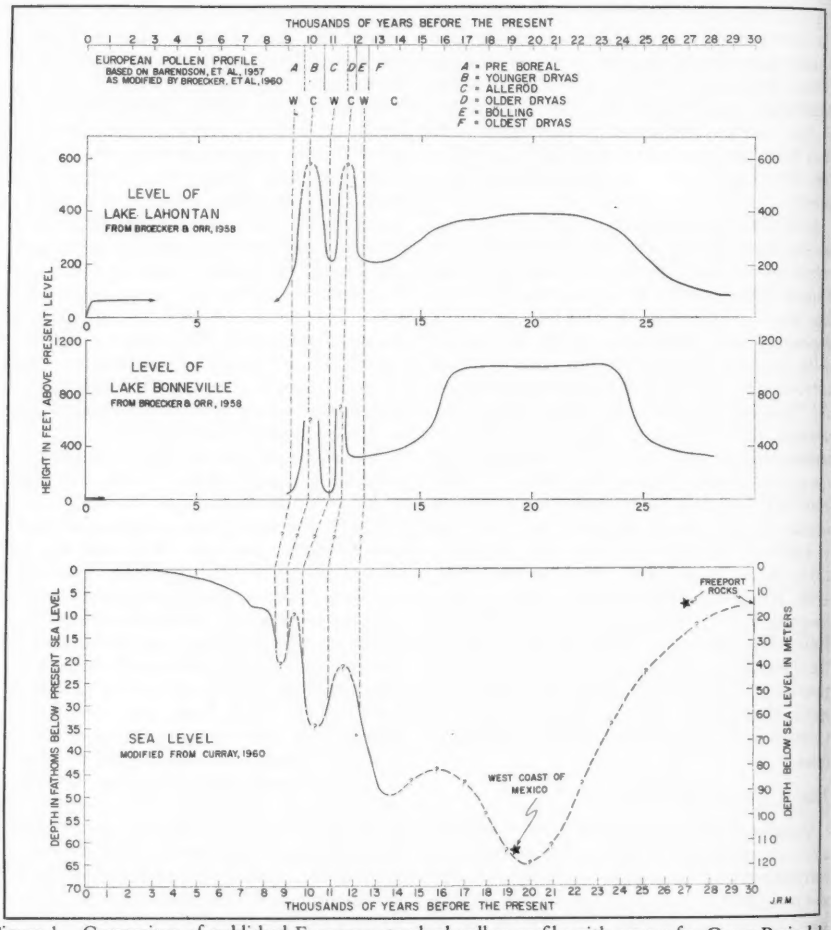

Figure 1. Comparison of published European standard pollen profile with curves for Great Basin lake levels and sea level. Curve for sea level modified to hit present level at 3000 B. P. on basis of Gould and McFarlan (1959), Byrne, LeRoy, and Riley (1959), and Jelgersma and Pannekoek (1960)

climatic change, as revealed by Great Basin lake levels and the European pollen profile, show a complex sequence of fluctuations. These fluctuations are not at all incompatible with the change in ocean-surface temperature and have been damped out of the record. The fluctuations appear to be present, however, in the record of sea level during approximately the period of time of most rapid rise, from about 15,000 to 7000 B.P. It would seem appropriate to re-examine the records of this period of time. We are probably attaching undue significance to the date 11,000 when we should be referring to a period of transition covering several thousand years, still rather abrupt in terms of the length of time involved in the Wisconsin.

Use of the time 11,000 B.P. seems particularly inappropriate in referring to the time of triggering the end of the glaciation by freezing over the Arctic Ocean (Ewing and Donn, 1956). Most of the published estimates of the position of sea level for this time agree that approximately half the water had been returned to the oceans from the late Wisconsin glaciers. Events at 11,000 could not, then, have triggered the end of the glaciation, but may instead have helped to complete a process already well started.

Prior to 15,000 B.P.

Broecker (1961) has rejected the negative argument by McFarlan that sea level was constant at a level of − 250 feet from sometime prior to 35,000 B.P. until about 18,500 B.P. He suggested the alternative hypothesis that sea level dropped between 25,000 B.P. and 18,000 B.P., citing as evidence the Great Basin lake levels (Broecker and Orr, 1958), studies of ice-sheet advances in the Lake Erie to southern Ohio area (Flint and Rubin, 1955), pollen sequences of northern Europe and the Paudorf interstadial (deVries, 1958), and oxygen-isotope and coarse-fraction studies of deep-sea cores (Emiliani, 1955; Broecker *et al.*, 1958). The study of the continental shelf off Texas further corroborates Broecker's suggestion of lowering of sea level following an interstadial prior to 25,000 B.P.

There is no evidence from the shelf off Texas of a long-continued stillstand of sea level at − 250 feet (42 fathoms). Such a stillstand would have had a profound effect on the continental shelves of the world and particularly on the areas such as parts of the eastern Texas shelf where present deposition is negligible. Extensive terraces and submerged deltas would have been formed at this depth; shore-line features and deposits would be widespread; and the banks in the Gulf of Mexico would show pronounced terraces cut into their sides, or else they would have been planed off to this level. Detailed bathymetry of the eastern Texas shelf (Curray, 1960, p. 226–227) shows marked changes in gradient at 35 fathoms (215 feet) and 65 fathoms (390 feet), but nothing at 250 or 300 feet. These latter depths lie on the slightly steeper outer shelf, devoid of significant escarpments or shore-line features. Although relict shore-line deposits are rather widespread on the sandy part of the shelf, there is no evidence of especially extensive development of such deposits in the 250- to 300-foot depth range.

The bathymetry of the rock, shell, coral, and Lithothamnion banks on this shelf was studied by Parker and Curray (1956) by plotting a histogram of the depths to the tops of 130 banks. The most frequent occurrences of bank tops are at about 9, 32, and 48 fathoms (54,192 and 288 feet), suggesting periods of erosion at or near sea level at these depths. Terraces observed in the sides of the better surveyed banks fall at approximately these same depths. If sea level had stayed at − 250 feet (42 fathoms) for more than 15,000 years, many of the banks would show flat tops or terraces at this level. The 48-fathom mode of the histogram of bank tops, and the occasional low escarpments in the sediments on the shelf at 45 to 50 fathoms (Curray, 1960, p. 259) do not suggest a long-continued stand of sea level.

A very recently obtained date from the continental shelf south of Mazatlan, Mexico, corroborates the suggestion (Curray, 1960, p. 258–259) that sea level was at about − 65 fathoms between 18,000 and 20,000 B.P. A sample (C-331) dredged by the writer from near the shelf edge at 62½ fathoms about 60 nautical miles south of Mazatlan (22° 06.7′ N. Lat., 106° 17.8′ W. Long.) consists of shells identified by Robert H. Parker (personal communication) as predominantly shallow-water organisms. A sample of *Strombus grannulatus*, with living depth range of 1 to 10 fathoms (Parker, personal communication), gave a C^{14} date of 19,300 ± 300 B.P.

Little is known of the stability of this Mexican shelf except from an uncompleted study of the morphology and sediments by the writer. Both the development of the wide strand plain along the coast and the depths of

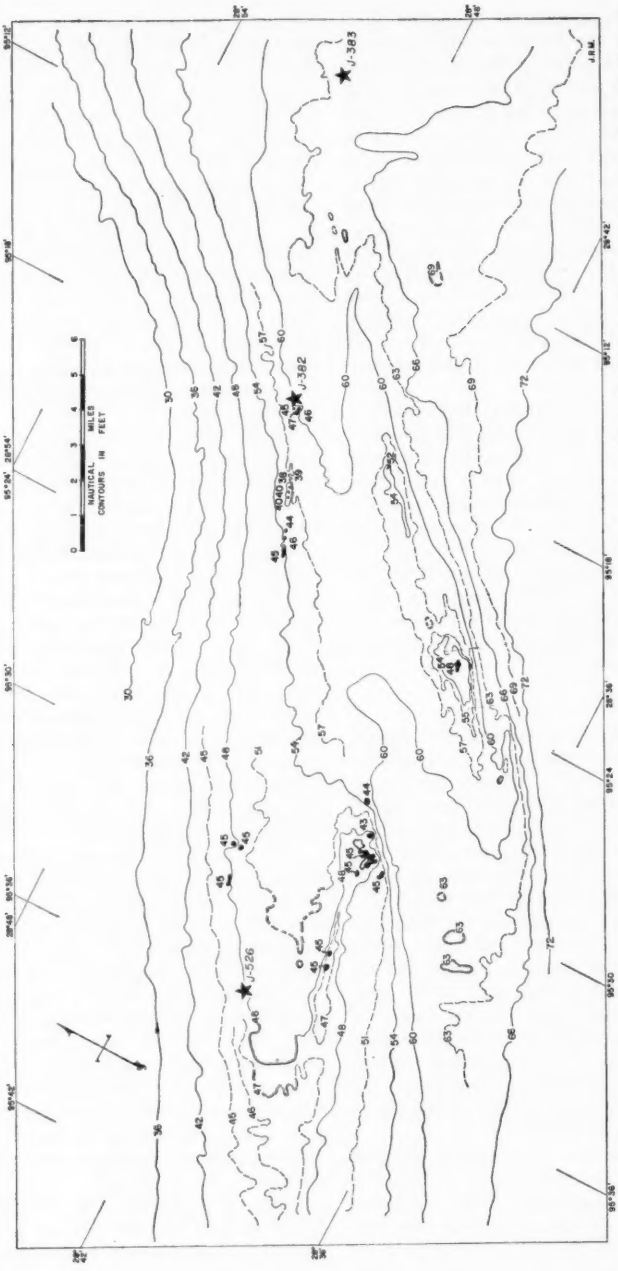

Figure 2. Bathymetric chart of Freeport bank and rock area, Texas. "Rock Pinnacles" shown in black with depths to tops in feet. Samples and observations at locations indicated with stars. Soundings from unpublished plotting sheets, Coast and Geodetic Survey

relict shore-line deposits on the shelf suggest, but certainly do not prove, that the area has been relatively stable during this time.

Some additional evidence on the position of sea level prior to 20,000 B.P. comes from dates from the shallow shelf off Freeport, Texas (Curray, 1960, p. 225, 255, 256). Two pre-Tazewell dates were obtained from a line of isolated rock pinnacles at about 8 fathoms in this area. The rocks on two pinnacles (J-382 and J-383) were examined by SCUBA diving and found to be calcareous-cemented beachrock and coquina. A radiocarbon date of 26,900 ± 1800 years was obtained on *Crassostrea virginica* selected by Robert H. Parker (sample J-383, Fig. 2). In line with these rocks and farther west is rough bottom of shells and coquina (J-526), which give a date of 32,500 ± 3500 B.P. from *Rangia cuniata* and *Crassostrea virginicia*, also selected by Parker.

The low sediment bank in the 60-foot contour off Freeport (Fig. 2) is probably a Holocene feature formed during the transgression. The rock pinnacles, rising to 15 feet above the adjacent bottom, are arranged in a line at an angle to the sediment bank. These rocks probably represent the few remaining remnants of a beach-line development from an interstadial approximately 30,000 years ago. Parts of the beach were cemented to form hard beachrock and coquina and survived the long subaerial exposure. The nature of the other "rocks" shown in Figure 2 has not been investigated, but they probably hold some of the record of a complex sequence of climatic and sea-level fluctuations.

Francis P. Shepard (personal communication) reports new dates on shells from 5- and 12-foot elevated terraces on Hawaii of 24,000 ± 700 and 31,400 ± 1200 B.P. respectively. The stability of Hawaii is certainly questionable, but these dates may indicate an approximation of the position of sea level at that time.

None of this evidence has any bearing on the probability of stands of sea level lower than − 65 fathoms, but no dates are yet available to determine when these low stands occurred. It is suggested here that these low stands may have occurred in the early Wisconsin, prior to the 25,000 to 30,000 year interstadial.

Conclusions

(1) The general trend of dates for the last 17,000 years presented by McFarlan agrees with published results of many other investigators.

(2) The sequence of climatic events "at about 11,000 years ago" was not a simple unidirectional change, but was instead a complex sequence of fluctuations in climate occurring between about 15,000 and 7000 B.P., which also affected sea level. Warming at 11,000 B.P. could not have triggered the end of the glaciation because by that time approximately half the water had been returned to the oceans by the glaciers. We should not refer to the end of glaciation as 11,000 B.P. because it was more probably a period of transition and fluctuation lasting several thousand years. The Holocene/Pleistocene sedimentary contact along our continental shelves and coastal plains is a time-transgressive unconformity, older than 11,000 on the outer shelves, and younger inside of approximately 25 to 35 fathoms.

(3) There is no corroborating evidence from the rather densely sampled and very well-sounded shelf off Texas of a stillstand of the sea at −250 feet (42 fathoms) for a duration of many thousands of years.

(4) Preliminary studies of the continental shelf off the west coast of Mexico corroborate previous suggestions that sea level was at about −65 fathoms between 18,000 and 20,000 years ago, at the height of the Tazewell glaciation.

(5) Isolated remnants of a shore-line deposit at a depth of 8 fathoms off Freeport, Texas, give radiocarbon dates suggesting an interstadial somewhere around 30,000 years ago.

Acknowledgments

This work was sponsored by the American Petroleum Institute Project 51. Francis P. Shepard, Robert H. Parker, and Tj. H. van Andel have contributed significantly to this study and to reviewing the manuscript.

References Cited

Barendson, G. W., Deevey, E. S., and Gialenski, L. J., 1957, Yale radiocarbon measurements III: Science, v. 126, p. 908–919

Bennema, J., 1954, Holocene movements of land and sea-level in the coastal area of the Netherlands: Geologie en Mijnbouw, v. 16e, (n. ser.), p. 254–264

Broecker, W., 1961, Radiocarbon dating of Late Quaternary deposits, south Louisiana: A discussion: Geol. Soc. America Bull., v. 72, p. 159–162

Broecker, W. S., and Orr, P. C., 1958, The radiocarbon chronologies of Lake Lahontan and Lake Bonneville: Geol. Soc. America Bull., v. 69, p. 1009–1032

Broecker, W. S., Ewing, M., and Heezen, B. C., 1960, Evidence for an abrupt change in climate close to 11,000 years ago: Am. Jour. Sci., v. 258, p. 429–448

Broecker, W. S., Turekian, K. K., and Heezen, B. C., 1958, The relation of deep sea sedimentation rates to variations in climate: Am. Jour. Sci., v. 256, p. 503–517

Byrne, J. V., LeRoy, D. O., and Riley, C. M., 1959, The chenier plain and its stratigraphy, southwestern Louisiana: Gulf Coast Assoc. Geol. Socs. Trans., v. 9, p. 237–260

Curray, J. R., 1960, Sediments and history of Holocene transgression, continental shelf, northwest Gulf of Mexico, p. 221–266 *in* Shepard, F. P., *et al., Editors,* Recent sediments, northwest Gulf of Mexico, 1951–1958: Am. Assoc. Petroleum Geologists, 394 p.

deVries, Hl., 1958, Radiocarbon dates for upper Eeem and Wurm-interstadial samples: Eiszeitalter und Gegenmark, Band 9, p. 10–17

Emiliani, C., 1955, Pleistocene temperatures: Jour. Geology, v. 63, p. 538–578

Ericson, D. B., Broecker, W. S., Kulp, J. L., and Wollin, G., 1956, Late-Pleistocene climates and deep-sea sediments: Science, v. 124, p. 385–389

Ewing, M., and Donn, W. L., 1956, A theory of the ice ages: Science, v. 123, p. 1061–1066

Fairbridge, R. W., 1958, Dating the latest movements of the Quaternary sea level: N. Y. Acad. Sci. Trans., ser. 2, v. 20, p. 471–482

—— 1960, The changing level of the sea: Scientific American, v. 202, p. 70–79

Flint, R. F., and Rubin, Meyer, 1955, Radiocarbon dates of pre-Mankato events in eastern and central North America: Science, v. 121, p. 649–658

Godwin, H., Suggate, R. P., and Willis, E. H., 1958, Radiocarbon dating of the eustatic rise in ocean-level: Nature, v. 181, p. 1518–1519

Gould, H. R., and McFarlan, E., Jr., 1959, Geologic history of the chenier plain, southwestern Louisiana: Gulf Coast Assoc. Geol. Socs. Trans., v. 9, p. 261–270

Jelgersma, S., and Pannekoek, A. J., 1960, Post-glacial rise of sea level in the Netherlands (A preliminary report): Geologie en Mijnbouw, v. 39, p. 201–207

McFarlan, E., Jr., 1961, Radiocarbon dating of Late Quaternary deposits, south Louisiana: Geol. Soc. America Bull., v. 72, p. 129–158

Parker, R. H., and Curray, J. R., 1956, Fauna and bathymetry of banks on continental shelf, northwest Gulf of Mexico: Am. Assoc. Petroleum Geologists Bull., v. 40, p. 2428–2439

Shepard, F. P., 1960, Rise of sea level along northwest Gulf of Mexico: p. 338–344 *in* Shepard, F. P., *et al., Editors,* Recent sediments, northwest Gulf of Mexico, 1951–1958: Am. Assoc. Petroleum Geologists, 394 p.

Shepard, F. P., and Suess, H. E., 1956, Rate of postglacial rise of sea level: Science, v. 123, p. 1082–1083

van Straaten, L. M. J. U., 1954, Radiocarbon dating and changes of sea level at Velzen (Netherlands): Geologie en Mijnbouw, n. ser., v. 16, p. 247–253

Scripps Institution of Oceanography, La Jolla, Calif.
Manuscript Received by the Secretary of the Society, April 24, 1961

Addendum

After this note was submitted, the following papers appeared or were called to the writer's attention:

Flint, R. F., and Brandtner, F., 1961, Climatic changes since the last interglacial: Am. Jour. Sci., v. 259, p. 321–328

Frye, J. C., and Willman, H. B., 1960, Classification of the Wisconsinian Stage in the Lake Michigan glacial lobe: Ill. Geol. Survey Circ. 285, 16 p.

—— 1961, Continental glaciation in relation to McFarlan's sea-level curves for Louisiana: Geol. Soc. America Bull., v. 72, p. 991–992

Each of these papers shows warmer climate or glacial retreat between approximately 25,000 and 30,000 years ago, colder climate or glacial maximum approximately 18,000 to 20,000 years ago, and short-period fluctuations between 15,000 and 7000 years ago, corroborating the sea-level curve proposed in this note.

JOHN B. DROSTE

CLAY MINERALS IN SEDIMENTS OF OWENS, CHINA, SEARLES, PANAMINT, BRISTOL, CADIZ, AND DANBY LAKE BASINS, CALIFORNIA

Abstract: Clay minerals are not affected significantly by diagenetic processes in the continental saline environment, and the clay suite is used to correlate basin-fill materials in Owens, China, and Searles lakes and in Bristol and Cadiz lakes.

The U. S. Geological Survey has obtained deep cores in two large groups of intermontane basins in southern California as part of a project to study various aspects of saline deposits in the Mojave Desert, and the gross lithology of these cores has been described in several parts of U. S. Geological Survey Bulletin 1045. Samples for clay-mineral analyses were obtained from these cores to test the use of clay suites in correlation problems and to gain information concerning clay-mineral diagenesis in continental sediments.

Owens Lake, China Lake, Searles Lake, and two playas in Panamint Valley are considered as one group in this study because these basins probably contained a more or less continuous system of lakes during pluvial times of the Pleistocene (Gale, 1914). Smith and Pratt (1957) suggested that the main source of water for these basins was from drainage on the eastern slopes of the Sierra Nevada. This water formed the Owens River, for which Owens Lake was the settling basin. When Owens Lake filled to about 200 feet above the present lake surface, overflow water cut a narrow gorge leading into Indian Wells Valley. A large, shallow lake, China Lake, formed in Indian Wells Valley and filled to a depth of about 640 feet above the present playa surface. At high-water stage China Lake overflowed into Searles Lake, and at maximum high water Searles Lakes and China Lake merged. Water from this large lake flowed around the south end of the Slate Range into Panamint Valley, and the lake formed in Panamint Valley rose to about 930 feet above the present basin floor (Fig. 1).

A second group of related basins, including Bristol, Cadiz, and Danby dry lakes, occupy a northwest-trending trough divided into basins by projecting mountain ranges (Fig. 2). The geologic setting and gross composition of basin sediments have been given by Bassett, Kupfer, and Barstow (1959).

Surface sediments of Bristol Dry Lake were described by Gale (1951), and the Danby Dry Lake surface sediments were described by Ver Planck (1954). A large flow from Amboy Crater (also called Bagdad Cinder Cone) has separated Bristol Lake Basin into Bristol Dry Lake on the east and Alkali Dry Lake (also called Bagdad Dry Lake) on the west. The surface sediments of Alkali Dry Lake are essentially identical to surface sediments of Bristol Dry Lake.

Bristol and Cadiz basins are separated by a divide about 52 feet above the present lowest part of the Bristol playa and about 104 feet above the lowest part of the present Cadiz playa. Thompson (1929) proposed the name Amboy Lake for a large body of water that he thought existed in the Bristol-Cadiz basin in Pleistocene time.

Danby Dry Lake is a sump of a separate basin called Ward Valley, and Thompson (1929) suggested that the Pleistocene lake in Ward Valley be called Ward Lake. Ward Lake may have overflowed to the Colorado River through a pass near Rice, California.

Bassett, Kupfer, and Barstow (1959) stated that

"in none of the three basins, however, have the writers found shoreline features, wave-cut terraces, or gravel bars, such as occur commonly around other desert basins that did contain overflowing Pleistocene Lakes, though these absences do not constitute proof that such lakes never existed. This evidence is in accord with the theoretical argument that such huge bodies of water would not be expected even during pluvial periods, because the entire drainage basin lies within one of the most

Geological Society of America Bulletin, v. 72, p. 1713–1722, 6 figs., November 1961

arid regions of the country. It seems likely that these basins contained only very shallow—perhaps ephemeral—lakes that did not overflow during the late Pleistocente epoch."

The clay-mineral composition of sediments in more than 60 desert basins in California, Nevada, and Oregon shows that the clay suites of desert lake basins strongly reflect the source rocks surrounding the basins (Droste, 1961; in press).

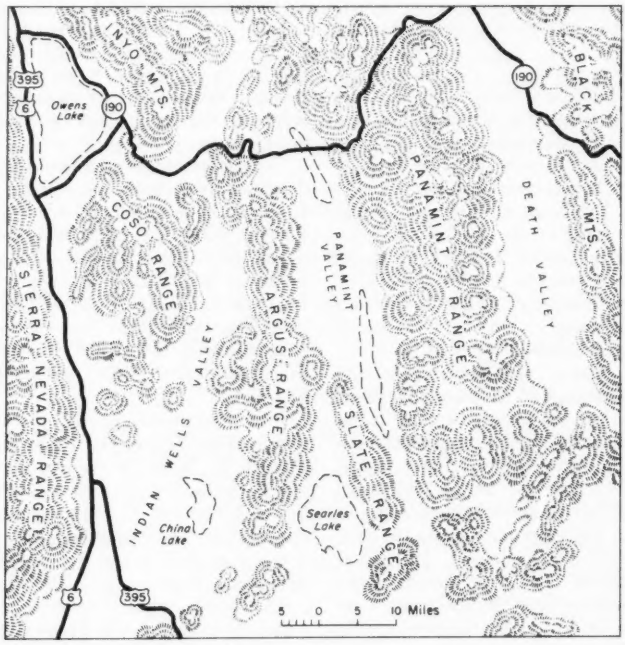

Figure 1. Index map of Owens, China, Searles, and Panamint basins

This work is part of a larger study of the effect of saline environments on clay minerals supported by a grant from the National Science Foundation, and some reports have already appeared (Droste, 1959; Harrison and Droste, 1959; Droste and Gates, 1959; Gates, 1959; Grim, Droste, and Bradley, 1961; Droste, 1961; in press). Without the co-operation of many commercial organizations and U. S. Geological Survey geologists, the study could not have been made.

Normal X-ray methods have been used in determining the clay-mineral composition of the samples studied. After complete removal of soluble salts (often very time consuming for the evaporite samples) the material less than 2 microns in size was removed by sedimentation in distilled water. Oriented clay aggregates were prepared on glass slides, and diffraction data from untreated, glycolated, and heated (400° C and 450° C for half an hour) slides were obtained on an XRD-5 General Electric diffractometer.

It was believed that some components of Owens Valley detritus could be recognized in the sediment of downstream deposits, and the clay minerals were considered the most likely to be carried from one lake to another.

The clay suites around each basin were determined, and it is assumed that the suites have been relatively constant throughout the time represented by the sediments in the cores.

The clay-mineral compositions of the material < 2 microns in size in the deep-core samples from the lakes are given in Figure 3. The ratio of clay minerals in detritus entering

Owens Lake is 2:7:1 for montmorillonite:illite: chlorite and/or kaolinite, respectively, and the variation in composition for the basin sediments in Owens Lake is produced by variation in the relative abundance of montmorillonite and illite. The increase in abundance of montmorillonite over illite is related to volcanic eruptions in Quaternary time. Those samples of silt and clay richest in montmorillonite contain fresh to thoroughly altered glass shards as well as layers of more or less pure volcanic glass.

The locally derived sediment entering China Lake has a montmorillonite:illite:chlorite and/or kaolinite ratio of 5:4:1, and most of the samples from China Lake also have this ratio. At two depths, 350 feet and 610 feet, the sediment in the China Lake core has the clay suite of the typical Owens River detritus. It is suggested that, when sediment was accumulating in Indian Wells Valley at 350 feet and 610 feet below the present surface, the Owens River carried detritus into China Lake. The 350-foot level in the China Lake core best correlates with the 200- to 370-foot interval in Owens Lake, and the 610-foot level in China Lake correlates with the 810- to 900+(?)-foot interval in Owens Lake. If the montmorillonite is directly related to volcanic ash, and if the ash from the same eruption fell into both lakes, the montmorillonite-rich layers in China Lake at 430 feet and 570 feet may correlate with the high montmorillonite material at 400–500 feet and 780 feet respectively in the Owens Lake core.

The use of clay-mineral composition to suggest times of China Lake and Searles Lake drainage integration is more tenuous than the correlation between Owens Lake and China Lake. The abundant montmorillonite at 800 feet and in the interval between 520 feet and 650 feet in Searles Lake may have resulted from the influx of typical montmorillonite-rich China Lake detritus or may have formed from devitrification of volcanic ash. If a correlation can be made, the most plausible suggestion is that these lakes were connected at the time represented by the sediments between 650 and 520 feet in Searles Lake and between 570 and 390 feet in China Lake. The greater abundance of montmorillonite in the Searles Lake sediment from the surface to 160 feet also suggests that in late Pleistocene and Recent time detritus from Indian Wells Valley has entered Searles Lake Basin.

The clay suites in the samples from the three deep cores in Panamint Valley show very little variation, and the montmorillonite:illite: chlorite and/or kaolinite ratio typically is 5:3:2. The source surrounding the Panamint Basin contributes sediment whose montmorillonite: illite:chlorite and/or kaolinite ratio ranges between 6:3:1 and 3:4:3. The uniformity of the

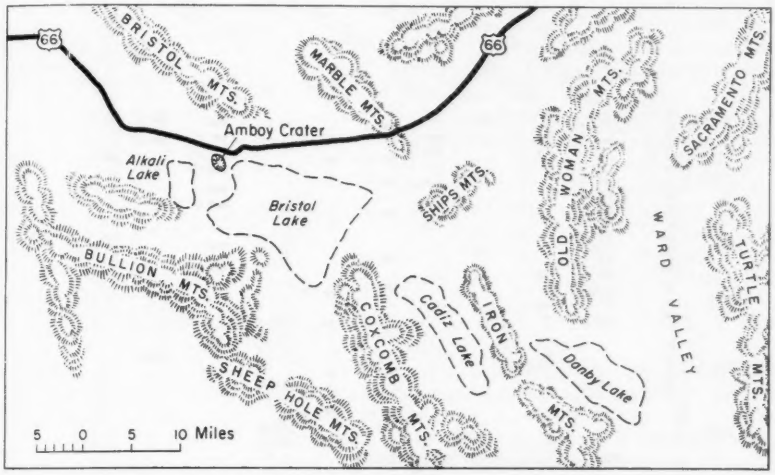

Figure 2. Index map of Bristol, Cadiz, and Danby basins

clay-mineral composition of the basin fill indicates thorough mixing of various source materials in the basin of deposition.

Searles Lake is a playa about 7 miles wide and 9 miles long; geophysical data (Mabey, 1956) indicated that the lake fill is about 3300 feet thick. About 12 square miles of the center of the lake is exposed halite; the remaining surface consists of wet, soft, silty mud. The shore facies are sand and gravel of beach and alluvial-fan deposits. Drainage into the playa is from the slopes of the Argus Range and from Indian Wells Valley to the west and Slate Range on the east.

Forty-one shallow drill holes in the saline deposits in the lake have been described by Haines (1959). These holes were drilled by the U. S. Geological Survey to obtain basic data on the shape, thickness, and character of the salt bodies, and the samples used in the present clay-mineral study were obtained from these cores. The minerals most often found in the saline bodies are halite, trona, hanksite, borax, thenardite, burkeite, and aphthitalite; mud and marl layers contain dolomite (probably detrital), gaylussite, pirrsonite, aragonite, nahcolite, and tychite; northupite and sulfohalite are found in both evaporite and mud layers.

The evaporite deposits are two beds of saline minerals separated by fine-grained clastic layers. The upper salt layer, locally called "upper salt," "upper structure," or "upper crystal body," is exposed in the central portion of the lake, and silty clay, locally called "overburden mud," overlies the upper salt. The mineral composition of the upper salt is predominantly halite, trona, hanksite, and borax. The lower salt layer ("lower salt," "lower structure," or "lower crystal body") is separated from the upper salt by the mud layer called the "parting mud." The parting mud contains dominantly disseminated crystals of gaylussite and pirssonite with halite, aragonite, trona, burkeite, northuptite, and borax and others in lesser amounts. The lower salt can be distinguished from the upper salt because: (1) the lower salt has more mud layers; (2) hanksite is

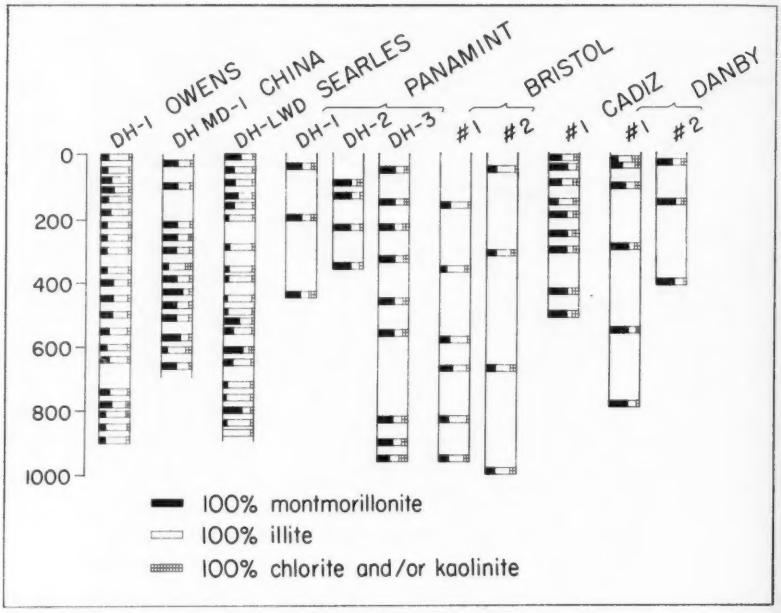

Figure 3. Clay minerals in sediment from cores in Owens, China, Searles, Panamint, Bristol, Cadiz, and Danby basins. Each bar represents the clay-mineral composition of the sediment at the depth indicated.

not found in the lower salt; (3) the lower salt contains northupite and burkeite, which are absent or rare in the upper salt; and (4) the lower salt has tychite and schairerite near its base. All the sediment below the bottom salt is called the "bottom mud." Figure 4 presents a

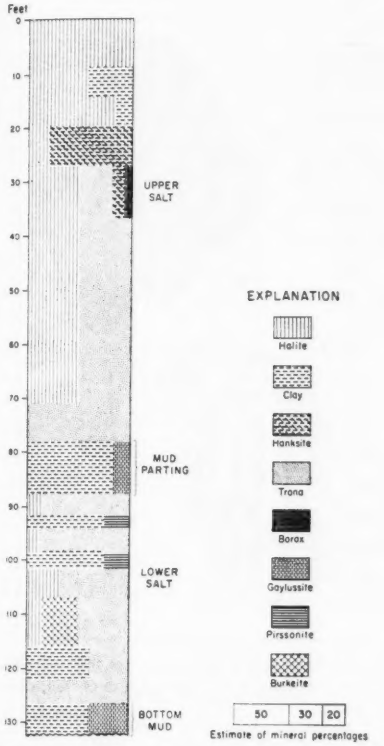

Figure 4. Generalized core log of the upper 130 feet of the sediments near the center of Searles Lake. After Haines (1959)

generalized typical core log of the upper 150 feet of the sediments near the center of the playa.

The clay-mineral composition of the shallow sediments in Searles Lake is shown in Figures 5 and 6. The overburden mud varies widely in clay-mineral composition but is commonly more montmorillonitic than the parting mud in the same location. The parting mud is generally less montmorillonitic than the bottom mud just below the lower salt. The clay-mineral composition of the bottom mud below 150 feet is shown in Figure 3.

Much of the 14 Å–7 Å material in Searles Lake is chlorite, but 8 of 20 surface samples contain kaolinite as well as chlorite. Kaolinite is not present without chlorite in any sample. Kaolinite and chlorite are difficult to differentiate in samples containing a small amount of either or both minerals, and conclusions concerning them are tentative.

The source of chlorite is dominantly from the Slate Range, the montmorillonite is derived from Indian Wells Valley, and the illite comes from most of the sources surrounding Searles Lake. Like illite, kaolinite is obtained from several sources.

The sporadic distribution of the clay suites in the shallow and surface sediments of Searles Lake is not readily explained, and the distribution of chlorite is the most perplexing. The inverse relationship of the illite and montmorillonite abundance is related to the source of the sediments, and minor variations that depend upon sedimentary dispersal processes exist between neighboring samples.

Several possibilities may account for the chlorite distribution:

(1) Diagenesis in the super saline desert environment is altering the chlorite to montmorillonite.

(2) The distribution is produced solely by agents of transportation and deposition.

(3) Chlorite is present in all samples, but it cannot be recognized because of its scarcity and/or low crystallinity.

Diagenesis in the supersaline environment probably is not a major factor in chlorite distribution, because chlorite is found in samples containing all combinations of evaporites. The chlorite in a few very salty samples is slightly degraded, but in other samples with the same salt content, the chlorite is not degraded.

The distribution of chlorite in the surface sediments is probably most closely related to normal sedimentary dispersal mechanisms. The montmorillonite-rich sediment from western sources (Indian Wells Valley) is not thoroughly mixed with the chlorite-rich sediment entering the basin from the east, and hence montmorillonite is more abundant in the western part of the playa deposits and chlorite in eastern sediments. The inverse abundance of montmorillonite and illite also suggests the strong source influence and incomplete mixing.

Normal sedimentary dispersion may explain the distribution of chlorite in the surface

samples of Searles Lake, but not the seeming lack of chlorite in many near-surface samples closely related to the upper and lower salt layers. Chlorite is probably present in all samples, but the abundance and crystallinity are so low that it is not recognized. Partially degraded chlorite is identified in some samples tween these two cores. Although two cores from Danby Dry Lake were between two commercial halite deposits in the north and south ends of the basin, halite was not penetrated by either core. The only correlation between the Danby cores was general: the upper 120–130 feet of sediment in both cores is yellowish-

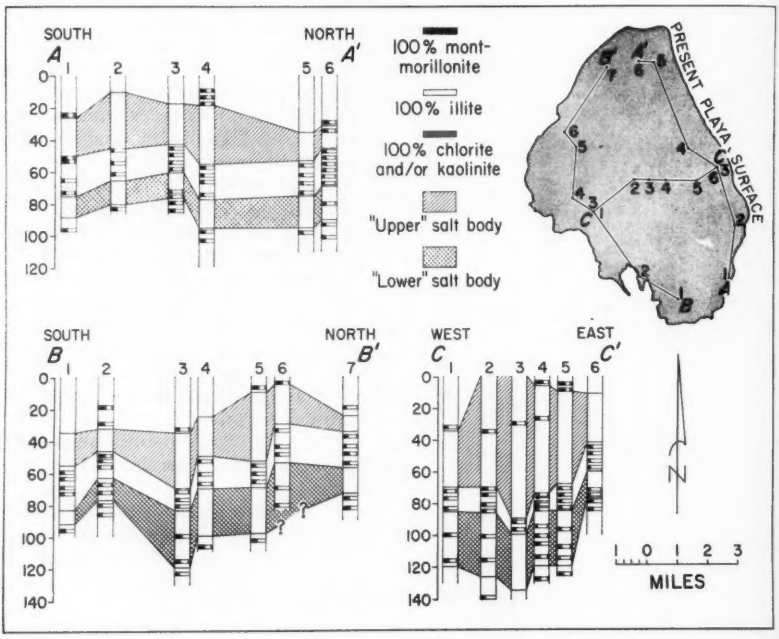

Figure 5. Clay-mineral data of shallow sediment in Searles Lake. Each bar represents the clay-mineral composition of the sediment at the depth indicated. The inset map shows the location of each core.

by the (003) X-ray reflection in untreated material and the (001) peak of glycolated material. The first- and third-order peaks disappear upon heating to 400° C, indicating that the chlorite is degraded. A small, weak, diffuse peak at 7 Å is present in most samples, but the mineral producing the peak is very scarce and is not included in the data in Figures 5 and 6.

Bassett, Kupfer, and Barstow (1959) have pointed out the difficulty in correlating sediments from two cores in a single basin as well as between two basins. For example, each of two deep cores (more than 1000 feet) about a mile apart in Bristol basin penetrate sediments of which 40 to 50 per cent are evaporite beds, but positive correlations were not made between these two cores. Although two cores from Danby Dry Lake were between two commercial halite deposits in the north and south ends of the basin, halite was not penetrated by either core. The only correlation between the Danby cores was general: the upper 120–130 feet of sediment in both cores is yellowish-brown silty clay, and below 120–130 feet the sediment is olive-gray clay with coarse sand grains. Both cores contain crystalline gypsum layers, but these layers vary widely in thickness and depth. The cores from Bristol and Cadiz dry lakes have no similarity according to Bassett, Kupfer, and Barstow (1959).

The clay-mineral data obtained from core samples in these basins are given in Figure 3. The clay-mineral composition of 40 surface samples from Bristol and Alkali dry lakes has a montmorillonite:illite:chlorite and/or kaolinite ratio ranging from 6:3:1 to 5:3:2. Detritus entering Bristol basin ranges from 6:3:1 to 3:5:2 in clay-mineral abundance, and the higher montmorillonite content comes directly from

volcanic terranes. Extrusive volcanism has taken place in late Pleistocene and Recent time in the Bristol Basin area. Samples of the surface sediment near the core sites show high montmorillonite. One sample taken at 35 feet thick) is reported at 667 feet in Bristol core no. 2, and relic shards are present in other samples. The brines associated with the salt layers may inhibit the devitrification of ash to montmorillonite, and the unique occurrence of

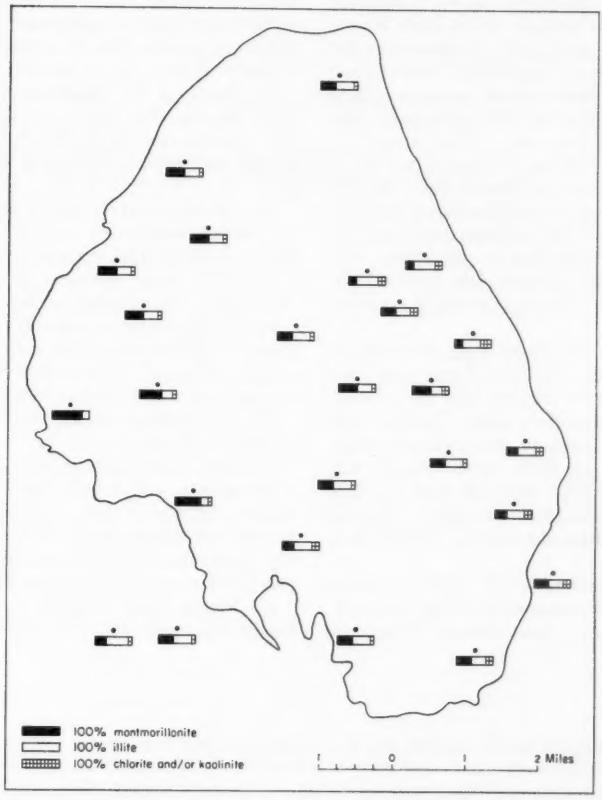

Figure 6. Clay-mineral data of surface sediments in Searles Lake. The sample location is indicated by a dot, and the bar represents the clay-mineral composition of the sediment at that location.

in the bottom of an exploration pit not far from the core locations had a 3:5:2 clay-mineral compositional ratio.

The uniform clay-mineral composition in the Bristol core samples suggests thorough mixing of detritus and that the volcanism that produced the high montmorillonite content of the surface samples did not take place until Recent time. The rather low montmorillonite content in the subsurface sediments of Bristol Dry Lake is a bit confusing. An ash bed (1 inch high calcium chloride brine in Bristol Basin may be the controlling influence.

The surface and subsurface clay-mineral distribution in the sediments of Cadiz Basin are very similar, and all but two samples (both subsurface) have a montmorillonite:illite:chlorite and/or kaolinite ratio ranging between 4:4:2 and 6:2:2. The sample from 150 feet in the Cadiz core has a clay-mineral ratio of 3:5:2, and it is suggested that if Cadiz Basin ever received detritus from the Bristol Basin it was

during deposition of this portion of the core.

The source rocks contributing material to Danby Basin furnish sediment that ranges from 3:5:2 to 6:3:1. Major northeastern sources yield sediments with the high montmorillonite content. In the surface sediments of Danby Dry Lake the range from 5:4:1 to 4:4:2 indicates that the detritus brought to the basin is only partially mixed in the site of deposition. Incomplete mixing of sediments from several sources has also produced the variation in clay-mineral composition in the uppermost sediments of Danby core no. 1. The composition of the sample of 10 feet in Danby core no. 1 may reflect overflow of Bristol Basin detritus into Danby Basin, but field evidence does not support this view. The uniform distribution in clay-mineral composition in the other subsurface samples from Danby Dry Lake is probably produced by thorough mixing in the basin of deposition.

Clay-mineral data might suggest that Cadiz and Danby basins may have been joined as a single lake, but the similar clay suites result from the fact that both basins received sediment from the same or similar source rocks. The sediments of both basins contain ash, zeolites, and opaline material, and the high montmorillonite content probably is directly related to ash falls and detritus derived from volcanic rocks.

Several conclusions can be made concerning the clay mineral composition of the basin sediments in Owens, China, Searles, Panamint, Bristol, Cadiz, and Danby Lakes, California:

(1) The clay-mineral composition of desert saline sediments of southern California is controlled almost entirely by the composition of the source rocks. The evaporites of this region are rich in sodium and calcium, and magnesium salts are extremely rare. The high sodium and calcium environment does not produce significant diagenetic change in the clay minerals deposited in these desert basins.

(2) Much of the variation in montmorillonite abundance is related to volcanic ash and aids in recognition of episodes of volcanism even though ash may not be seen in pure layers of glass.

(3) The degraded chlorite in the surface and near-surface samples in Searles Lake may or may not result from diagenesis in the supersaline environment. If diagenetic alteration has taken place, the modification is very slight.

(4) The high calcium chloride content in the brines of Bristol Dry Lake may be the controlling influence in retarding devitrification of glass into montmorillonite-rich clay sutes.

(5) Clay-mineral composition can be used to correlate rock sequences.

(6) Clay data indicate that Owens Basin sediment has spilled over into Indian Wells Valley, and China Basin sediment has overflowed into Searles Basin. The clay suites do not suggest that Searles Basin sediment has been transported into the Panamint Valley.

(7) Bristol Basin sediment may have overflowed into Cadiz Valley for one brief interval.

References Cited

Bassett, A. M., Kupfer, D. H., and Barstow, F. C., 1959, Core logs from Bristol, Cadiz, and Danby dry lakes, San Bernardino County, California: U. S. Geol. Survey Bull. 1045-D, p. 97–138

Droste, J. B., 1959, Clay minerals in playas of the Mojave Desert, California: Science, v. 130, p. 100

—— 1961, Clay mineral composition of sediments in some desert lakes in Nevada, California, and Oregon: Science, v. 133, p. 1928

—— in press, Clay minerals in playa sediments of the Mojave Desert California: Calif. Div. Mines Special Report 69

Droste, J. B., and Gates, G. R., 1959, Attapulgite in lacustrine sediments of southern California (Abstract): Geol. Soc. America Bull., v. 70, p. 1593

Gale, H. S., 1914, Salines in the Owens, Searles, and Panamint basins, southeastern California: U. S. Geol. Survey Bull. 580-L, p. 251–323

—— 1951, Geology of the saline deposits, Bristol Dry Lake, San Bernardino County, California: Calif. Div. Mines Special Rept. 13, 22 p.

Gates, G. R., 1959, Clay minerals composition of borate deposits and associated strata at Boron, California: Science, v. 130, p. 102

Grim, R. E., Droste, J. B., and Bradley, W. F., 1961, Diffraction data of a regular mixed-layered clay mineral in an evaporite: Proc. Eighth National Clay Conference, Clay and Clay Minerals, Pergamon Press, p. 228–236

Haines, D. V., 1959, Core logs from Searles Lake, San Bernardino County, California: U. S. Geol. Survey Bull. 1045-E, p. 139–317

Harrison, J. L., and Droste, J. B., 1960, Clay partings in gypsum deposits in southwestern Indiana: Seventh Nat. Conf. on Clays and Clay Minerals, Pergamon Press, p. 195–199

Mabey, D. R., 1956, Geophysical studies in intermontane basins in Southern California: Geophysics, v. 21, p. 839–853

Smith, G. I., and Pratt, W. P., 1957, Core logs from Owens, China, Searles, and Panamint basins, California: U. S. Geol. Survey Bull. 1045-A, p. 1–62

Thompson, D. G., 1929, The Mojave Desert region, California: U. S. Geol. Survey Water-Supply Paper 578, 759 p.

Ver Planck, W. L., 1958, Salt in California: Calif. Div. Mines Bull. 175, p. 168

Dept. Geology, Indiana University, Bloomington, Ind.
Manuscript Received by the Secretary of the Society, April 17, 1961

JOSEPH A. VANCE

ZONED GRANITIC INTRUSIONS— AN ALTERNATIVE HYPOTHESIS OF ORIGIN

Abstract: Certain granitic intrusions exhibit a gradational compositional zoning from relatively mafic margins to more leucocratic and potassic cores. Previous explanations of this zoning, including that of assimilation, are discussed and rejected. The proposed hypothesis involves: (1) crystallization from the margins inward, sealing in the released volatile phase which is forced downward with further crystallization; (2) migration downward of alkalis and silica, with the volatiles, and their enrichment in the magma at depth, leaving behind a more mafic residuum.

Recent studies of several granitic batholiths of demonstrated magmatic origin have revealed regular zonal compositional variations that are systematically related to the contacts. The zones are parallel to and roughly concentric with the contact and pass gradationally from relatively mafic quartz dioritic or granodioritic rocks at the margin to more leucocratic and potassic granitic rocks in the core. Although differing in some details, these zoned plutons show remarkable similarity in their over-all mineralogical and compositional progression. From margin to interior all show a decrease in total mafic minerals matched by a proportional increase in potassium feldspar and, to a lesser extent, quartz. Plagioclase tends to decrease sympathetically with the mafic minerals and becomes increasingly sodic toward the interior of the intrusions. Decrease in mafic minerals is accompanied by a falling hornblende–biotite ratio.

The degree of compositional variation and the rock types involved differ considerably among these zoned bodies, although the over-all progression is much the same. The latitude of this variation is shown by three examples for which detailed modal analyses are available. The Bald Rock batholith, California, described by Compton (1955), exhibits continuous gradations from a tonalitic border zone through granodiorite and trondhjemite to a leuco-trondhjemite core. The White Creek batholith, British Columbia (Reesor, 1958), grades inward from biotite granodiorite to hornblende-biotite granodiorite, quartz monzonite, and leuco-quartz monzonite. In both these intrusions, the compositional variation is strongly marked. Somewhat less pronounced variations are shown by the Bald Mountain batholith, Oregon (Taubeneck, 1957), which grades from a broad tonalite margin to a granodiorite interior.

Gradations of this kind have traditionally been attributed to marginal assimilation of mafic country rock by silicic magma of essentially the same composition as the interior of the body. The assimilation hypothesis does, upon first analysis, seem to explain the compositional zoning and has not often been seriously challenged, perhaps largely because no more satisfactory explanation has been forthcoming. It is suggested here that the assimilation mechanism may be open to question, and an alternative theory is proposed.

Other possible explanations include multiple intrusion, differential diffusion within the melt (Soret effect), and settling out of the mafic minerals in the deeper parts of the intrusion leaving the earlier crystallized margins relatively richer in these constituents. None of these, however, appears to account adequately for both the gradational zoning and the magnitude and detail of the compositional variations.

It is also difficult to accept the hypothesis of Hess (Walker, 1956, p. 450) by which Larsen and Poldervaart (1961, p. 87) explain the zoning of the Bald Mountain batholith. According to this theory, crystallization of more mafic minerals in the marginal zones of an intrusion may continue into the final stages of consolidation when the action of convection currents brings new melt into contact with the early crystallizing minerals. Such a mechanism seems possible at the floor of an intrusion where crystals may accumulate by settling and continue to grow in contact with a liquid moving across them. It is improbable, however, that crystals near the roof could remain suspended in fixed position as the surrounding melt sweeps

Geological Society of America Bulletin, v. 72, p. 1723–1728, November 1961

by, at least until such an advanced stage of crystallization is reached that a rigid crystalline mesh is produced, and at this stage the possibility of either convection or appreciable differentiation would be greatly limited. Carr (1954, p. 373) has shown that some of the Skaergaard plagioclase has participated with the melt in several convective cycles. The general tendency must be for melt and crystals in a moving magma to remain together, except as modified by differential vertical movements occasioned by differences in specific gravity.

For the Bald Rock batholith, Compton (1955, p. 54) postulates assimilation of amphibolitic country rock by an initial trondhjemitic magma. While assimilation could indeed produce compositional variations of the kind observed, several difficulties remain. Larsen and Poldervaart (1961) in their recent reinterpretation of the Bald Rock batholith have pointed out several objections. The most cogent relates to the energy problem. The assimilated country rock would have to be about one-fourth the volume of the batholith. It is doubtful that the magmatic body as a whole, much less the marginal parts alone, possessed sufficient energy to make over this amount of country rock. In addition the trend of compositional variation and especially of the plagioclase composition differs from that to be expected from assimilation of mafic country rock. They also find very marked differences in the abundance and crystal habit of zircon in the marginal and interior portions of the batholith. Two more objections to assimilation theory may be added. (1) According to Compton's description, the minerals of the marginal facies of the body, and the plagioclase especially, have igneous textural characteristics. This aggravates the energy problem, as these features imply actual fusion of the assimilated material rather than simple reaction in the solid state. (2) The general absence of gradation, either textural or compositional, between the amphibolitic wall rock and the marginal tonalites is clearly unfavorable to the assimilation hypothesis.

Larsen and Poldervaart (1961) have developed an elaborate hypothesis to account for the compositional zoning of the Bald Rock batholith without recourse to assimilation. They postulate (1) differential fusion of basaltic parent material at depth to give a mobile "migma-magma." (2) During its rise this body segregates into a largely crystalline, but still mobile, mafic outer zone which is gradational into a core of trondhjemitic magma. (3) During the ascent of this column of material, the outer portions recrystallize, and the different crystal habit of the zircon is produced. The writer agrees that the zoning of the batholith is probably not the result of assimilation, but he finds it difficult to accept their alternative. If the marginal facies of the batholith represents a residuum of the original basaltic material from which the trondhjemitic core separated after differential fusion, it should, by reaction, have become more mafic than the original material (*i.e.*, ultramafic rather than tonalitic). In addition, the postulated extensive recrystallization of the marginal tonalites is incompatible with their predominantly igneous textural characteristics. (Incidentally, there appears to be little, if any, physicochemical basis upon which to postulate such complete recrystallization.) The writer would also question whether such a rising column of partially fused mobile material would separate into a magmatic core and a largely crystalline marginal zone. If the magmatic core were sufficiently mobile to segregate itself, would it not separate largely or entirely from the migma phase and be emplaced independently at a higher level? And, even had some such gradational zoning developed at depth, it would be remarkable for it to preserve its integrity under forceful intrusion and conform so regularly to the present contacts.

Reesor (1958, p. 48) has interpreted the compositional zoning of the White Creek batholith in terms of assimilation. The energy problem involved in assimilation may again be raised. Moreover, in this instance the country rock consists of siliceous sediments, chiefly quartzites and argillites. Incorporation of such material could scarcely make a quartz monzonitic magma more mafic.

The compositional variations of the Bald Mountain batholith, Oregon, are attributed by Taubeneck (1957, p. 237) to differentiation in place after intrusion, but he does not discuss the mechanism. From his description assimilation may be ruled out, for the zoning of the batholith does not in any way reflect the compositional heterogeneity of the rocks intruded.

These three intrusions show that strikingly similar zoning has developed in very different lithologic environments. This is a final argument against assimilation, since the zoning is in two cases unrelated to, and in the third (the Bald Rock batholith) may be only accidentally related to, wall-rock lithology. In view of these

difficulties, the assimilation hypothesis must be rejected as a general explanation of such zoning.

The writer believes that a fairly simple mechanism of differentiation *in situ* may be responsible for at least some examples of this type of zoning. The suggested mechanism involves progressive downward migration of volatiles, as a magma having the composition of the present marginal facies crystallizes inward from the contact. Alkalis and silica are carried along with the descending volatiles or diffuse through the volatiles and are enriched in the magma at depth. Volatiles, following the pressure gradient, must in general migrate upward. Under the conditions envisioned here, however, upward movement may be inhibited, and temporary downward movement may ensue. Early crystallization of the cooler upper and outer portions of the intrusion may produce a solid crystalline envelope which prevents upward escape of the volatile constituents subsequently released in the crystallization of the melt immediately below. The released volatile phase will tend to collect in the upper part of the remaining magma body just below the crystalline shell. At deeper levels, owing to the less advanced stage of crystallization of the magma and, to a lesser extent, to their greater solubility at higher pressure, the volatiles will have not yet begun to separate from the melt as a distinct phase. Progressive crystallization inward and downward will produce increasing amounts of the volatile phase, which is sealed in and forced downward by the thickening outer shell. With continued crystallization, one may visualize a downward-moving front of water saturation preceded by a gradient of water concentration which diminishes with depth in the unsaturated deeper melt. The migrating volatiles are redissolved at depth, accelerating saturation of the melt at depth with respect to its stage of crystallization. Volatiles will thus tend to accumulate in increasing amount with depth and with time.

It is well known that at moderate pressures the potassium silicates show continuous solubility with water (Morey and Fenner, 1917; Tuttle and Bowen, 1958, p. 85) and that similar relations probably apply to sodium silicate as well (Tuttle and Friedman, 1948). There is little question that comparable solubility relations occur between alkalis and silica and the vapor phase in water-saturated magmas. Transfer of alkalis and silica by the volatile phase has, of course, long been suspected and has recently been demonstrated experimentally in systems approaching the composition of natural granitic magmas (Tuttle and Bowen, 1958, p. 89). Such solution and transfer is especially to be expected in granitic magmas where advanced fractional crystallization has led to separation of the volatile phase and concentration of alkalis and silica in the residual melt.

It is suggested that selective transfer of alkalis and silica from the marginal to the interior and deeper portions of the melt has occurred in the zoned intrusions considered here. Extraction of these constituents would leave the marginal rocks more mafic than the original magma. By addition, the melt below would become increasingly silicic and richer in alkalis with depth. The volatiles and the substances dissolved in them could be redissolved at depth and modify the composition of the melt directly, or they could act on the already crystallized portions of the deeper magma to produce late magmatic and deuteric changes. By this theory the early crystallized margins of the intrusion should most nearly reflect the composition of the initial magma. Below this undifferentiated shell there might be a concentric residual, more mafic zone from which alkalis and silica have been differentially removed. Such a mafic zone appears to be developed in the White Creek batholith (Reesor, 1958). The undifferentiated marginal zone may vary considerably in thickness and could even be absent, provided the alkali-silica removal process has been active from the start—for instance, where the country rock itself was impermeable to volatiles at the time of intrusion. Tuttle and Bowen (1958, p. 91) supply convincing experimental evidence for a differentiation mechanism of this kind, and John Adams (Personal communication) believes that it may have operated on a large scale to produce a mafic border zone on the Black Peak intrusion in Washington.

Downward migration of volatiles as outlined depends upon the presence of an impermeable crystalline shell which thickens downward with progressive crystallization. Consequently, fracturing and joint formation in these chilled margins, whether due to further impulses of movement after initial emplacement or simply to contraction on cooling, will tend to permit upward or sideward escape of volatiles and to terminate differentiation. Eventually, of course, volatiles in excess of the amounts bound in the

hydrous minerals must escape upward or sideward at depth. The aplite dike swarms so typically associated with magmatic quartz diorites and granodiorites must owe their formation to such a late history of fracturing in which volatiles and residual interstitial melt migrate into newly opened joints. Separation of additional volatiles from the melt in the lower-pressure environment of the joints leads to rapid crystallization of the fine-textured aplites. Such differentiation is not to be expected in all granitic intrusions. Intrusions with a history of nearly continuous fracturing could not develop zoning by the mechanism outlined. Another critical factor is the initial water content of the melt. In very dry melts low volatile content will preclude much differentiation by this mechanism. In water-rich melts extensive differentiation may be possible. The timing of fracturing and jointing will also determine the extent to which the differentiation may operate. It seems probable that irregularities and recurrences in the zoning sequence could result from interruption and later re-establishment of the differentiation process (*e.g.*, because of temporary upward escape of volatiles with fracturing). Deformation during differentiation could lead to movement of the still mobile deeper phases producing local intrusive relationships across the zoning sequence.

The hypothesis outlined here, although intentionally generalized, is believed to be compatible not only with the over-all zoning sequence of the plutons cited, but also with most of their individual detailed relations. In the Bald Rock batholith, for instance, stoping in the early stages of emplacement of a largely crystalline tonalite magma, prior to initiation of differentiation, is required to account for the disappearance of large amounts of mafic wall rock, the development of flow structures, and local inclusion swarms as described by Compton. The writer has not formed any hypothesis to explain the variation in zircon characteristics in the Bald Rock batholith. Inasmuch, however, as the factors controlling the development of zircon habit are not at present understood, this variation in itself serves no more to invalidate the present hypothesis than it does to demonstrate the hypothesis of Larsen and Poldervaart. While the zircon characteristics do indicate an environmental difference between the crystallization of the rim and the core, the significance of this difference is unclear.

It may be argued that the enormous transfer of alkalis and silica by the volatile phase demanded by this hypothesis is unlikely. This objection is valid to the extent that quantitative experimental data on the solubility of these constituents in the hydrous phase are not yet available. The experiments of Tuttle and Bowen (1958, p. 89) are encouraging, however, and, if their suggestion that alkalis and silica may migrate rapidly through the volatile phase by diffusion is correct, large-scale movement of these constituents is clearly possible.

Although the hypothesis presented is in several respects speculative, it does account for the detailed features of the zoning and, the writer believes, satisfies more conditions than any other theory thus far proposed. The mechanism requires no participation of country rock so that zoned intrusions may develop independently of wall-rock lithology. The hypothesis avoids the excessive energy requirements involved in fusing or making over the country rock into granite. Finally, the process is entirely magmatic and is in harmony with the igneous textural characteristics of the marginal facies.

Acknowledgments

The writer wishes to thank John Adams and J. Hoover Mackin of the University of Washington and Robert R. Compton of Stanford University for critical reading of the manuscript.

References Cited

Carr, J. M., 1954, Zoned plagioclases in layered gabbros of the Skaergaard intrusion, east Greenland: Min. Mag., v. 30, p. 367–375

Compton, R. R., 1955, Trondhjemite batholith near Bidwell Bar, California: Geol. Soc. America Bull., v. 66, p. 9–44

Larsen, L. H., and Poldervaart, A., 1961, Petrologic study of the Bald Rock batholith, near Bidwell Bar, California: Geol. Soc. America Bull., v. 72, p. 69–91

Morey, G. W., and Fenner, C. N., 1917, The ternary system H_2O-K_2SiO_3-SiO_2: Am. Chem. Soc. Jour., v. 39, p. 1123–1229

Reesor, J. E., 1958, Dewar Creek map-area with special emphasis on the White Creek batholith, British Columbia: Geol. Survey Canada Mem. 292, p. 1–78

Taubeneck, W. H., 1957, Geology of the Elkhorn Mountains, northeastern Oregon, Bald Mountain batholith: Geol. Soc. America Bull., v. 68, p. 181–238

Tuttle, O. F., and Bowen, N. L., 1958, Origin of granite in the light of experimental studies in the system $NaAlSi_3O_8$-$KAlSi_3O_8$-SiO_2-H_2O: Geol. Soc. America Mem. 74, 153 p.

Tuttle, O. F., and Friedman, I., 1948, Liquid immiscibility in the system H_2O-Na_2O-SiO_2: Am. Chem. Soc. Jour., v. 70, p. 919–926

Walker, F., 1956, The magnetic properties and differentiation of dolerite sills—a critical discussion: Am. Jour. Sci., v. 254, p. 433–434; Discussion by H. H. Hess, p. 446–451

Dept. Geology, University of Washington, Seattle, Wash.
Manuscript Received by the Secretary of the Society, October 13, 1960

Back Stock of GSA Bulletin

Arrangements were recently completed whereby The Geological Society of America appointed the firm of Walter J. Johnson, Incorporated, international dealers of scientific periodicals, as distributors for the remaining back stock of Volumes 37–65 of the Bulletin.

Orders for this back stock should be directed to Walter J. Johnson, Inc., 111 Fifth Avenue, New York 3, New York. The prices for back volumes of the Bulletin are $25 per volume and $2.50 per single issue.

Orders for back stock may also be placed with the distributor's branch offices: California Office, 1901 West Eighth Street, Los Angeles 57; British Office, 17 Old Queen Street, London S. W. 1; German Agency, Minerva, G.m.b.H., Holbeinstrasse 25–27, Frankfurt am Main; Italian Office, Periodici Scientifici, Via Gran Sasso 24, Milano.